AD-A093 795 ILLINOIS STATE WATER SURVEY URBANA F/G 4/2
BOUNDARY LAYER STRUCTURE AND ITS RELATION TO PRECIPITATION OVER--ETC(U)
OCT 80 G L ACHTEMEIER NSF-ATM78-08865
UNCLASSIFIED SWS-CR-241 ARO-15529.4-GS NL

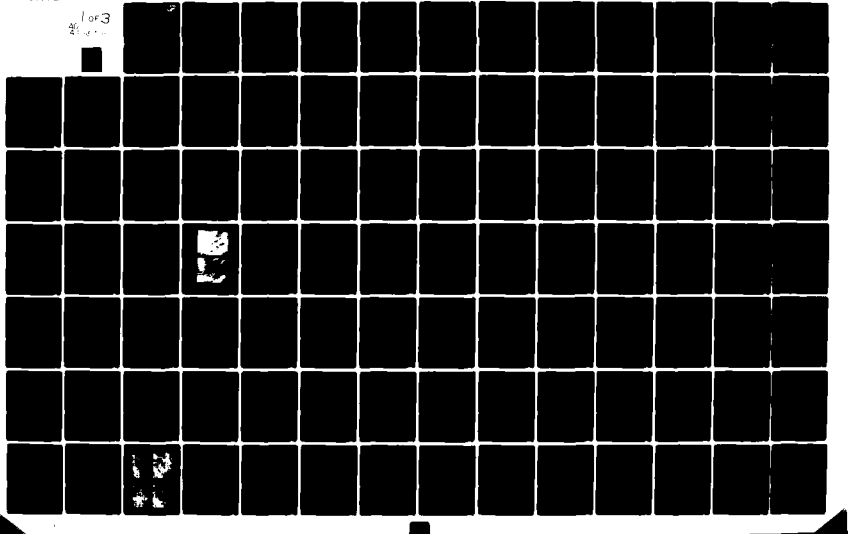

LEVEL II

State Water Survey Division
METEOROLOGY SECTION
AT THE
UNIVERSITY OF ILLINOIS

SWS Contract Report 241

Illinois Institute of Natural Resources

BOUNDARY LAYER STRUCTURE AND ITS RELATION TO PRECIPITATION OVER THE ST. LOUIS AREA

Gary L. Achtemeier
Meteorology Section
Illinois State Water Survey

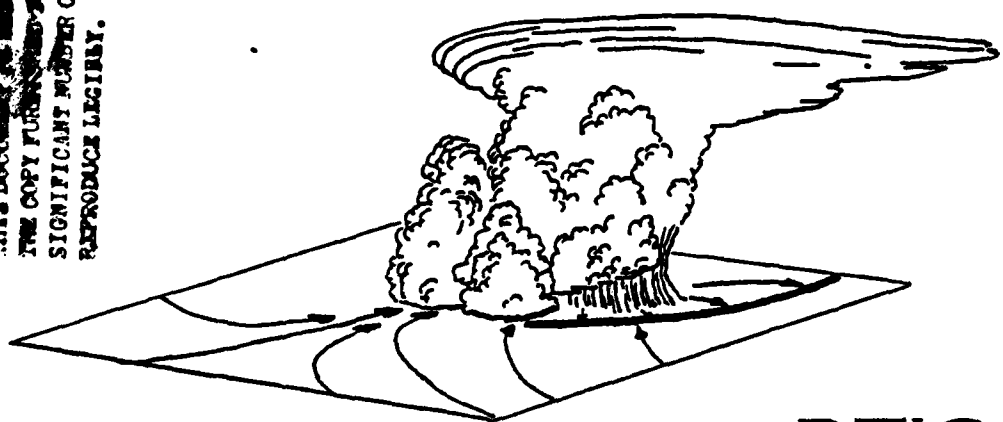

Technical Report 2
NSF Grant ATM 78-08865
Low Level Convergence and the
Prediction of Convective Precipitation
October 1980

Urbana IL 61801

The project "Low-level Convergence and the Prediction of Convective Precipitation" is a coordinated research effort by the State Water Survey Division of the Illinois Institute of Natural Resources, the Office of Weather Modification Research in the National Oceanic and Atmospheric Administration, and the Department of Environmental Sciences of the University of Virginia. Support of this research has been provided to the State Water Survey by the Atmospheric Research Section, National Science Foundation, through grant ATM-78-08865. This award includes funds from the Army Research Office and the Air Force Office of Scientific Research of the Department of Defense.

DISCLAIMER NOTICE

THIS DOCUMENT IS BEST QUALITY PRACTICABLE. THE COPY FURNISHED TO DTIC CONTAINED A SIGNIFICANT NUMBER OF PAGES WHICH DO NOT REPRODUCE LEGIBLY.

UNCLASSIFIED

SECURITY CLASSIFICATION OF THIS PAGE (When Data Entered)

REPORT DOCUMENTATION PAGE	READ INSTRUCTIONS BEFORE COMPLETING FORM
1. REPORT NUMBER: 15529.4-GS (19) (10) AD-A093 795	2. GOVT ACCESSION NO. / 3. RECIPIENT'S CATALOG NUMBER
4. TITLE (and Subtitle): Boundary Layer Structure and its Relation to Precipitation Over the St. Louis Area,	5. TYPE OF REPORT & PERIOD COVERED: Technical / 6. PERFORMING ORG. REPORT NUMBER
7. AUTHOR(s): (10) Gary L. Achtemeier	8. CONTRACT OR GRANT NUMBER(s): ARO MIPR 20-78, 21-78
9. PERFORMING ORGANIZATION NAME AND ADDRESS: University of Illinois, Urbana, IL 61801	10. PROGRAM ELEMENT, PROJECT, TASK AREA & WORK UNIT NUMBERS
11. CONTROLLING OFFICE NAME AND ADDRESS: U. S. Army Research Office, Post Office Box 12211, Research Triangle Park, NC 27709	12. REPORT DATE: Oct 80 / 13. NUMBER OF PAGES: 225
14. MONITORING AGENCY NAME & ADDRESS (if different from Controlling Office)	15. SECURITY CLASS. (of this report): Unclassified / 15a. DECLASSIFICATION/DOWNGRADING SCHEDULE

16. DISTRIBUTION STATEMENT (of this Report)

Approved for public release; distribution unlimited.

17. DISTRIBUTION STATEMENT (of the abstract entered in Block 20, if different from Report)

NA

18. SUPPLEMENTARY NOTES

The view, opinions, and/or findings contained in this report are those of the author(s) and should not be construed as an official Department of the Army position, policy, or decision, unless so designated by other documentation.

19. KEY WORDS (Continue on reverse side if necessary and identify by block number)

boundary layers
rainfall
precipitation(meteorology)
meteorology
wind(meteorology)
temperature

20. ABSTRACT (Continue on reverse side if necessary and identify by block number)

Rainfall, wind and temperature data at the surface and winds in the lower 1-2 km for a mesoscale area surrounding St. Louis, Missouri, for 7 summer days in 1975 were used in a study to determine the relationship between the surface kinematic fields and the occurrence and intensity of rainfall, and to determine if the surface kinematic fields are representative of the subcloud layer. It was found that, on some case days, patterns of convergence collocated favorably with rain-cells, were predictive of rainfall onset, and were positively related with

DD FORM 1 JAN 73 1473 EDITION OF 1 NOV 65 IS OBSOLETE

UNCLASSIFIED

SECURITY CLASSIFICATION OF THIS PAGE (When Data Entered)

15529.4-GS

20. ABSTRACT CONTINUED

rainfall amount. However, the relationships were nonexistent or negative on other case days. The statistics support the premise of the predictability of rain amount or rain mass based upon the preceding convergence on the cell scale and on the scale of the network, especially if some method that stratifies the convergence-rainfall relations can be found. Subsynoptic and/or mesoscale disturbances that tend to increase the potential for convective precipitation were present on all 7 case study days. These disturbances formed over the dense St. Louis surface network on three case study days. Although occurring under different synoptic conditions, these systems were similar structurally, being strongest near the surface and extending through a depth of 550 to 750 meters.

BOUNDARY LAYER STRUCTURE AND ITS
RELATION TO PRECIPITATION OVER THE ST. LOUIS AREA

Gary L. Achtemeier

TABLE OF CONTENTS

LIST OF TABLES

APPENDIX

LIST OF FIGURES

BOUNDARY LAYER STRUCTURE AND ITS RELATION TO PRECIPITATION OVER THE ST. LOUIS AREA

Gary L. Achtemeier

ABSTRACT

Rainfall, wind and temperature data at the surface and winds in the lower 1-2 km for a mesoscale area surrounding St. Louis, Missouri, for 7 summer days in 1975 were used in a study to determine the relationship between the surface kinematic fields and the occurrence and intensity of rainfall, and to determine if the surface kinematic fields are representative of the subcloud layer. It was found that, on some case days, patterns of convergence collocated favorably with raincells, were predictive of rainfall onset, and were positively related with rainfall amount. However, the relationships were nonexistent or negative on other case days. The statistics support the premise of the predictability of rain amount or rain mass based upon the preceding convergence on the cell scale and on the scale of the network, especially if some method that stratifies the convergence-rainfall relations can be found.

Subsynoptic and/or mesoscale disturbances that tend to increase the potential for convective precipitation were present on all 7 case study days. These disturbances formed over the dense St. Louis surface network on three case study days. Although occurring under different synoptic conditions, these systems were similar structurally, being strongest near the surface and extending through a depth of 550 to 750 meters.

ACKNOWLEDGMENTS

The research described in this report was carried out under grant ATM 78-08865 from the Atmospheric Science Division of the National Science Foundation. This grant award included funds from the Army Research Office and Air Force Office of Scientific Research.

This study utilized surface and upper air data collected in Project METROMEX by the Illinois State Water Survey with funding from the National Science Foundation under grant ENV 73-07796, the Department of Energy on Contract EY-76-S-02-1199 and with support from the State of Illinois. Additional data were provided by the St. Louis City and County Air Pollution Boards and by the U. S. Environmental Protection Agency from their Regional Air Pollution Study data bank. The cooperation of these agencies are appreciated.

Several people provided valuable assistance during the course of the research and preparation of the report. Most of the computer programming and data processing was done by Marilyn Schweitzer. Nancy Westcott reviewed, analyzed and edited several data banks, to provide a reliable final set which could be used in the analysis. Bernice Ackerman reviewed the manuscript. The figures were drafted and mounted by the Water Survey Graphics Unit under the direction of John Brother. Debbie Hayn typed the report from early draft to final manuscript.

A. INTRODUCTION AND METHODS OF ANALYSIS

INTRODUCTION

Over the years, evidence has been accumulating that low level convergence plays an important role in the development of precipitating convective systems. Convective systems, which vary in size, depth, intensity, and duration, are the main producers of precipitation over large parts of the world, from the tropics through the high latitudes. They range from the light rains falling from cumulus congestus to the intense driving rain, hail and strong winds of the squall line. In between is a hierarchy of convective systems, with the intensity of the rainfall tending to increase with increasing size of the system.

The occurrence of convective precipitation requires as a necessary but not sufficient condition, convective instability in the lower atmosphere, which must be released by some "triggering" mechanism. This triggering mechanism may be diabatic heating, differential advection of temperature or moisture, dynamic or mechanical lifting, acting independently or in combination. Unless the heating is localized, insolation acting alone will result in a more or less random distribution of cumulus clouds. However, in general, convective showers in the central part of the United States tend to occur in groups or in lines. This strongly suggests that dynamic mechanisms other than heating are also causing destabilization and/or convection to organize.

A number of researchers have found good correlation between precipitating convection and pre-existing convergence on the subsynoptic or mesoscale. Byers and Braham (1949) found that convergence developed at the surface up to one-half hour before the appearance of the first radar echo. Copeland and Hexter (1957) found a similar lead time in their study of frontal precipitation bands. On some thunderstorm days in eastern Colorado, the convergence preceded the precipitation by up to 5 hours (Anderson and Uccellini, 1974). Using findings on the lag between the convergence at the surface and precipitation for convective systems over the middle west, Achtemeier and Morgan (1975) and Changnon and Morgan (1976) introduced "cumulative lift," a parameter based on an integration (over time) of the surface divergence, as a predictor variable for the onset time and the location of thunderstorm areas in Illinois.

The above-mentioned studies have all noted the qualitative relationship between convergence and precipitation. Ulanski and Garstang (1978) in their study of surface kinematic fields on the cloud-scale in Florida, sought quantitative relationships between surface convergence and precipitation. Their results, still to be verified, suggest that quantitative estimation of time of onset of rainfall, total accumulations, and extent of precipitation may be possible from surface data.

Purpose of this Study

The Illinois State Water Survey research effort under the cooperative study of the link between low level kinematics and rain-cloud development included the analysis of rainfall, wind and temperature at the surface and winds in the lower 1-2 km for a mesoscale area around St. Louis, Missouri.

The goals of the research were a) to study the relationship between the surface kinematic fields and the occurrence and intensity of rainfall, b) to try to determine if the surface kinematic fields are representative of the subcloud layer, and c) to develop baseline information for the design of a field program for the measurements needed to quantize these relationships.

Activities fell into three progressive tasks: 1) the assembly of a uniform, good-quality data set for surface winds and temperature from a number of varied data bases, and selection of networks of wind, temperature, and rainfall stations; 2) objective analysis of the three data sets; and 3) the correlation and case study analysis of the objectively analyzed kinematic, thermodynamic, and rainfall fields. The first task utilized all data from the sources available for the summer of 1975. The correlation and case study research were based on seven rain days: five within the period 12-19 July, 30 July, and 14 August 1975. Ten periods of rain were selected for the case studies. Individually, they varied in duration, amount, and time of occurrence. They also varied as to the number of individual raincells within the total rainstorm, their intensity and their areal coverage. Further, they occurred under diverse synoptic and regional scale conditions.

Assemby of the Data Sets

Digitized 15-min rainfall values were available for the high density (one gage per 9 mi^2) 5000 km^2 raingage network operated in the St. Louis area by the ISWS during the METROMEX project (Semonin and Changnon, 1974). In the summer of 1975, three independent wind networks with a total of 41 stations existed within the area covered by the ISWS raingage network. These networks, operated by the U.S. EPA, the St. Louis city and county Air Pollution Control Boards, and the ISWS, were quite diverse in the types of instruments. Thus, the data from all three sources had to be carefully reviewed before they could be merged into a single data set. Details of the data editing are presented in the Appendix.

Analysis of the Surface and Upper Air Fields

The data from each of the mesoscale networks were analyzed objectively by the method described in Achtemeier et al. (1978). Whenever rain fell over the 227-station METROMEX raingage network during the 7-day study period, the 15-min rainfall amounts were objectively analyzed onto an 80 x 80 km mesh with 5-km grid spacing (Fig. A1). Data void areas are lined out. Adjustable parameters were set in the rainfall analysis so that the influence of any one data point dropped off rapidly with distance because rainfall is usually poorly correlated in space. The spatial smoothing by the objective analysis was also minimal so that maximum point amounts were almost totally restored.

The surface wind and temperature data were objectively analyzed for a smaller 40 x 40 km grid, with the same 5-km grid spacing. This grid was interior to, but compatible with, the rain mesh so that the rainfall wind and temperature data were presented at the same gridpoints. Fifty-five raingages were contained within the 40 x 40 km surface wind and temperature network (identified by square in Fig. A1).

The u and v components at each gridpoint in the wind network were used to calculate divergence and vorticity and the fields were stored on tape. This analysis was done for every 15-min interval for the 7-day analysis period.

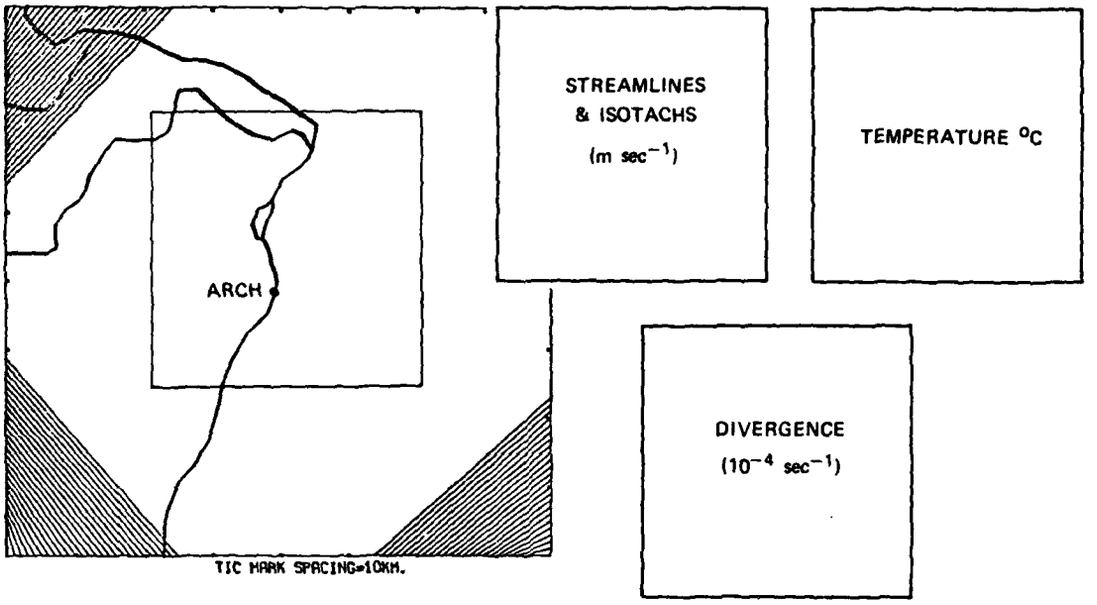

Figure A1. Format used for presentation of rainfall, streamlines and isotachs, temperature and convergence.

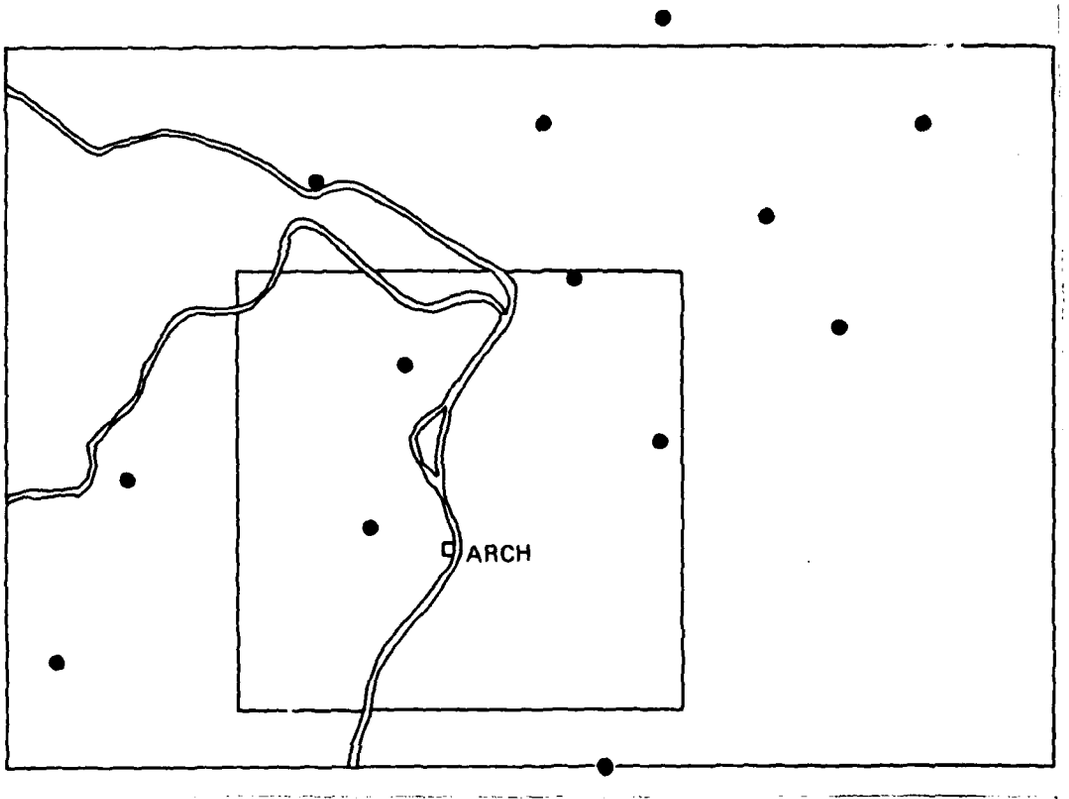

Figure A2. Map showing pibal sites (black dots) and outline of surface wind field network.

From the stored data, streamline and isotach patterns and contours of divergence and vorticity were objectively calculated and computer plotted. The method for calculating the streamlines has been described by Achtemeier (1978). The format for the presentation of the rainfall, streamline, isotachs, convergence and temperature is shown in Fig. A1.

The pibal data were analyzed objectively at 50 m height intervals from roughly 50 to 75 meters above the surface to cloud base. The upper-air mesh was 20 x 14, with 5-km grid spacing. All 3 meshes have common gridpoints in the overlapping areas. The location of the pibal network relative to the St. Louis area and the surface network is given in Fig. A2. The times the pibal data were available for the seven case study days are given in Table A1.

The hourly surface regional wind data were objectively analyzed onto a 15 x 18 grid with 48.55 km spacing that enclosed a 56,000 sq. km area bounded by northeastern Oklahoma, south-central Minnesota, western Michigan, central Tennessee, and northeastern Oklahoma (Fig. A3). Convergence fields were calculated from the u and v components at the gridpoints. The resulting regional scale wind analyses were objectively plotted as streamline and convergence fields. The divergence (positive) part of the fields was not plotted so that the convergence zones could be more easily identified.

METHODS OF ANALYSIS

Two analysis approaches, case study and statistical, were used in this investigation of rainfall and convergence. Most time was devoted to the case study approach which provided insights necessary to develop the statistical relationships between convergence and rainfall.

Case Study Approach

The rainfall/convergence part of the case study approach was to determine: 1) if there was any spatial relationship between patterns of convergence and rainfall measured at the ground; 2) if the amount of rainfall was proportional to the strength of the convergence; and 3) if the convergence could be used to predict the locations and amount of the rainfall. This study used rainfall maps and mesoscale fields of surface wind streamlines, isotachs, convergence and temperature.

Table A1. Times of Pibal Ascents for the Seven Rain-Case Study Days.

Day		Hour CST				
July	12	----	----	----	----	----
	13	1130	1200	1300	1400	1500
	17	----	----	----	----	----
	18	1100	1200	1300	1400	1500
	19	1100	1200	1300	----	----
	30	1100	1200	1300	1400	1500
August	14	----	1200	1300	1400	1500

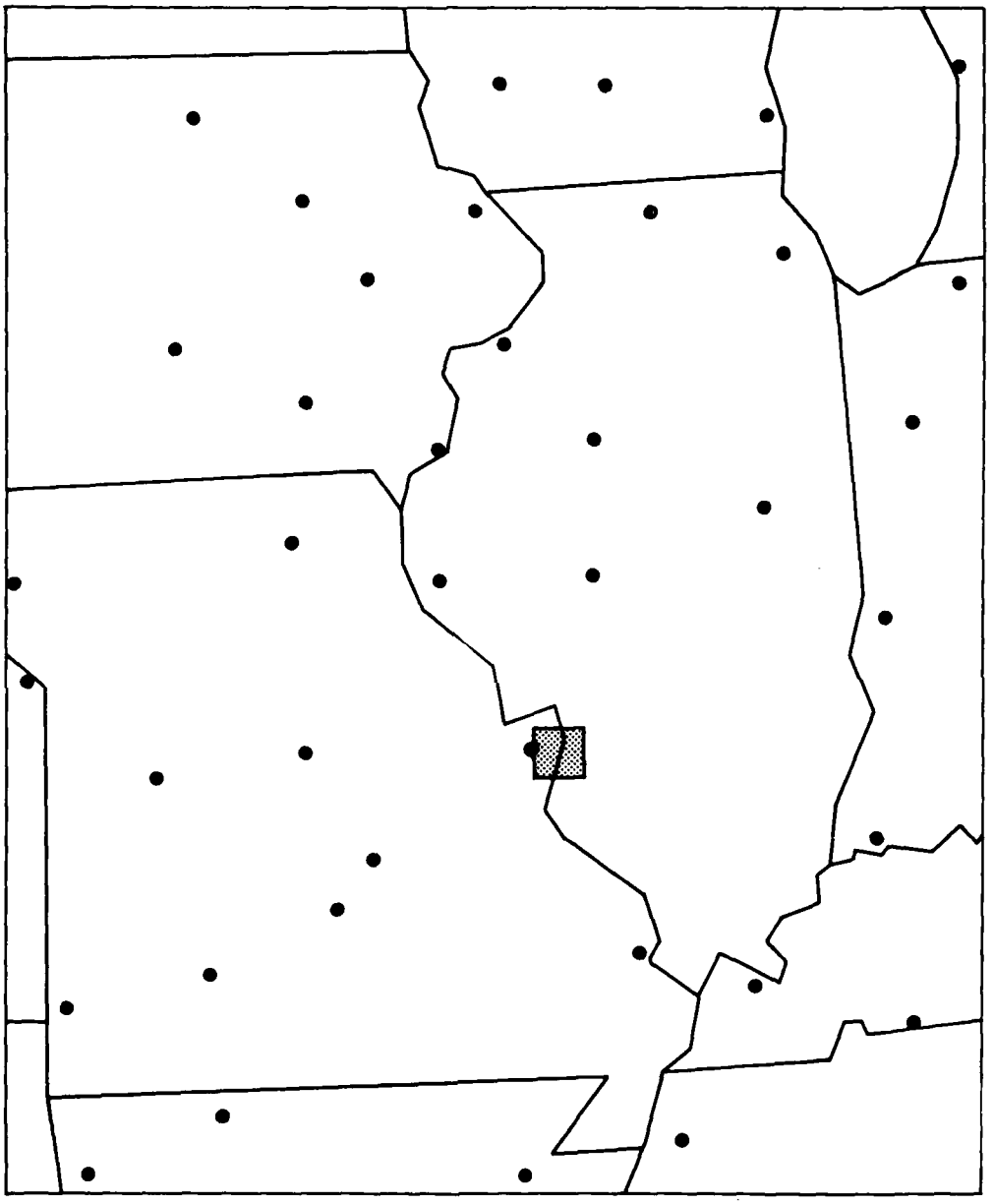

Figure A3. Base map for the regional scale wind field analyses.

The boundary layer part of the case study approach was to determine to what heights features in the surface wind and convergence fields could be found in the boundary layer. The pibal wind data were used to develop objectively analyzed fields of streamlines and isotachs, and wind divergence at selected levels from 250 m to 1350 m. These fields were compared with the surface analyses through pattern recognition and through vertical profiles of mean divergence, mean maximum and mean minimum divergence, and point maximum and point minimum divergence. (Minimum divergence values are equivalent to maximum convergence.)

The system part of the case study approach was to determine the scale and type of weather system (synoptic scale, regional scale, large mesoscale, thunderstorm scale) that was mostly likely responsible for the initiation of deep precipitating convection over the St. Louis network. A careful examination of synoptic weather maps, regional scale objective surface wind analyses and the St. Louis network surface and boundary layer analyses revealed a number of diverse precipitation causing systems. Time series of the St. Louis network scale convergence helped in determining the scale of the convergence. The results proved helpful in the stratification of weather types for which convergence and rainfall were poorly related.

As part of the case study approach, it was necessary to develop techniques to simplify some analyses and to clarify others. Rather than find the total raincell rainfall, we used a quantity defined as the "cell strength," the summation of the maximum point rainfalls at each analysis time. For example, if a raincell that lasted for two 15-min periods produced a maximum point rainfall of 1.0 mm for the first period and produced a maximum point rainfall of 3.5 mm for the second period, its cell strength would be 4.5 mm.

A similar approach was used to determine the strength and duration of the convergence centers that existed prior to the collocated development or passage of raincells. For example, if the convergence preceding the raincell covered three analysis periods and had magnitudes of respectively, 1U*, 2U, 2U, the convergence strength would be 5U and the convergence duration would be 45-min.

It was found that divergence of both signs was always present over large areas of the St. Louis network, including the prolonged rainless periods. This "background" convergence was due to a number of non-rain factors that perturbed the surface winds. Some possible causes of local wind variations are; general gustiness, flow over unlevel terrain including a city, channeling along a river valley, obstructions by trees or by man-made structures, and variations in instrument elevation (AGL). Background convergence patterns tended to persist when the winds were steady. Convergences were required to exceed the background (usually -4U) as indicative of non-background meteorologically significant circulations. Exceptions were when local convergence centers changed the character of the overall convergence patterns and/or when wind speeds were very light.

*Divergence and convergence are expressed in terms of units, U, throughout this report where $U = 1 \times 10^{-4}$ sec^{-1}.

As an example of background convergence and divergence, Fig. A4 shows the time series for the maximum and minimum point divergence for 19 July. At no time during this day did the peak divergence of either sign approach zero although there was a long rainless period between 0730-1330 CST. There were numerous short duration peaks in both time series, some of which were associated with rainfall and some of which were not. However, none of these peaks were considered significant until they exceeded 4U. Those peaks (pointing downward) that exceeded background in the convergence time series are identified by the arrows.

The Statistical Approach

The statistical analysis was concerned with determining the strength of the relationship between network scale convergence and network scale rainfall variables and determining the strength of the relationships between the convergence and the rainfall from raincells selected from several of the case studies. Temporal fields of correlation coefficients were developed by several methods. This analysis made it possible to follow the evolution of the convergence relative to the raincells and to find the magntiude and persistence of correlation coefficient extreme.

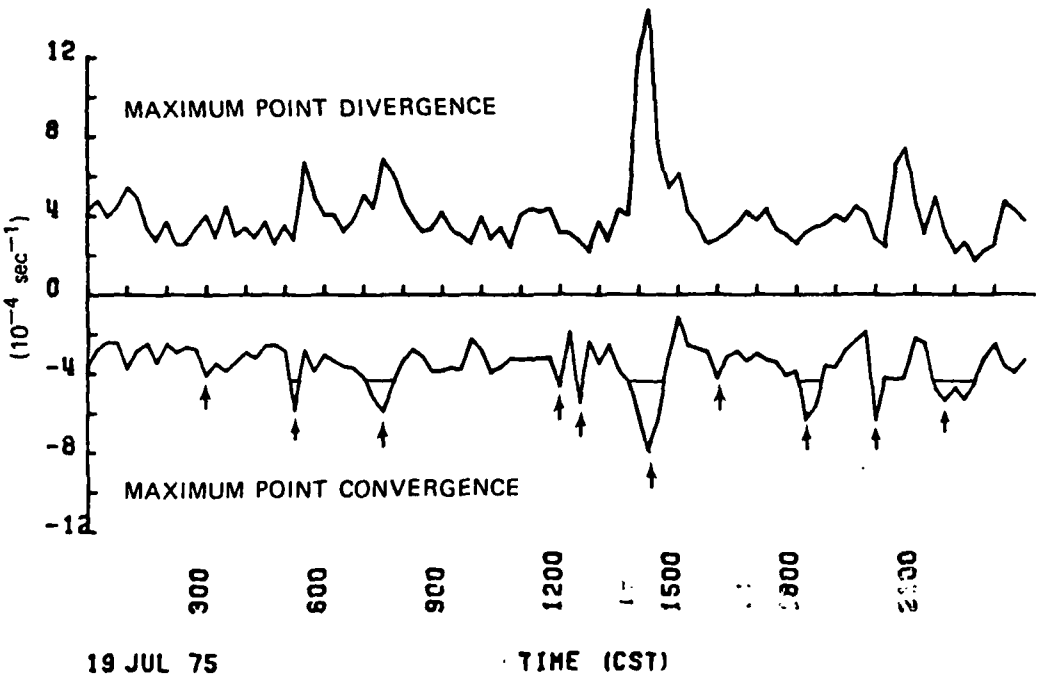

Figure A4. Time series of the maximum and minimum point divergence for 19 July 1975.

B. SUMMARY OF RESULTS

The various case study analyses and the statistical studies are summarized in this section. The section begins with the search for dynamic precipitation producing weather systems and concludes with the statistical studies. Detailed analyses and results of the 7 case studies are given in the following sections, C through I.

SCALES OF PRECIPITATION PRODUCING WEATHER SYSTEMS

It has been found from other studies (Ackerman, 1978 and 1979) that surface and boundary layer convergences on dry days may be as large as convergences on days with convective precipitation. The differences between moist and wet days is in the larger scale environment which is more favorable for showers because of greater instability (leading to airmass showers) and/or because convective instability is released by some dynamic weather disturbance (producing organized areas or lines of showers).

Table B1 summarizes the search for weather systems that could have started the rainfall within the St. Louis network and the surrounding areas during the case study period. It was found that some possible synoptic, regional, or mesoscale rainfall-causing mechanism was present for all 10 rain periods studied.

The synoptic scale circulations contributed to possible shower development through an upper level cyclone which brought a deep layer of unstable cold air into the Midwest on 12-13 July. During the period 17-19 July, there was no discernible synoptic scale precipitation forcing mechanisms. Weak positive vorticity advection (PVA) at 700 mb on 30 July and 14 August could have developed ascending motions that led to increased convective instability. However, the suggestion of PVA on 30 July is based upon the 700 mb flow and was not supported by satellite photographs which showed synoptic scale cloud areas confined south of Missouri. The 14 August situation was the more classic 700 mb trough passage.

Although synoptic scale systems contributed to precipitation initiation on some of the case days, possible regional scale and mesoscale (network scale) precipitation initiating disturbances were present on all rain periods. None of these disturbances could be considered as typical of frontal passages and frontal related precipitation which are the major precipitation producers in the upper Midwest (Huff, 1977). Precipitation on 12 July occurred behind a secondary cold front, and rainfall on 14 August was triggered within unstable airmasses about 150 km south of a stationary front. Frontal zones were not present in the network vicinity at the other times.

With the exception of rain periods 1 19 July (possible gravity waves) and 2 19 July (850 mb convergence), well defined convergence areas and/or squall lines were present at the surface. The convergence zones tended to appear up to 2 hours prior to the initiation or intensification of rain systems as determined from the satellite photographs. In some instances showers occurred near the edge of the convergence areas. During the 13 July rain periods, cumulus clouds within the convergence area (as revealed in satellite photos) grew progressively deeper as air flowed downwind through the convergence area and developed into the cumulonimbus stage at the far downwind edge.

Table B1. Scales of Weather Systems Associated with the Rainfall Periods.

No.	Date	Period	Synoptic	Regional Scale	Network Scale
1	12 July	1100-1930	Unstable cold low	Secondary cold front	none
2	13 July	1200-1700	Unstable cold low	500 mb trough	Surface low/ convergence zone
3	17 July	1130-1700	none	Surface convergence area	Possible urban circulation
4	18 July	1130-1530	none	Surface convergence area	Convergence zone
5	19 July, I	0000-0300	none	none	Gravity waves?
6	19 July, II	0500-0700	none	850 mb convergence	none
7	19 July, III	1330-1500	none	Surface convergence area	none
8	30 July	1215-1800	Weak PVA at 700 mb	300 mb trough, surface convergence zone	Convergence zone
9	14 Aug.	0730-1000	Weak PVA at 700 mb	Convergence zone	Squall line
10	14 Aug.	1530-1700	Weak PVA at 700 mb	Convergence zone	Convergence Zone

In some cases, the evolution of the convergence areas revealed the physical mechanism for its development. For example, rain period III 19 July formed within a convergence area that developed over southern Missouri in response to differential vertical momentum transport, a process that brought increasing amounts of westerly momentum from to a low-level wind maximum (jet) to the surface in northern Missouri, but brought down lesser amounts of westerly momentum in southern Missouri where the jet was not present. This resulted in general confluence of northward flowing airmasses with eastward flowing airmasses over central Missouri.

The convergence area over Missouri on 30 July, well correlated with deep convective clouds, may have been coupled with circulations in the trough at 300 mb that developed over the same area, although such a coupling was not obvious in the routine analyses.

Twenty-seven prominent raincells and their associated convergence areas (if any) (Table B2) were part of a study to determine the mesoscale system (if any) that caused convergence within the St. Louis network. The selection was not based upon the presence of convergence but, rather, favored those cells that were prominent by cell strength and were separated from neighboring cells. Seven of the 27 raincells (26%) were not preceded by discernible convergence. All seven occurred during the 18-19 July period.

The wind field and temperature analyses showed convergence centers along boundaries between gust fronts and the ambient air, at the intersection of gust fronts, and at the intersection of gust fronts with pre-existing mesoscale convergence zones. In addition, there were convergence generating mechanisms not caused by rainshowers; possible urban induced circulations and, mesoscale convergence zones.

The convergence centers associated with the raincells in Table B2 were classed as follows: 0 - no apparent convergence; 1 - convergence along a gust front; 2 - convergence at intersecting gust fronts; 3 - convergence at intersection of a gust front and a mesoscale convergence zone; 4 - convergence within possible urban circulations; and, 5 - convergence within mesoscale convergence zones. As has already been noted, 7 raincells were classed under category 0. Only 3 raincells could be classed as having been formed along a gust front. This compared with 7 raincells formed at the intersection of gust fronts and 4 raincells formed at the intersection of a gust front and a mesoscale convergence zone. The suspect urban circulation accounted for 1 raincell and the mesoscale convergence zone accounted for 5 raincells.

Some additional explanation of these figures is necessary. Clearly, the category 4 and 5 raincells forming in the absence of gust fronts or their intersections with mesoscale convergence zones are rare because once a raincell has formed, its gust front will spread outward and greatly reduce the area in which another category 4 or 5 storm can form. Also the importance of the mesoscale convergence zone in raincell development cannot be overstressed. The formation of 9 raincells were in some manner associated with mesoscale convergence zones. In some instances, particularly with the 61 mm storm at 1600 on 14 August, a mesoscale convergence zone existed nearby for more than one hour before interaction with the gust front from a neighboring raincell triggered the storm. A similar condition existed for the raincells that developed between 1215-1230 17 July except the precursor was an apparent urban circulation.

Table B2. Convergence and Rainfall Information for 27 Raincells.

Date	Cell ID	Cell Strength	Time of Maximum 15-min Rainfall	Convergence Strength	Duration	Apparent Cause
12 July	M	11mm	1900 CST	4U	30 min	1
13 July	H	7	1630	31	60	5
17 July	C	38	1215	5	45	4
	D	10	1230	22	105	2
	G	38	1245	8	30	2
	I	8	1330	20	45	2
	K	28	1345	8	30	2
	L	19	1415	14	45	2
	M	12	1430	12	30	2
	T	9	1615	2	15	1
18 July	E	13	1215	0	0	0
	G	2	1230	4	15	1
	N	7	1345	0	0	0
	O	14	1400	0	0	0
19 July	B	3	0500	0	0	0
	D	12	0530	0	0	0
	B	4	1400	0	0	0
	C	11	1415	0	0	0
	F	3	1430	10	60	2
30 July	E	9	1345	18	75	3
	H	6	1430	8	45	3
	Q	13	1745	9	45	3
14 August	A	24	0745	2	15	5
	C	18	0800	2	15	5
	F	13	0845	2	15	5
	B	20	1530	22	195	5
	D	61	1600	18	45	3

[1] See text for description of causes.

Mesoscale Convergence Studies

The 15-min convergence, wind field, and temperature analyses for rain, pre-rain, and non-rain periods were studied in detail to determine a) if there was a spatial relationship between convergence and rainfall, b) if there was a relationship between convergence and rainfall amount, and c) if the relationship between convergence and rainfall was predictive of rainfall. In general, it was found that the convergence/rainfall relationship was highly variable from day to day and from storm to storm. There was no straightforward quantitative method to express the relationship in a manner free from ambiguity.

Because of this variability, a full understanding of the convergence rainfall relationship for these case days cannot be realized without a review of the original analyses. To accomplish this, details of the surface and boundary layer analyses have been presented for each case day in the following sections. The remainder of this section will briefly summarize the general aspects of the convergence rainfall relationship.

Very strong convergence centers were present during some rain periods and were almost totally absent during other periods. Some raincells developed near areas of weak convergence but were absent within areas of strong convergence. During other periods the convergence/rainfall relationships were excellent in both location and intensity of convergence and rainfall. Some convergence areas persisted for over an hour before rain was recorded at the ground. Other convergence areas appeared almost simultaneously with the rainfall.

Summaries of the convergence rainfall relationship by day and/or rain event for the seven case days are presented below.

12 July

Precipitation occurred within an unstable Canadian airmass behind a secondary cold front. The airmass was relatively dry and cool and it is likely that much of the precipitation was evaporated before it fell to the ground. The raincells, which began at 1100 and lasted through 1930, were characterized by light rainfalls, strong divergent outflows and weak or nonexistent convergent inflows. Fourteen raincells were included in the 12 July study. Eight of these moved onto the network. Two of the remaining six raincells formed near the boundaries of the wind network where data were insufficient to determine the convergence.

The maximum cell strength for the four cells that formed within the data dense part of the network was only 1.5 mm. Convergence centers accompanied three of these cells. The maximum convergence strength was only 2U, less than the background convergence for the 12th. The average cell strength for the four raincells was 1.1 mm, the average convergence strength was 1U and the average duration was 15-min. There were too few raincells to determine a relationship between convergence strength and cell strength.

With regard to a spatial relationship between convergence and rainfall, convergence was favorably located for the development of three of the four raincells that formed over the data dense part of the St. Louis network. These centers were weak and of short duration, being present only 15-30 min

prior to raincell formation. Possible explanations for the short lead times are 1) the convergence centers were not related to the developing raincells, i.e., the spatial collocation was chance, 2) the data were not dense enough to resolve the convergent inflows until the developing storms passed close enough to a single wind site to perturb the wind speed and direction, and 3) the storms initially drew from heat and moisture at the top of the mixed layer and it was only later in the development stage that the cloud circulations extended down to the surface.

There were eight other convergence centers that occurred during the rain period but were not associated with rainfall. Seven of the eight centers had convergence strengths equal to or greater than 4U and durations greater than 30-min. Thus, they were stronger and more persistent than the convergence centers that were thought to be associated with rainfall. The strongest convergence center that occurred during this period persisted for 60-min and had a strength of 10U.

Only three of eleven convergence centers were possibly associated with rainfall. These were among the weakest and shortest duration of the centers. Therefore, on this day, there apparently existed little if any predictive relationship between the convergence centers, either in location and/or in strength, and the raincells.

13 July

The synoptic weather conditions on the 13th were much the same as they were on the 12th as the unstable Canadian airmass persisted over the St. Louis area. Regional and mesoscale convergence systems combined to make conditions favorable for showers which fell from 1200-1700. Fifteen raincells developed over or sufficiently near the St. Louis network to influence the wind field. Twelve of these were within the data-dense areas where the convergence could be accurately determined.

Cell strengths ranged from 0.5 to 13.0 mm. Convergence centers preceded eleven of the twelve cells. The maximum convergence strength was 31U with a duration of 60-min. The average cell strength was 3.0 mm, the average convergence strength was 9.1U, and the average convergence duration was 30-min.

The spatial relationship between the raincells and the convergence centers was quite good for the 13th. The centers persisted for 30-min or longer for 8 of the 12 raincells. Thus the convergence centers were fairly predictive of the future location of raincells and with few false alarms - only 3 convergence centers were not associated with rainfall. These centers had strengths and durations of, respectively, 4U (15-min), 8U (30-min), and 20U (45-min).

Eight of the twelve raincells produced cell strengths less than 1.5 mm. The cell strengths and convergence strengths for the remaining four raincells were, respectively, 2.0 mm (10U), 5.0 mm (0U), 7.0 mm (31U), and 13.0 mm (20U). One 1.5 mm raincell was associated with a 16U convergence center. For the remaining weak raincells, convergence strengths were less than 10U. Thus, with some scatter, a positive relationship between convergence strength and cell strength was apparent on the 13th.

17 July

Copious amounts of moisture came to the St. Louis area with deep southerly flow. An area of convergence that persisted over southern Missouri for about 4 hours from mid-morning until early afternoon apparently initiated the convective showers which lasted from 1130 to 1700. No fronts were in the area. Showers were of the airmass variety at the beginning of the rain period and became organized into a squall line near the end of the period.

Thirteen of the fifteen raincells that formed over the St. Louis network were preceded by convergence centers for periods up to 105-min. Cell strengths ranged from 0.5 to 38.0 mm. The average cell strength was 15.4 mm, the average convergence strength was 8.9U, and the average pre-rain convergence duration was 36-min. Five convergence centers not associated with raincell development had strengths and durations of, respectively, 2U (15-min), 4U (15-min), 10U (45-min), and 22U (105-min).

The spatial relationship between the convergence centers and the raincells was quite good for the 17th. Convergence preceded raincells by 30-min or greater for 10 of the 15 raincells. This along with the finding of only five "false alarm" convergence centers is suggestive of a fairly good predictive relationship. There was no apparent relationship between cell strength and convergence strength.

18 July

Showers developed from 1130 to 1530 on the 18th after an area of convergence developed and persisted over southeastern Missouri. There were no fronts in the area and the showers appeared at scattered locations over the network. Twenty raincells developed over or sufficiently near the network to influence the wind field. Of these, 10 either moved onto the network or formed near the boundaries in areas where the data was not sufficient to define the convergence field accurately.

The cell strengths for the 10 raincells which developed in the network ranged from 0.5 to 14.5 mm. Overall, the precipitation was lighter on the 18th than on the 17th. The average cell strength was 5.3 mm, the average convergence strength was 1.2U, and the average convergence duration was only 6-min. The relationship between cell strength and convergence strength, if any, was negative.

Only four of the ten raincells were preceded by convergence. None of the convergence strengths exceeded 4U and none of the durations exceeded 15-min. The two strongest raincells (strengths of 13.0 and 14.5 mm) were not preceded with convergence. With only four of the ten raincells preceded by weak, short-duration convergence, the spatial relationship was considered as poor.

Eighteen convergence centers not associated with rainfall occurred over the network during the rain period. Seven persisted for 30-min or longer and one persisted for 150-min, with a strength of 32U. Further, with ten raincells and 22 convergence centers occurring during the same time period, it is likely that several raincells would be favorably located in space and time with convergence centers by chance.

Given that 60% of the raincells were not associated with convergence and that 82% of the convergence centers were not associated with rainfall, the predictive relationship between convergence and rainfall must be judged as very poor.

19 July

The weather conditions were disturbed on the 19th and three rain periods occurred. The first was a 3-hour period of light rain showers that began at midnight. The second rain event occurred over a 2-hour period beginning at 0500 CST and apparently was associated with a convergence producing disturbance at 850 mb. It produced five raincells over the St. Louis network with strengths ranging from 2.0 mm to 12.0 mm. The average cell strength was 6.8 mm.

No convergence centers preceded the raincells although seven convergence centers with strengths upto 8U and durations to 60-min occurred during the same period. Thus, there was no relationship between convergence and rainfall for this early morning rain event.

The third rain event began at 1330 CST and lasted for 1.5 hours. It formed within an area of convergence over southern Missouri which was not unlike the convergence system that produced rainfall on the 18th. Seven raincells formed over the network but only two were associated with surface convergence. The average cell strength was 6.0 mm, the average convergence strength was 1.7U and the averge convergence duration was 11-min. The strongest raincells (11.0 mm and 21.0 mm) were not preceded by convergence. During this same period, there were six other convergence centers with strengths ranging from 2U to 18U and durations ranging from 15-min to 120-min.

There was no apparent spatial relationship between convergence centers and rainfall. The relationship between cell strength and convergence strength, if any, was negative. The convergence centers apparently were not predictive of raincell formation on this day.

30 July

A weak convergence zone, possibly associated with a 300 mb trough, developed over the St. Louis network along an old frontal zone that was distinguished only by a sharp contrast in haze. Showers with relatively light rainfall amounts and with short durations formed in a scattered fashion beginning at 1200 CST and were active until 1800 CST. Ten raincells with strengths ranging from 0.5 mm to 13.0 mm formed over the network. The average raincell strength was 3.6 mm, the average convergence strength was 4.9U, and the average convergence duration was 33-min.

All ten raincells were preceded by convergence. The convergence durations equal to or exceeding 30-min were found for seven of the ten cells. Four convergence centers with strengths and durations of, respectively, 4U (15-min), 4U (30-min), 6U (30-min), and 10U (30-min) were not associated with rainfall. The strongest convergence associated with rainfall was 18U and it lasted 75-min.

The spatial relationship between raincells and centers of convergence was excellent. The centers preceded rainfall for 30-min or longer for 7 of the 10 storms. Thus, on this day, the convergence centers were fairly predictive of the future location of raincells and there were only 4 false alarms.

There appeared to be a signficant qualitative relationship between convergence strength and raincell strength for the 30th. Convergence strengths for the lighter raincells (strengths equal to or less than 3.0 mm) did not exceed 4U. Raincell strengths and convergence strengths for the heavier raincells were, respectively, 5.5 mm (8U), 9.0 mm (18U), and 13.0 mm (9U). The relationship was also apparent in the convergence durations which ranged from 45-min to 75-min for the stronger storms and ranged from 15 to 30-min for the lighter storms.

14 August

A weak 700 mb disturbance produced three periods of rainfall over the St. Louis network on the 14th. These rain events occurred within warm, humid, unstable airmasses 150 km south of a stationary front. The first period of rain began at 0115 CST and lasted for 45-min. The raincells formed along the southern boundary of the St. Louis network over an area where the data was insufficient to resolve the wind field. The second rain event began at 0730 CST and lasted for 2.5 hours. Moderate amounts of precipitation fell from an aged squall line that died out within the network. The squall line reactivated to produce rainfalls of cloudburst proportions from 1530 to 1700 CST.

Seven raincells with strengths ranging from 1.5 mm to 24.0 mm formed over the network during the second period of rain. The average cell strength was 12.6 mm, the average convergence strength was 2.0U and the average duration was 15-min. Convergence preceded six of the seven raincells but only one had a duration exceeding 15-min. Two convergence centers with strengths and durations of, respectively, 2U (15-min) and 12U (60-min) were not associated with rainfall.

The spatial relationship between the convergence centers and the raincells was very good. Because of the short durations of the convergence centers (15-min or less for 6 of the 7 cells) the appearance of convergence centers was not considered to be predictive of the raincell development. Furthermore, there was no apparent relation between cell strength and convergence strength for these early morning storms.

Five raincells formed during the third rain event, one with a strength of 61.0 mm. The average cell strength was 31.2 mm, the average convergence strength was 12.0U, and the average duration was 66-min. Four of the five raincells were preceded by convergence which persisted for 30-min or longer. The fifth raincell was in a location to receive moisture that had been lifted within the convergence zone of the reactivating squall line and carried by the 500 m winds. There was one convergence center (16U and 60-min) that was not accompanied by rainfall.

The spatial relationship between the raincells and the convergence centers was very good. The convergence centers were also predictive of the location of raincell formation. There was no apparent relationship between the convergence strengths and the strengths of the raincells.

Other Results

Some other findings of the surface convergence/rainfall study were as follows:

a) The nocturnal raincells were more weakly reflected in the surface wind field than were the daytime raincells.

b) With some exceptions, convergence magnitudes prior to raincell development were within the range of -2U to -4U. After raincell development and ensuing strengthening of wind field by downdrafts, the convergence magnitudes frequently increased to -6U to -8U. A number of other raincells were found to produce considerable divergence but little convergence. A possible explanation may be in the 15-min averaging for the winds. With rapidly moving gust fronts, strong local convergence occurs at any one location for a very short period as the gust front passes and then the flow may become strongly divergent. When the winds are averaged over 15-min, the convergence may be averaged out.

c) The analysis of the surface temperature field proved to be helpful in locating the gust fronts and determining the strength of outflows. Raincells didn't develop within strong convergence areas within rain cooled airmasses on most case study days. This indicates that a heated surface layer is a factor in raincell development.

VERTICAL STRUCTURE OF THE BOUNDARY LAYER

Objectively analyzed streamline, isotach, and convergence fields from pibal wind data at selected levels within the boundary layer were used a) to describe the vertical structure of significant weather systems, and b) to relate the vertical structure to the more densely sampled surface patterns. In general, there was a wide variety of wind field perturbations, and except for the mesoscale circulations, the relationship with rainfall and surface convergence patterns was ambiguous because of differences in station spacing (20 km pibal vs. 5 km surface) and gustiness in the boundary layer winds. Average boundary layer inflows into the surface network were generally consistent with the calculated surface inflow. Descriptions of the vertical structure have been included in the daily case summaries given in the following chapters.

Mesoscale convergence zones were most easily identified by wind direction confluence within the streamline fields. The three confluence zones that were observed (18 and 30 July, 14 August) were similar in their vertical structure. These systems were 550-750 m deep and persisted for several hours. The confluence was strongest at the surface and gradually diminished upward. The 30 July convergence zone maintained its structure after shower outflows lifted it, from the lowest one-half kilometer to levels above 750 m.

STATISTICAL RELATIONSHIPS BETWEEN CONVERGENCE AND RAINFALL

Several methods for the statistical analysis of the relationship between the surface convergence and rainfall have been tried. These include statistical analysis on the network scale and statistical analysis on the raincell scale.

Statistical Analysis on the Network Scale

The objective analysis produced gridded values of rainfall and divergence at each of 81 points of the 9 x 9 wind network mesh. Three rainfall and 5 divergence variables were defined from the gridded fields. The rainfall variables were correlated with the divergence variables, each having been defined at 15-min intervals for each case day. The correlation analysis is thus based on 672 values of each parameter.

The field variables are:

a) Network average rainfall (RAVG) defined as the average rainfall for all the gages with rain within the network.

b) Network total rainfall (RTOT) defined as the sum of all the gridpoint rainfall amounts.

c) The largest 15-min rain rate (RMAX) at any gridpoint in the wind network.

d) Network average divergence (DAVG) defined as the average of the gridpoint divergences. From continuity considerations, DAVG should be approximately equal to the inflow into the area, calculated by the line integral of the normal flow along the grid boundaries.

e) Network average negative divergence (DMNA) defined as average of all the negative values of divergence over the grid, zero excluded (thus the average of the convergence values).

f) Network average positive divergence (DMXA) defined as the average of all the positive values of divergence over the grid, zero excluded.

g) Point minimum divergence (DMIN) defined as the largest absolute value of negative divergences (strongest gridpoint convergence) anywhere within the grid.

h) Point maximum divergence (DMAX) defined as the largest positive divergence at a gridpoint anywhere within the grid.

The correlation coefficients for the 5 "characteristic" divergence parameters and the 3 rainfall variables are shown for various lag times in Table B3. (Lag time is defined as time of rain minus time of divergence.) All 15-min values for the 7 case days were used in these calculations. For a large fraction of the time there was no rain and during these periods the rainfall parameters were constant (zero). Since the divergence was not constant during the non-rain periods, one must expect relatively low correlation coefficients, and indeed they seldom exceeded 0.6.

Table B3. Pearson correlation coefficients between rainfall and divergence parameters for lags ± 75 mins. Lag time = time of rain value minus time of divergence, thus positive (negative) lags are for rains following (preceding) divergence. See text for definitions of variables.

Log (min)	DAVG RAVG/RTOT/RMAX	DMNA RAVG/RTOT/RMAX	DMIN RAVG/RTOT/RMAX	DMXA RAVG/RTOT/RMAX	DMAX RAVG/RTOT/RMAX
+75[1]	.01/-.08/-.01	-.27/-.30/-.30	-.29/-.33/-.33	.21/ .16/ .21	.22/ .16/ .22
+60	.03/-.05/ .01	-.32/-.35/-.37	-.32/-.38/-.38	.28/ .24/ .31	.30/ .22/ .30
+45	.05/-.04/ .04	-.37/-.43/-.45	-.38/-.44/-.45	.32/ .30/ .39	.34/ .29/ .39
+30	.05/-.03/ .05	-.43/-.53/-.53	-.46/-.52/-.53	.39/ .38/ .47	.39/ .39/ .47
+15	.11/ .04/ .11	-.43/-.55/-.55	-.42/-.51/-.52	.43/ .47/ .51	.42/ .49/ .54
0	.19/ .16/ .20	-.42/-.49/-.52	-.39/-.42/-.46	.51/ .58/ .59	.51/ .56/ .59
-15	.28/ .30/ .31	-.42/-.37/-.45	-.42/-.32/-.43	.55/ .58/ .62	.54/ .53/ .61
-30	.34/ .35/ .37	-.33/-.26/-.36	-.30/-.20/-.32	.51/ .48/ .58	.47/ .44/ .53
-45	.41/ .37/ .42	-.23/-.15/-.24	-.19/-.10/-.21	.46/ .37/ .47	.44/ .36/ .45
-60	.43/ .35/ .42	-.16/-.06/-.16	-.14/-.03/-.13	.43/ .27/ .41	.42/ .29/ .41
-75	.41/ .32/ .41	-.09/ .00/-.07	-.07/ .03/-.04	.31/ .18/ .30	.31/ .21/ .32

[1] For lags greater than +75, all coefficients were less than .3 for DMNA, DMIN and less than .2 for DMXA and DMAX.

The correlation between rainfall and divergence was consistently greater for the "sub-network" divergence parameters, and smallest for the network average, DAVG, a measure of the net mass inflow into the area. This suggests a dependency of the relationships between rainfall and divergence on the sizes of the grid over which the average is taken and of the storm circulations.

At times the divergence and convergence both tended to maximize during periods of rainfall and DAVG was often a small difference between two large quantities and no larger than it was for the non-rain periods. This suggests that the circulations that linked with convective rainfall occurred over areas smaller than the 1600 sq. km wind network.

The correlation between the DAVG and rain was very small for positive lags but increased with increasing negative lags (divergence following rain). They were also positive, reaching the highest value of 0.42 for 45-min after the rain. This indicates that, as the rainfall increased, the flow over the network became increasingly divergent and the net outflow out of the network increased, but for this size network there was a response time of 30-min to an hour.

The dense mesoscale network of wind stations permitted the resolution of divergence scales smaller than that defined by the network perimeter. The divergence patterns were used to calculate the average and point maxima for the convergence (negative only) and divergence (positive only). Table B3 shows that these correlated with the rainfall variables better than the network-scale divergence (DAVG). The correlation coefficients were also larger for the rainfall variable that was the least area dependent (15-min point maximum).

The correlation between the rainfall variables and the convergence parameters (DMNA, DMIN) maximized at lags of 15 and 30-min (rain following divergence). Moreover, there was a significant change occurring in these correlations as early as 75 to 90-min before the rain. The correlation tended to be largest for the rain variables most indicative of rain mass (i.e., total rain, RTOT, and highest point rain, RMAX). These results suggest promise for the predictability of rain mass based on preceding convergence in the wind field over the area.

The correlation between the rainfall variables and the divergence (positive only) variables, DMXA, DMAX, was largest for negative lags of 0 to 15-min for DMAX and 0 to 30-min for DMXA. This difference is to be expected since the storm outflow is felt at the surface very shortly after rain locally, but then takes some time to move out across the network. Again the correlation tends to be larger for the rain variables more indicative of the rain mass than of the network average.

Statistical Analysis on the Raincell Scale

The statistical analysis on the raincell scale was a semi-objective scheme similar to the subjective approach used by Ulanski and Garstang (1978). The method was applied to 19 raincells for the period 12-19 July. The raincell was defined as a rainfall entity that could be tracked continuously across the network. The raincell was allowed to merge with other raincells and its

rainfall included in the total as long as it was definable within the merged system. The gridpoint rain amounts for each raincell were summed to form the cell rainfall.

The raincell starting point was defined as that gridpoint at which rain first fell. If the rain started simultaneously at more than one gridpoint, the one having the heaviest rainfall was used as the reference location, and when the initial rainfall was equal at all gridpoints in a raincell, the easternmost gridpoint was used.

The magnitudes of the divergence in a 25-point sub-grid surrounding the raincell starting point were recorded for lag zero (defined as the gridpoint rain event start time) and for four 15-min lags, beginning 1 hour prior to the raincell starting time. The sub-grid had a local origin centered at the selected gridpoint and was oriented along the direction of motion of the raincell. This allowed the convergence values to be compared with respect to the rainfall "flanks."

An example of the relationship between the gridpoint rain event and the 25-point sub-grid is given in the first panel of Fig. B1. The schematic raincell first appears at the gridpoints marked A and B. Since the heavier rain fell at A, the 25-point sub-grid is centered over A and the divergence extracted for the five time periods.

The average patterns of divergence and correlation coefficients between divergence and rainfall for the 19 raincells reveal a convergence history within the 25-point sub-grid shown in the remaining 5 panels of Fig. B1. At lag 60 the field was strongly divergent near the raincell starting point. Lag 45 was a transition between the divergent field and the convergent field apparent at lag 30. The convergence 7-10 km southwest of the starting point at lag 30 moved to within 5 km and intensified to -1.5U at lag 15. Lag 0 reveals a rapid transition from convergence to divergence as the rainfall commenced. Convergence was displaced to the upper right hand corner of the sub-grid.

Although the divergence patterns were characterized by spatial and temporal continuity, correlations with rainfall remained small until lag 15. Fig. B2 shows the divergence-rainfall correlations for the 25-point sub-grid at the 5 lags. Correlations at lags 60 and 45 were unrelated to the divergence patterns. The -1.0U convergence center southwest of the raincell starting point at lag 30 shows almost no correlation with rainfall amount. At lag 15 a center of moderately large negative correlations (rainfall increasing with increasing convergence) is nearly coincident with the center of convergence. The correlation coefficient of -0.55 at the raincell starting point indicates that the convergence explains up to 30% of the rainfall variance. The center of high correlations progressed northeastward with the convergence center at lag 0 and explains up to 45% of the rainfall variance. These findings for only 19 raincells are hardly significant but they strongly suggest physically meaningful relationships between rainfall and mesoscale wind patterns on this scale.

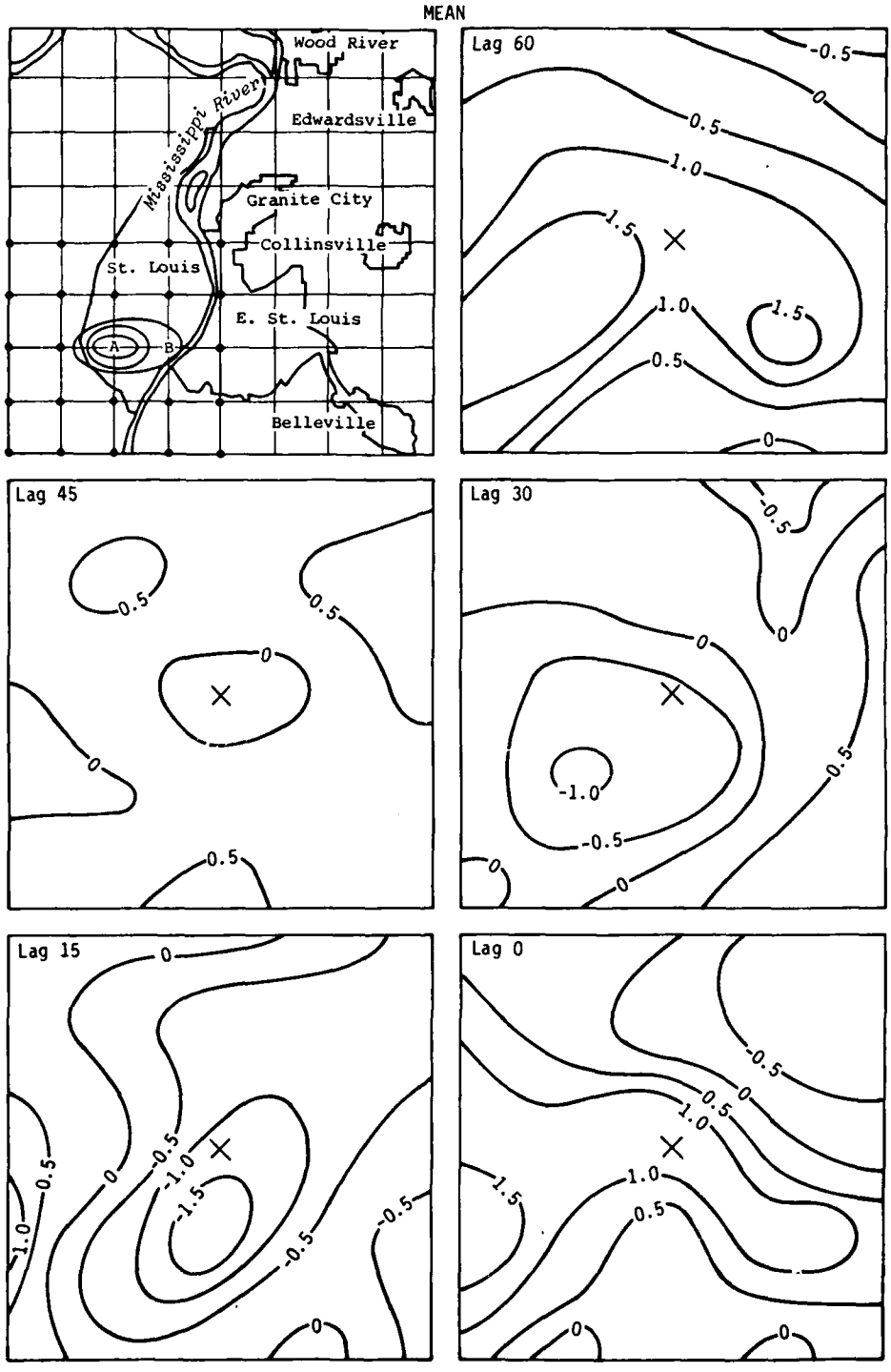

Figure B1. First panel: Map of St. Louis surface network showing a 25-point subgrid used for calculating correlations between convergence and rainfall centered over a schematic raincell. Other panels: Patterns of mean divergence at 5 lag times prior to rainfall.

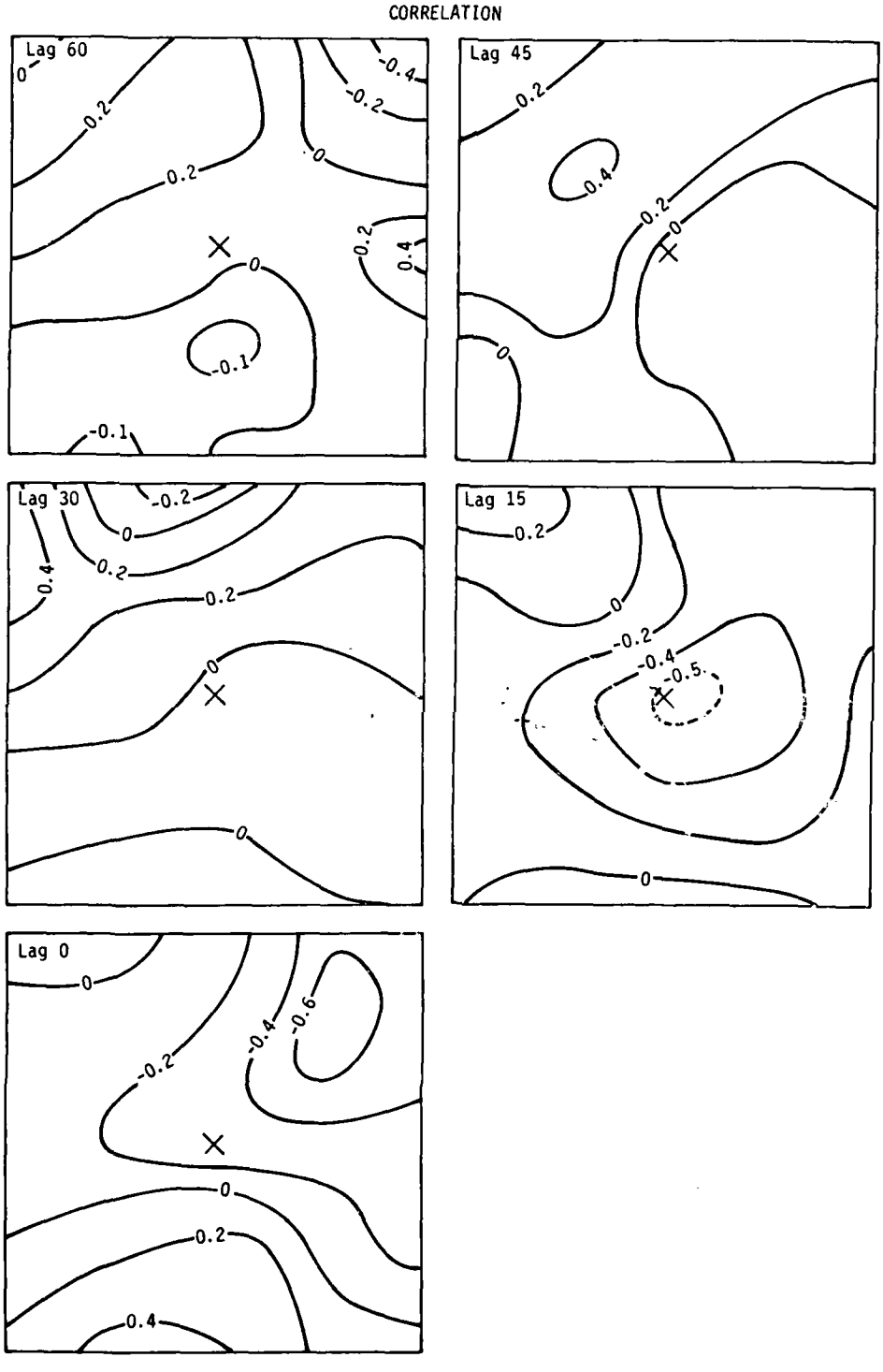

Figure B2. Maps of correlation coefficients between divergence and rainfall for 5-pre-rain lags for the 25-point subgrid.

GENERAL SUMMARY OF RESULTS

The case studies and statistical analysis of the convergence-rainfall relationship in the vicinity of St. Louis suggests that a physically meaningful relationship with rainfall and convergence does exist at the raincell level and also at the network scale. These results are not viewed as conclusive in view of the relatively weak statistical relationships.

Much more investigation on the convergence-rainfall relationship is needed. This study has shown that, qualitatively, the convergence collocates favorably with raincells, is predictive of rainfall onset, and is positively related with rainfall amount on some case days. The relationships are nonexistent or negative on other case days. Methods need to be found so that the periods with good convergence relationships can be stratified from those periods with poor convergence-rainfall relationships. The reasons for so great a variation in the relationships from one day to the next, even under similar synoptic conditions (see for example 12-13 July, 17-18 July case studies) should be sought.

In addition, quantitative methods to represent the cell scale convergence fields need to be refined. The 25-point sub-grid centered about the raincell at the location of its first appearance appears to be a potentially useful approach. Otherwise, subjective methods to develop convergence parameters and relate them to rainfall can be prohibitively time-consuming.

Subsynoptic and/or mesoscale disturbances that tend to increase the potential for convective showers were present on all case study days. These disturbances were found over the dense St. Louis surface network during the time the boundary layer wind profiles were taken on three of the case study days. Although occurring under different synoptic conditions, these systems were similar structurally, being strongest near the surface and extending through a depth of 550-750 meters.

C. CASE STUDY: 12 JULY 1975

SYNOPTIC SITUATION

A cold-core cyclone in the middle troposphere brought unseasonably cold air into the Midwest. At 0600 CST, the cyclone was centered over Wisconsin (Fig. C1). Missouri was beneath deep northwesterly flow from the surface to 500 mb, a flow pattern that is usually accompanied by dry stable weather conditions over the Midwest. The low moved to southern Wisconsin by 1800 CST (Fig. C2). Strong cold advection within the northwesterly flow at 850 mb established a short wave trough that extended southwestward from the low center through Iowa at 0600 CST (thick dashed line in Fig. C1b). This weak 850 mb trough moved slowly through the St. Louis area (black dot) during the day (Fig. C2b).

At the surface was a complex pattern of low pressure centers, troughs, and fronts, in association with the upper level low. The main polar front had pushed through the St. Louis area on the 11th and was located across the Gulf Coast States by 0600 on the 12th (Fig. C1a). The Pacific airmass behind the front had dewpoints in the middle 50's. A secondary cold front indicated in Fig. C1a as a weak trough from the low center over southern Lake Michigan to central Missouri separated the Pacific air to the south from Canadian air with dewpoints in the upper 40's. The surface trough had pushed about 200 km southeast of St. Louis by 1800 CST (Fig. C2a).

REGIONAL SCALE SITUATION

There were cyclonically swirled cloud masses within the circulation of the middle troposphere cyclone (Fig. C3a). The cloud band extending from Lake Michigan to central Missouri (arrows) was collocated with the surface position of the Canadian cold front (Fig. C1a). By 1200 CST, the cloud band (see arrows A, Fig. C3b) had pushed mostly southeast of St. Louis.

Deep cumulus clouds developed within the Canadian airmass over central Missouri to the northwest of the frontal cloud band (see arrow B). Special radiosonde ascents taken within this airmass at 1100, 1300 and 1500 CST by the ISWS at three sites surrounding the St. Louis network revealed the troposphere to be convectively unstable (K-index 26.0-34.5) though fairly dry (precipitable water 1.8-2.5 cm). The weak vertical motions within the middle level trough were apparently sufficient to release the convective instability.

The regional scale surface streamline and convergence analyses (Fig. C4) show that two mesoscale troughs passed through the St. Louis network during the morning of 12 July. At 0800 CST, the first trough (A) which caused the winds to shift from southerly to westerly was over southeast Illinois within a zone of 3×10^{-5} sec^{-1} (3U) convergence. The secondary trough (B), approaching the network from the northwest, shifted the winds from westerly to northerly. After 0800 CST, the wind field behind trough B became strongly deformed by local shower outflows.

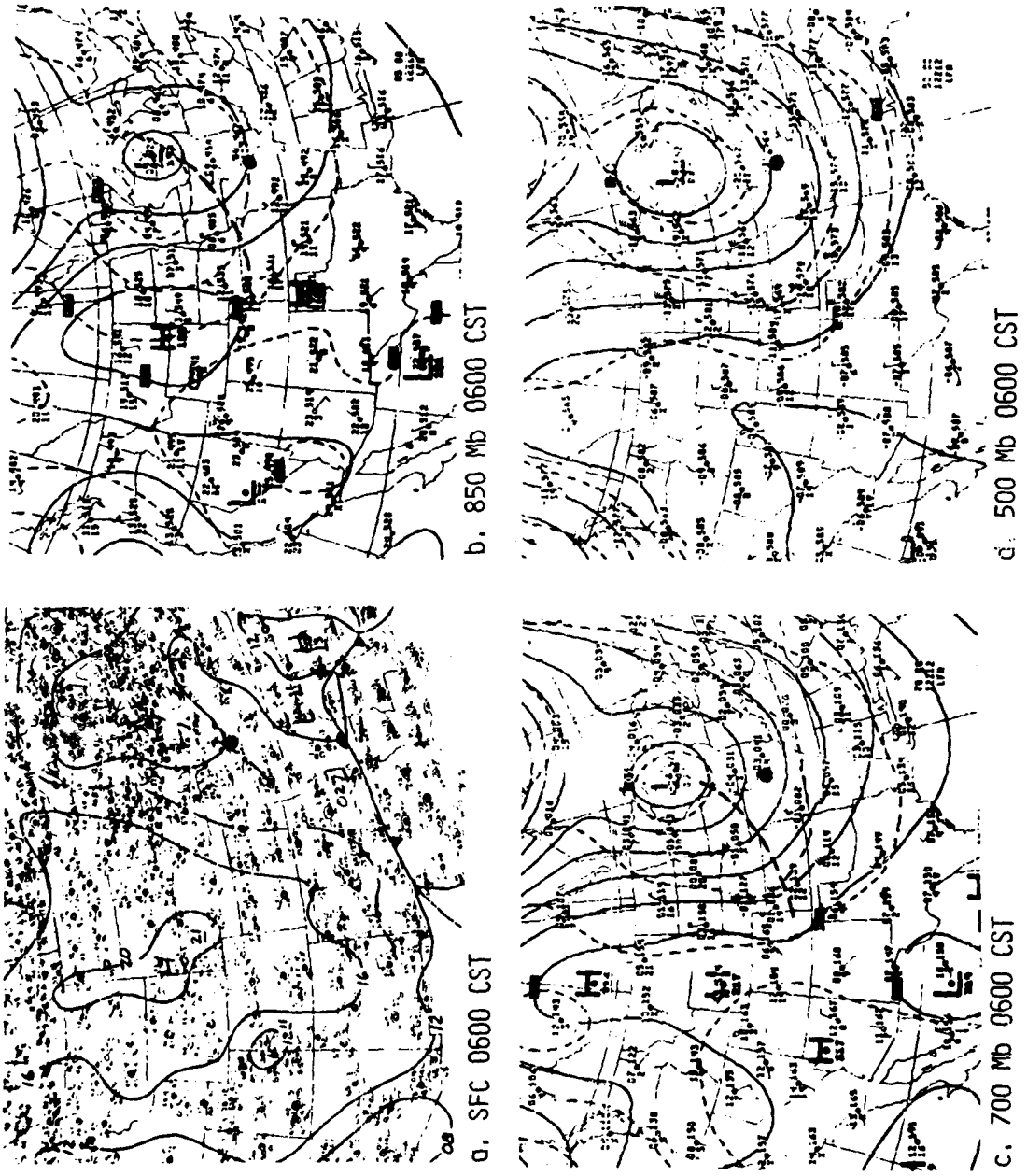

Figure C1. National Weather Service synoptic analyses for 0600 CST 12 July 1975. St. Louis area identified by black dot.

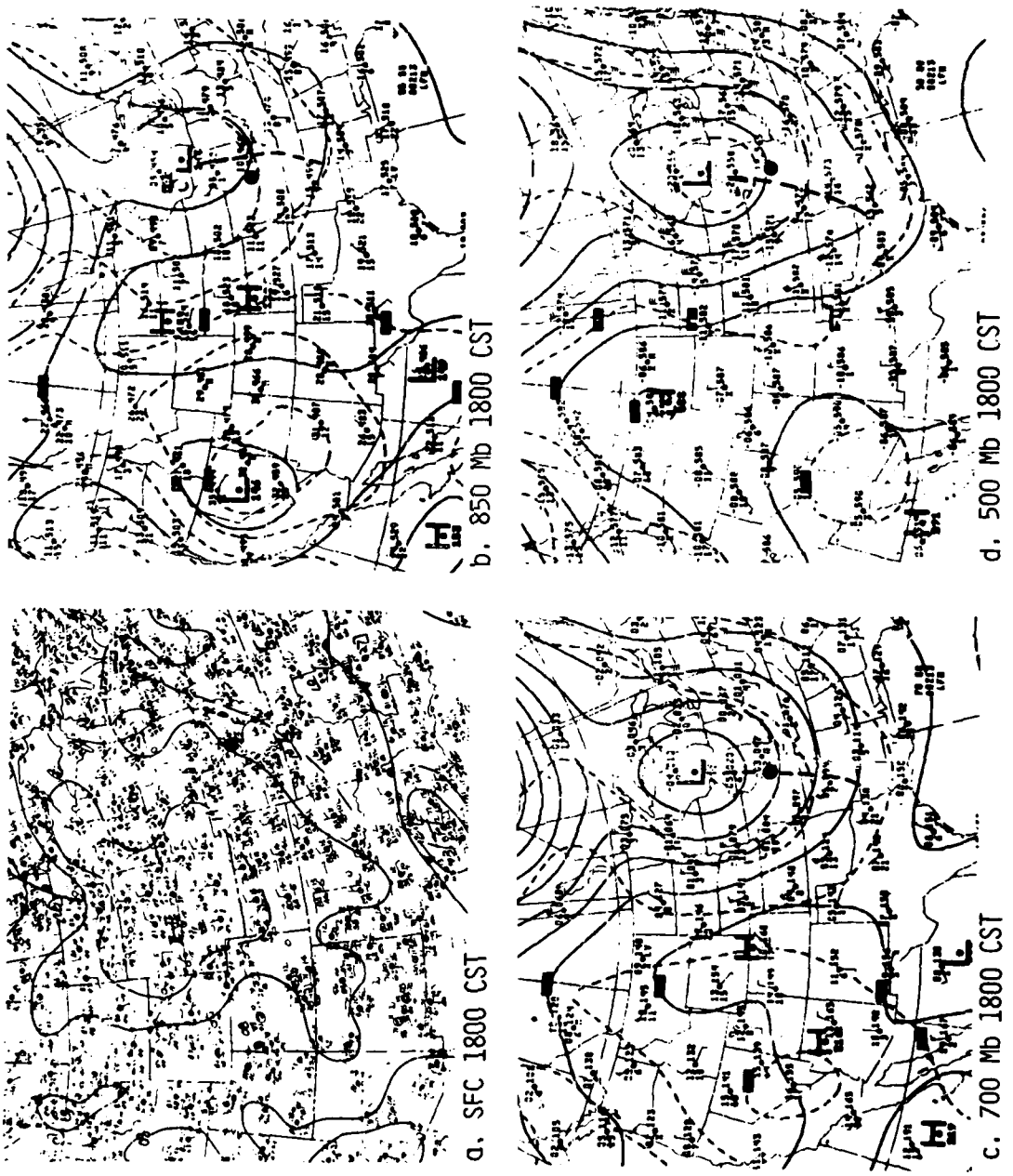

Figure C2. National Weather Service synoptic analyses for 1800 CST 12 July 1975.

a. 0800 CST

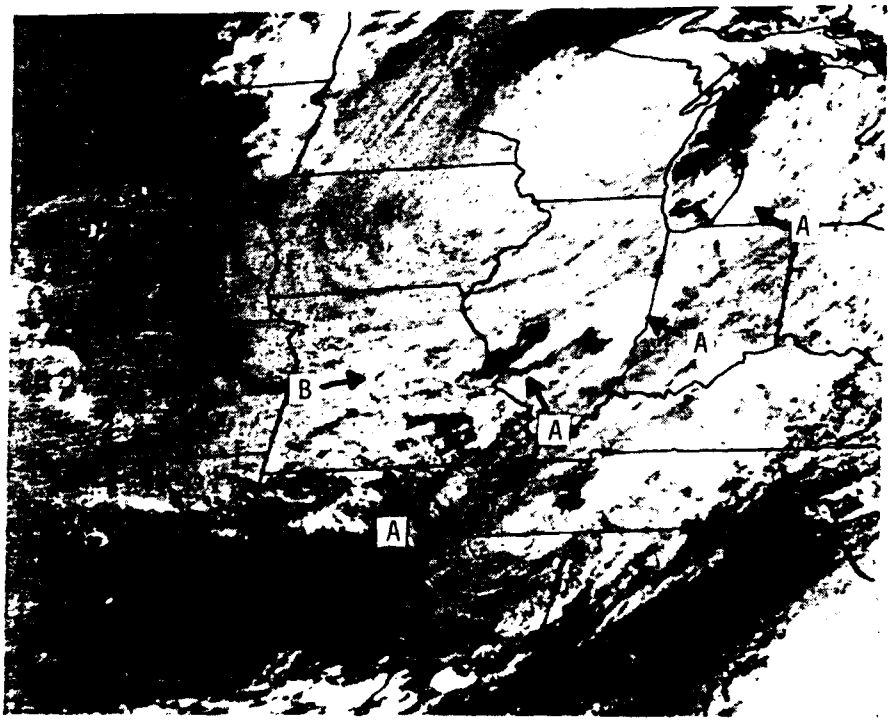

b. 1200 CST

Figure C3. GOES satellite photograph of the Midwest at 0800 and 1200 CST showing synoptic scale cloud bands and convective clouds that produced precipitation over Missouri.

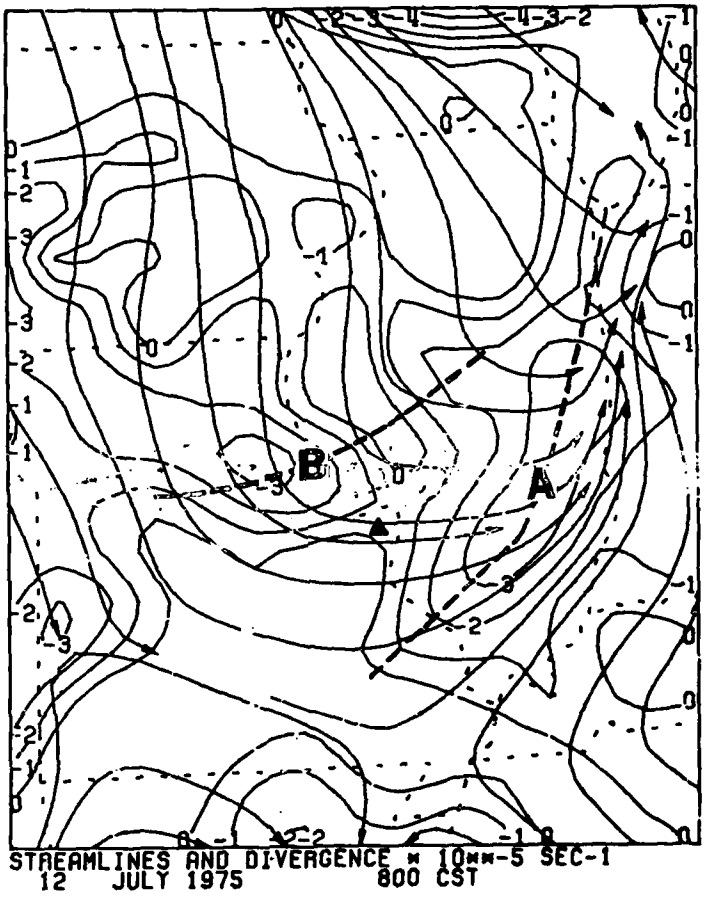

Figure C4. Regional scale analysis of surface wind field at 0800 CST.

EVOLUTION OF DIVERGENCE AND RAINFALL

Post-frontal convective showers that fell over the St. Louis network from 1115-1930 CST were small in areal coverage and light in rainfall amounts. Figures C5a-C5c show time series for the number of gridpoints that reported rain, the average 15-min rainfall for the gridpoints reporting rain, and the network mean divergence. Fewer than five gridpoints reported rain at any one time and the 15-min averages were less than 3.0 mm.

Prior to the beginning of the rainfall, there was net convergence into the network (Fig. C5c). Convergence increased to 0.5U during the passage of regional scale trough A (arrow A) shortly before 0600 CST. A brief return to southwesterly flow over part of the network led to another convergence peak around 0800 CST. Convergence reached to 0.7U during the passage of trough B (arrow B). After 1200 CST, shower outflows disturbed the wind field and produced peaks of varying signs depending upon where the flow was predominantly divergent or convergent.

Network mean convergence preceded the rainfall by 2 hr (arrow B). Following a lull in the rainfall, convergence appeared briefly at 1315 (arrow C) about 15-min before a weak shower (C). Convergence from 1345-1415 (arrow D) preceded another peak in the rainfall (D).

Figures C5d-C5f give the time series of the maximum 15-min point rainfall and the maximum point divergence, minimum point divergence (convergence). These values are taken anywhere within the network and the locations of divergence and convergence maxima are not necessarily collocated with the rainfall. The background peak divergences approach +/- 4U through most of the 12th. Convergence centers associated with the passage of trough A (arrow A) did not exceed background levels. Convergence centers exceeded 4U during the passage of trough B (arrow B) through the network. Convergences in excess of the background occurred briefly several times during the showery period (arrows).

The divergences (arrows) were stronger and more persistent than the convergences. Divergences exceeding the background began as trough B passed through the network and tended to peak during the periods of heaviest rainfall.

MESOSCALE SITUATION

The second regional scale trough (B) strengthened as it moved southeastward across the St. Louis network beginning shortly after 0900. Figure C6 shows the wind and temperature fields from 1000-1030 as the trough pushed over the southern one-half of the network. Convergence along the trough strengthened from 4U at 1000 to greater than 6U by 1030. The trough was not as well defined in the wind field at 1045 and 1100 as it pushed out of the network with convergences of approximately 2U (Figs. C7a and C7b).

Raincells A and B (Fig. C7c) appeared in areas that had been weakly convergent during the passage of the trough. However, cell B was located downwind from the 6U convergence center at 1030 (Fig. C6). Meanwhile, a weak gust front from cell C north of the network pushed into the northwestern areas. Cell B dissipated by 1130 (Fig. C7d). The gust front from C pushed to within 10 km of the Arch and produced two 2U convergence centers.

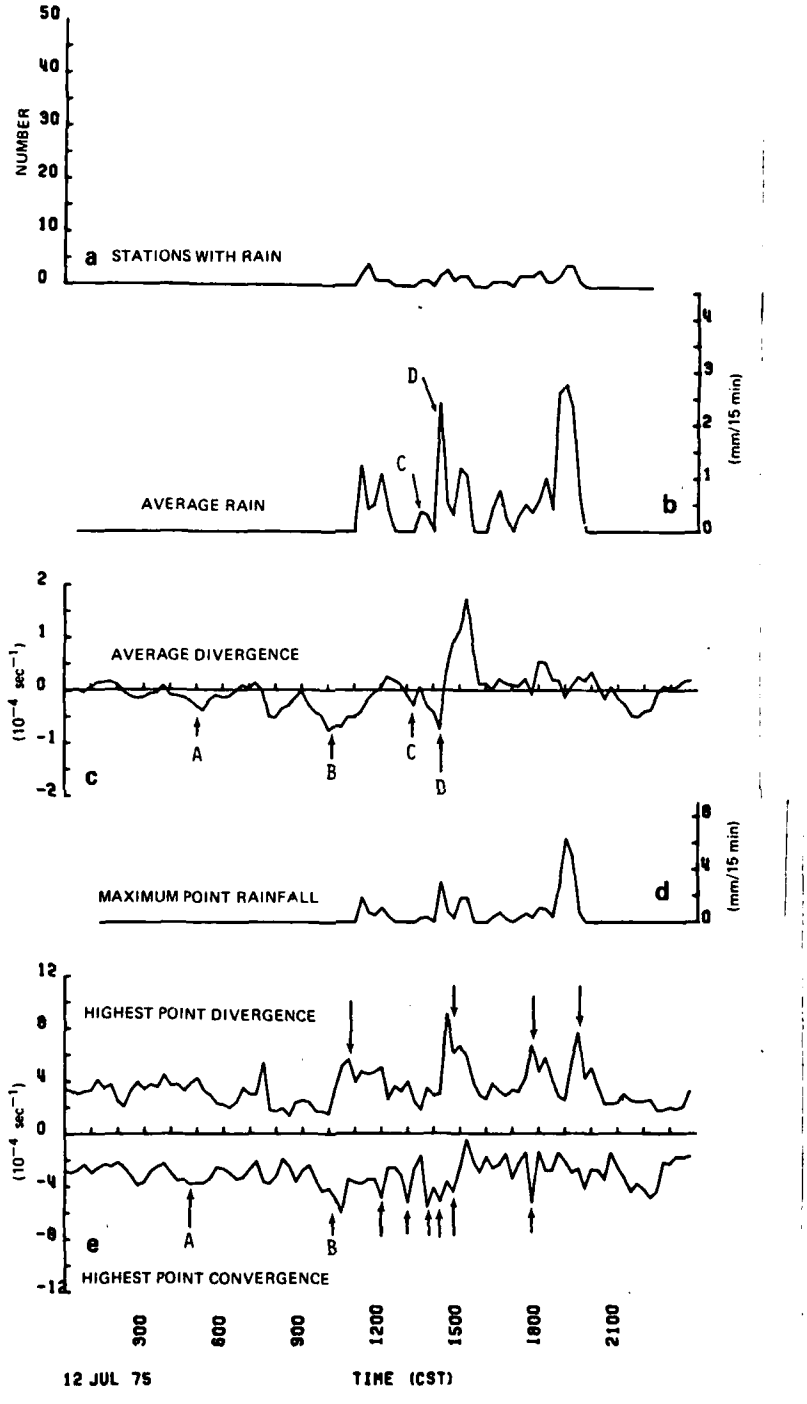

Figure C5. Time series of divergence and rainfall variables.

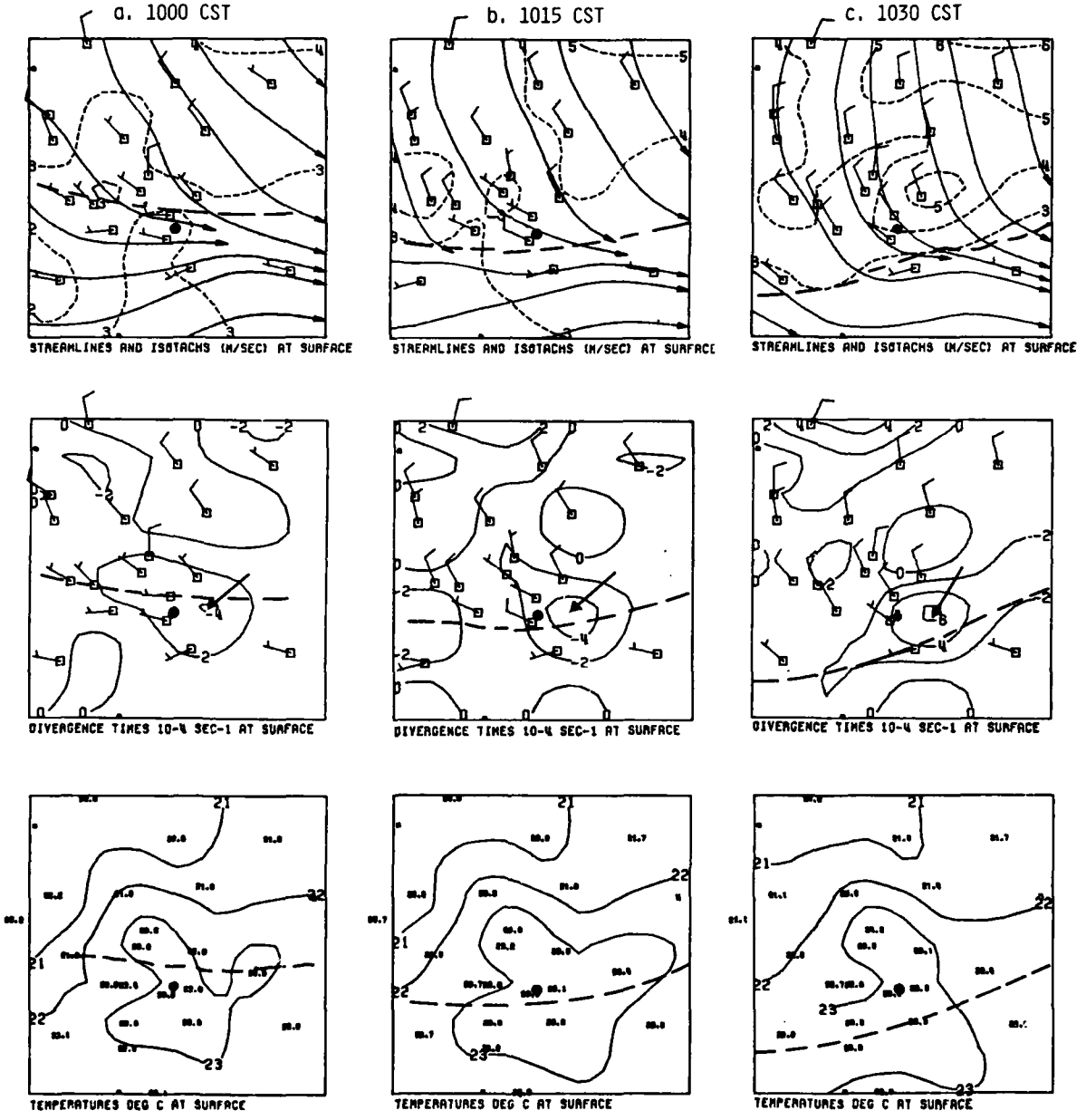

Figure C6. Composite of the objective wind field isotachs and streamlines (upper maps), divergence (middle maps), and temperature (lower maps) for 1000-1030 CST. St. Louis Arch identified by black dot.

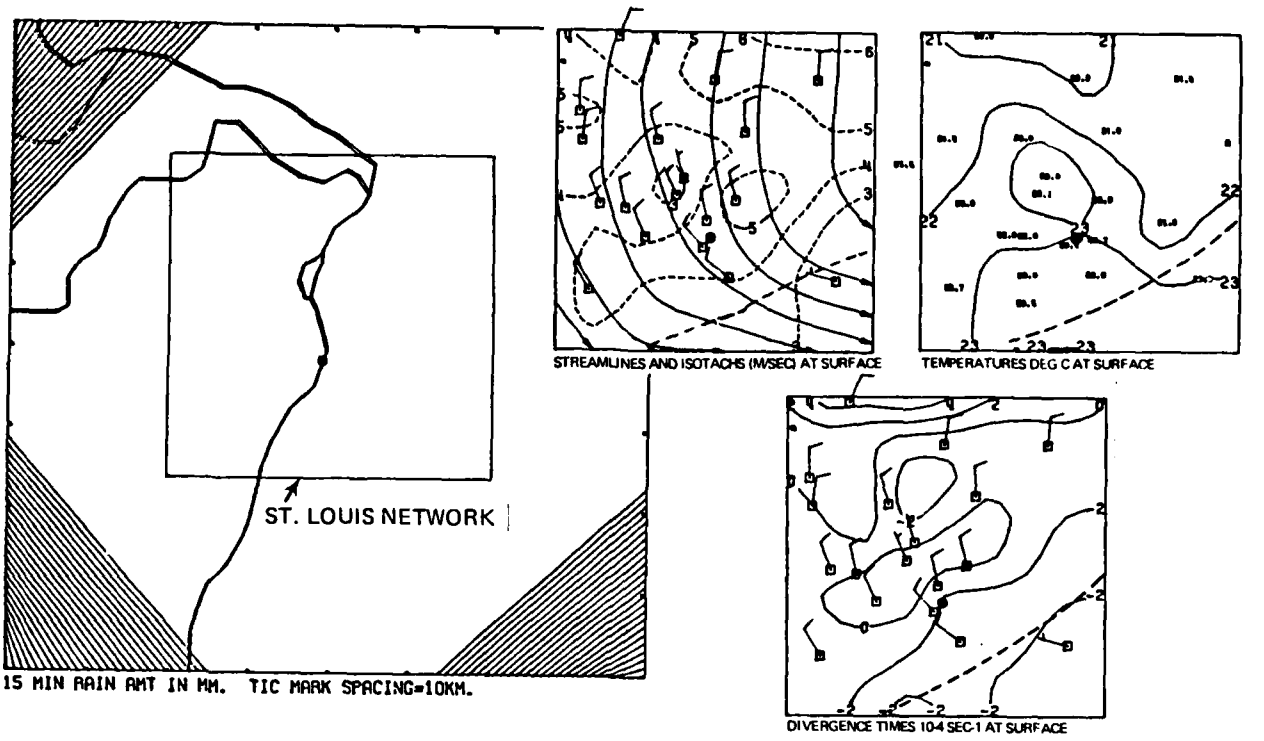

a. 1045 CST

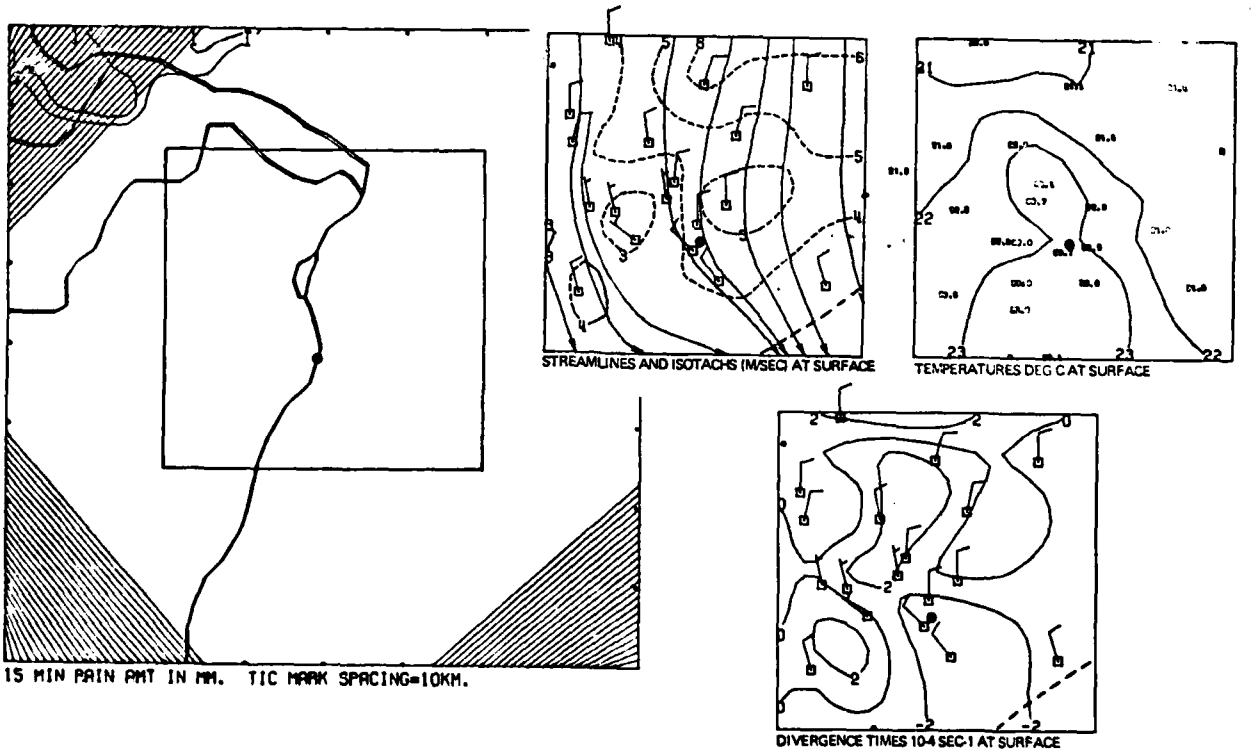

b. 1100 CST

Figure C7. Composite of the objective isotachs and streamlines, divergence, temperature, and rainfall for 1045-1130 CST.

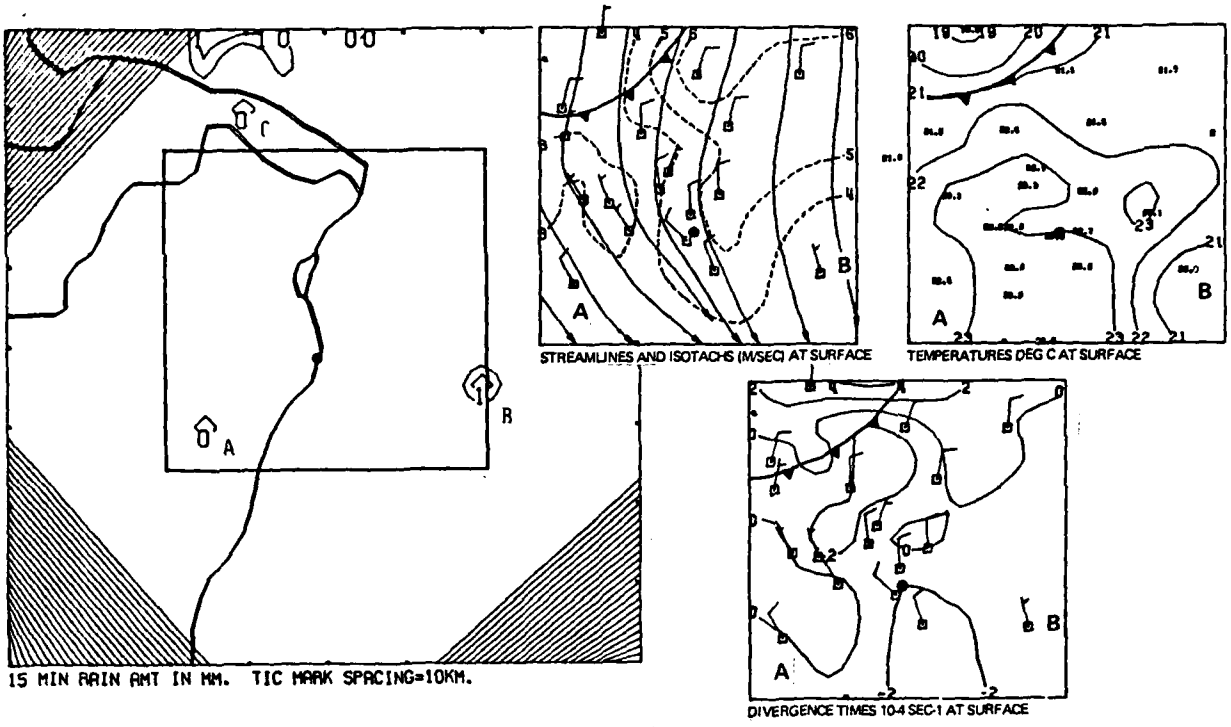

c. 1115 CST

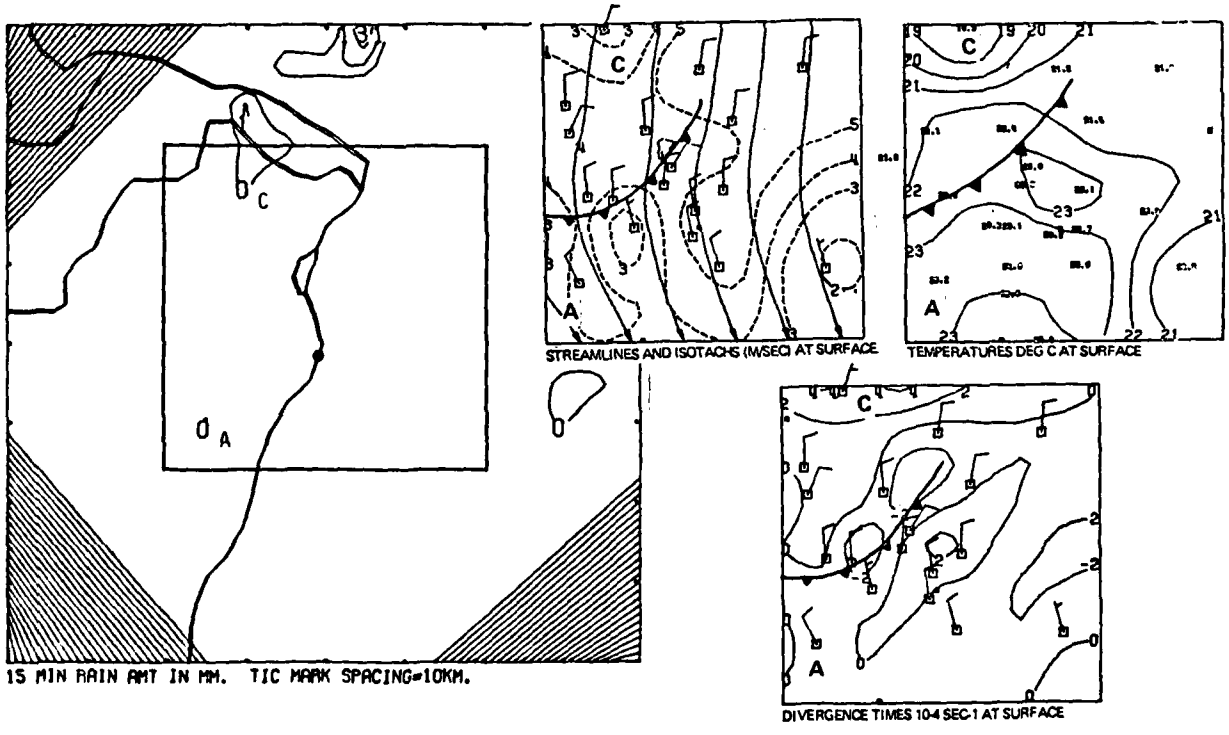

d. 1130 CST

Figure C7. Concluded

Both cells A and C dissipated after 1130. There was no new raincell development along the gust front.

Convective showers resumed at 1330 (Fig. C8a) when cell D formed over the southern part of the network where there had been weak convergence for half an hour. At 1345 (Fig. C8b) a 4U convergence center appeared about 10 km northwest of the Arch (arrow) and moved to the southeast (arrow, Fig. C8c). Meanwhile, cell E was producing 4 mm/15-min rainfall northwest of the network and its gust front had moved into the network. Cell E moved into the network at 1415 (Fig. C8d). A zone of 4U convergence developed as its gust front accelerated the northwesterly flow. Cell F formed within the convergence zone and just behind the gust front at 1430 (Fig. C8e). Cell G developed 15 km northeast of the Arch at 1500 (Fig. C8g) in divergent flow but in an area where airmasses could have been lifted by the gust front from cell E between 1430-1445.

Convergence was not apparent over the southeast part of the network prior to cell H which developed ahead of the cell E gust front. The gust front moved through the network by 1515 (Fig. C8h) and the post gust-front flow was generally divergent.

A third brief period with showers within the network began at 1730 (Fig. C9a) when cell J formed 15 km northwest of the Arch where the wind field was weakly divergent at 1700. Cell I developed within a data void area along the western network boundary. A gust front, presumably from a shower 10 km further west entered the network near the location of cell I. The gust front spread eastward to undercut cell J at 1745 (Fig. C9b). Meanwhile, cell K formed at 1745, probably along the logical extension of a gust front that pushed southeastward from a raincell north of the network at 1730. A 4U convergence area (arrow, Fig. C9b) formed along this gust front ahead of cell K.

Cell J dissipated by 1800. Cell L formed in an area undercut by the eastward moving gust front (Fig. C9c). There was no significant convergence in the vicinity of L during the gust front passage.

A 2U convergence zone formed when the two gust fronts merged over the network at 1815 (Fig. C9d). The convergence zone persisted through 1845 (Figs. C9e and C9f) but no raincells developed along or downwind from it. A gust front from cell M (Fig. C9g) pushed into the network as a slight increase in wind speed and developed a weak convergence zone with convergence exceeding 2U (Fig. C9h). The convergence zone spread southeastward but no new raincells developed after 1915.

SUMMARY OF SHOWER DEVELOPMENT ON 12 JULY

Precipitation occurred within an unstable Canadian airmass behind a secondary cold front. The airmass was relatively dry and cool and it is likely that much of the precipitation was evaported before it fell to the ground. The raincells were characterized by light rainfalls, strong divergent outflows and weak or nonexistent convergence inflows. Fourteen raincells were included in the 12 July study. Eight of these moved onto the network. Two of the remaining six raincells formed near the boundaries of the wind network where data were insufficient to determine the convergence.

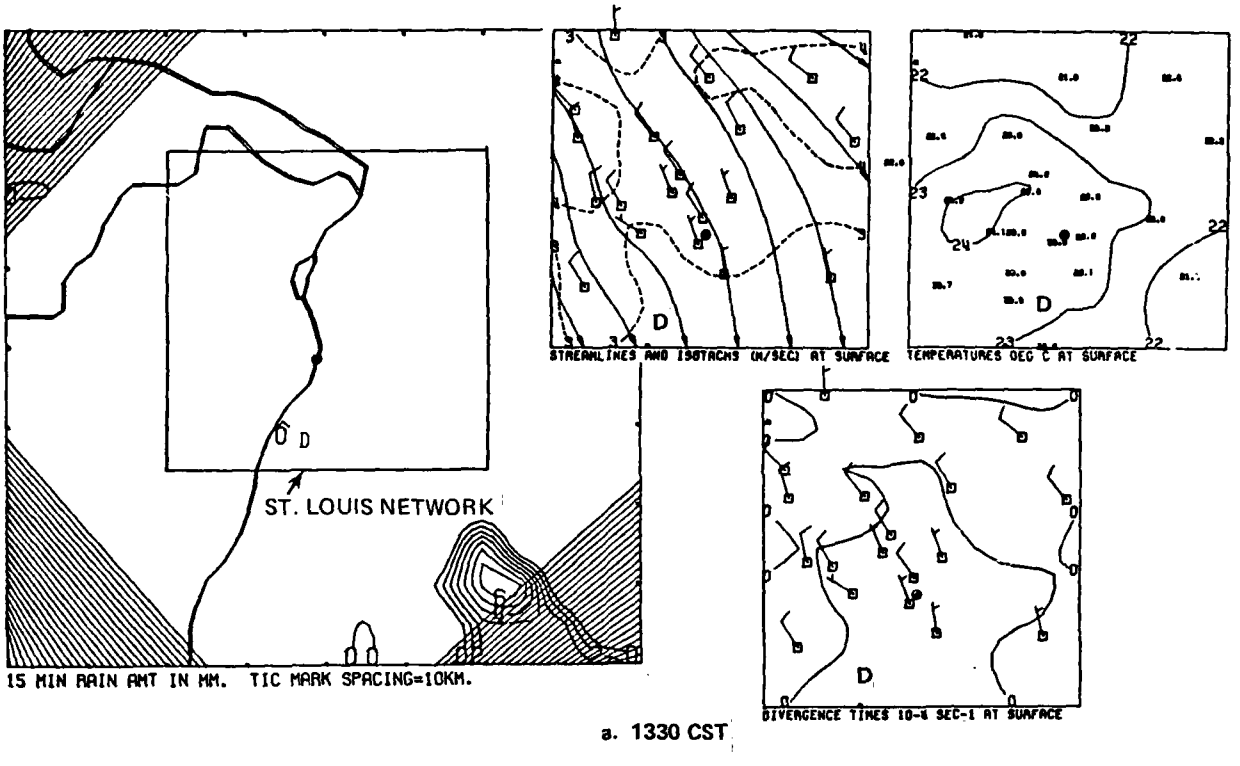

a. 1330 CST

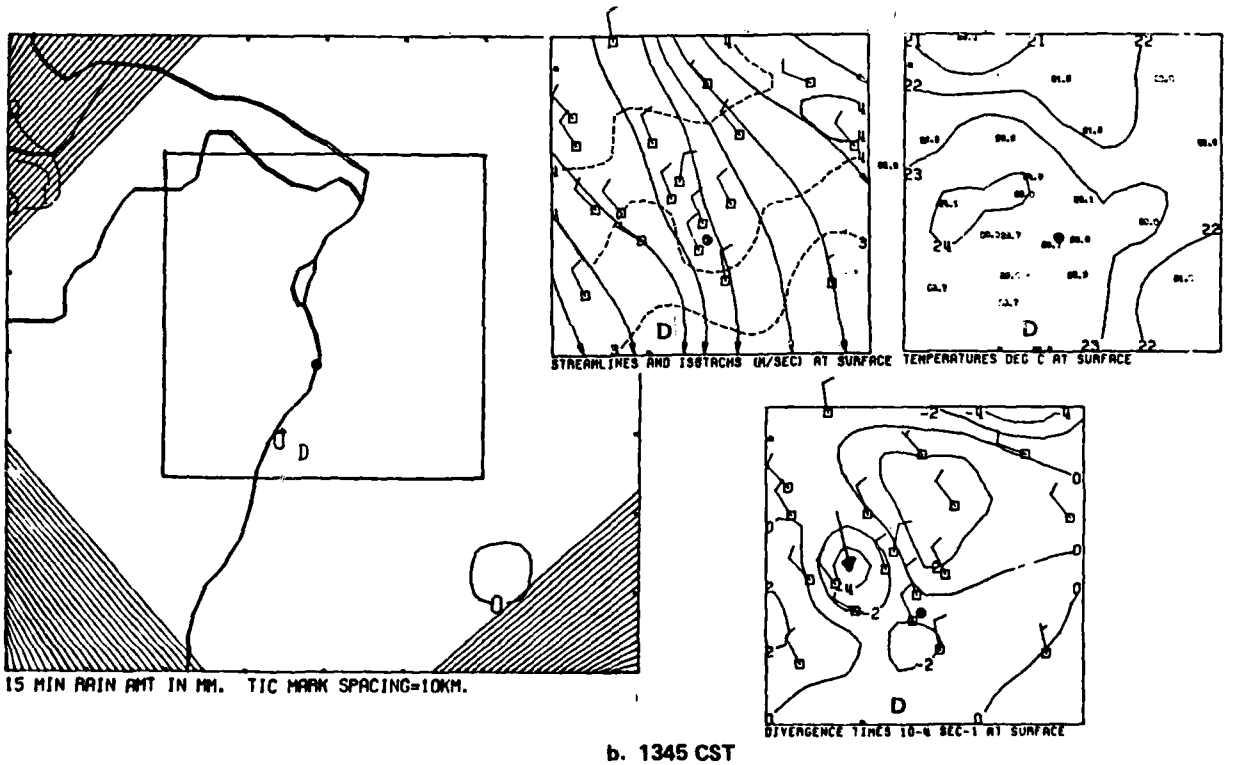

b. 1345 CST

Figure C8. Composite of the objective isotachs and streamlines, divergence, temperature, and rainfall for 1330-1515 CST.

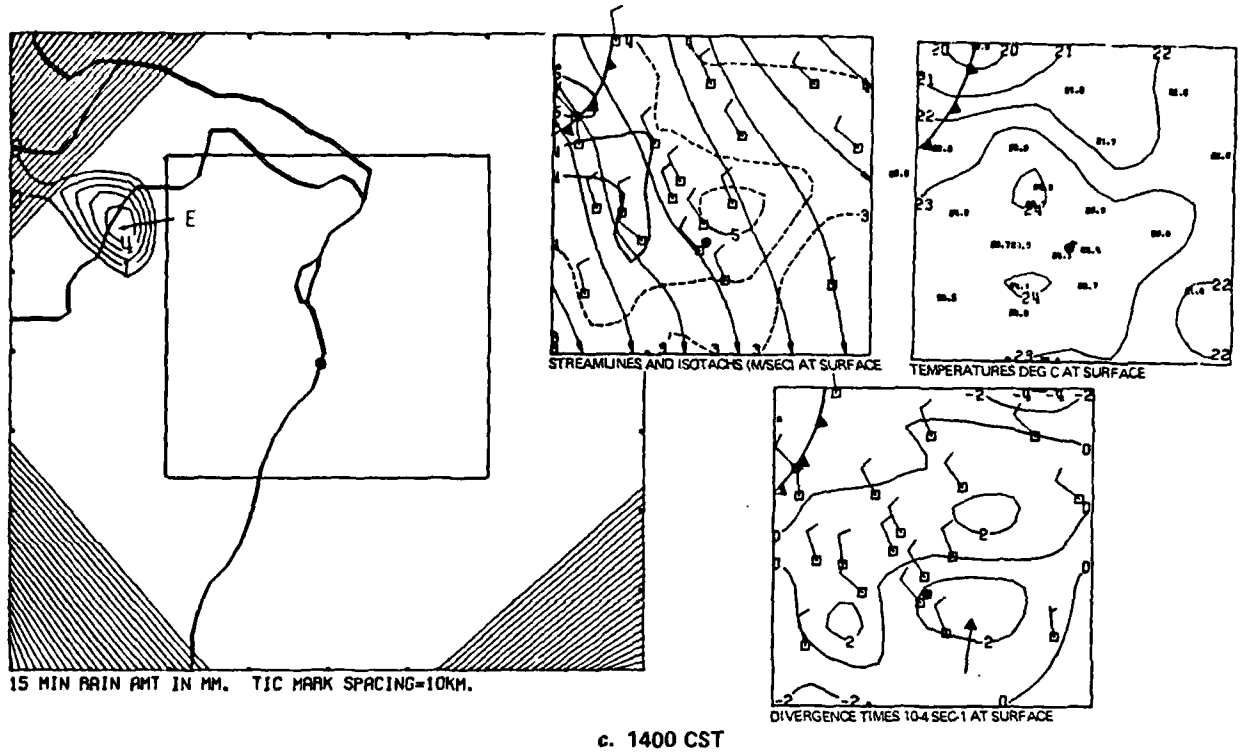

c. 1400 CST

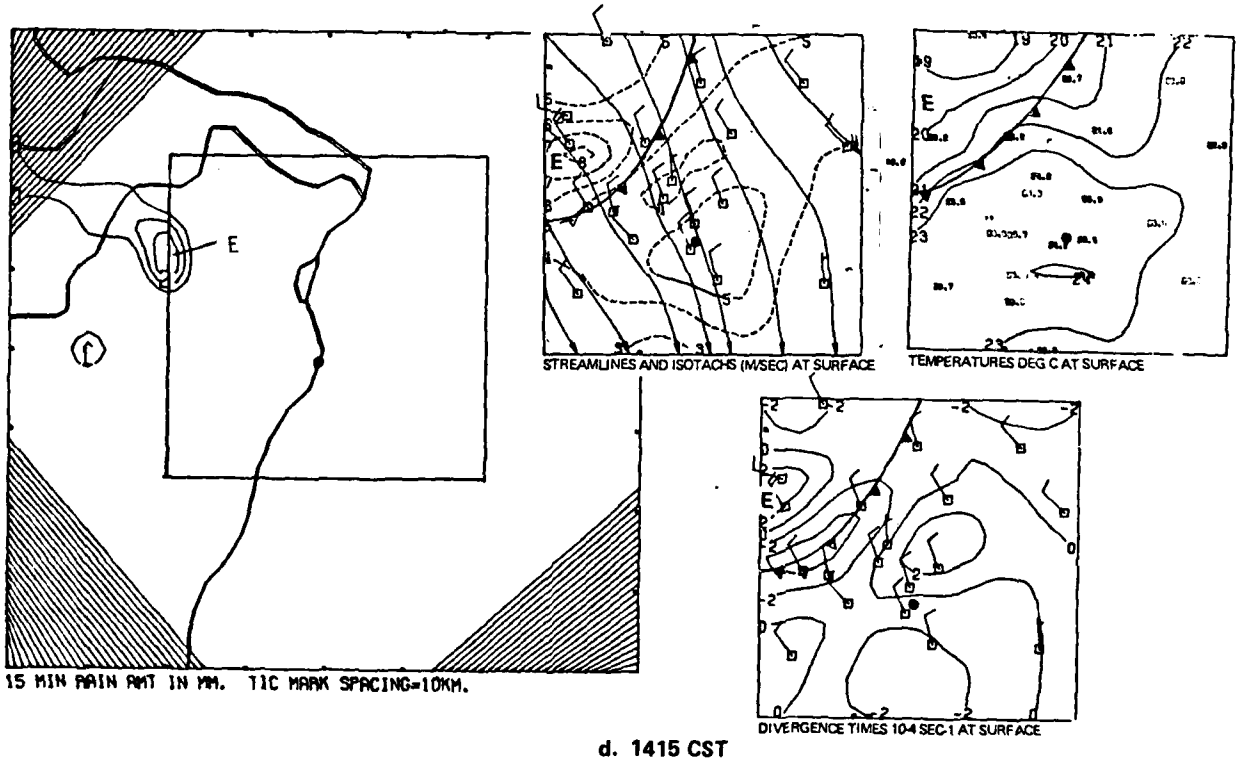

d. 1415 CST

Figure C8. Continued

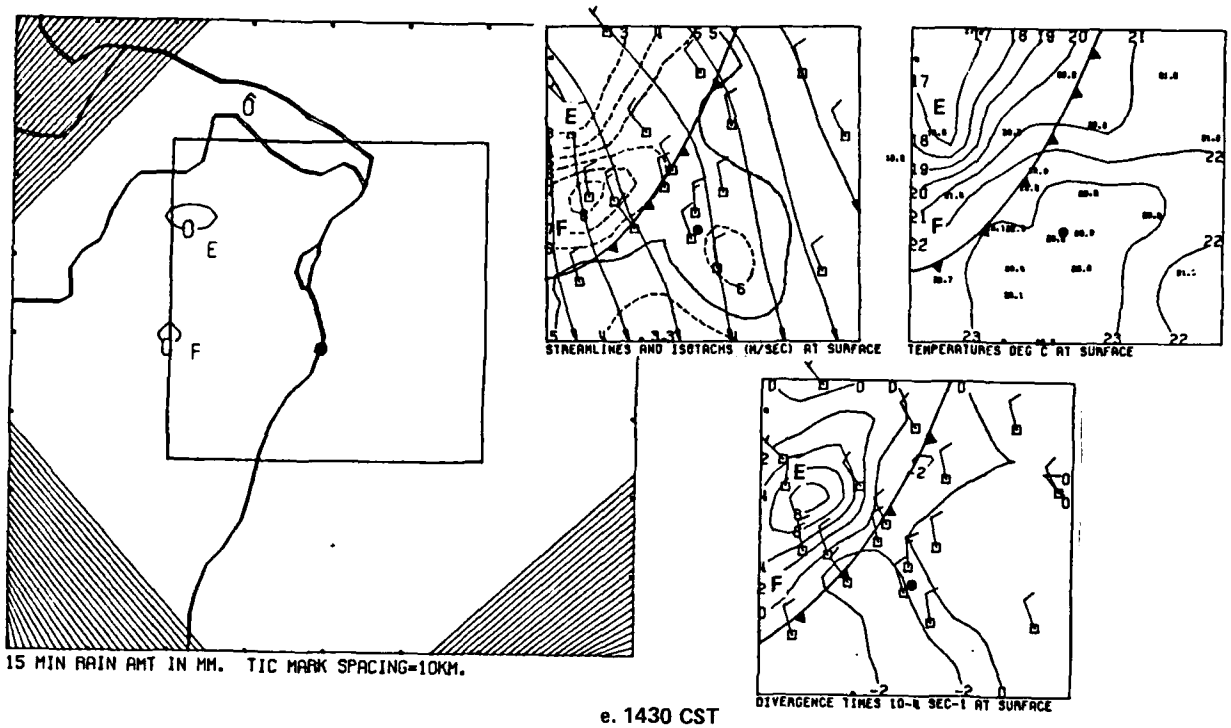

e. 1430 CST

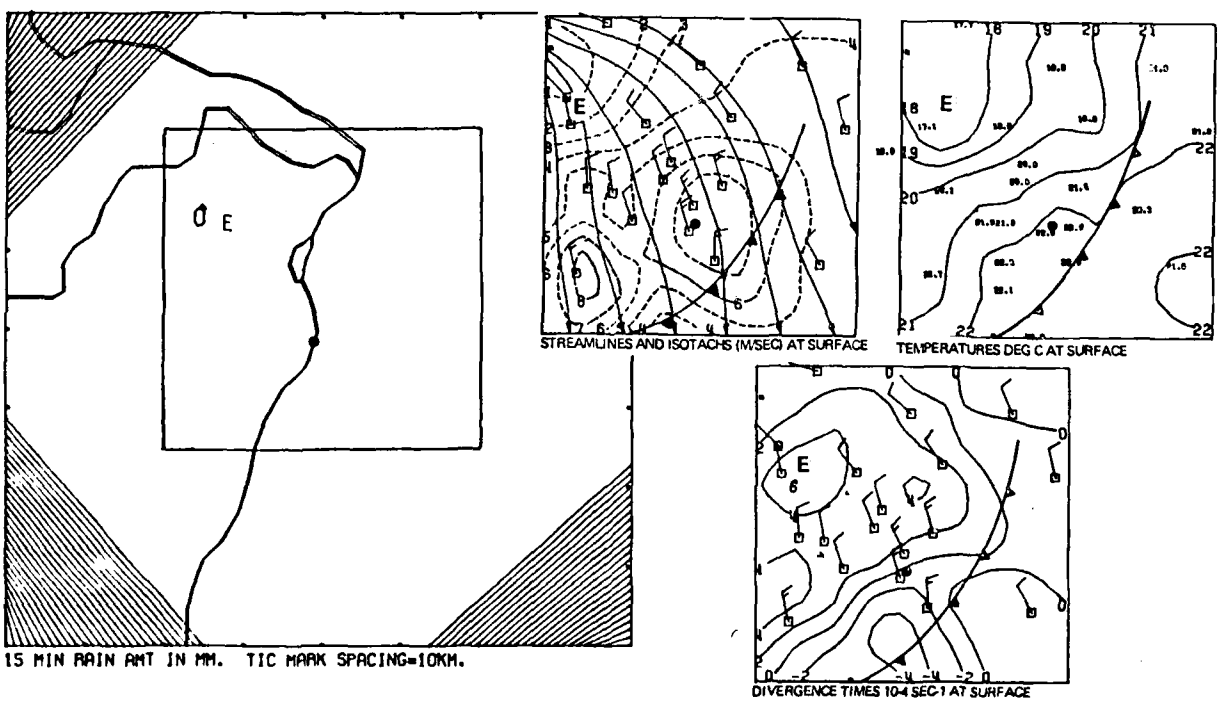

f. 1445 CST

Figure C8. Continued

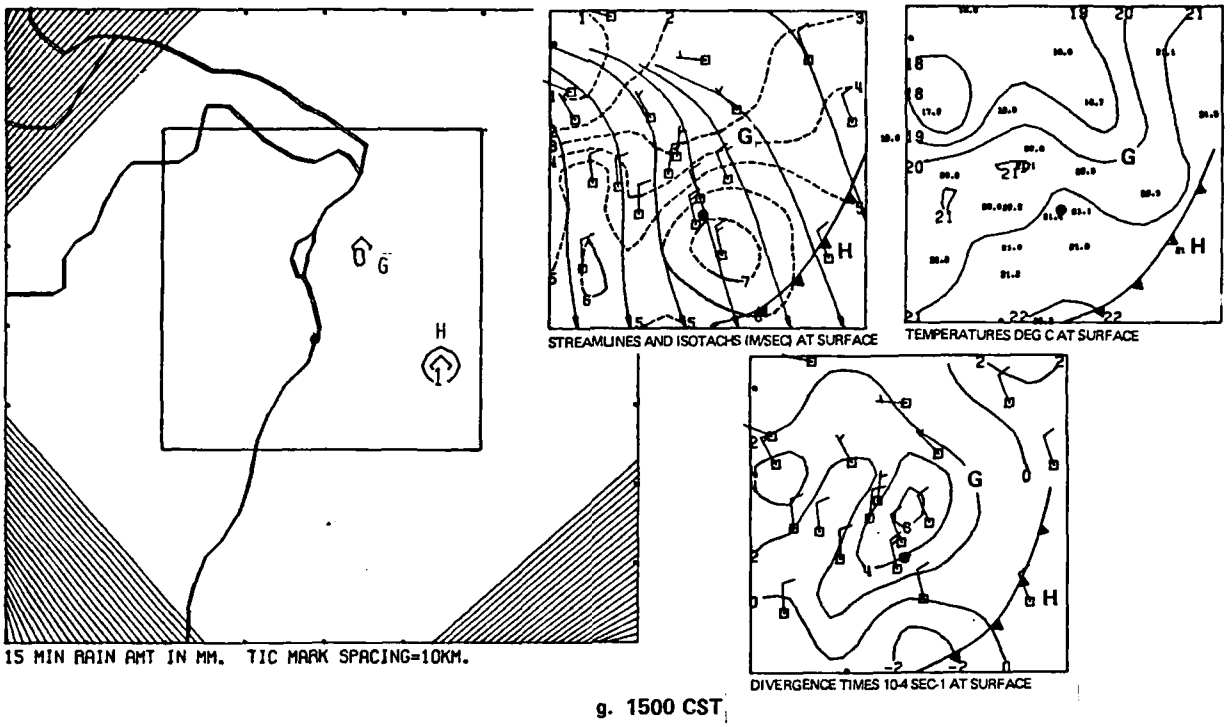

g. 1500 CST

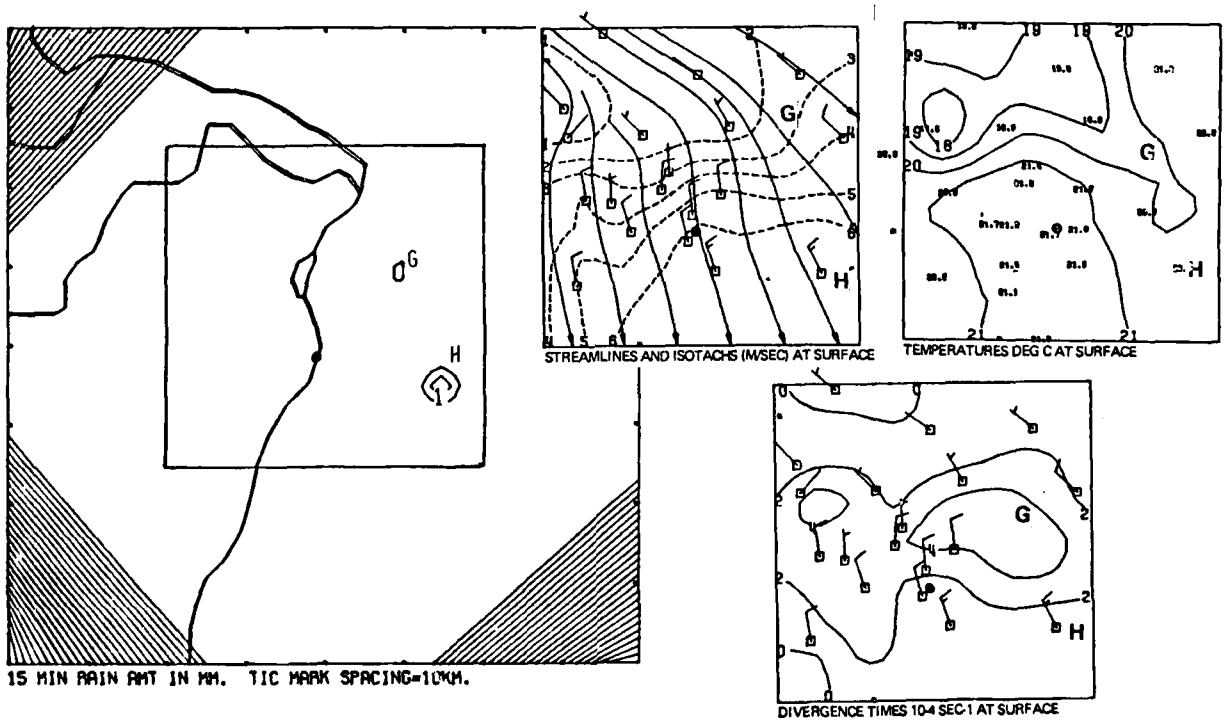

h. 1515 CST

Figure C8. Concluded

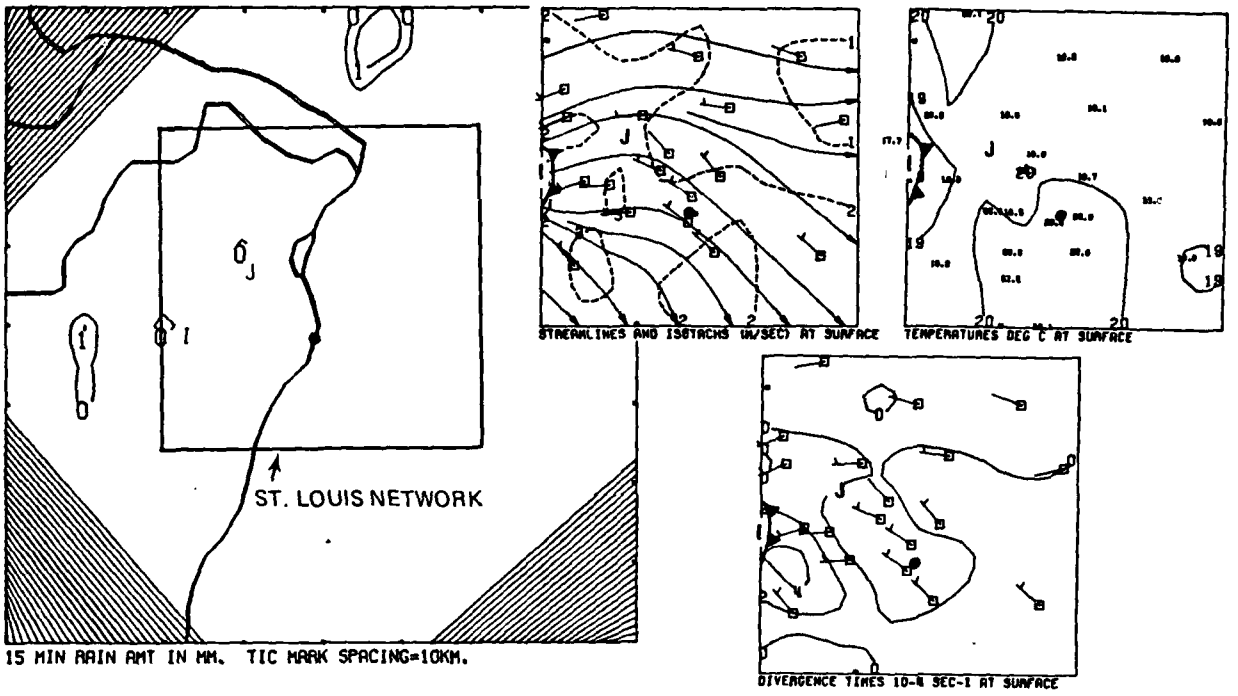

a. 1730 CST

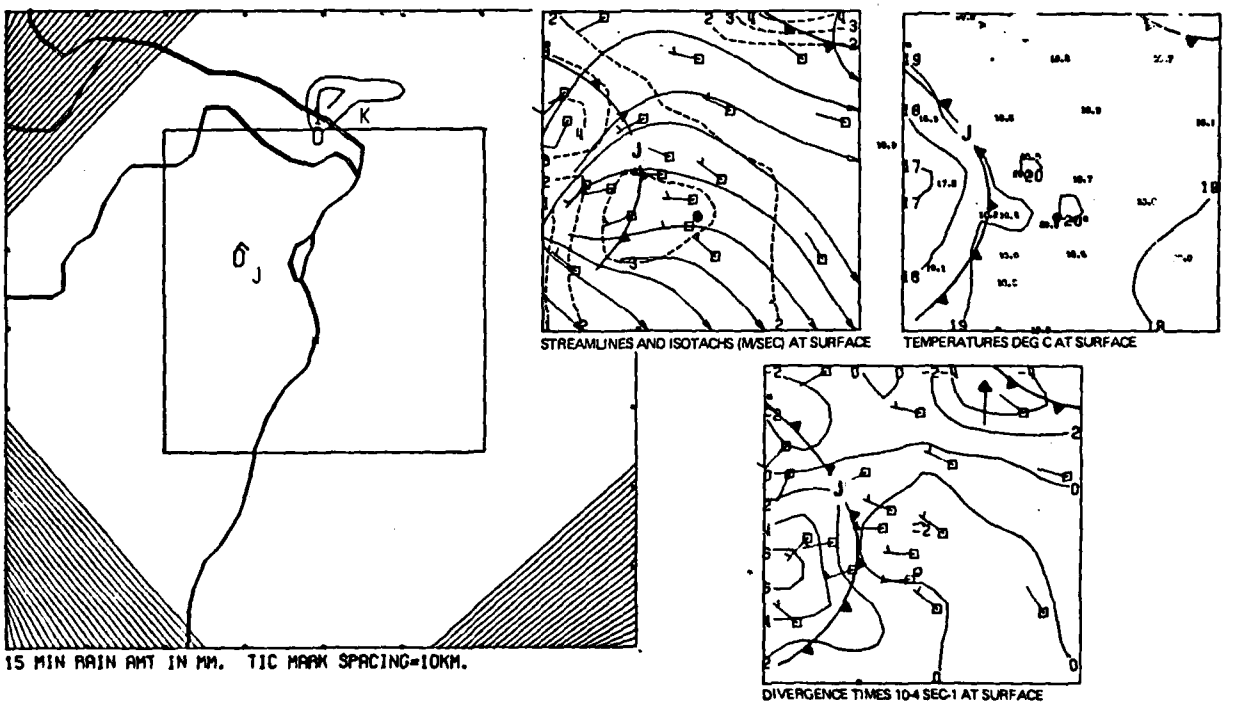

b. 1745 CST

Figure C9. Composite of the objective isotachs and streamlines, divergence, temperature, and rainfall for 1730-1915 CST.

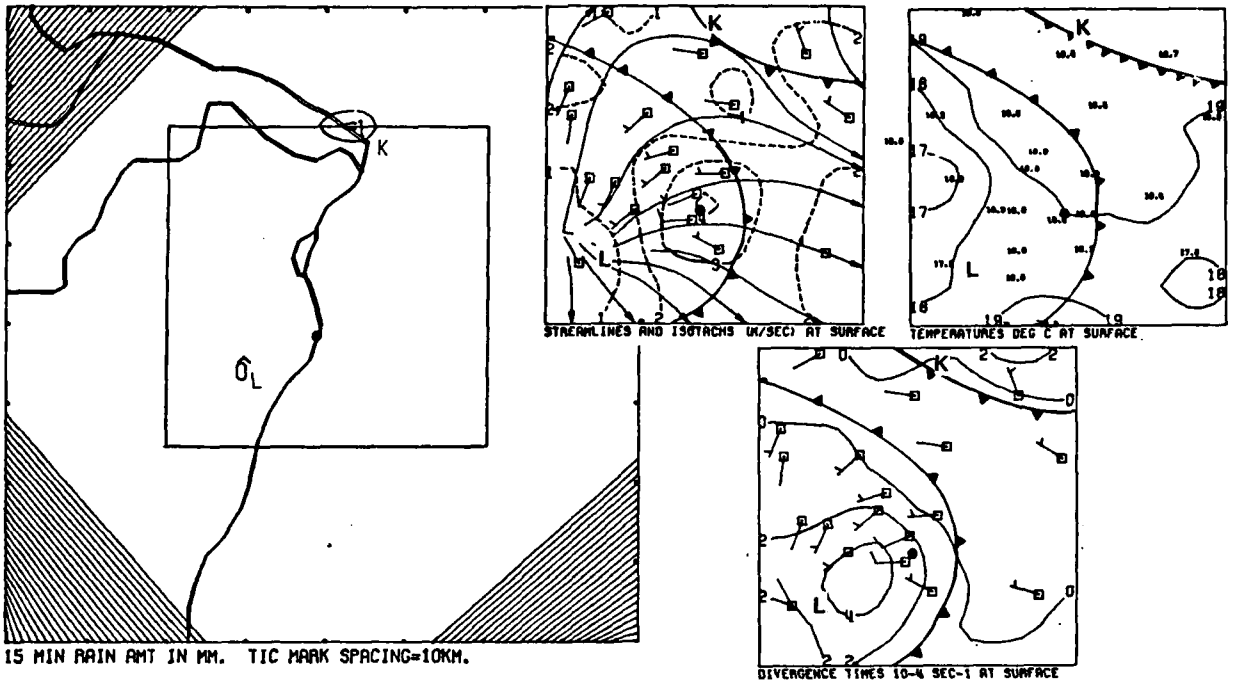

c. 1800 CST

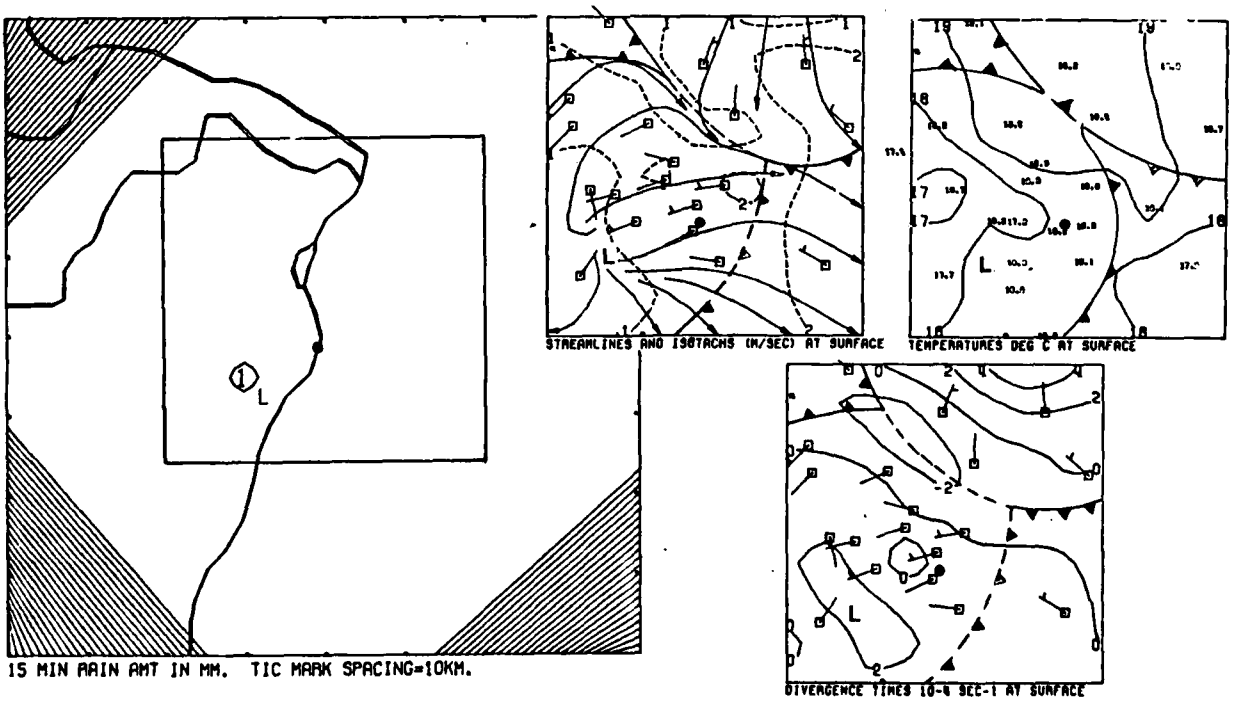

d. 1815 CST

Figure C9. Continued

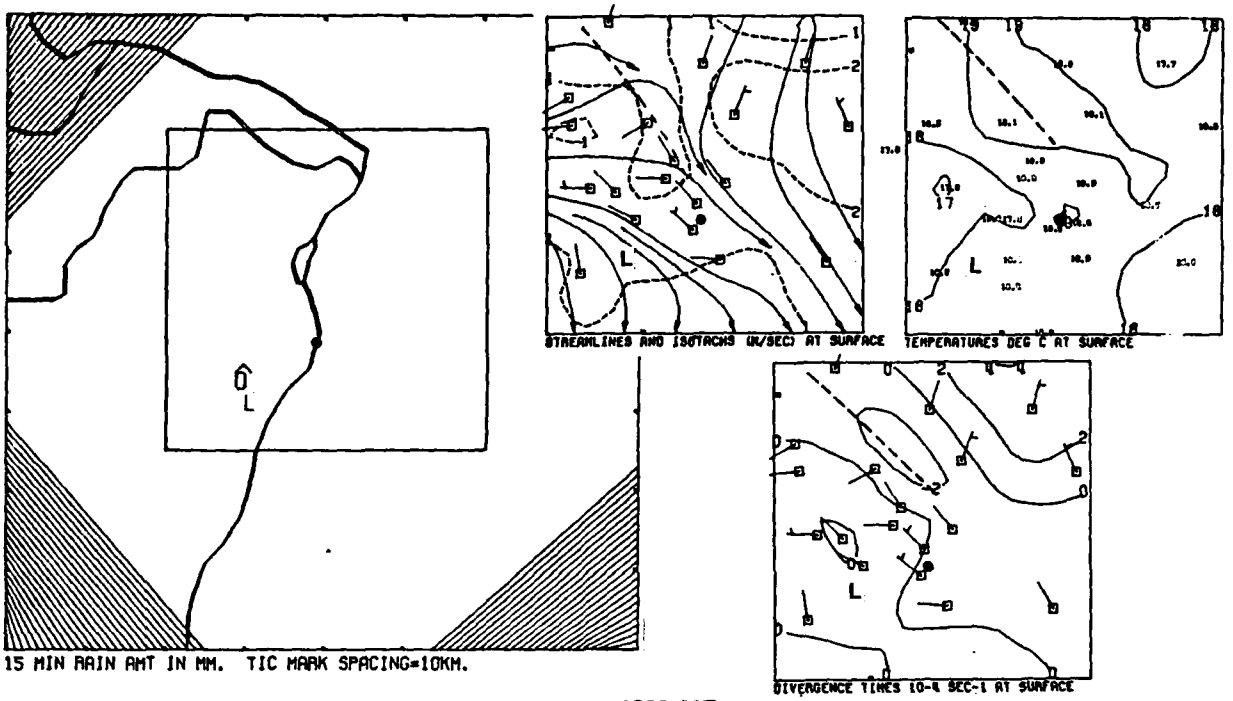

e. 1830 CST

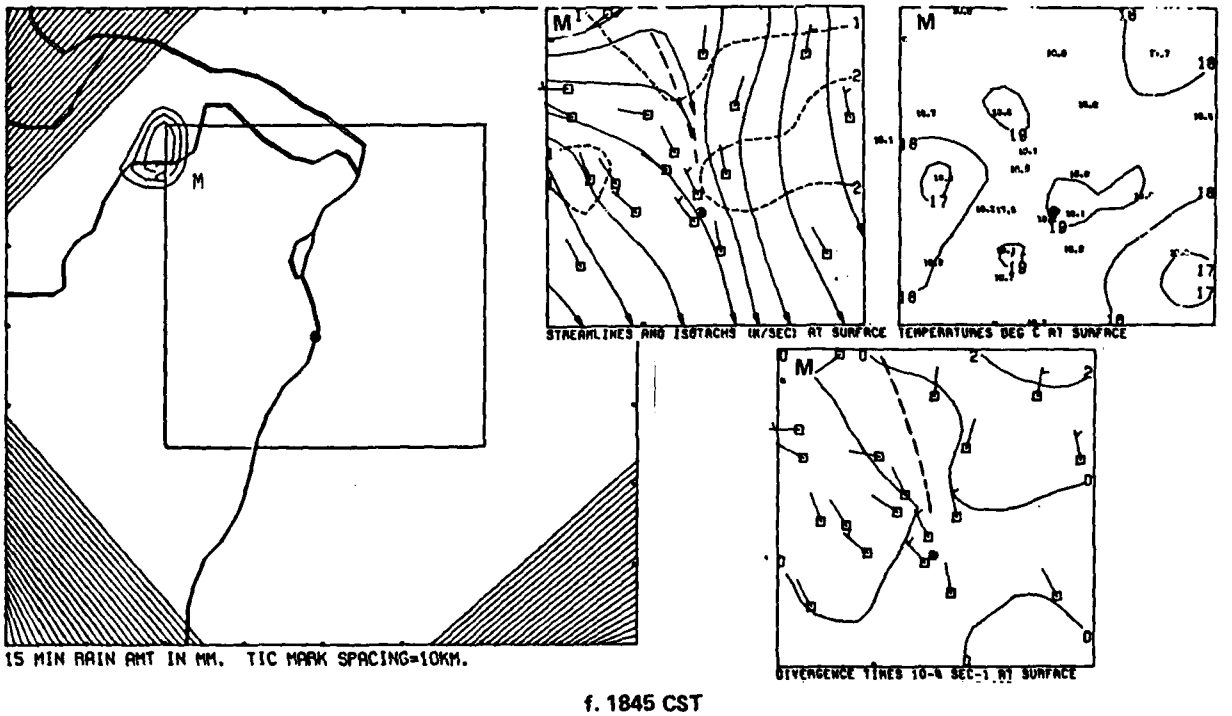

f. 1845 CST

Figure C9. Continued

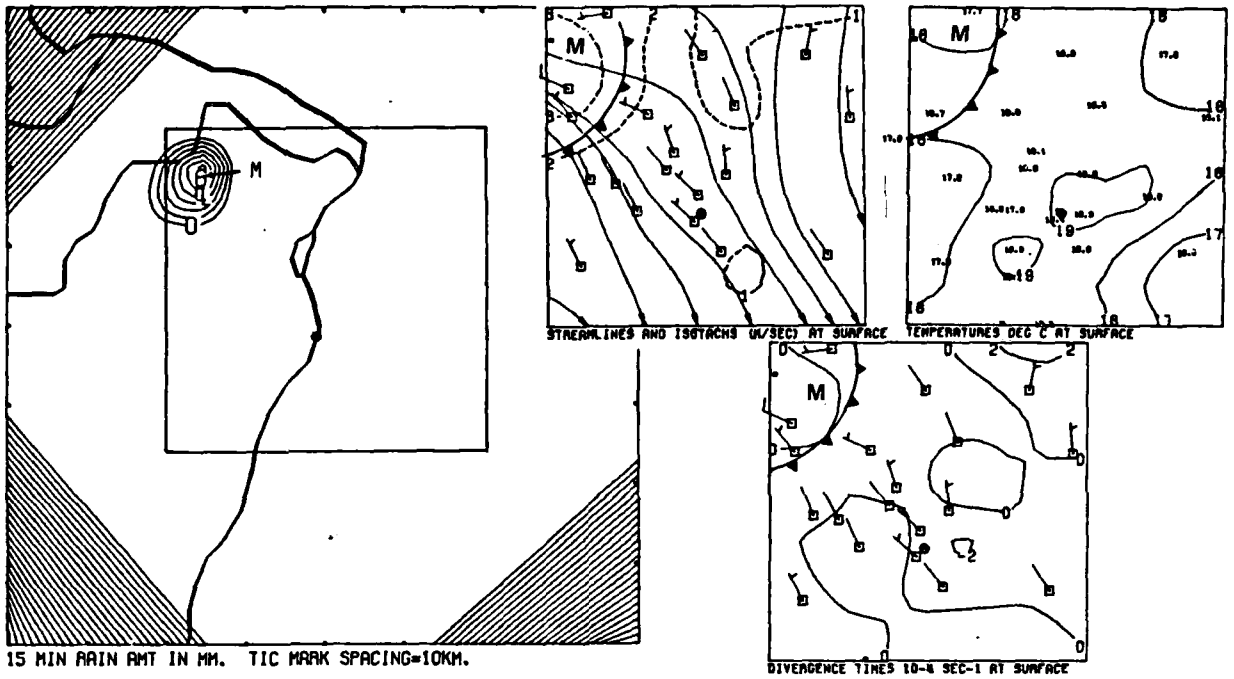

g. 1900 CST

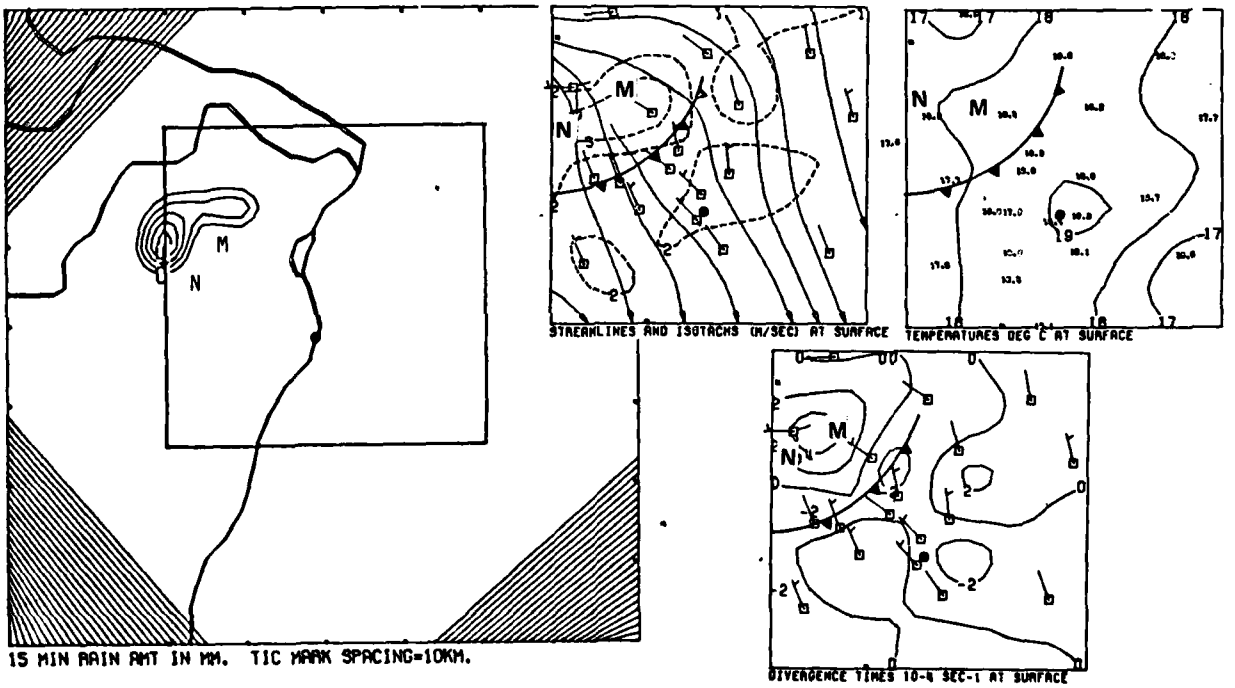

h. 1915 CST

Figure C9. Concluded

The maximum cell strength for the four cells that formed within the data-dense part of the network was only 1.5 mm, Table C1). Convergence centers accompanied three of these cells. The maximum convergence strength was only 2U, less than the background convergence for the 12th. The average cell strength for the four raincells was 1.1 mm, the average convergence strength was 1U and the average duration was 15-min.

There were eight other convergence centers that occurred during the rain period but were not associated with rainfall. Seven of the eight centers had convergence strengths equal to or greater than 4U and durations greater than 30-min. Thus, they were stronger and more persistent than the convergence centers that were thought to be associated with rainfall. The strongest convergence center that occurred during this period persisted for 60-min and had a strength of 10U.

With regard to a spatial relationship between convergence and rainfall, convergence was favorably located for the development of three of the four raincells that formed over the data dense part of the St. Louis network. These centers were weak and of short duration, being present only 15-30 min prior to raincell formation. Possible explanation for the short lead times are 1) the convergence centers were not related to the developing raincells, i.e., the spatial collocation was chance, 2) the data were not dense enough to resolve the convergent inflows until the developing storms passed close enough to a single wind site to perturb the wind speed and direction, and 3) the storms initially drew from heat and moisture at the top of the mixed layer and it was only later in the development stage that the cloud circulations extended down to the surface. There were too few raincells to determine a relationship between convergence strength and cell strength.

Only three of eleven convergence centers were possibly associated with rainfall. These were among the weakest and shortest duration of the centers. Therefore, on this day, there apparently existed little if any predictive relationship between the convergence centers, either in location and/or in strength, and the raincells.

Table C1. Cell strengths, Convergence Strengths, and Convergence Durations for Raincells that formed within the St. Louis Network on 12 July.

Cell ID	Cell Strength	Convergence Strength	Convergence Duration
D	1.0mm	1U	15 min
G	0.5	2	15
J	1.5	2	30
L	1.5	0	0

D. CASE STUDY: 13 JULY 1975

SYNOPTIC SITUATION

The middle tropospheric cyclone that developed over southern Wisconsin on 12 July, moved to northwest Illinois by 0600 CST on the 13th (Fig. D1). The 500 mb temperatures at Peoria (-24C) and Salem (-22C), Illinois, were unusually cold for the middle of July. The 700 mb and 850 mb cyclone positions were almost identical with the 500 mb position, a vertical structure typical of mid-latitude cyclones in the late occlusion stages. Moderate amounts of moisture, as indicated by temperature-dewpoint depressions between 3-8C, were present over most of Illinois and Missouri in the 850-700 mb layer. The 0600 CST surface winds were light and variable in response to the flat pressure gradient. Surface dewpoints were mostly in the upper 40's.

With the exception of a small eastward displacement of the low aloft (Fig. D2), no significant changes occurred in the circulations aloft between 0600 and 1800 CST. A weak low pressure center formed at the surface over southeastern Iowa and was accompanied by significant precipitation over eastern Missouri and western Illinois. The low was found over northern Missouri by 1800 CST (Fig. D2a).

REGIONAL SCALE SITUATION

Radar summary charts showed that light rain showers developed over northern Illinois before 0100 CST on the 13th. These showers expanded in areal coverage (area enclosed by scalloped lines) to include the St. Louis area by 1200 CST (Fig. D3a). Figure D3 also shows that winds over northern Missouri switched to westerly south of a convergence zone (dashed line) that extended from western Illinois westward along the Missouri-Iowa border. The surface low pressure center (Fig. D2a) developed within this convergence zone. Also included in Fig. D3 are the reported radar echo tops in thousands of feet.

The convergence zone pushed southward and had developed cyclonic circulation about 150 km northwest of St. Louis by 1500 CST (Fig. D3b). Convergence with magnitudes exceeding 4×10^{-5} sec^{-1} covered the northeastern one third of Missouri and parts of western Illinois. Precipitation fell over the eastern one-half of the convergence area. The tallest storms were located along its eastern edge.

Special radiosonde ascents taken at 1500 CST indicated westerly flow of 4-7 m sec^{-1} between the surface and 850 mb within the convectively unstable airmass (K-index 27.5-32.0) over St. Louis. Air flowing through the convergence zone was subjected to a prolonged period of vertical displacement. The deepest moist layer would be found within airmasses along the eastern edge of the convergence zone, airmasses that had been subjected to the greatest net vertical displacment. This was also the location of the deepest precipitating clouds.

By 1700 CST (Fig. D3c), the boundary (dashed line) between eastward moving relatively warm, unstable airmasses and westward moving rain cooled airmasses

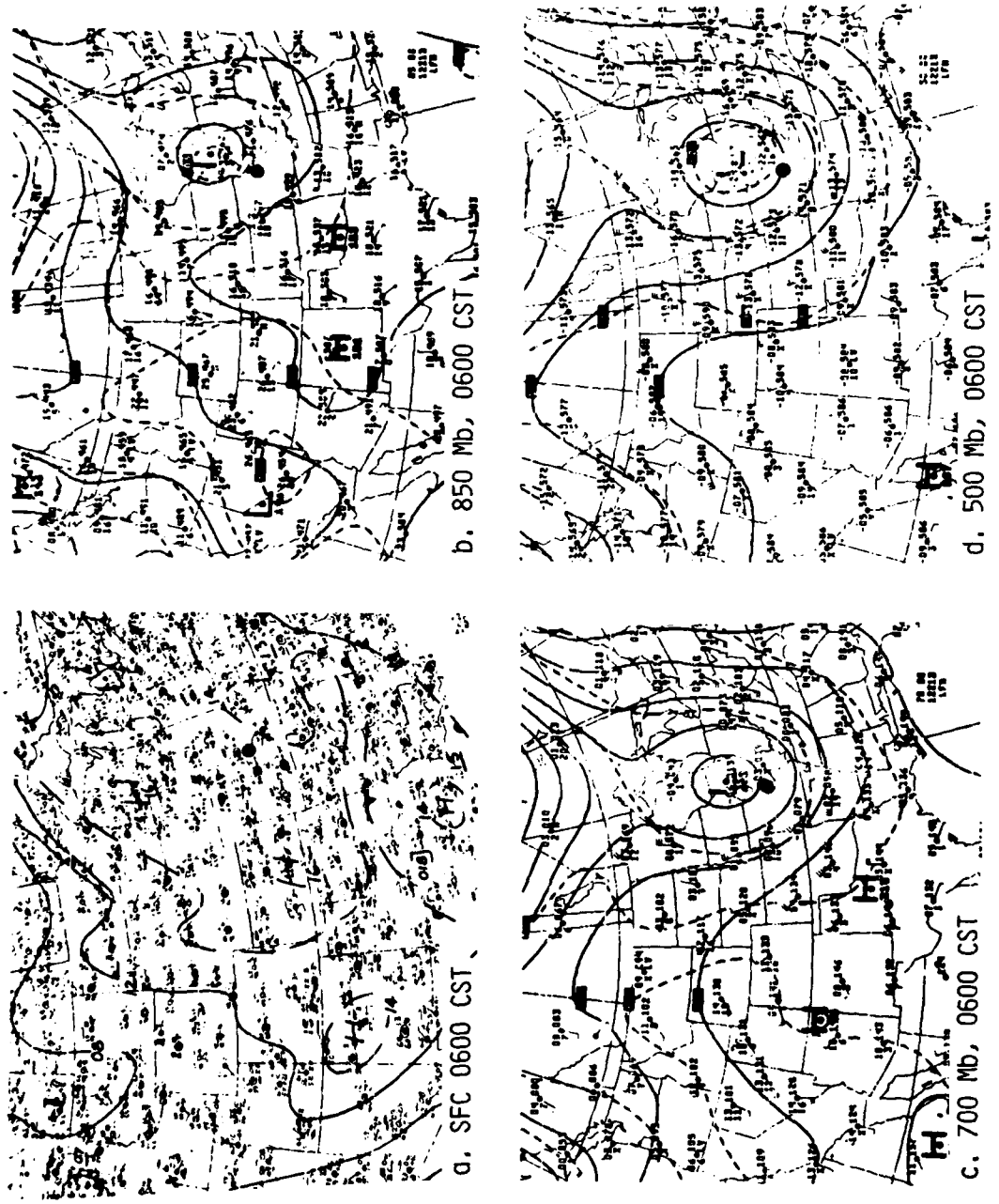

Figure D1. National Weather Service synoptic analyses for 0600 CST 13 July, 1975. St. Louis area identified by black dot.

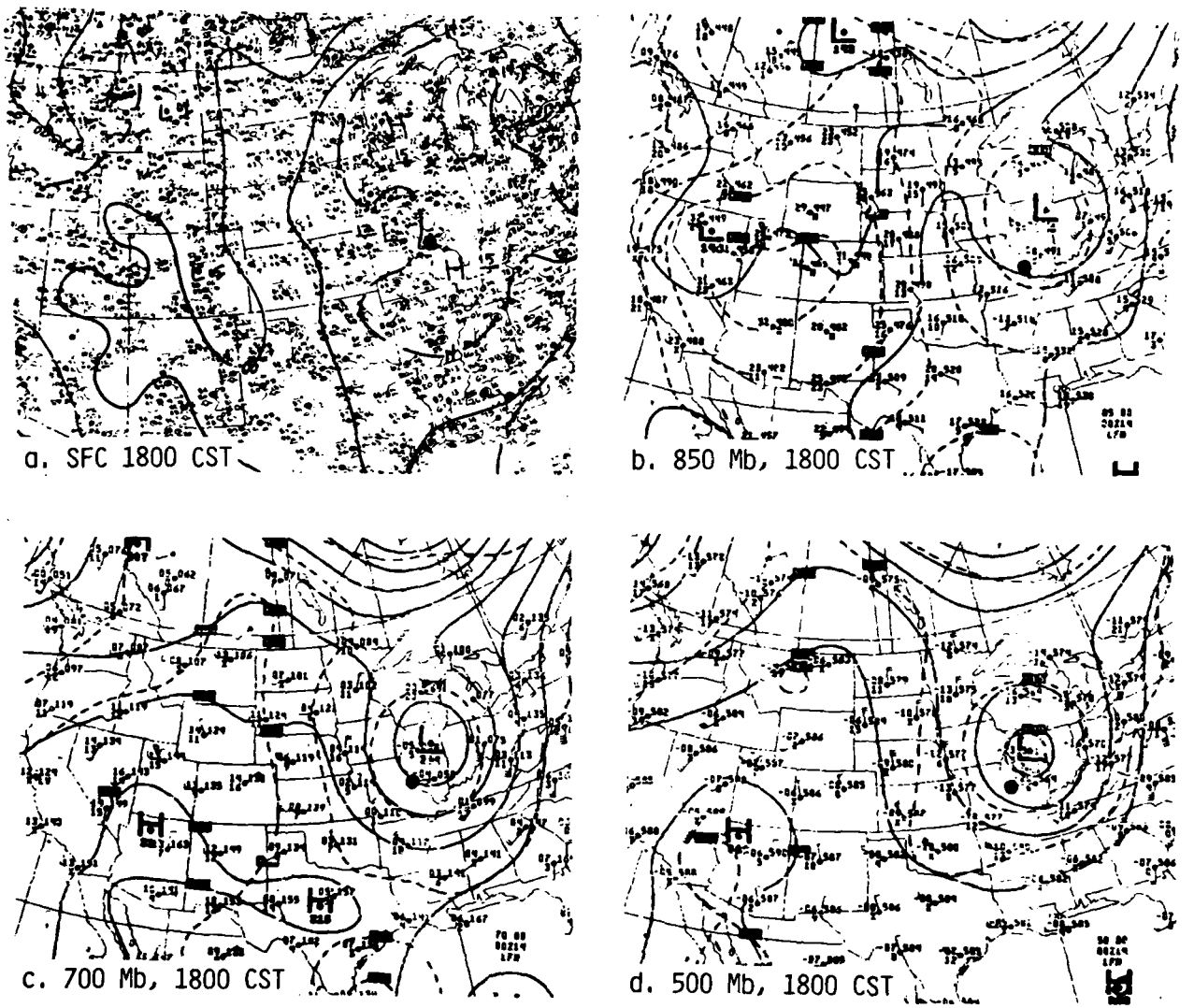

Figure D2. National Weather Service synoptic analyses for 1800 CST 13 July, 1975.

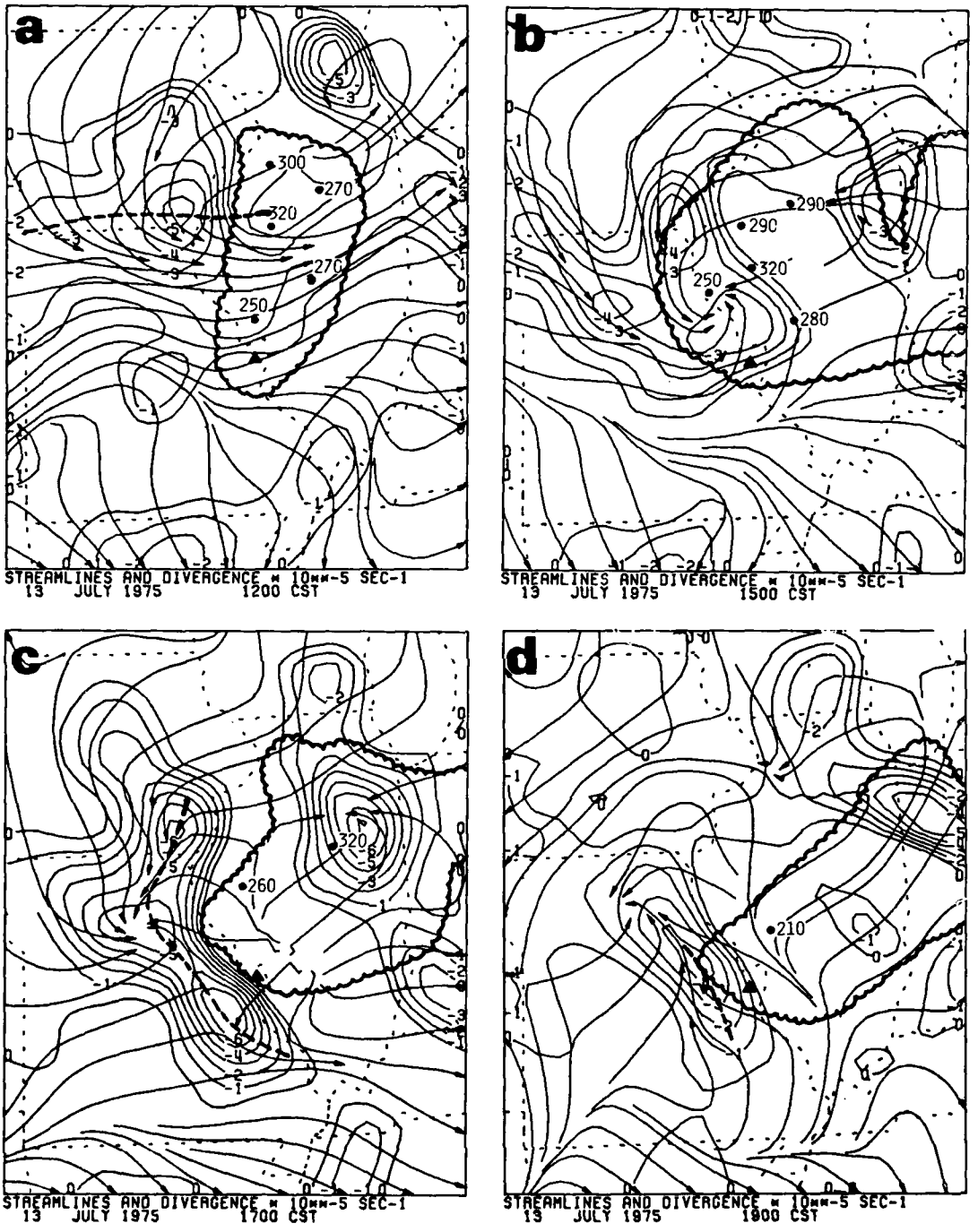

Figure D3. Regional scale analyses of surface streamlines and convergence.

had pushed westward across St. Louis to a location 50-100 km west of the Mississippi River leaving the network within rain cooled divergent flow. This pattern, though diminishing by 1900 CST, persisted for the remainder of the 13th.

TIME SERIES OF DIVERGENCE AND RAINFALL

The time series for the number of gridpoints with rainfall, the average 15-min rainfall for the gridpoints reporting rain, and the network mean divergence are shown in Fig. D4a-4c. Scattered rainshowers began at about 1200 CST and persisted until 1700 CST whereupon there was a rapid transition to widespread light rainfall. Until 1330 CST, the network average divergence oscillated about zero with a period of approximately 2 hr. Divergences were less than +/- 0.5U. Then the average divergence increased to 1.2U (arrow A) as showers became active over the network. There were no indications of network scale increases in convergence prior to the rainfall.

From 1600 to 1700, network scale convergence up to 1.5U (arrow B) occurred as moderate rain showers developed along the boundary of cool outflow from a shower area north and east of the network. The outflow pushed south-westward across the network by 1700 and was followed by the area of general light rainfall. The network average divergence was variable after 1700 CST but divergence predominated more frequently and was stronger than the convergence.

Figures D4d-4e give the time series for the maximum 15-min rainfall, the maximum point divergence, and the minimum point divergence (convergence). The convergence peaks almost simultaneously with the rainfall. However, some of these convergences were found within the network in areas not spatially related to the rainfall. The background point divergence was approximately +/- 3U for the 13th. Convergences exceeded background several times between 0900-1000 and persistently exceeded it after 1200 CST when wind field perturbations were increased by shower outflows (see following section). The perturbations reached maximum strength around 1330 CST to produce peaks in maximum divergence and convergence (arrows A). The network scale flow was divergent at this time (Fig. D4c). At 1600 CST, convergence increased to exceed 12U (arrow B) as the heaviest showers of the day developed within the network. After 1700 CST, both the divergence and convergence frequently exceeded background, an indication that the areas of light rainfall were perturbing the surface wind field.

MESOSCALE SITUATION

The strong outflow system that pushed over the network shortly after midday on the 13th was unique in that it was not accompanied by measurable precipitation over the network. The dry unstable weather conditions on the 13th were similar to the conditions on the 12th during which evaporation of falling rain led to strong outflows accompanying light rainfall amounts.

A weak convergence zone (dashed line) with two embedded 2U centers (arrows) extended from the western edge of the network to near the Arch at 1100 (Fig. D5). This convergence zone persisted through the next hour during which a convergence center exceeding 4U was observed (Fig. D5b). A trace

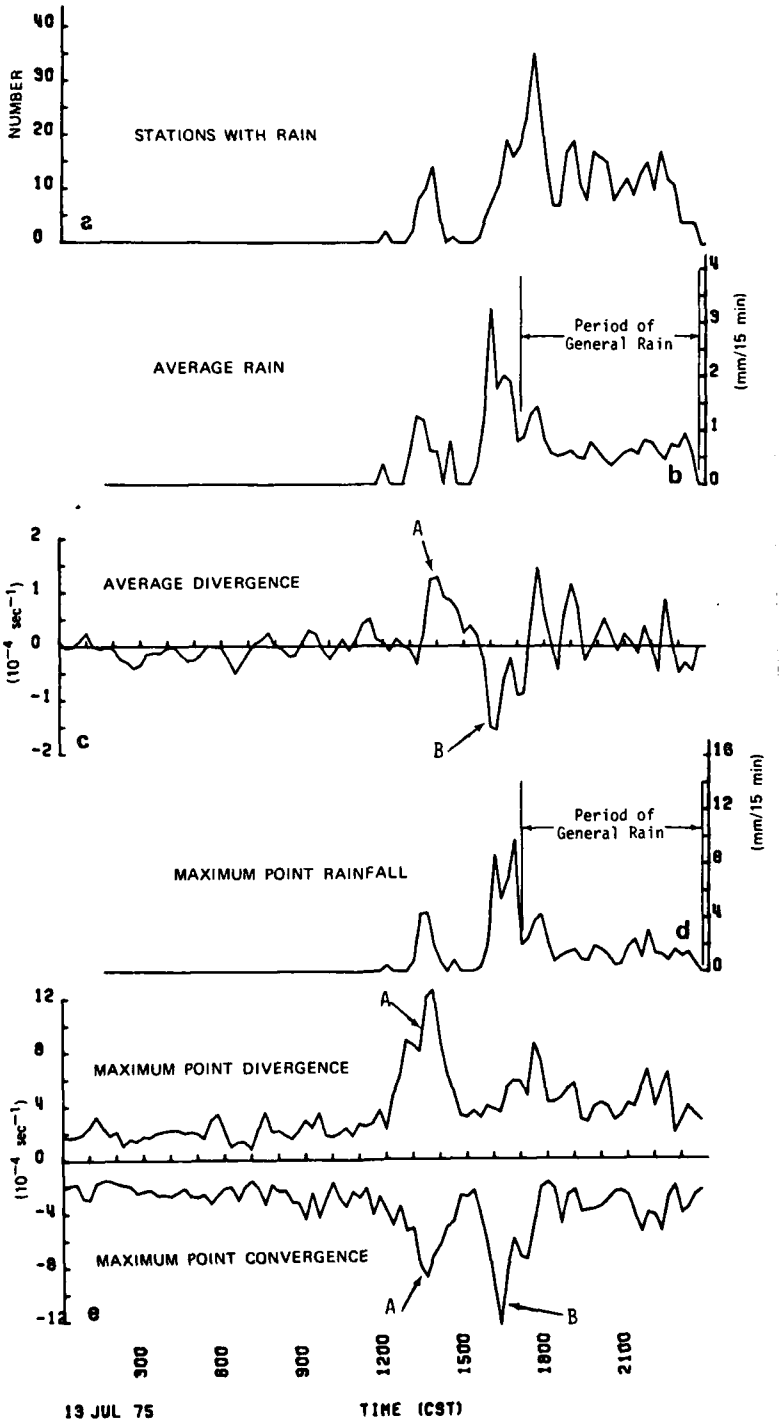

Figure D4. Time series of divergence and rainfall variables.

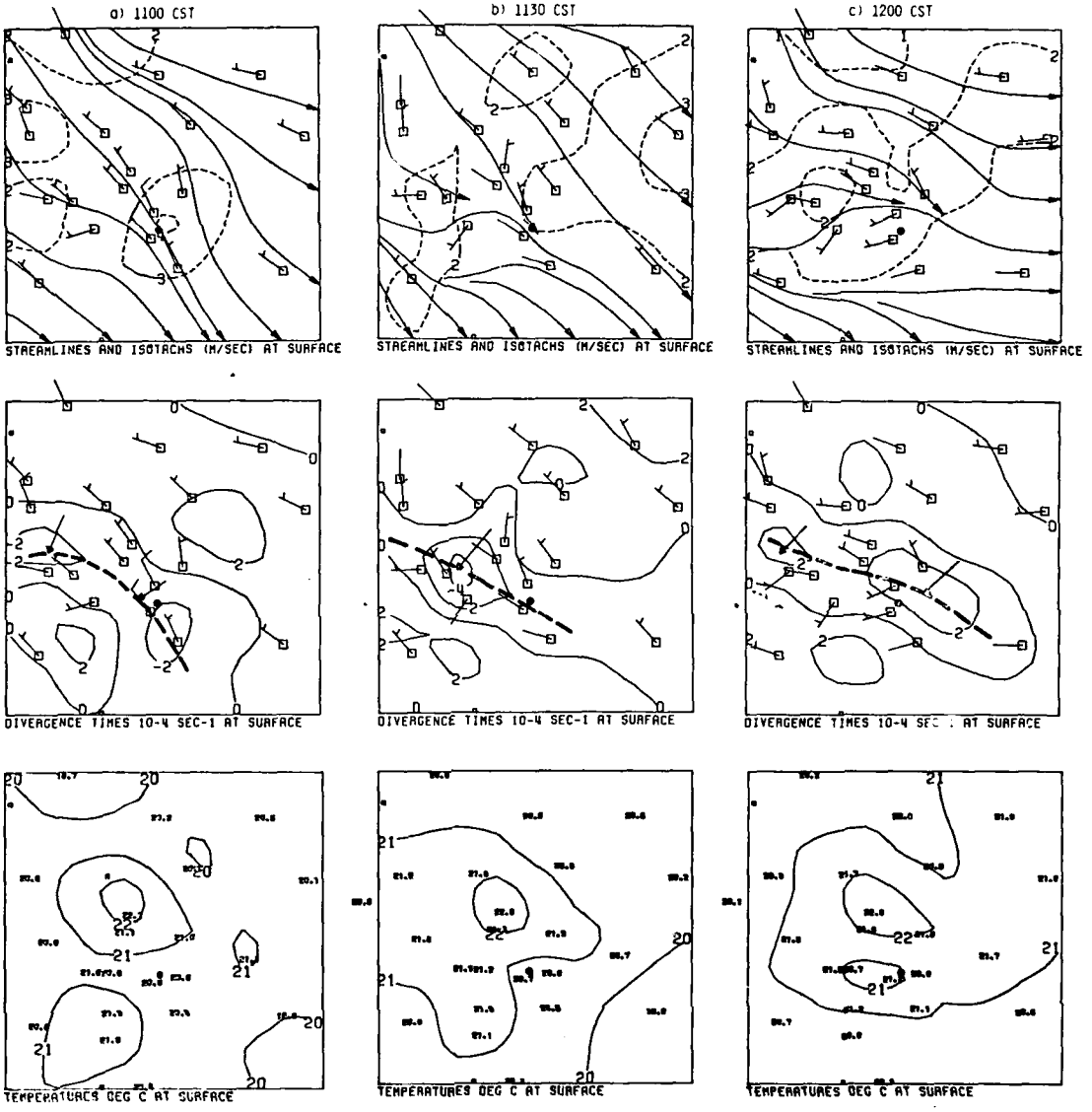

Figure D5. Composite of the objective wind field isotachs and streamlines (upper map), divergence (middle map), and temperature (lower map) for 1100-1200 CST. St. Louis Arch identified by the solid circle.

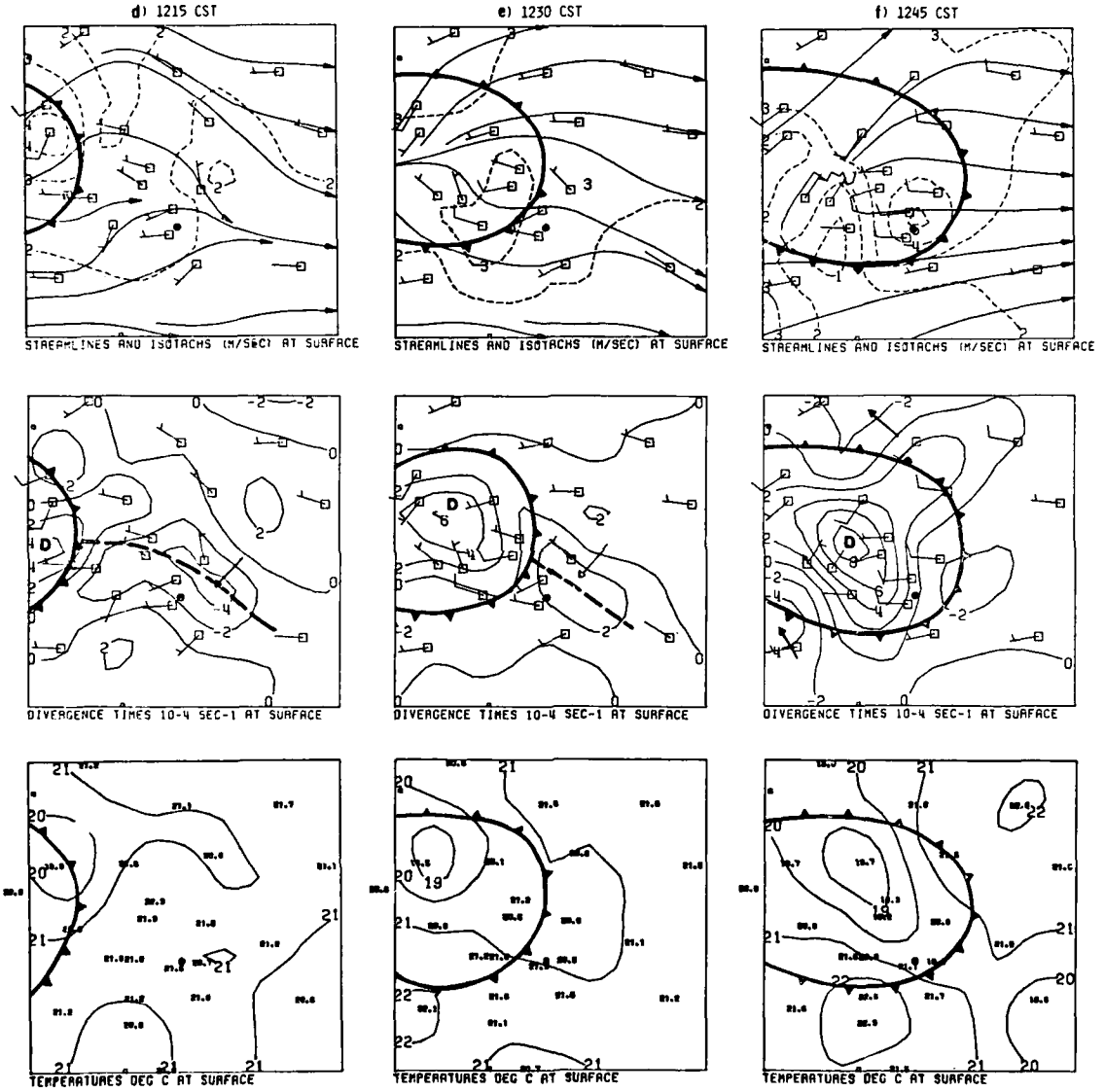

Figure D5. Concluded

amount of precipitation was recorded along the convergence zone at the western edge of the network at 1200. A gust front followed by a strong divergence center followed the convergence zone across the network beginning at 1215 (Fig. D5d). The divergence center D strengthened from 4U to 8U between 1215 and 1245, an indication that downdrafts had increased. The downdrafts were likely strengthened by the evaporation of falling rain.

The vertical motions analyzed from the surface and boundary layer convergence show that strong subsidence up to 30 cm sec^{-1} at 950 m (Fig. D6) was located over the strong surface outflow.

By 1300 (Fig. D7a) raincells were approaching the northern and southwestern boundaries of the St. Louis network. Convergence areas (arrows) preceded these storms. Outflow from both complexes merged with each other and merged with the dissipating gust front from the first outflow to produce three 4U or greater convergence centers (arrows) at 1315 (Fig. D7b). Cell A formed near a 4U convergence area found at 1245 and 1300 (see arrows, Fig. D5f and Fig. D7a) at the southwest corner of the network. Cell B propagated into a convergent area over the northern part of the network (arrows) that was also present for a half an hour.

The two new gust fronts merged progressively southeastward across the network to produce a convergence zone that exceeded 8U at 1330 (Fig. D7c) and 6U at 1345 (Fig. D7d). Cell C developed near the network's southern boundary downwind from a 4U convergence center at 1315 (arrow, Fig. D7b). Cells D and E formed at 1345 (Fig. D7d) as Cell B's gust front undercut a convergence center near the position of the first gust front (arrow, Fig. D7b).

No raincells developed along the convergence zone which weakened after 1345. All wind field perturbations subsided from 1415-1500 and the convergence zone vanished by 1500. Temperatures returned to near pre-rain levels and the winds shifted to southerly as the subsynoptic low over northeast Missouri controlled the circulation (Fig. D3b).

The period from 1500-1630 was characterized by the most notable convergence buildup in advance of rain cell development found in the seven case studies. At 1500 (Fig. D8a) winds over the southwest and central part of the network shifted to southwesterly and a convergence zone began to form over the northeastern part of the network. A 2U convergence center (arrow) at 1515 strengthened to exceed 4U by 1530.

A large center of ascent existed along an axis east of the Arch (arrow, Fig. D9) from the surface to 1350 m at 1500. The increasing vertical velocities with height indicates that the surface convergence zone extended through a deep layer in the lower troposphere.

An area of rain moved to the northern border of the network at 1545 (Fig. D10a). The convergence zone was in the path of the southeastward moving storm. Cell F formed within an area of 2U convergence that, though separate from the major convergence zone, had persisted since 1500. It appeared as the gust front from the northern cell complex including newly developed Cell G pushed into the network (Fig. D10b). Convergence increased to 8U where the gust front merged with the pre-existing convergence zone.

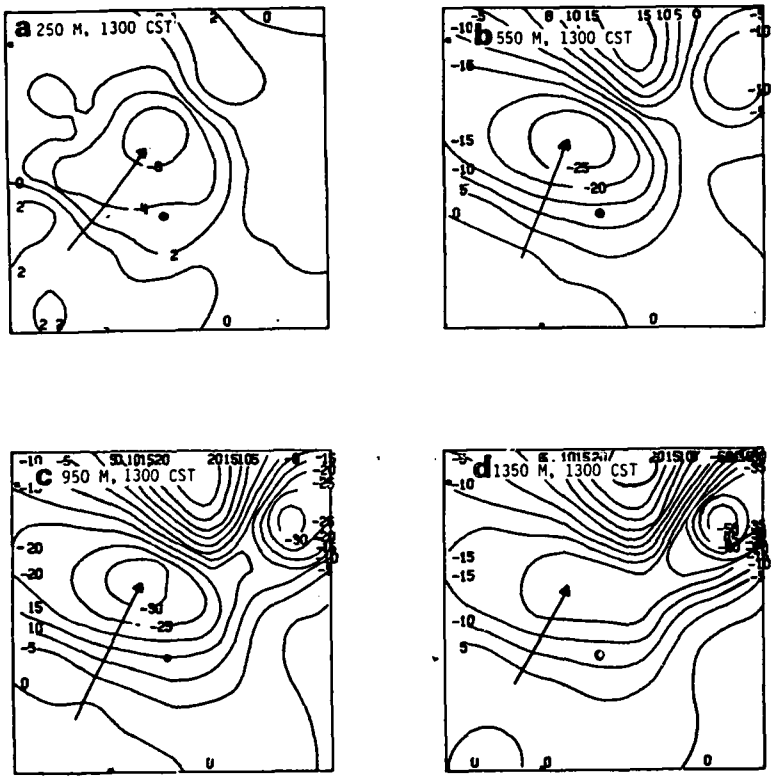

Figure D6. Vertical velocity maps (cm sec^{-1}) for 1300 CST.

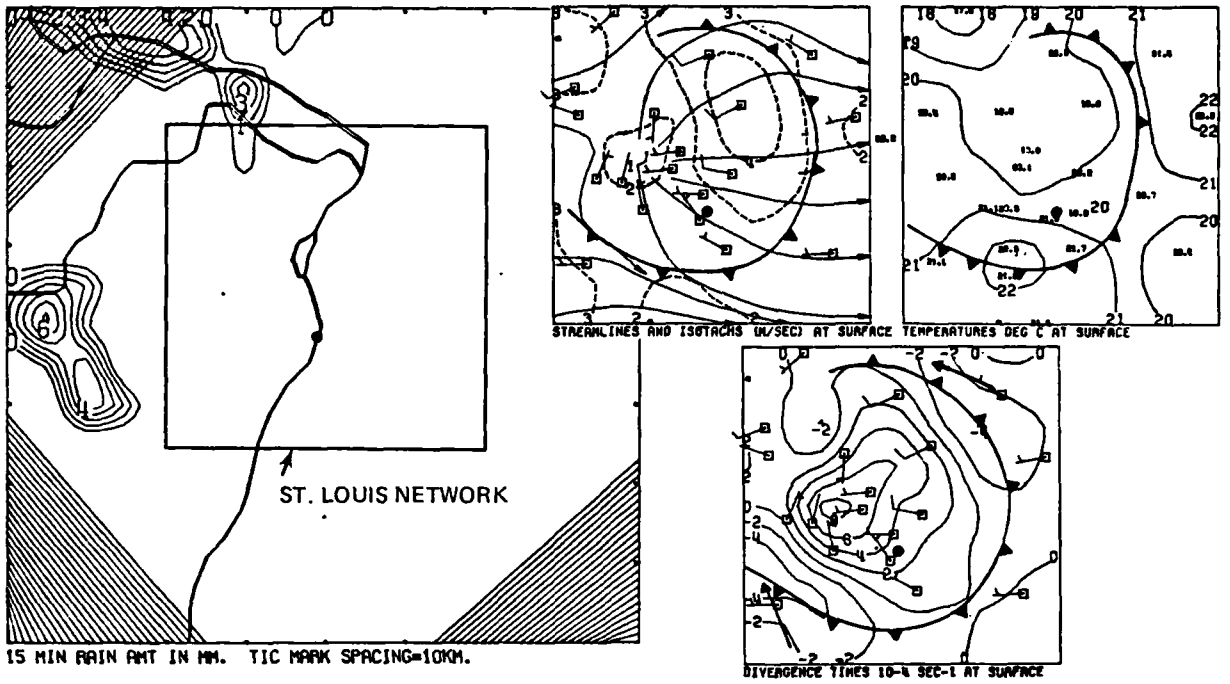

a. 1300 CST

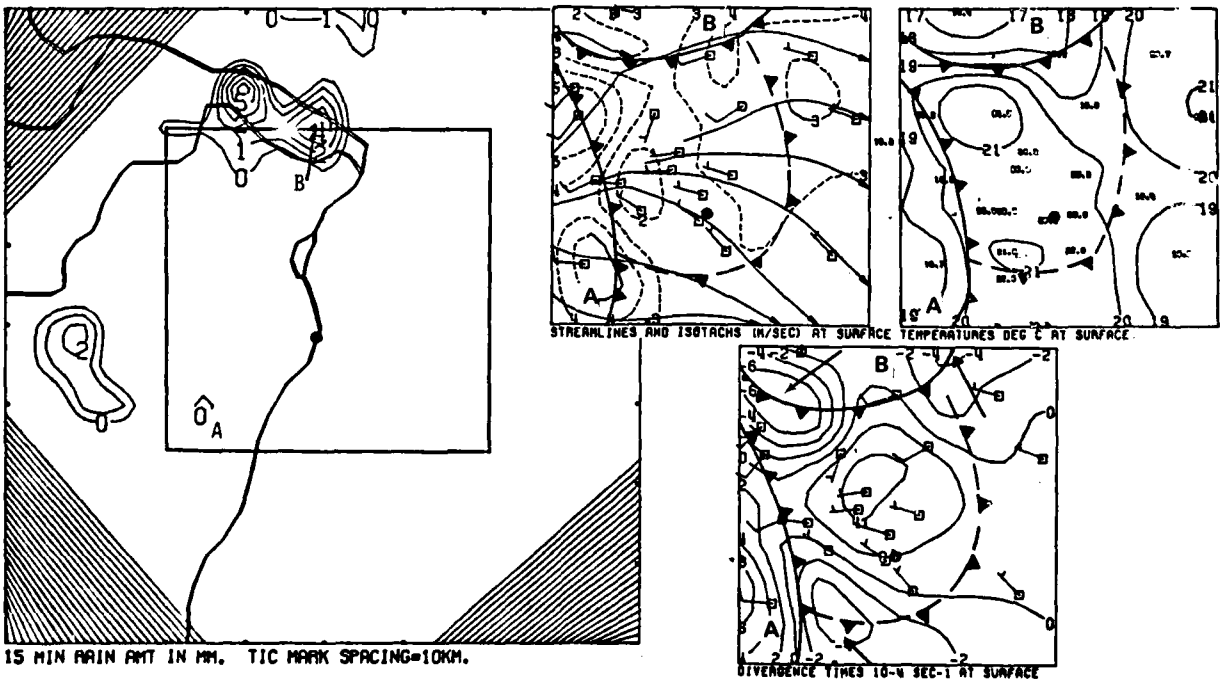

b. 1315 CST

Figure D7. Composite of the objective isotachs and streamlines, temperature, divergence and rainfall for 1300-1345 CST.

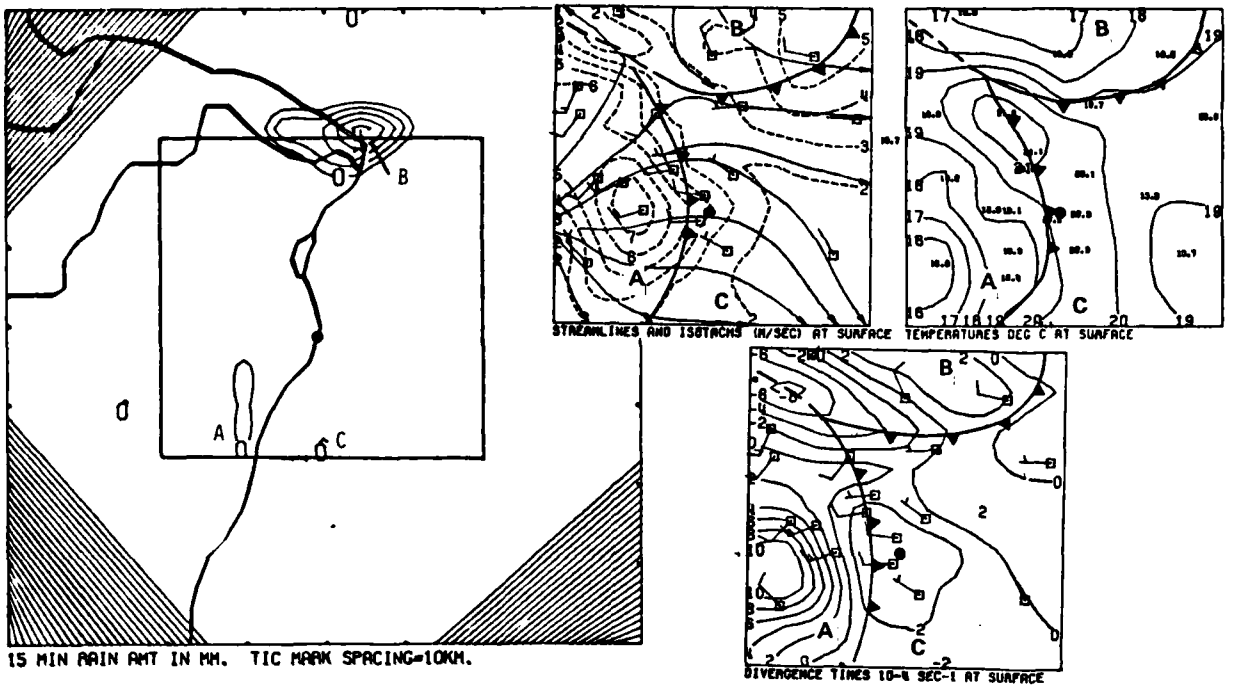

c. 1330 CST

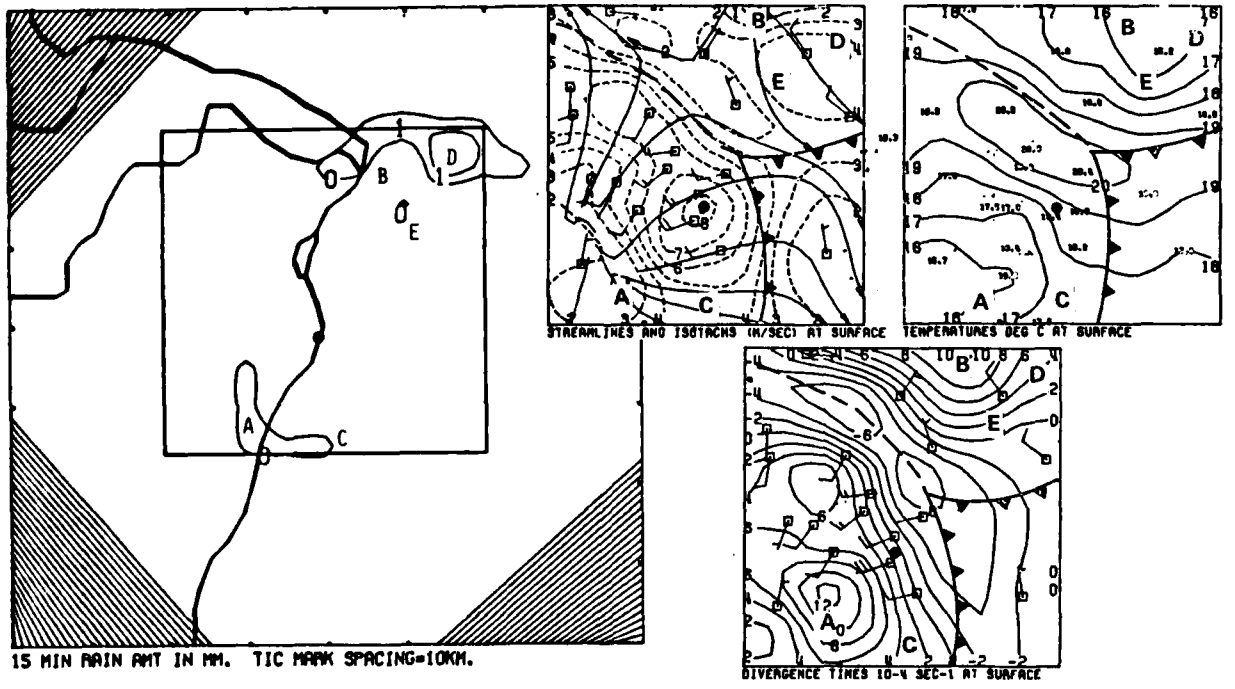

d. 1345 CST

Figure D7. Concluded

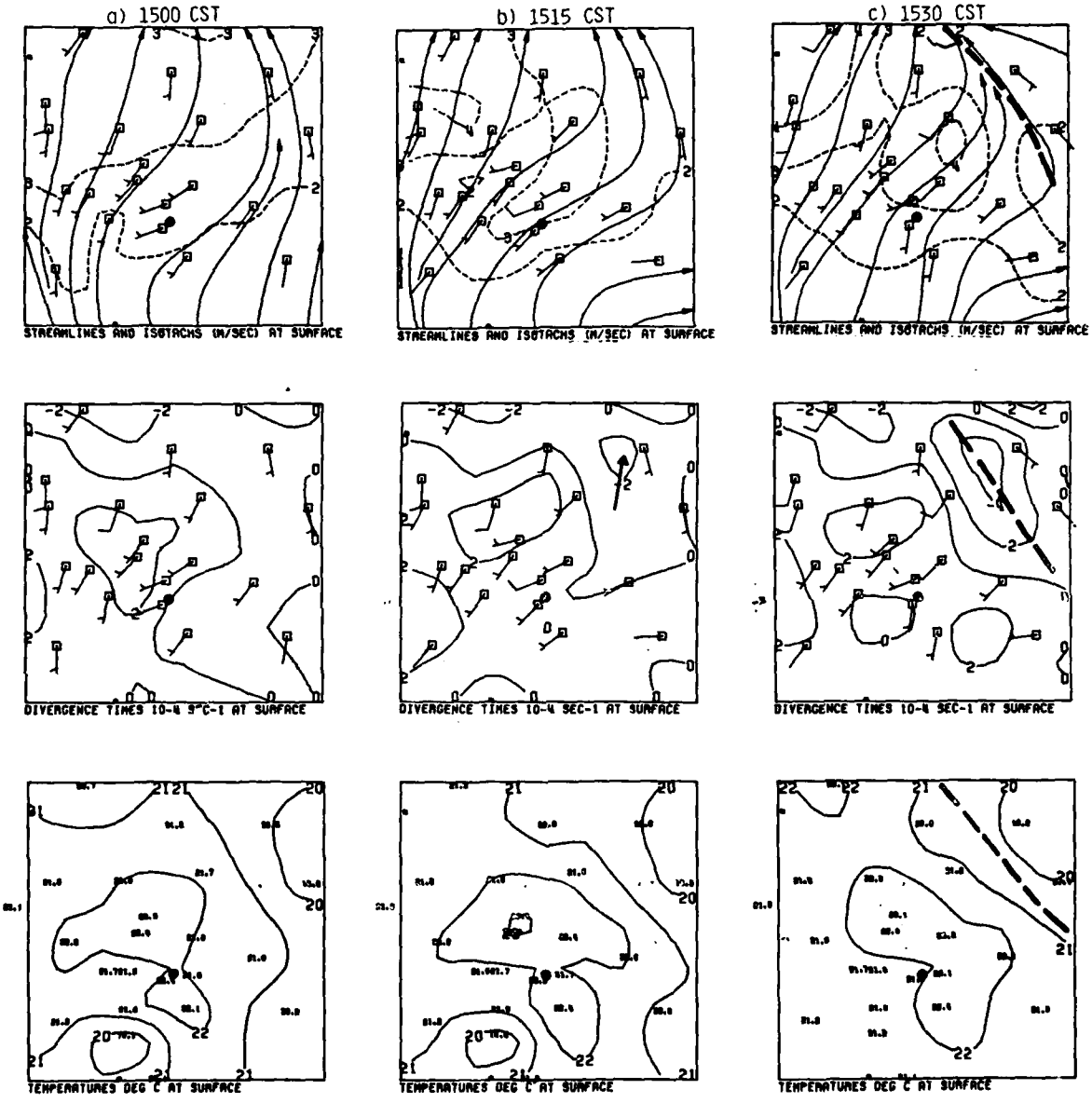

Figure D8. Composite of the objective isotachs and streamlines, temperature, divergence and rainfall for 1500-1530 CST.

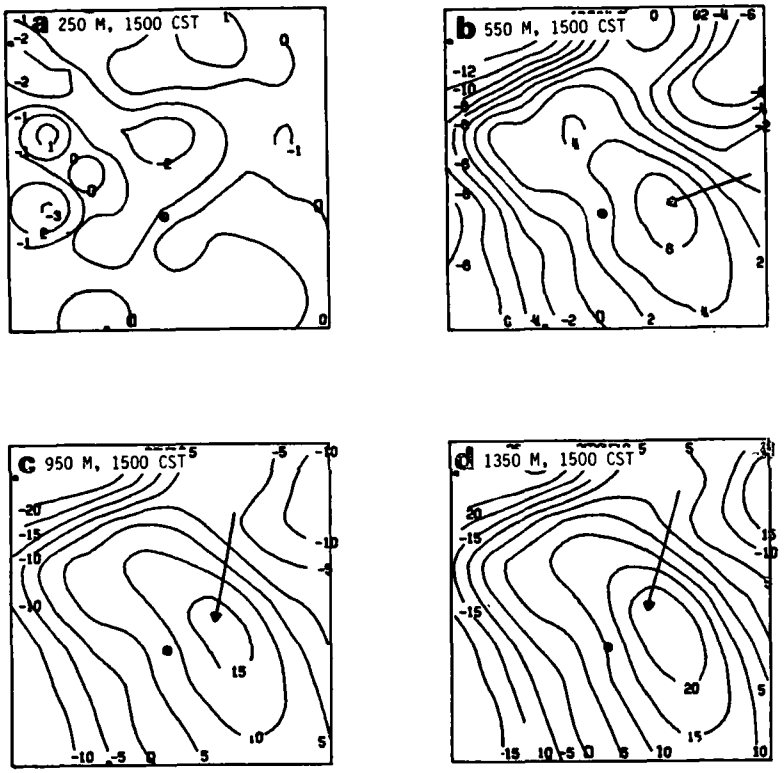

Figure D9. Vertical velocity maps (cm sec^{-1}) for 1500 CST.

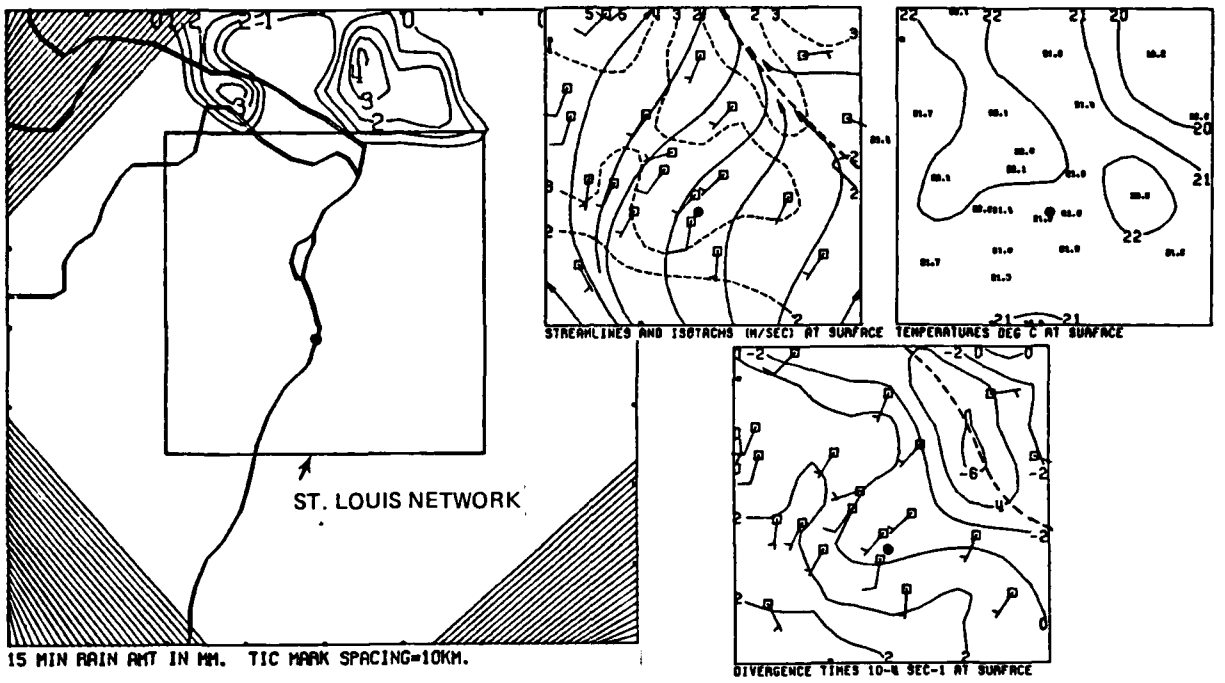

a. 1545 CST

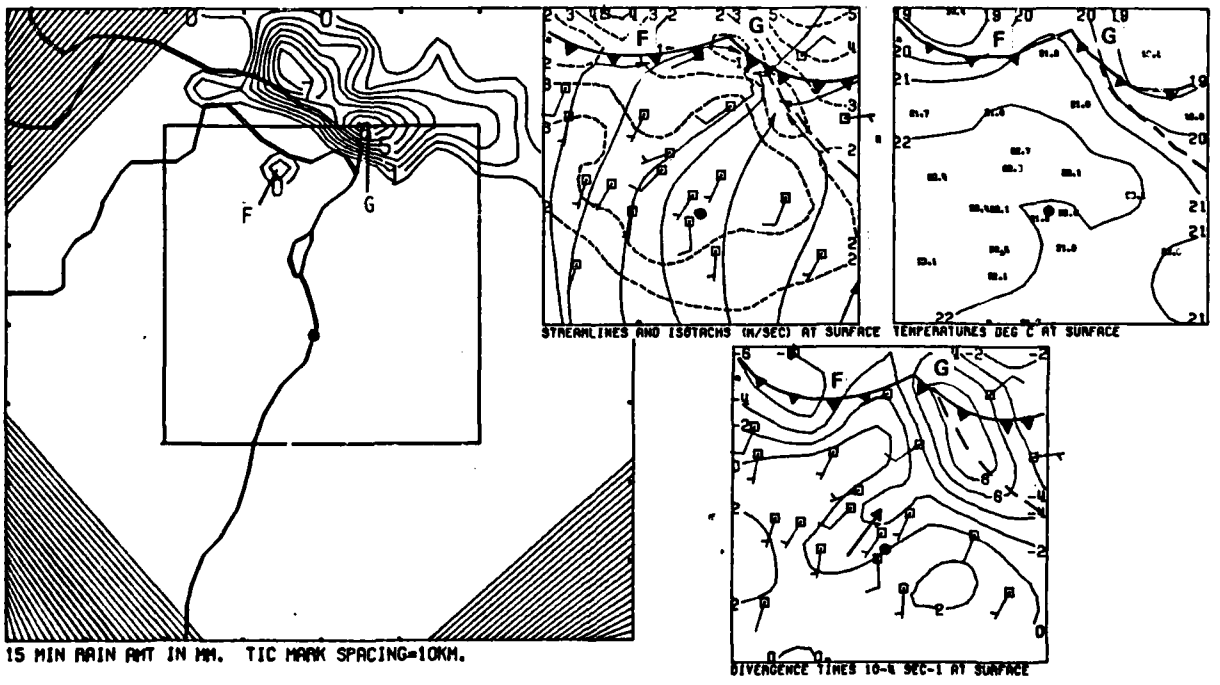

b. 1600 CST

Figure D10. Composite of the objective isotachs and streamlines, temperature, divergence and rainfall for 1545-1745 CST.

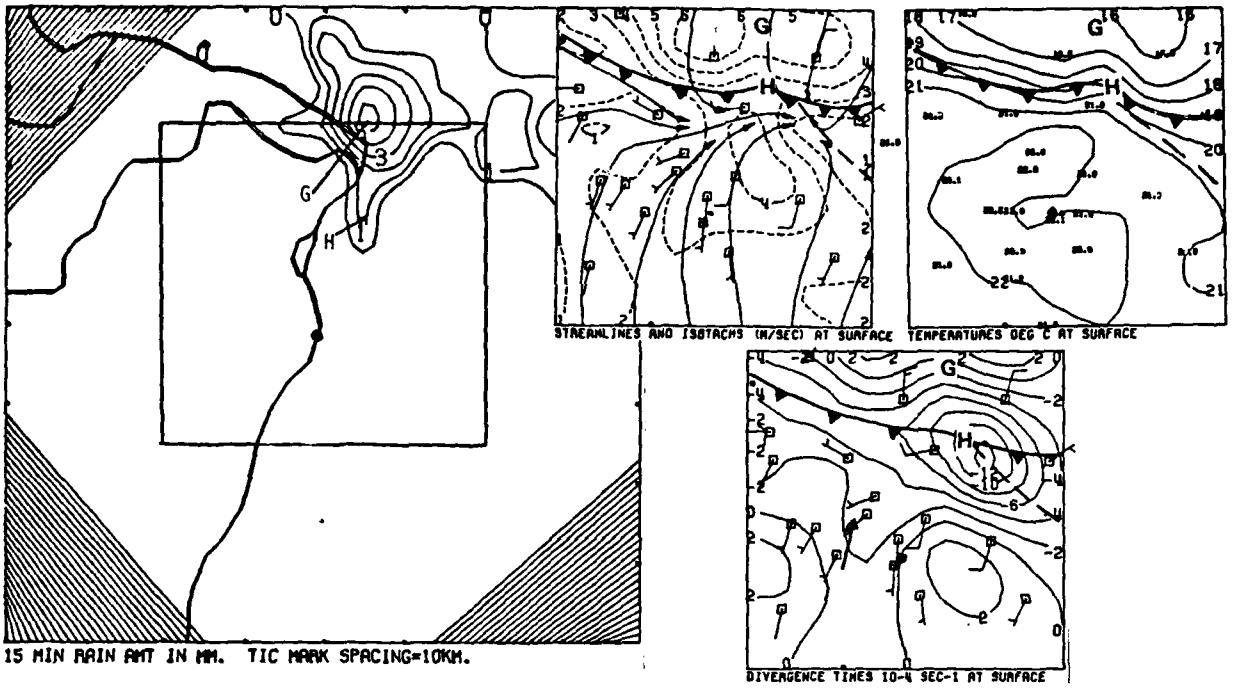

c. 1615 CST

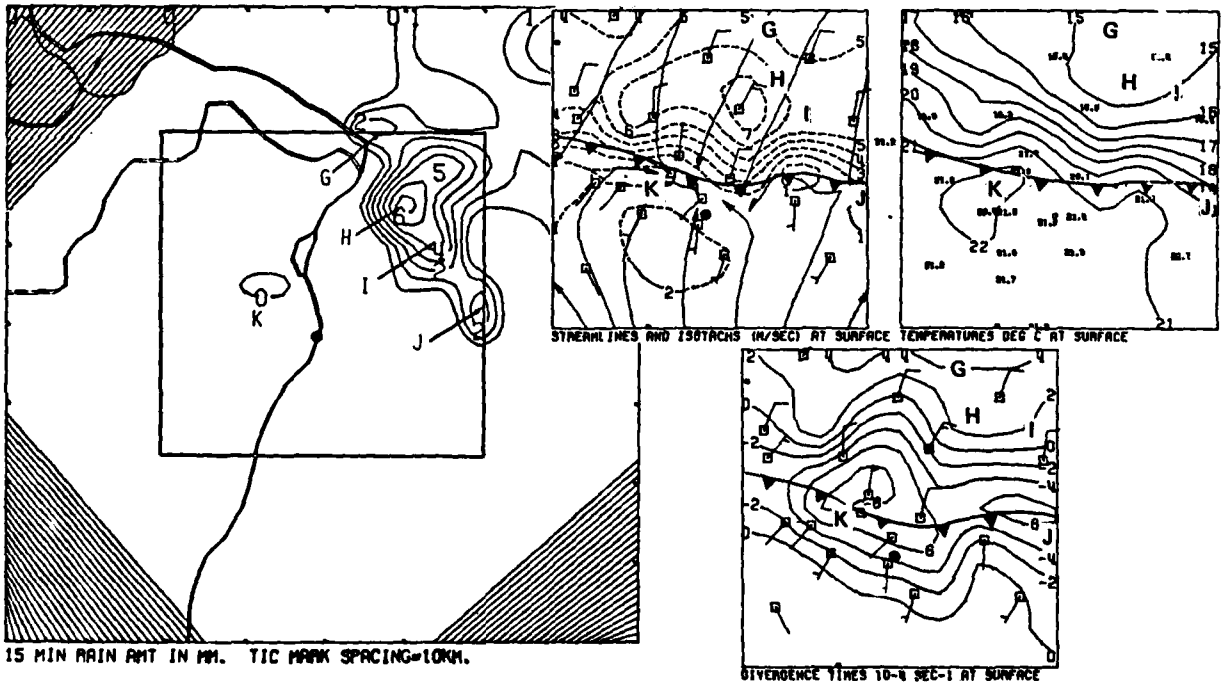

d. 1630 CST

Figure D10. Continued

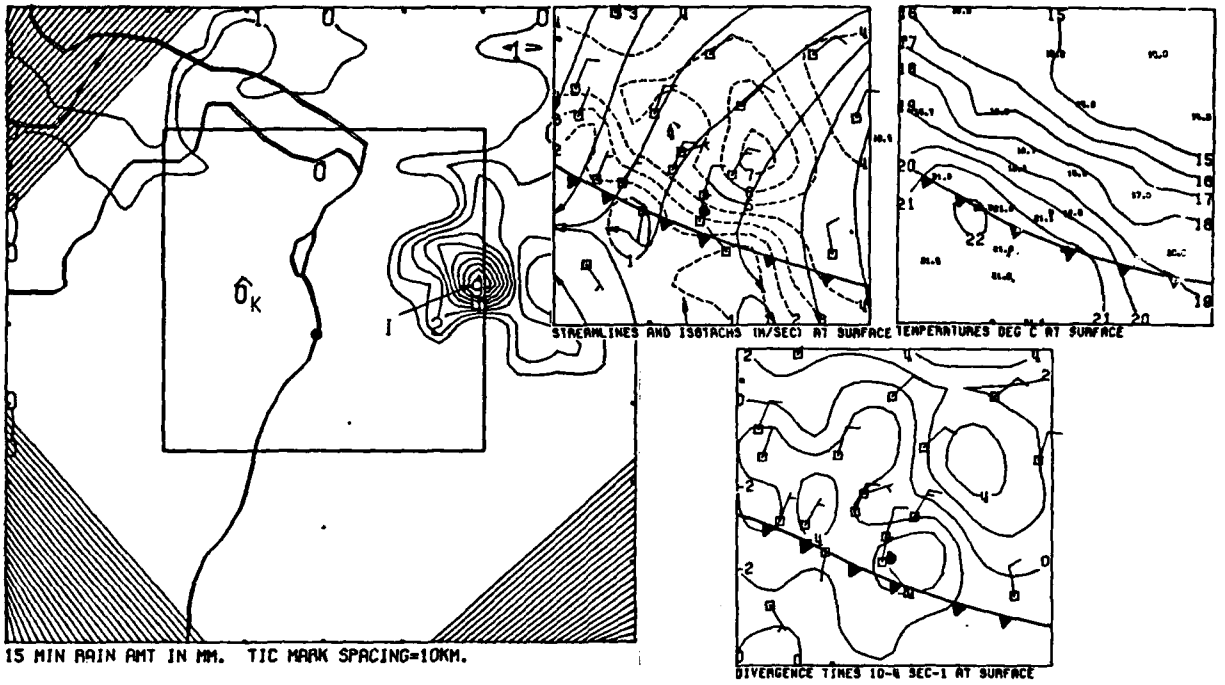

e. 1645 CST

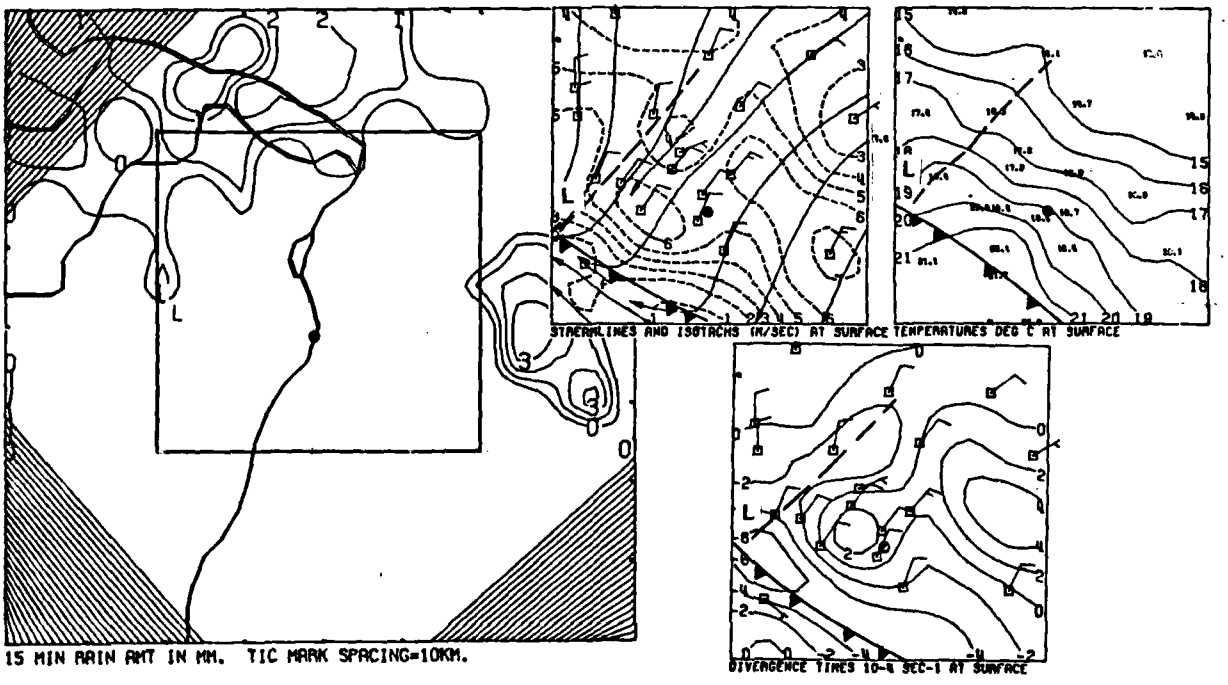

f. 1700 CST

Figure D10. Continued

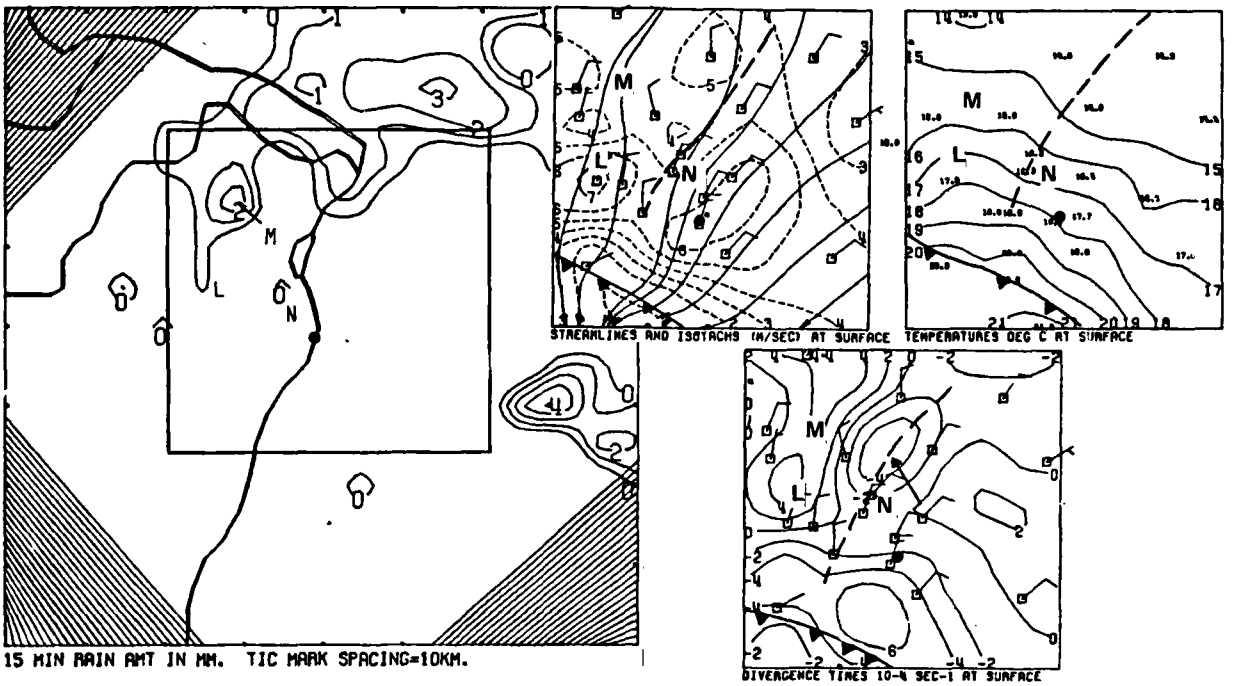

g. 1715 CST

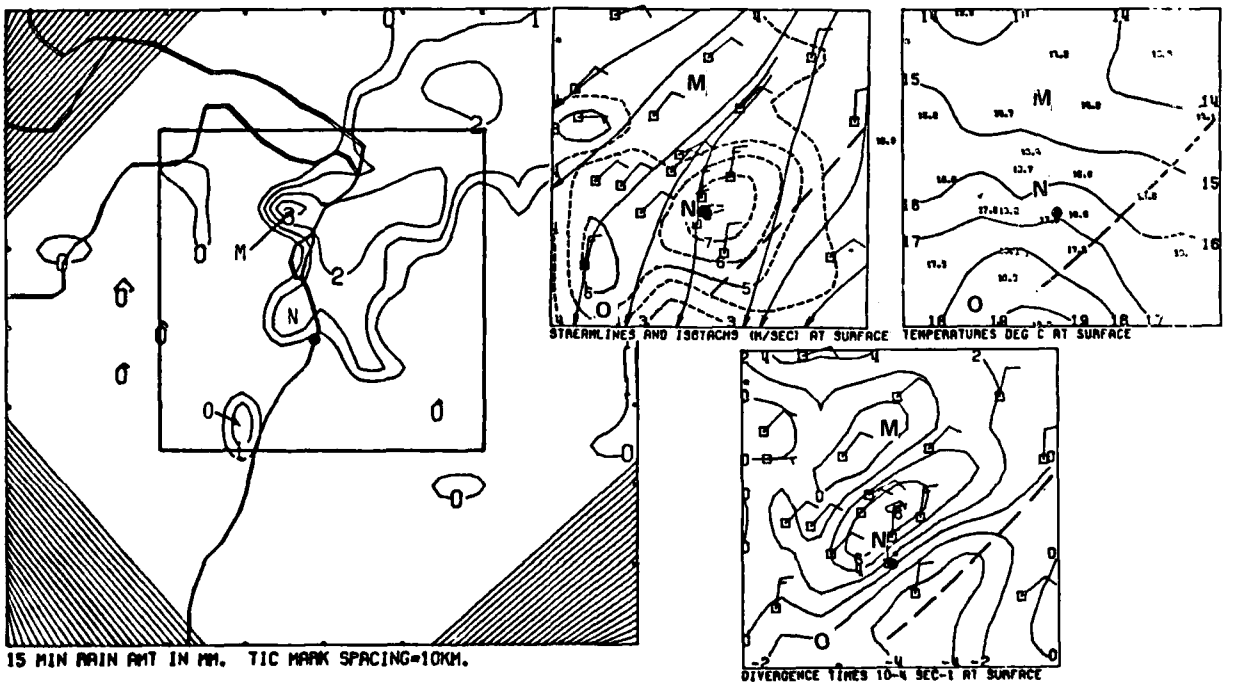

h. 1730 CST

Figure D10. Continued

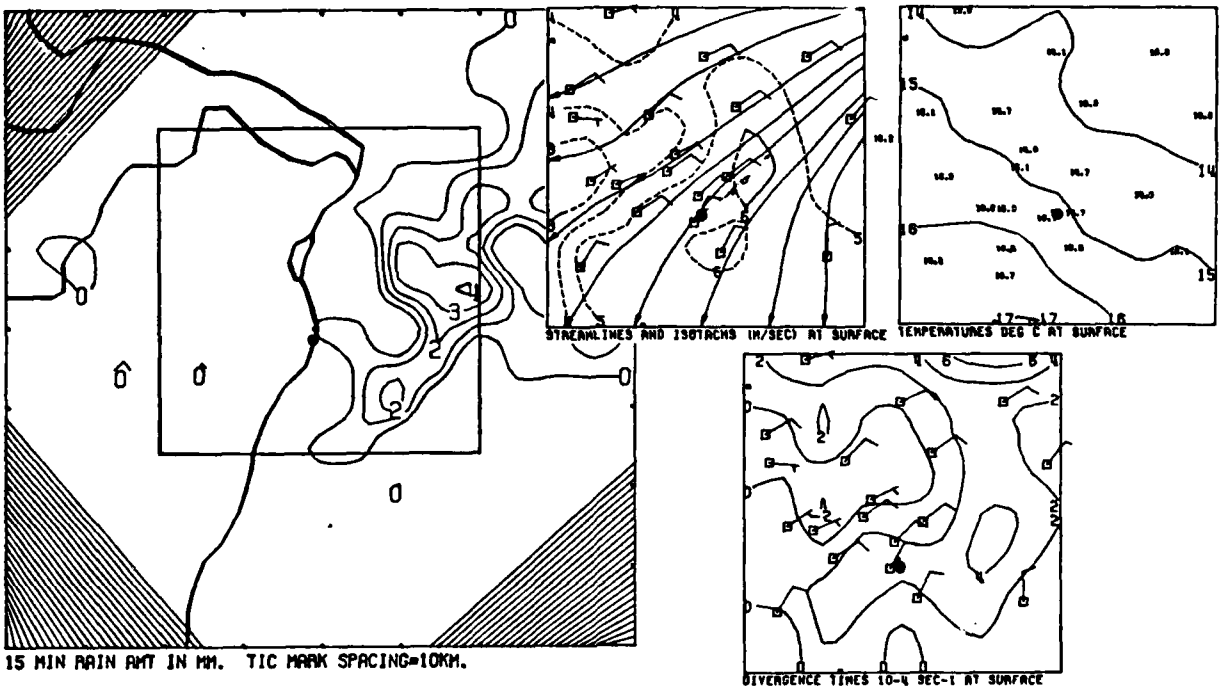

i. 1745 CST

Figure D10. Concluded

The gust front continued southward with convergence greater than 4U along its length within the network (Fig. D10c). Moderate south and southwesterly winds to 4 m sec^{-1} combined with the gust front and the convergence zone to increase convergence to 12U at the point of merger. Cell H formed near this intersection and increased to 6 mm/15-min (Fig. D10d). Cells I, J, appeared along the convergence zone southeast of Cell H.

A small tongue of 2U convergence extended southwestward from the convergence zone to about 5-10 km northwest of the Arch at 1600 and 1615 (arrows, Figs. D10b, 10c). Cell K developed within this area at 1630 as the gust front swept through with 8U convergence.

The cold outflow from the G, H, I, and J storm complex pushed southwestward past the Arch at 1645 (Fig. D10e). Cell I remained at the eastern edge of the network. Meanwhile, an area of light rain approaching the network from the northwest moved over the raincooled surface air behind the gust front (Fig. D10f). A convergence zone developed between the northerly outflow from the light rain area and the northeasterly post-gust-front flow. Cell L appeared near its junction with the gust front.

Cells M and N developed at 1715 (Fig. D10g). By 1730 Cell M moved to the location of a 4U convergence zone at 1715 and persisted while the rain area moved southeastward. Cell N formed within the convergence zone and merged with the rain area as it moved southeastward as a line following the surface convergence zone (Figs. D10h and D10i).

Cell O appeared at 1730 and was probably triggered by the southward moving gust front. Convergence had exceeded 4U for one half hour prior to cell O's appearance.

SUMMARY OF RAINCELL DEVELOPMENTS ON 13 JULY

Weather systems on different scales combined to produce conditions favorable for an outbreak of convective showers over the St. Louis network during 30 July. The area was located within a deep layer of northwesterly flow from the surface to 500 mb, conditions usually unfavorable for convective showers. However, the cold temperatures aloft and moderate amounts of moisture combined to create convectively unstable conditions. Convective instability was further increased by lifting of airmasses within a regional scale convergence area that developed over northern Missouri and moved southward during the day.

Strong outflows and light rainfall amounts accompanied the first of the showers. This was an indication that much of the rain was evaporating before reaching the ground. The first outflow system moved over the network without any measurable rainfall. By 1600, the most notable pre-rain convergence zone found in the seven case studies developed convergence to 12U. The network-average convergence reached 1.5U during this same period.

The convective showers were followed by a period of light rain that lasted to the end of the day. Outflows from the heavier showers had pushed south and west of the network leaving the network within a rain cooled airmass. The

convergence zone persisted west of St. Louis (Fig. D3d) and it is possible that warm air flowing over the cold surface air was the source of moisture of these rains.

Raincell development over the St. Louis network was apparently highly dependent upon surface convergence. Fifteen raincells developed over or sufficiently near the network to influence the wind field. Convergence extended into the network ahead of Cells B, G, and L which formed outside of the network. The light raincells tended to form along gust fronts and the heavier raincells formed in presistent convergence areas or at the intersections of convergence zones with gust fronts. Except for the light rain period, raincell development decreased once the surface layer was cooled and then increased after surface temperatures increased to near pre-rain levels.

Table D1 summarizes the cell strengths, convergence strengths, and convergence durations for the raincells that formed within the network. Cell strengths ranged from 0.5 to 13.0 mm. Convergence centers preceded eleven of the twelve cells. The maximum convergence strength was 31U with a duration of 60-min. The average cell strength was 3.0 mm, the average convergence strength was 9.1U, and the average convergence duration was 30-min.

Three other convergence centers occurred during the rain period but were not associated with rainfall. These centers had strengths and durations of, respectively, 4U (15-min), 8U (30-min), and 20U (45-min).

The spatial relationship between the raincells and the convergence centers was quite good for the 13th. The centers persisted for 30-min or longer for 8 of the 12 raincells. Thus, the convergence centers were fairly predictive of the future location of raincells and with few false alarms - only 3 convergence centers were not associated with rainfall.

Eight of the twelve raincells produced cell strengths less than 1.5 mm. The cell strengths and convergence strengths for the remaining four raincells were, respectively, 2.0 mm (10U), 5.0 mm (0U), 7.0 mm (31U), and 13.0 mm (20U). One 1.5 mm raincell was associated with a 16U convergence center; for the remaining weak raincells convergence strengths were less than 10U. Thus, with some scatter, a positive relationship between convergence strength and cell strength was apparent on the 13th.

Table D1. Cell Strengths, Convergence Strengths, and Convergence Durations for Raincells that formed within the St. Louis Network on 13 July.

Cell ID	Cell Strength	Convergence Strength	Convergence Duration
A	1.0mm	8U	30 min
C	0.5	4	15
D	1.5	2	15
E	0.5	2	15
F	1.5	16	45
H	7.0	31	60
I	13.0	20	60
J	2.0	10	45
K	1.0	5	30
M	5.0	0	0
N	0.5	4	30
O	1.5	8	30

E. CASE STUDY: 17 JULY 1975

SYNOPTIC SITUATION

The precipitation regime that produced rainfall over the St. Louis network from 1130-1700 CST was observed by satellite in various stages of development. At 1000 CST, the middle west was largely cloud free. Several small cloud bands (arrows A, Fig. Ela) were present over southern Missouri and parts of Illinois. A large field of cumulus clouds had developed over Missouri and southeast Iowa by 1200 CST. Large cumulus clouds were found from near St. Louis southwestward to the Arkansas border (arrows B, Fig. Elb). Radar summaries indicated that some of these clouds were producing showers.

Continued development led to numerous showers within the St. Louis network and southwestward by 1300 CST (arrows C, Fig. Elc). The network was found at the northern edge of an extensive anvil canopy by 1530 (arrows D, Fig. Eld).

At 0600 CST the St. Louis area was beneath southwesterly flow from the surface to 700 mb (Fig. E2). The flow switched to northwesterly by 500 mb where the circulation over St. Louis was controlled by a cold-core cyclone centered over the Indiana-Ohio border. During the day, a short wave trough (dashed line) moved from the High Plains into Minnesota (Figs. E2 and E3). A strong low-level jet stream at 850 mb (shaded area) extending from Texas through the High Plains and into southwestern Minnesota moved slowly eastward ahead of the trough. Circulations (if any) associated with this wind maximum had no apparent influence on the local St. Louis area as the jet stream remained well to the west throughout the day.

The surface maps for 0600 and 1800 CST (Figs. E2 and E3) show the cold front in the High Plains that accompanied the upper level short wave. An associated trough of low pressure that extended from the Dakotas southward through eastern Colorado and western Texas spawned numerous showers and thunderstorms later in the day. These storms remained west of the development that occurred over Missouri.

Increased convective instability caused by the flow of warmer and more moist air at 850 mb beneath the circulation of the cold-core cyclone in the middle troposphere over Indiana helped to initiate the convective showers over the St. Louis area. One to two degree temperature increases occurred at Salem and Peoria, Illinois, between 0600-1800 CST. Dewpoints increased from 7-9C at 0600 to 13-14C at 1800 (Figs. E2b and E3b). The low at 500 mb moved slowly eastward during the day but kept the St. Louis area within its circulation (Figs. E2d and E3d).

The wind fields at the levels from the surface to 500 mb were searched for subsynoptic scale weather systems that could have initiated the showery weather that occurred over the St. Louis area about midday. None were identified as the flow at both 0600 and 1800 CST appeared to be generally undisturbed and anticyclonic over Missouri.

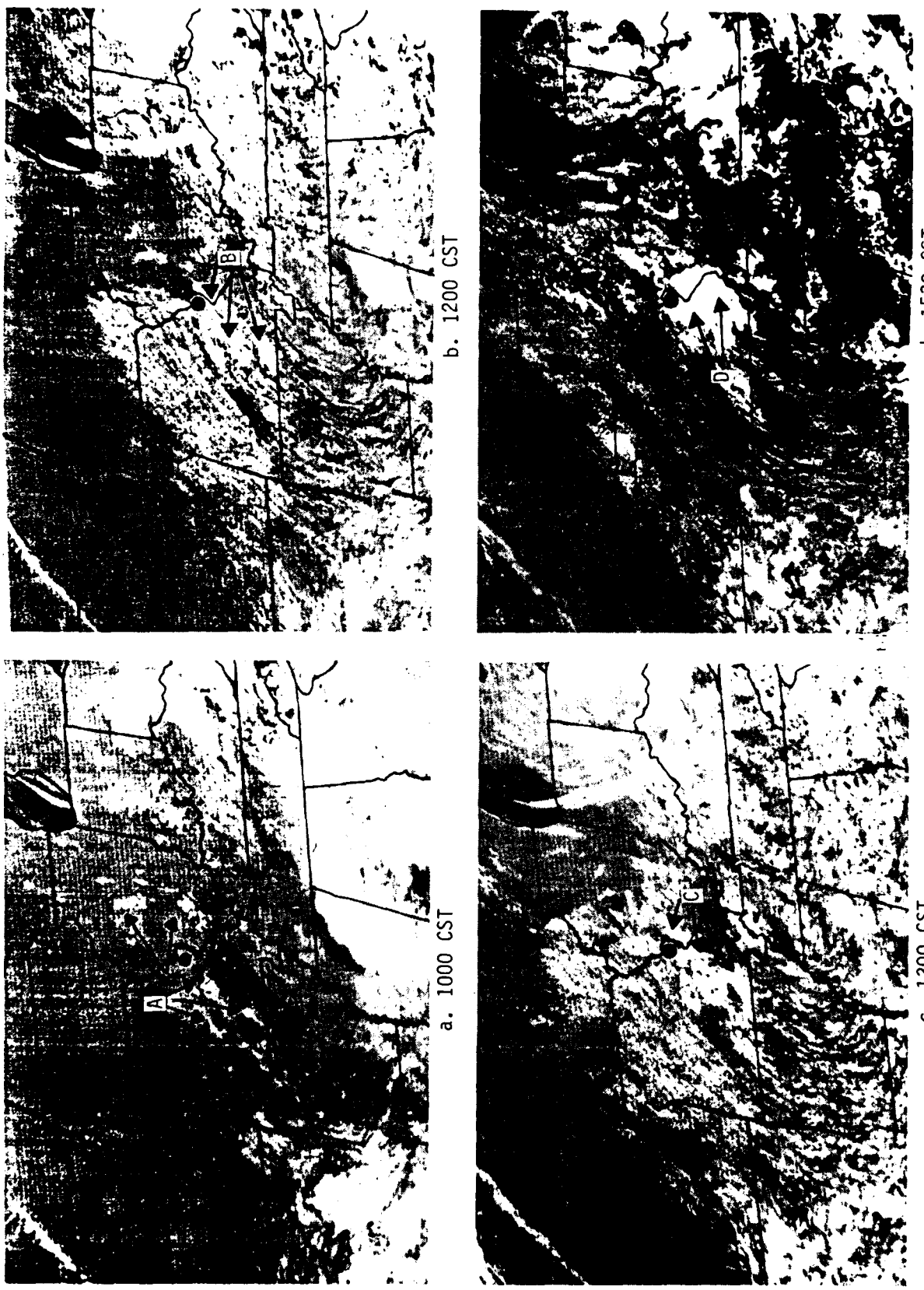

Figure E1. GOES satellite photographs of the Midwest on 17 July showing the evolution of deep cumulus clouds over southeastern Missouri. St. Louis area identified by black dot.

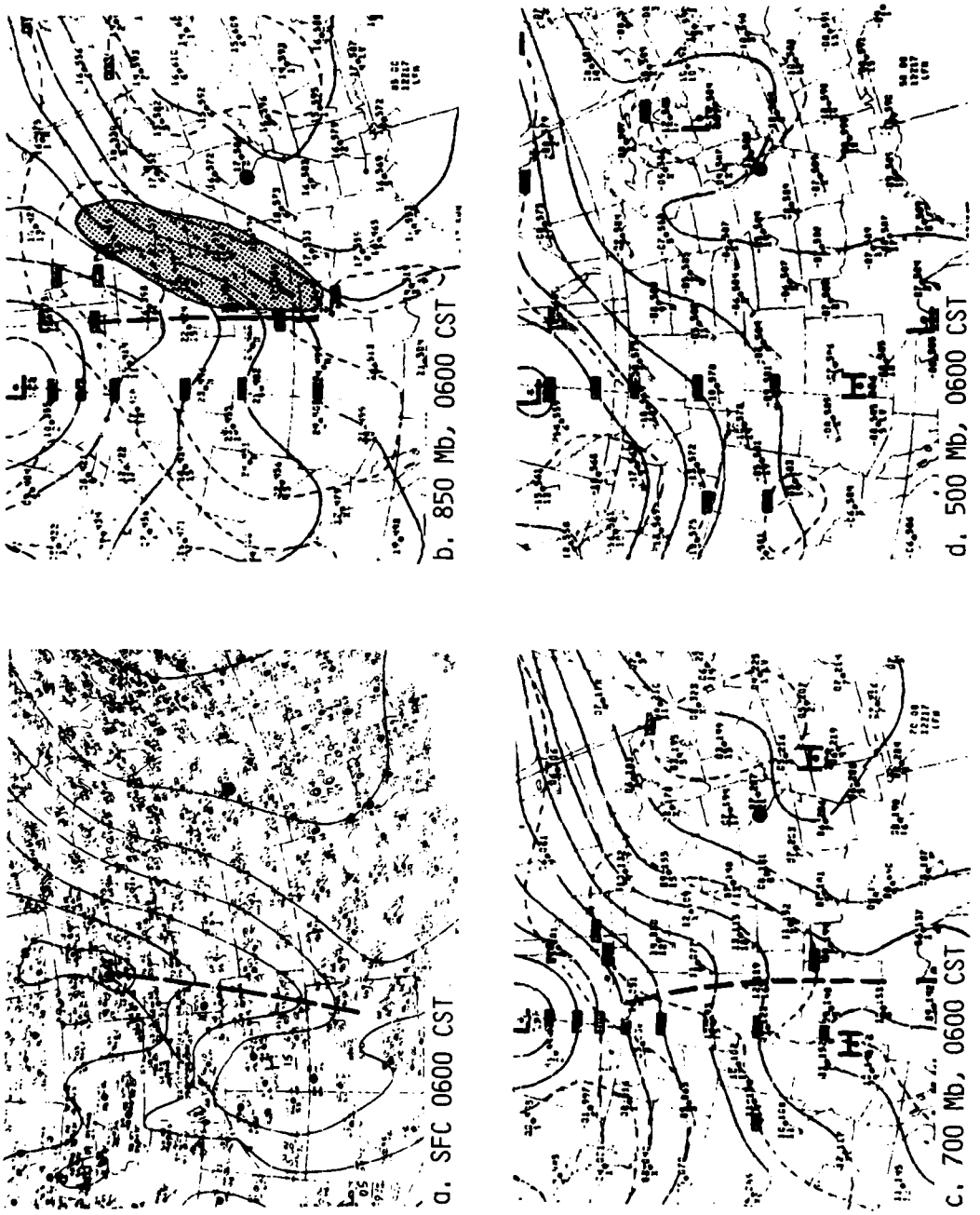

Figure E2. National Weather Service synoptic analyses for 0600 CST 17 July 1975. St. Louis area identified by black dot.

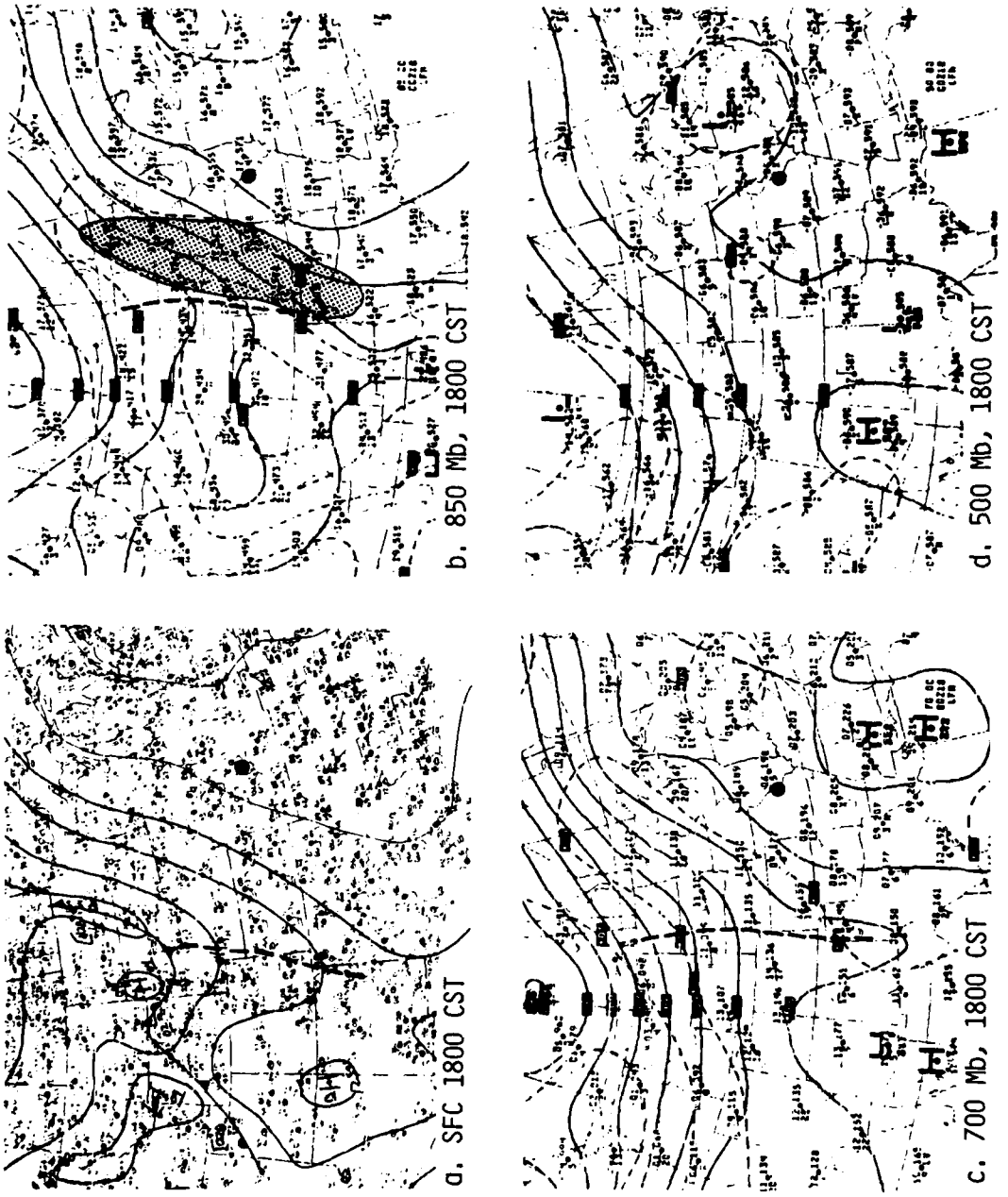

Figure E3. National Weather Service synoptic analyses for 1800 CST 17 July 1975. St. Louis area identified by black dot.

REGIONAL SCALE SITUATION

Hourly surface streamline and convergence analyses (Fig. E4) indicate that generally southwesterly flow was interrupted by a number of perturbations, some that apparently triggered showers and others that apparently were caused by the showers. Perhaps the most significant of these perturbations with regard to precipitation within the St. Louis network appeared over southern Missouri at about 0900 CST (arrow A) as a general zone of convergence with magnitude up to 0.3U. It developed as southerly flow over northern Arkansas and extreme southeastern Missouri converged into southwesterly flow over much of central Missouri. The convergence persisted through 1300 CST, sufficient time for significant deepening of the moist layers through regional scale ascent. The St. Louis area was at the northern edge of the convergence zone.

The satellite observation at 1000 CST (arrows A, Fig. E1) shows several lines of towering cumulus over southeastern Missouri within the area where the regional scale surface analysis identified the convergence zone. Further, the satellite observations also show that the showery area remained stationary over southeastern Missouri through 1500 CST. This is the location of the convergence center (arrow A, Fig. E4) which remained stationary through 1300 CST.

With southwesterly winds of 10 m sec^{-1} from near the surface to 3 km, moist air lifted within the convergence area in southern Missouri would likely have been carried over the St. Louis area. The K-index calculated from the 1025 CST radiosonde in St. Louis was 35.0, an indication that abundant moisture and considerable convective instability were present and therefore, a high potential existed for showers during the heated part of the day.

EVOLUTION OF DIVERGENCE AND RAINFALL

Figures E5a-E5c shows the time series for the the number of gridpoints reporting rainfall, the average 15-min rainfall for the gridpoints reporting rain and the network mean divergence. Weak network-scale convergence was present from midnight until 1215 CST when divergence increased in response to the outflows from heavy showers. The maximum pre-rain convergence was 0.5U at 1015 and 1115 CST. There were two peaks in the number of gridpoints with rain, (Fig. E5a) one occurring at 1400 CST (A) and other at 1630 CST (B). There were corresponding peaks in the mean divergence (Fig. E5c); the first, a two peaked maximum between 1300-1500 CST (A) and the second at 1630 CST (B). These peaks lagged the peaks in average rainfall by approximately half an hour (Fig. E5b). The network scale convergence reappeared after the shower related wind field disturbances subsided at about 1730 CST.

A possible 1.5 hr lead time in the network scale convergence before the onset of major convective activity is suggested by this time series. The time series of the point maximum rainfall (Fig. E5d) and the point maximum and minimum divergence (Figs. E5e and E5f) shows that the maximum convergence (minimum divergence) began exceeding the $\pm$3.0U background shortly after 1000 CST, about 1.5 h before the rain started. The point maximum convergence remained above the background for most of the period (A) during which heavy rain fell.

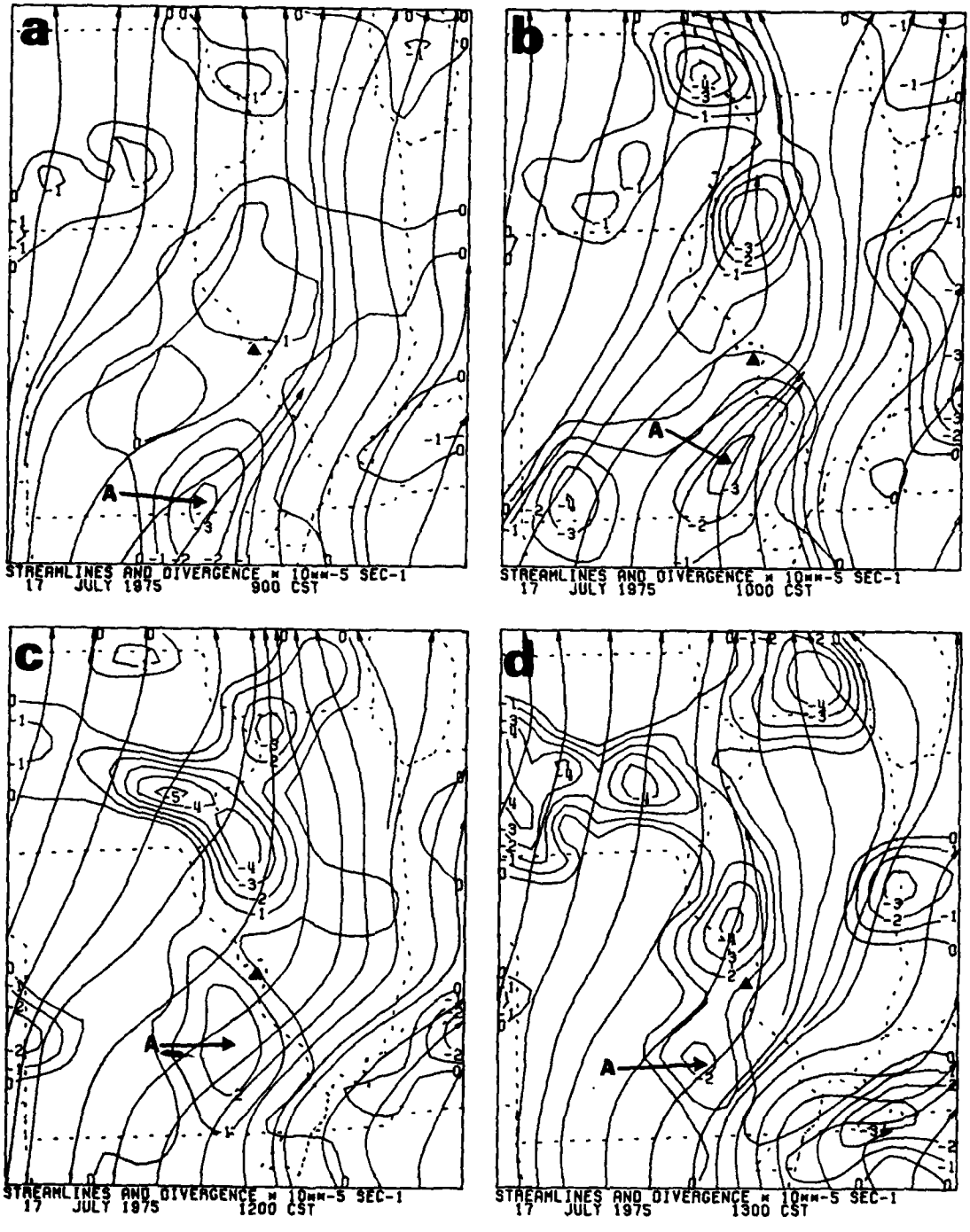

Figure E4. Regional scale analyses of surface wind field, 0900-1300 CST.

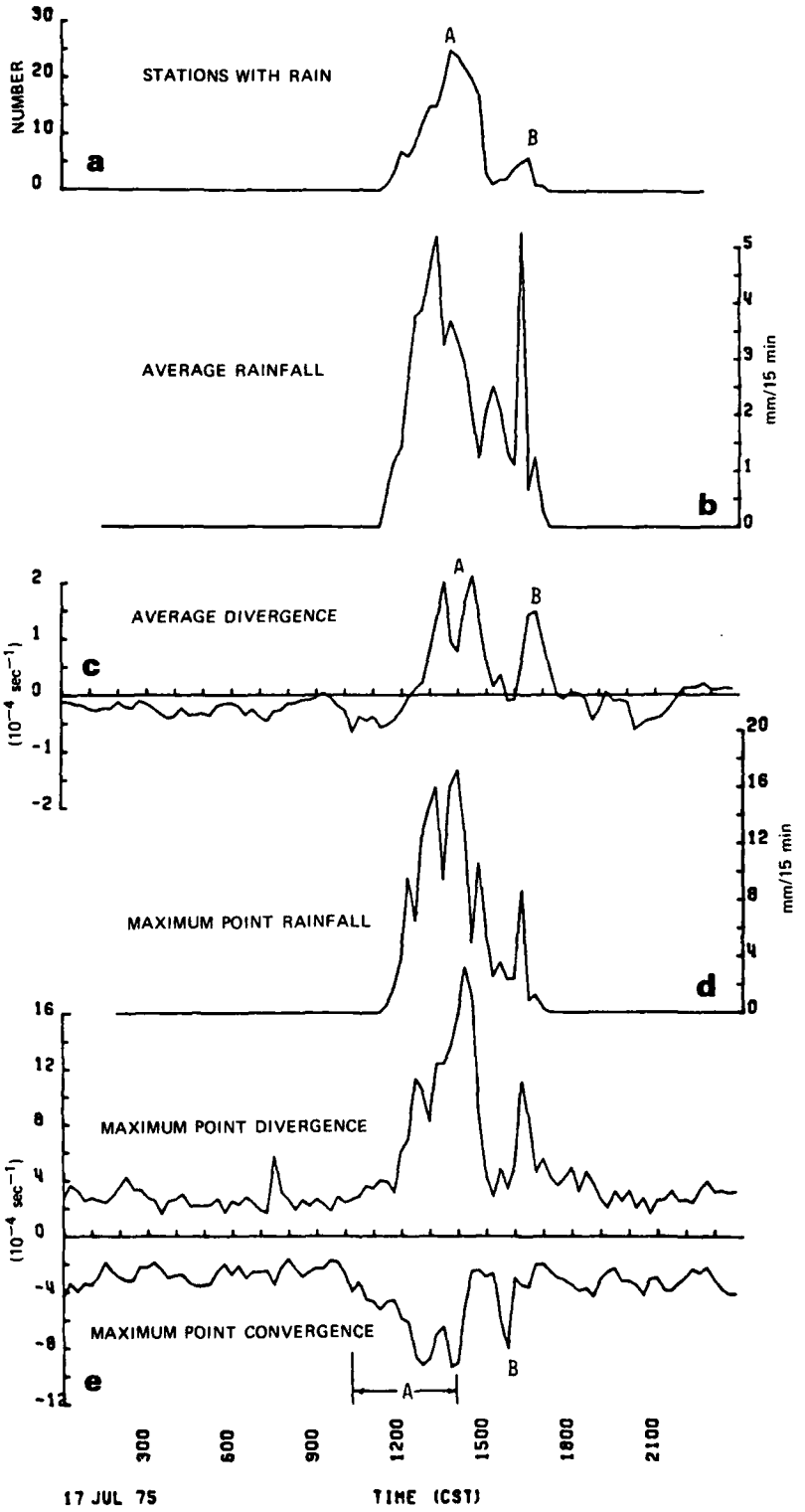

Figure E5. Time series of divergence and rainfall variables.

With the onset of heavy rainshowers, indicated by the increase in rainfall rates at 1200 CST (Fig. E5d), raincell scale outflows caused notable increases in the maximum convergence and these tended to peak out at approximately the same time as the maximum rainfall rates (Fig. E5f). For example, at 1245 and at 1345, there are peaks observed in both the rainfall amounts and in the maximum convergence. Convergence approached 9U.

The convergence initially within a mesoscale circulation (discussed in the next section) increased the convergence over the background to 4U-5U. Then shower outflows caused further increase to above 8U as winds associated with the strong outflow either interacted with other outflows or with the mesoscale convergence zone.

A secondary peak in the convergence at 1545 CST (B) preceded a peak in the rainfall at 1615 CST. But the analysis to follow will show that this convergence center occurred well away from the area in which rain fell. Thus, in some cases, it is necessary to consult the detailed spatial analyses in order to define the convergence rainfall relationship.

MESOSCALE SITUATION

Prior to 1030 CST, winds over the St. Louis network were generally southerly with speeds of 4 m sec^{-1} or less. Winds at sites in the west and northwest sections of St. Louis shifted to more westerly and caused a narrow convergence zone (dashed line, Fig. E6). The convergence zone persisted and increased in strength reaching 4U 5 km west of the Arch at 1100.

At 1115 showers formed over the larger METROMEX raingage network southwest of the wind field network (Fig. E7a). These showers developed northeastward along the probable extension of the convergence zone to reach the southwestern corner of the network at 1130 (Fig. E7b). Raincell A intensified to 6 mm/15-min at 1145 (Fig. E7c) and Cell B formed at the western edge of the network. The gust front from Cell A spread northeastward into the convergence zone and a 4U convergence center appeared at their intersection at 1145 and again at 1200 (Fig. E7d).

Cell C formed near the eastern end of the convergence zone in an area where southwesterly flow aloft would have carried moisture displaced vertically within the convergence zone. Its gust front pushed southwestward into the convergence zone (Fig. E7e) and increased the convergence to 6U. Meanwhile, Cell D formed 5 km west of the Arch at the intersection of the convergence zone and the northeastward moving gust front from cells A and B.

A complex gust front structure evolved from the outflows from the new raincells (Fig. E7f). Cell E formed along the Cell A gust front and its gust front pushed northeastward onto the network. Cell F formed within the 6U convergence center at 1215 (Fig. E7e) and was collocated with an 8U convergence center formed by the intersection of Cell C and Cell D gust fronts at 1230 (Fig. E7f).

Cell G merged with Cells C, D, and F to develop a complex which produced 10U surface divergence about 10 km north of the Arch (Fig. E7g). Its eastward

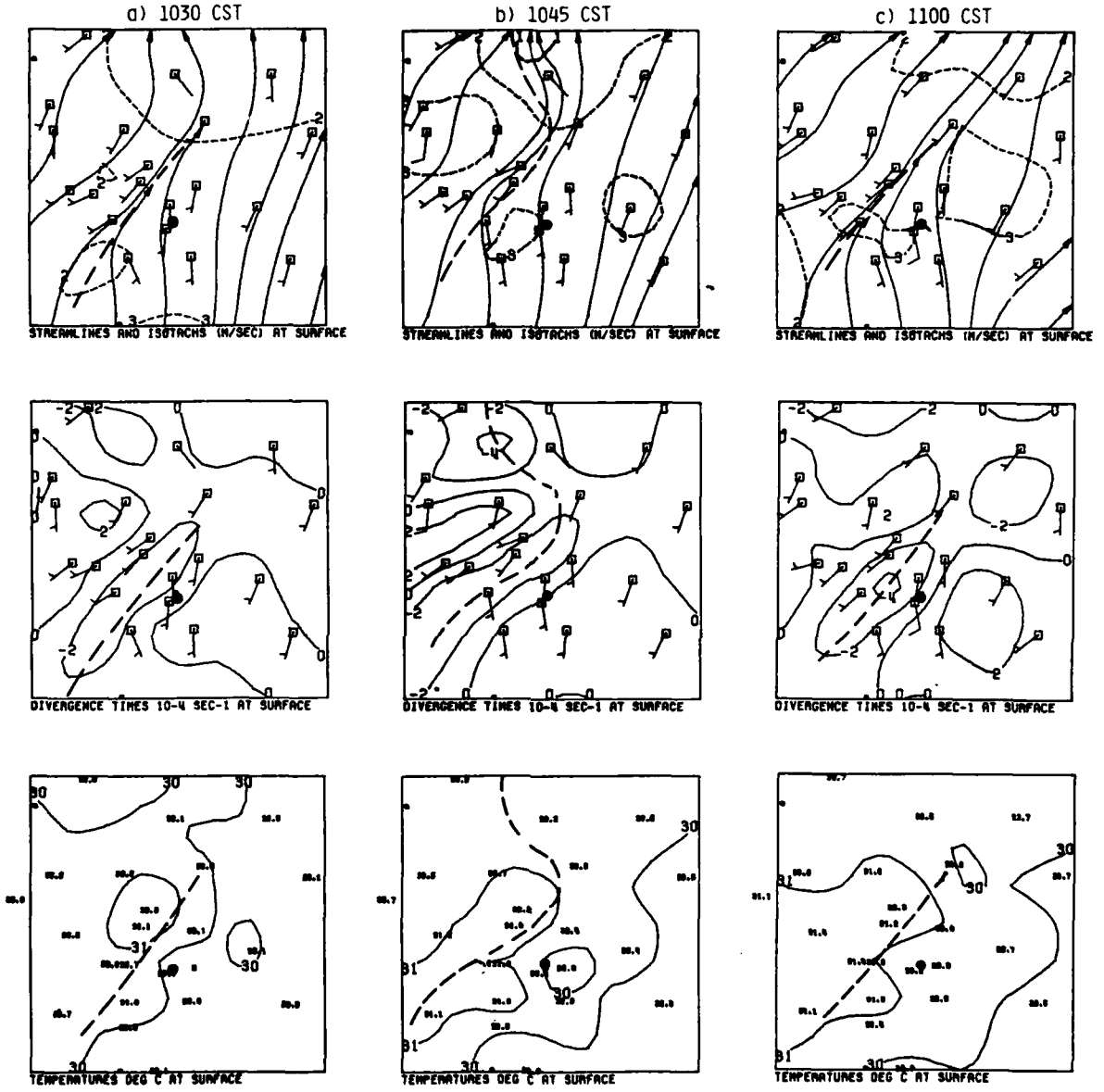

Figure E6. Composite of the objective wind field isotachs and streamlines (upper maps), divergence (middle maps), and temperature (lower maps) for 1030-1100 CST. St. Louis Arch identified by black dot.

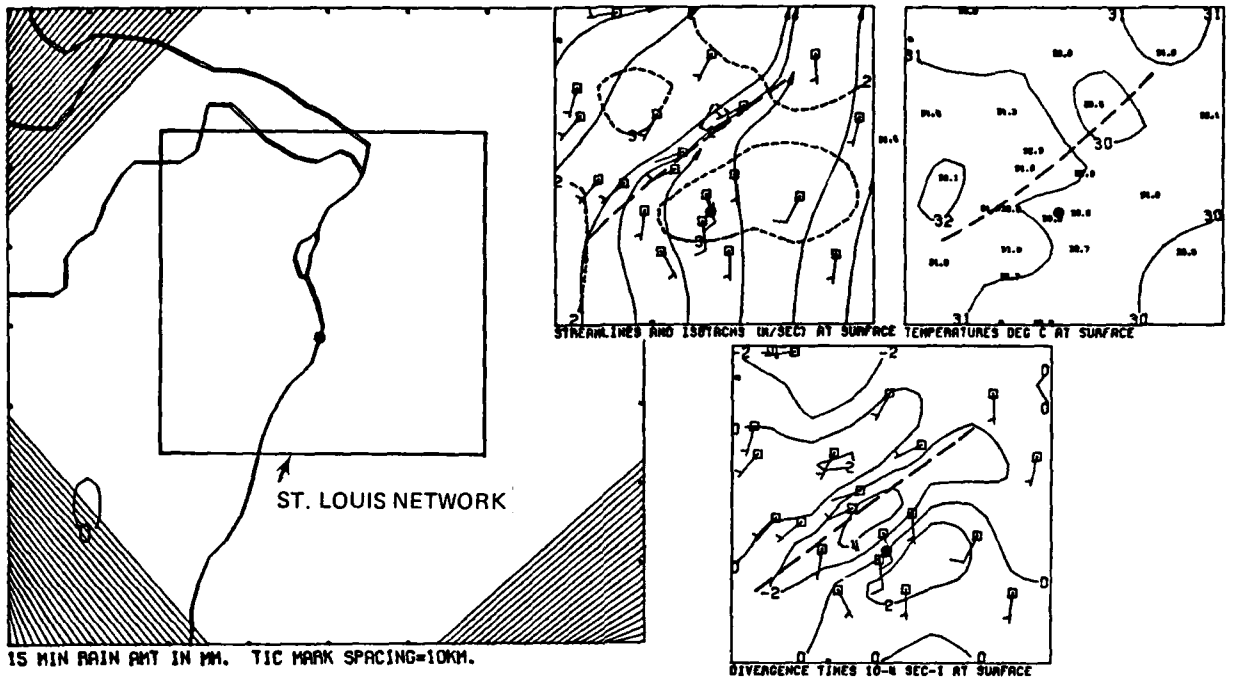

a. 1115 CST

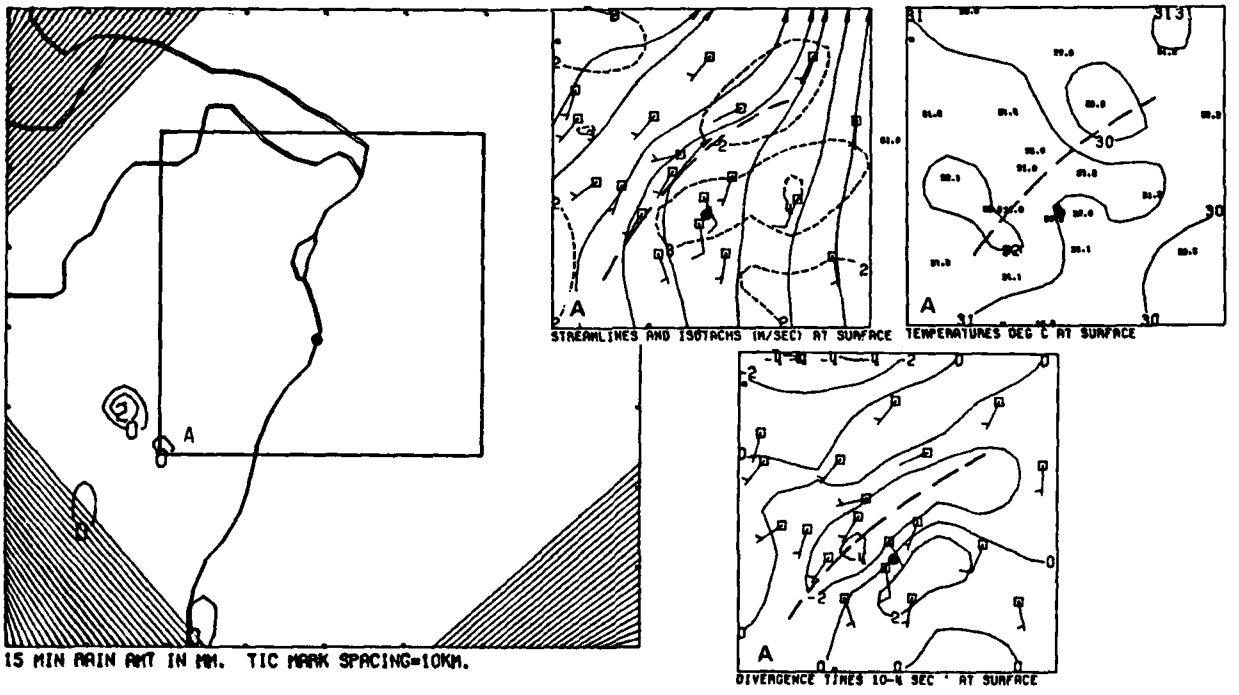

b. 1130 CST

Figure E7. Composite of the objective isotachs and streamlines, temperature, divergence and rainfall for 1115-1445 CST.

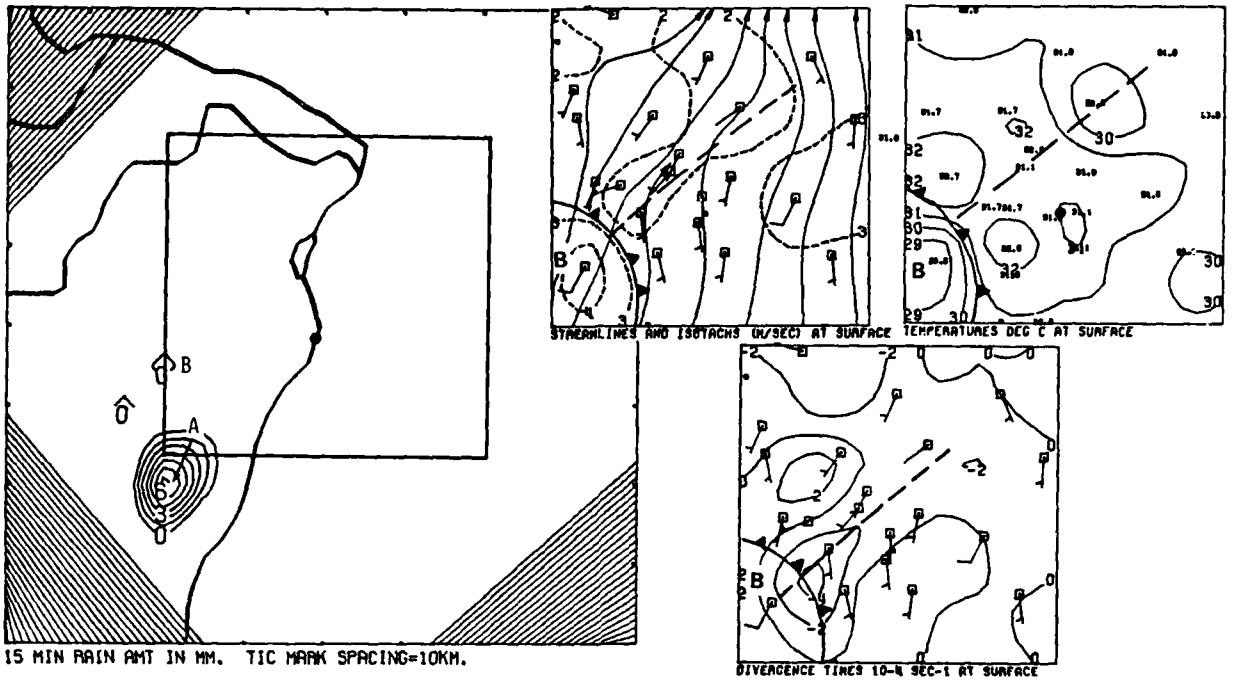

c. 1145 CST

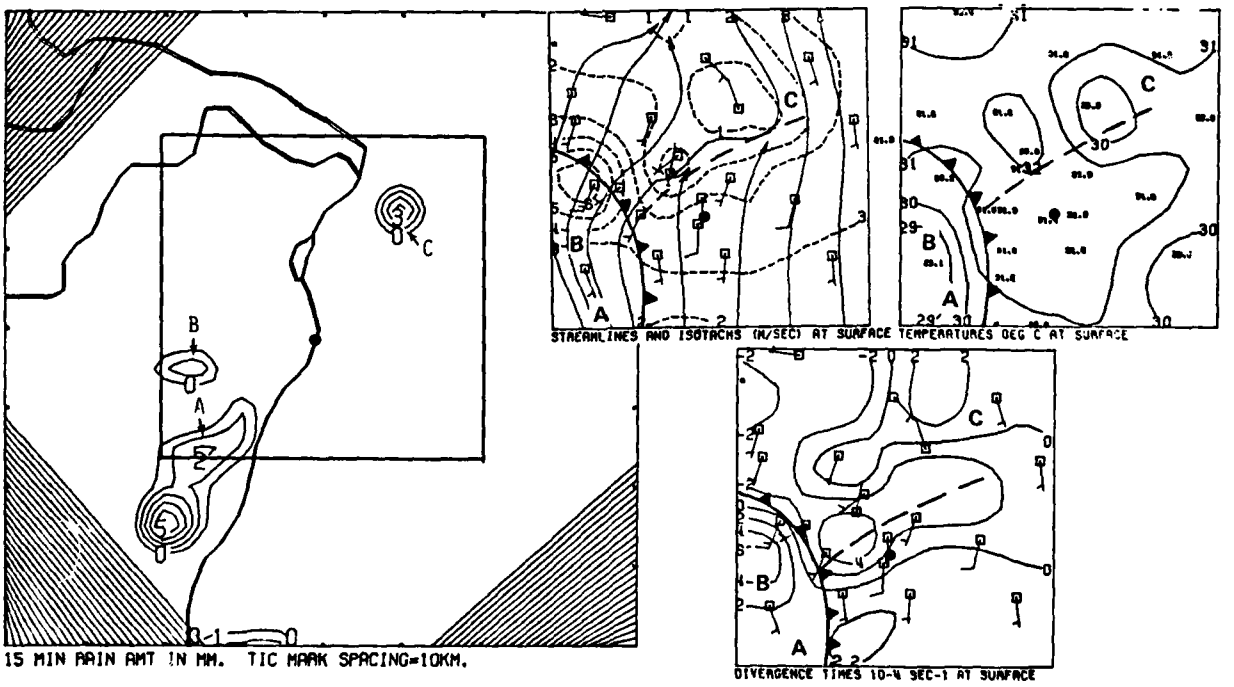

d. 1200 CST

Figure E7. Continued

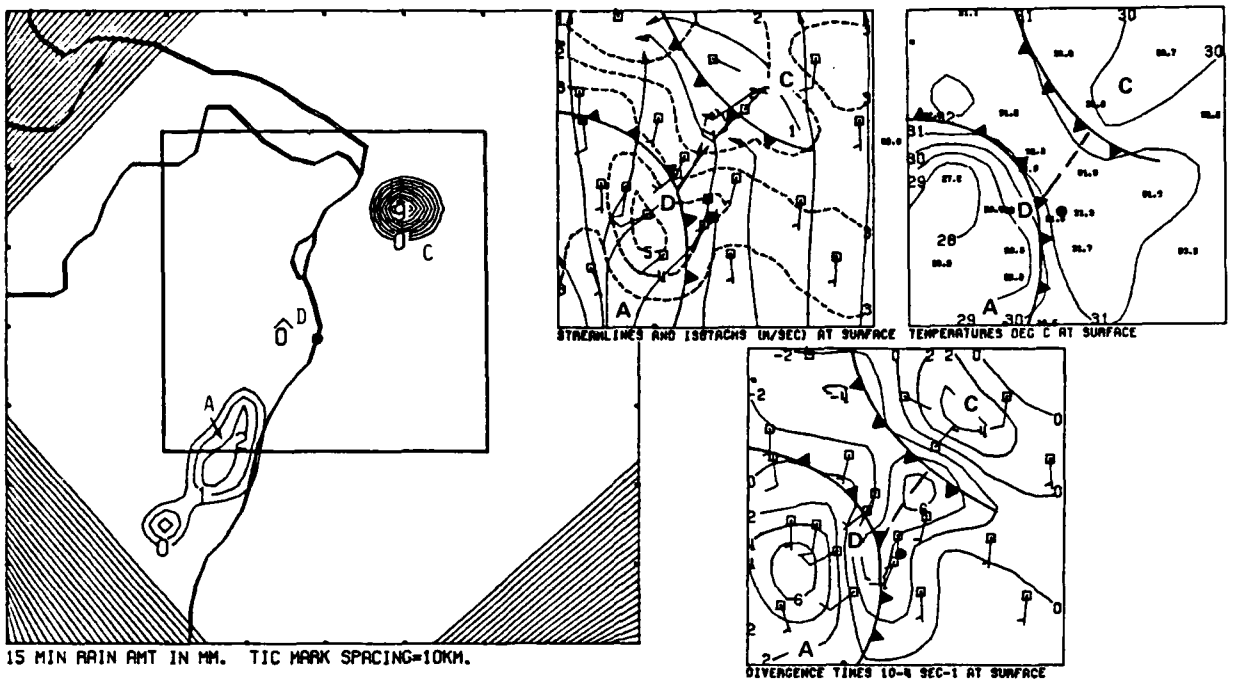

e. 1215 CST

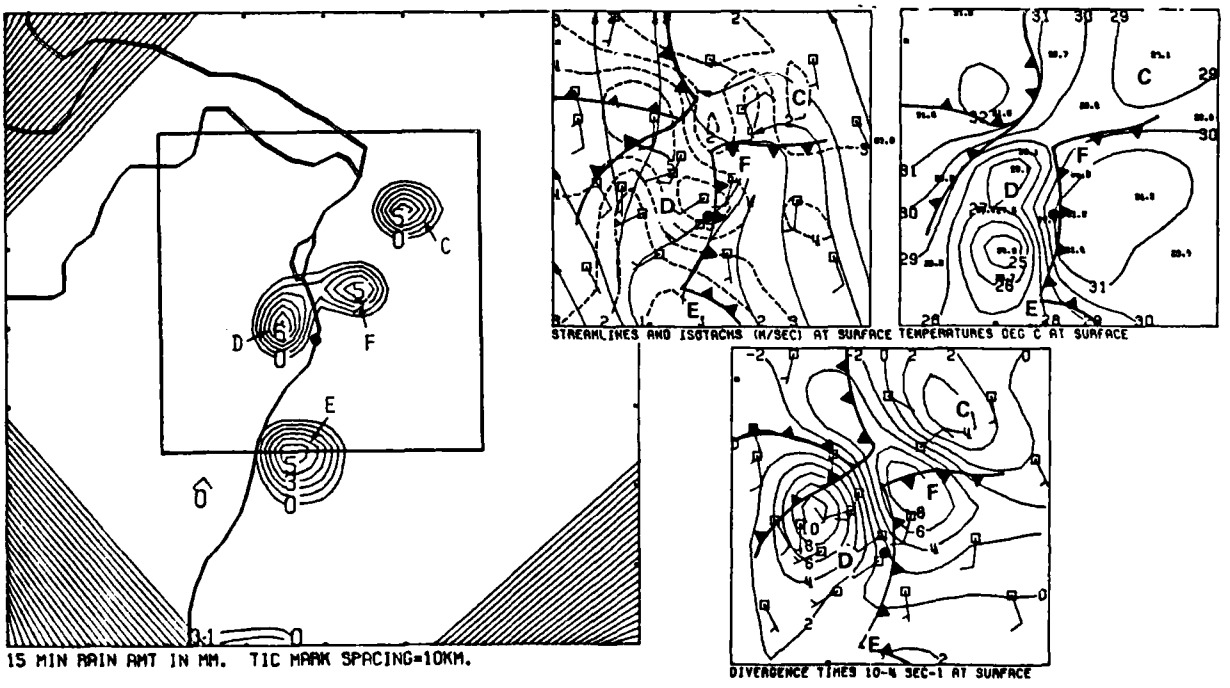

f. 1230 CST

Figure E7. Continued

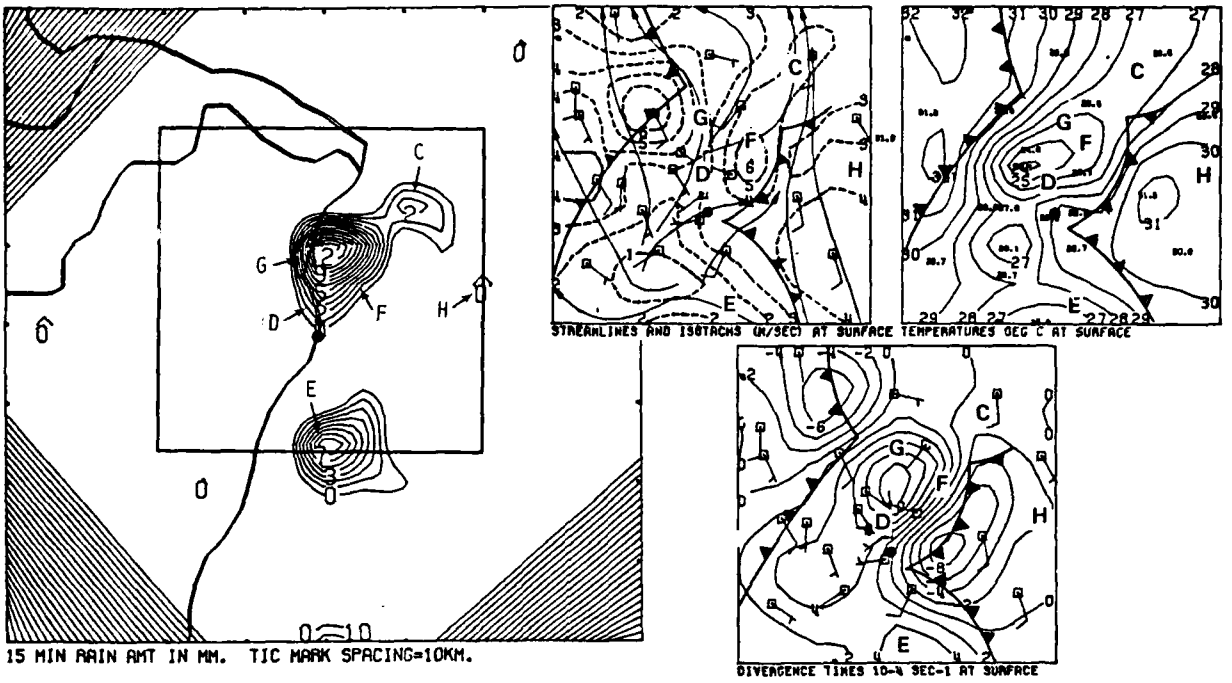

g. 1245 CST

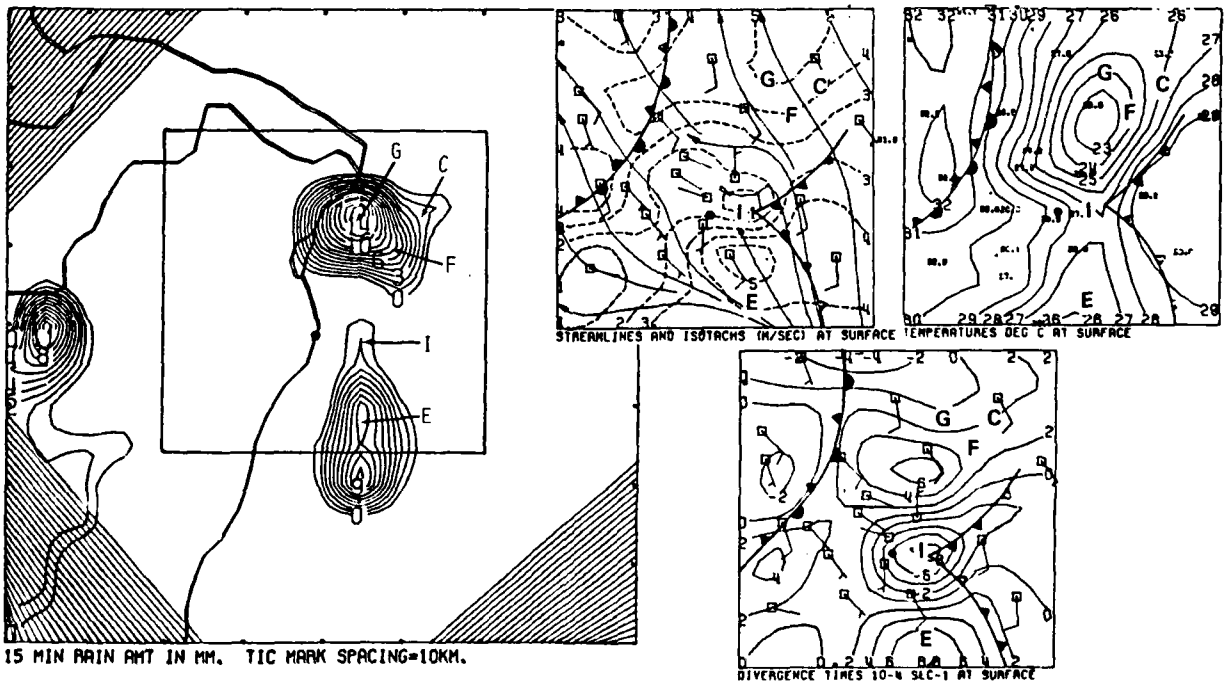

h. 1300 CST

Figure E7. Continued

AD-A093 795 ILLINOIS STATE WATER SURVEY URBANA F/G 4/2
BOUNDARY LAYER STRUCTURE AND ITS RELATION TO PRECIPITATION OVER--ETC(U)
OCT 80 G L ACHTEMEIER NSF-ATM78-08865
UNCLASSIFIED SWS-CR-241 ARO-15529.4-GS NL

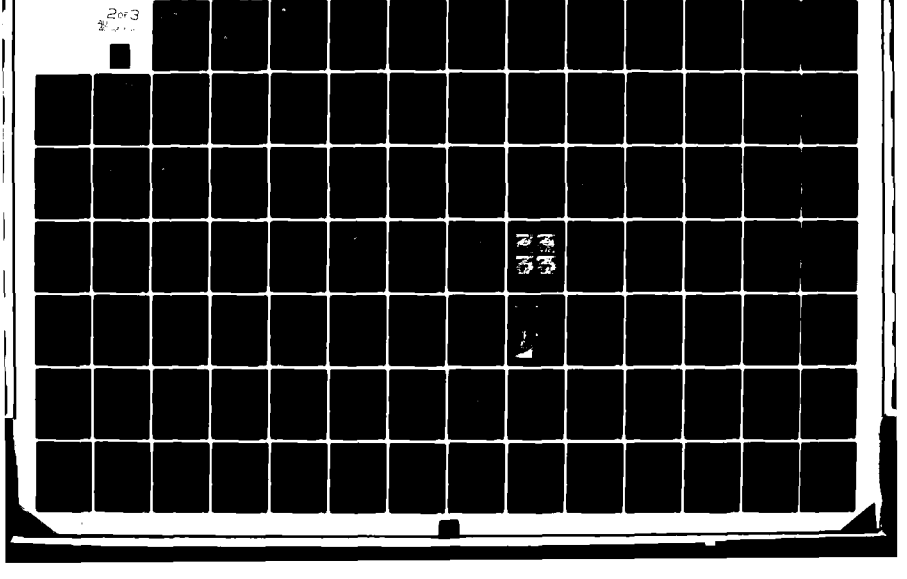

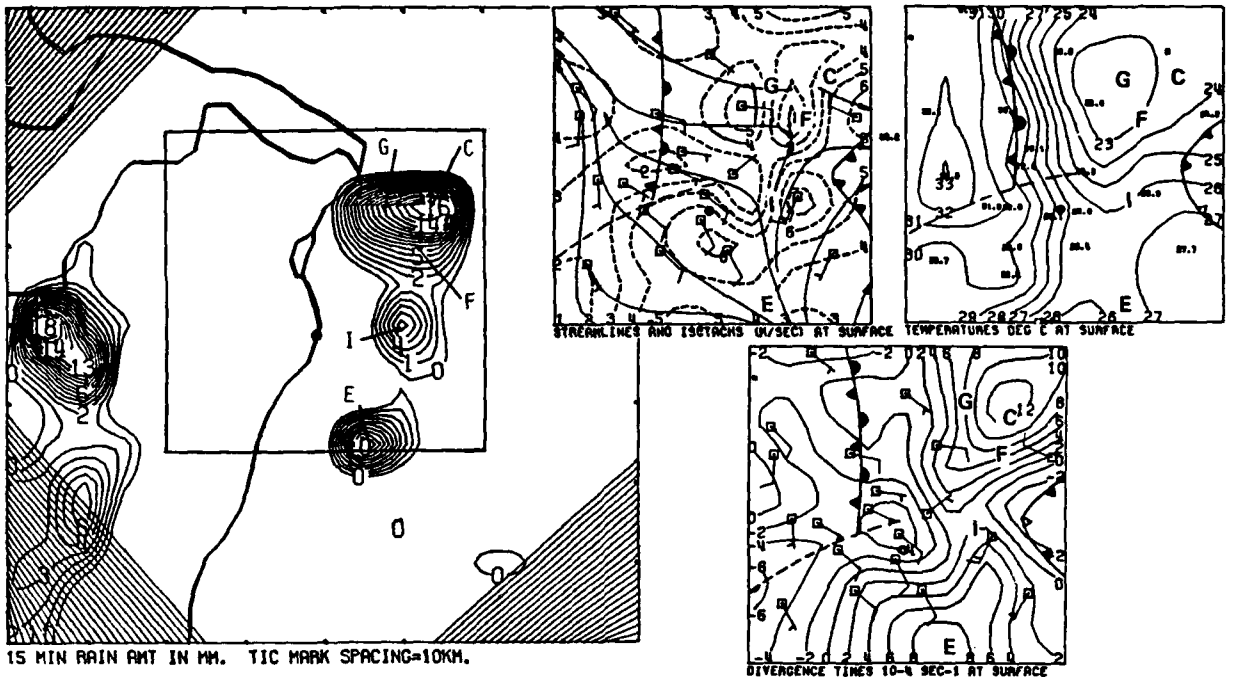

i. 1315 CST

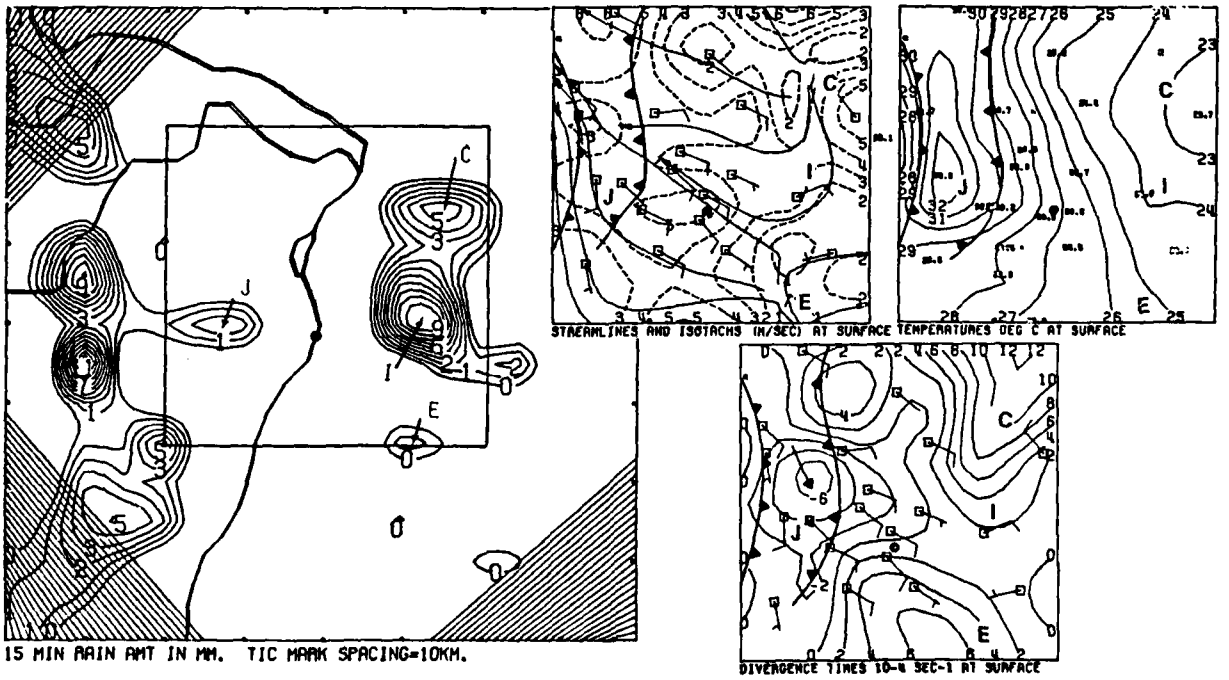

j. 1330 CST

Figure E7. Continued

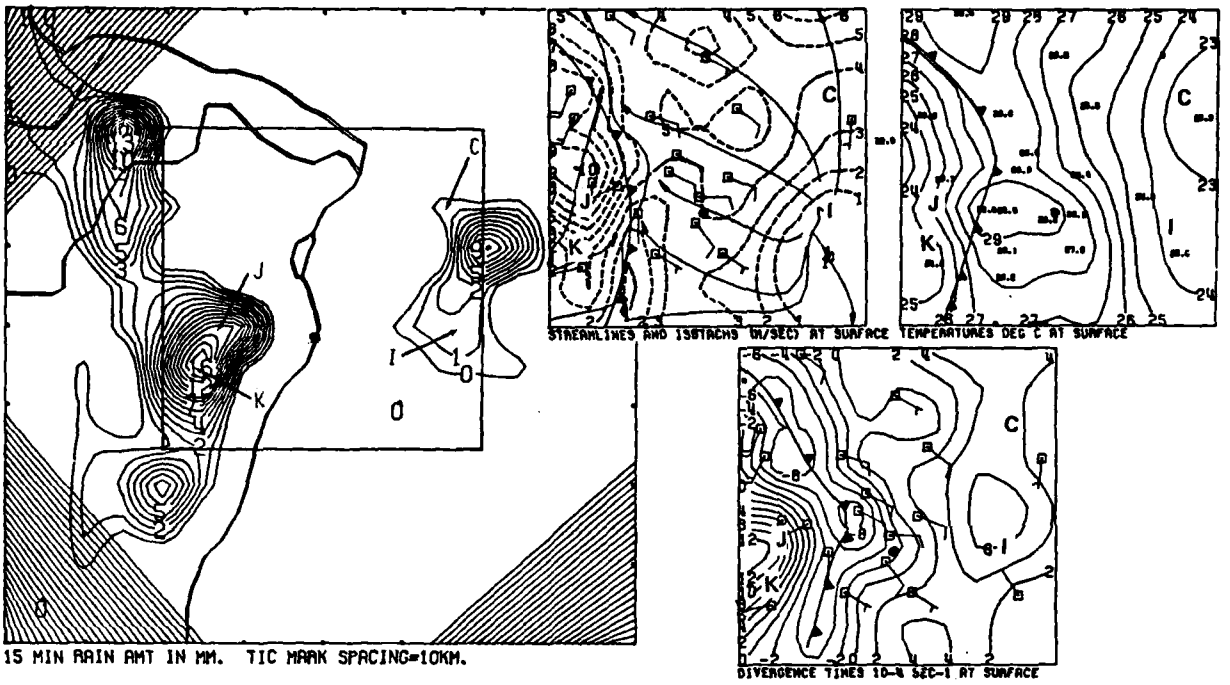

k. 1345 CST

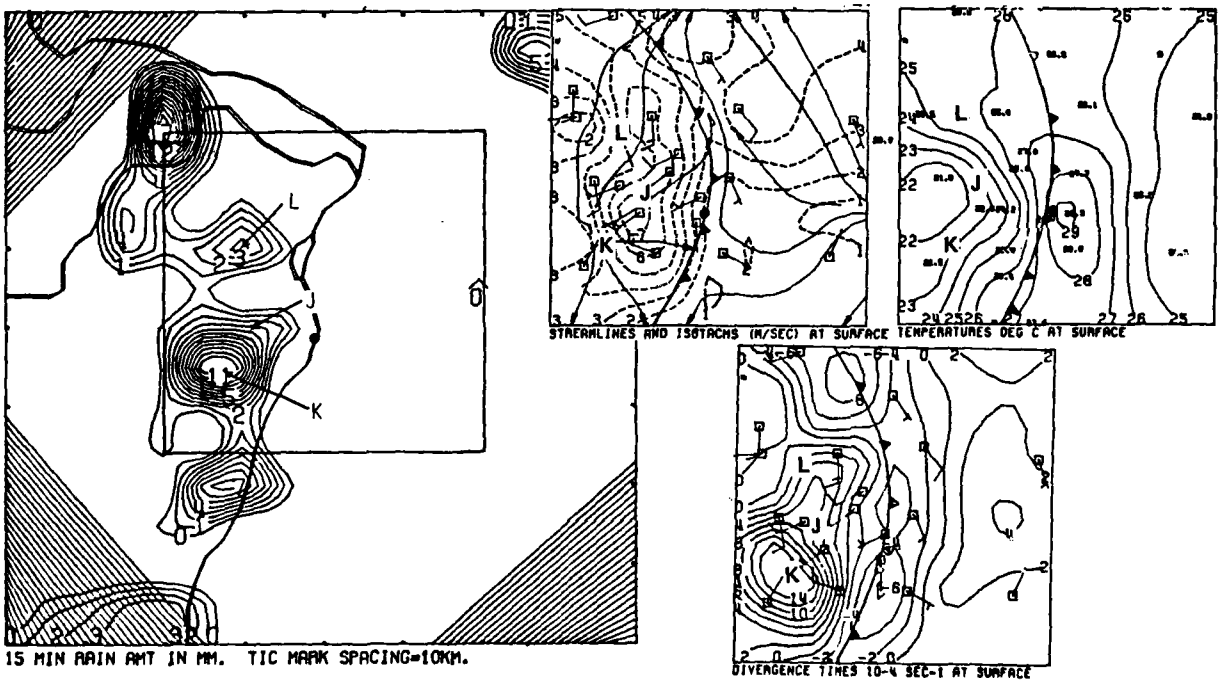

l. 1400 CST

Figure E7. Continued

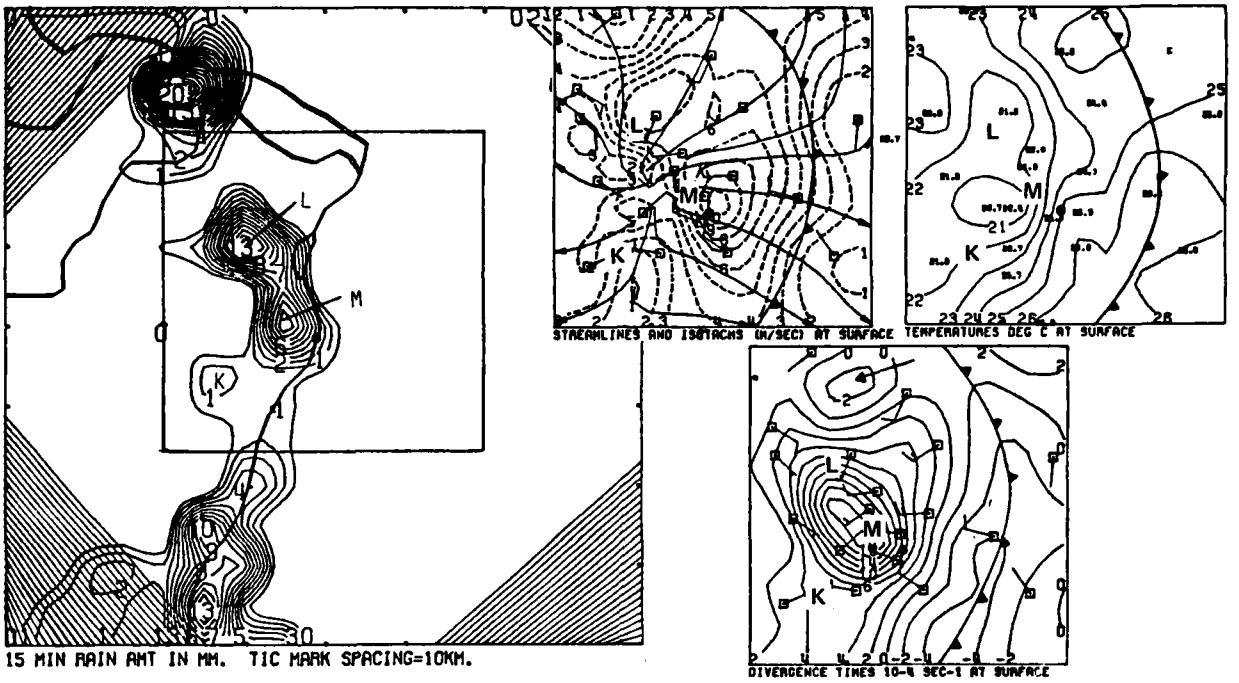

m. 1415 CST

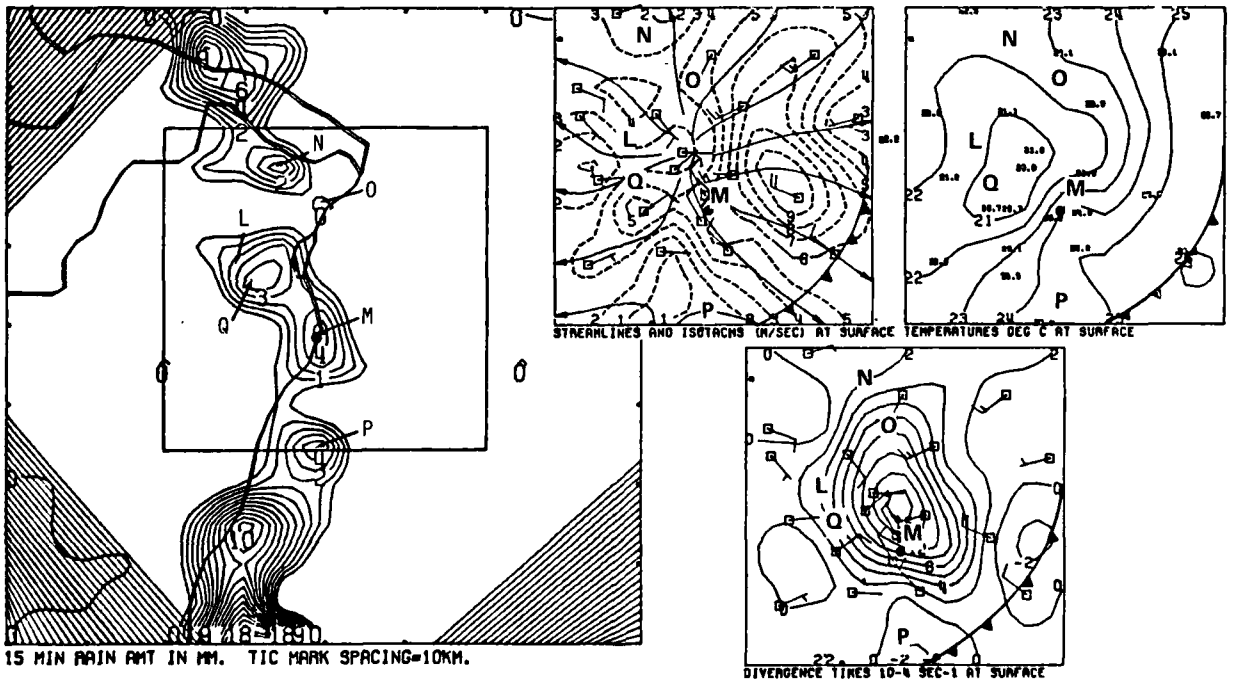

n. 1430 CST

Figure E7. Continued

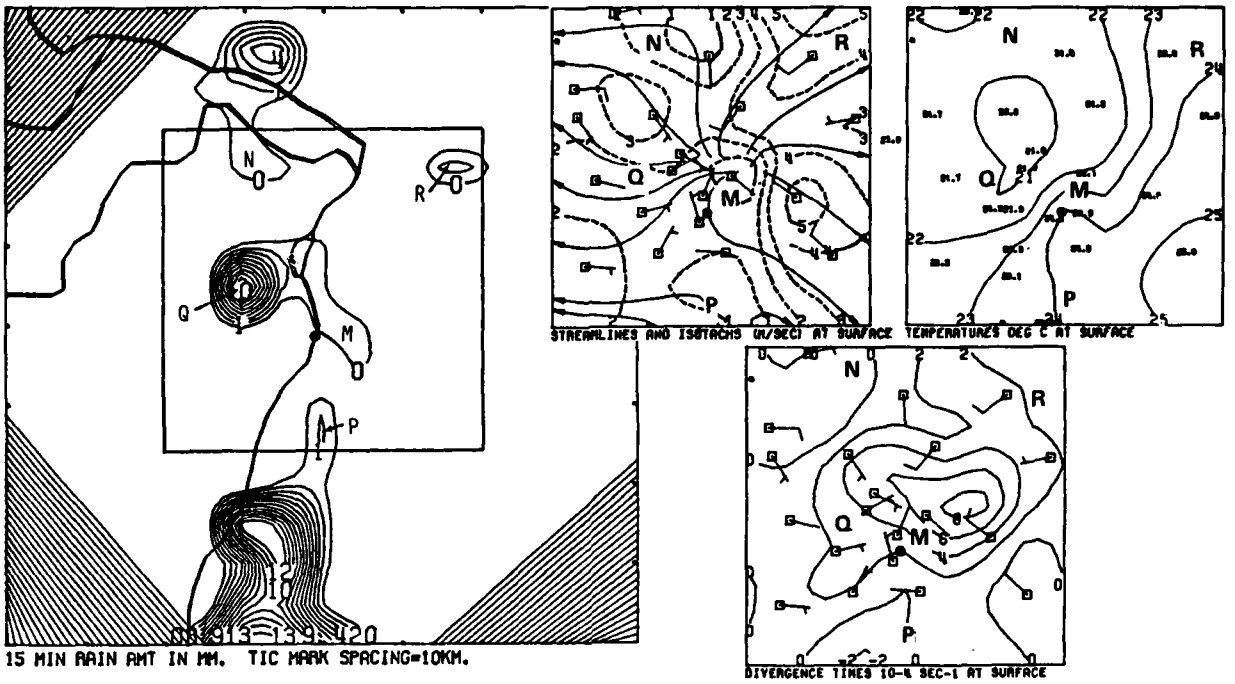

o. 1445 CST

Figure E7. Concluded

moving gust front intersected Cell E's northeastward moving gust front to produce an 8U convergence center 10 km east of the Arch. Cell H was a light shower which formed within a 2U convergence area at 1230 (Fig. E7f).

Cell I (Fig. E7h) developed at the intersection of the cell complex C, D, and F gust front with the Cell E gust front. The five cells (C, E, F, G, and I) formed a broken line of heavy raincells that moved slowly eastward and dissipated at the eastern boundary of the network by 1400 leaving the eastern two thirds of the network within a rain cooled airmass, 8-10C colder than the airmass outside the rainy area.

Meanwhile, a line of strong raincells moved onto the western edge of the METROMEX network at 1300 (Fig. E7h). Unlike the raincells that formed over the city, these cell were organized into a squall line which propogated eastward by the formation of new cells along its leading edge (Fig. E7i and E7j).

Beginning at 1230 (Fig. E7f), temperatures over the western third of the network increased, reaching pre-rain levels by 1315 (Fig. E7i). A convergence zone (dashed line) extended from near the Arch southwestward through the warm areas toward the squall line. Convergence reached 6U at the western edge of the network.

The intensification of the outflow from cells, C, E, and I pushed the rain cooled air westward as the gust front in advance of the squall line pushed in from the west (Fig. E7j). Cell J developed near a 6U convergence center (arrow) located in the warm airmass between the two gust fronts. Cell K formed along the squall line which at 1345 had merged with the outflow from the eastern storms to produce a convergence zone with several centers exceeding 8U (Fig. E7k). Cell L (Fig. E7l) appeared in an area where moderate to strong convergence had persisted for 45-min prior to gust front passage. Cell M (Fig. E7m) developed along the gust front near the 8U convergence center at 1345 (Fig. E7k). Meanwhile, a 2U convergence area (arrow) persisted some 15 km behind the gust front near the network's northern boundary. Cell N developed within this convergence area at 1430 (Fig. E7n) and minor Cells O and P formed upon the passage of the gust front.

Convergences along the gust front decreased to 4U as the gust front decelerated within the rain cooled airmasses from the storm complex that preceded it. Cell Q developed over strongly divergent surface flow adjacent to cell L (Fig. E7o) and Cell R formed as the gust front pushed through the northeastern part of the St. Louis network.

Divergence generally prevailed from 1500-1530 as the network was within rain cooled air produced by the squall line outflow. All raincells except Cell Q dissipated. By 1530 (Fig. E8a) new raincells moved onto the larger METROMEX raingage network west of the wind field network. Southerly winds had returned to the west and south parts of the network and developed two convergence areas (arrows), one a 6U center along the confluence between the southerly flow and an airmass with light and variable winds, and the other, a 2U center within the southerly flow along the western part of the grid.

The 6U convergence center to the east weakened as southerly flow increased over the northeastern part of the grid (Fig. E8b). The western center increased to 6U in advance of a strong raincell west of the network. A

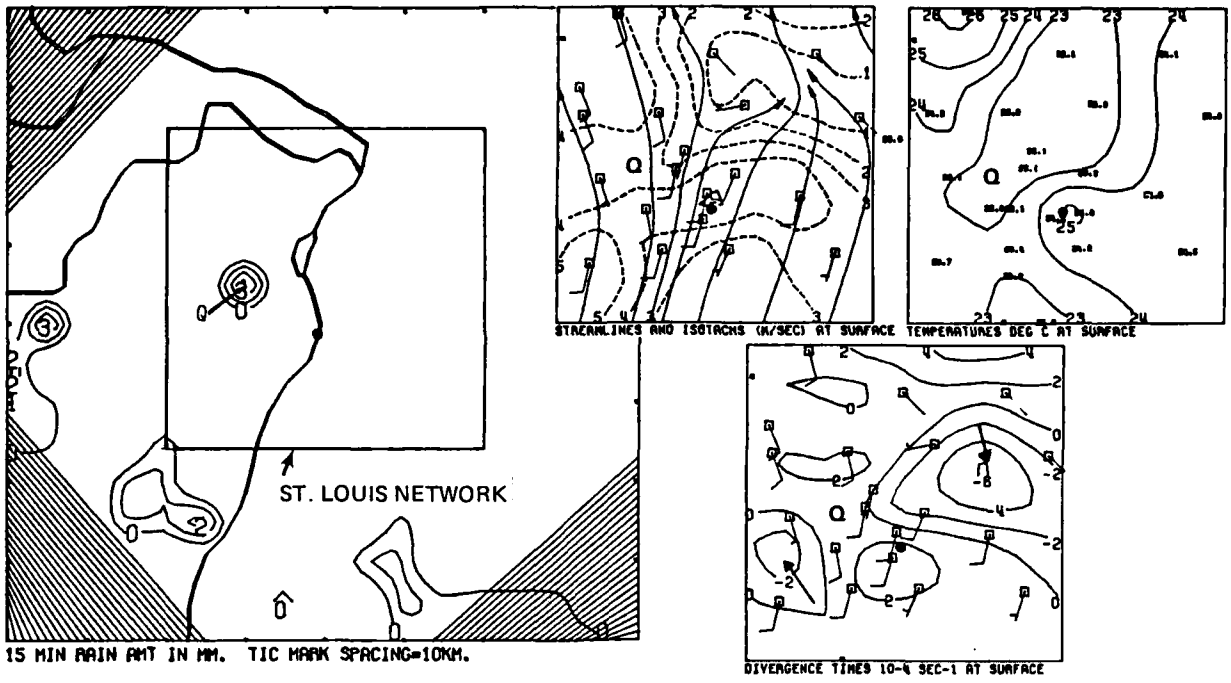

a. 1530 CST

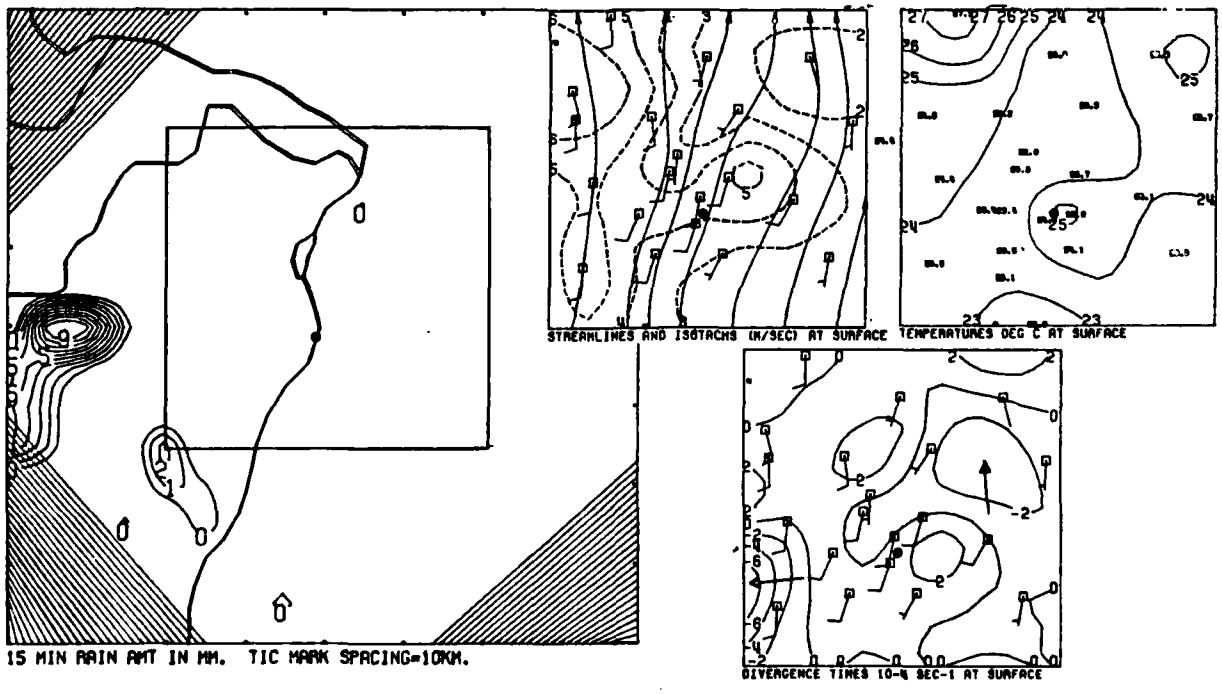

b. 1545 CST

Figure E8. Composite of the objective isotachs and streamlines, temperature, divergence and rainfall for 1530-1630 CST.

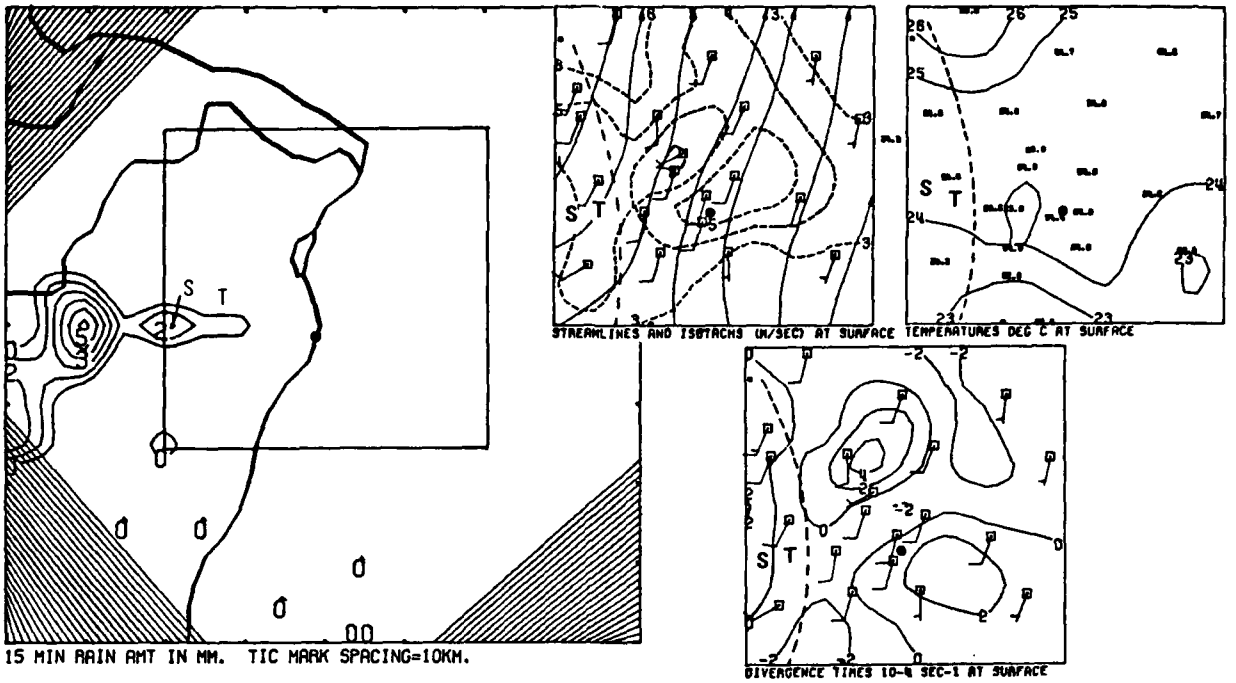

c. 1600 CST

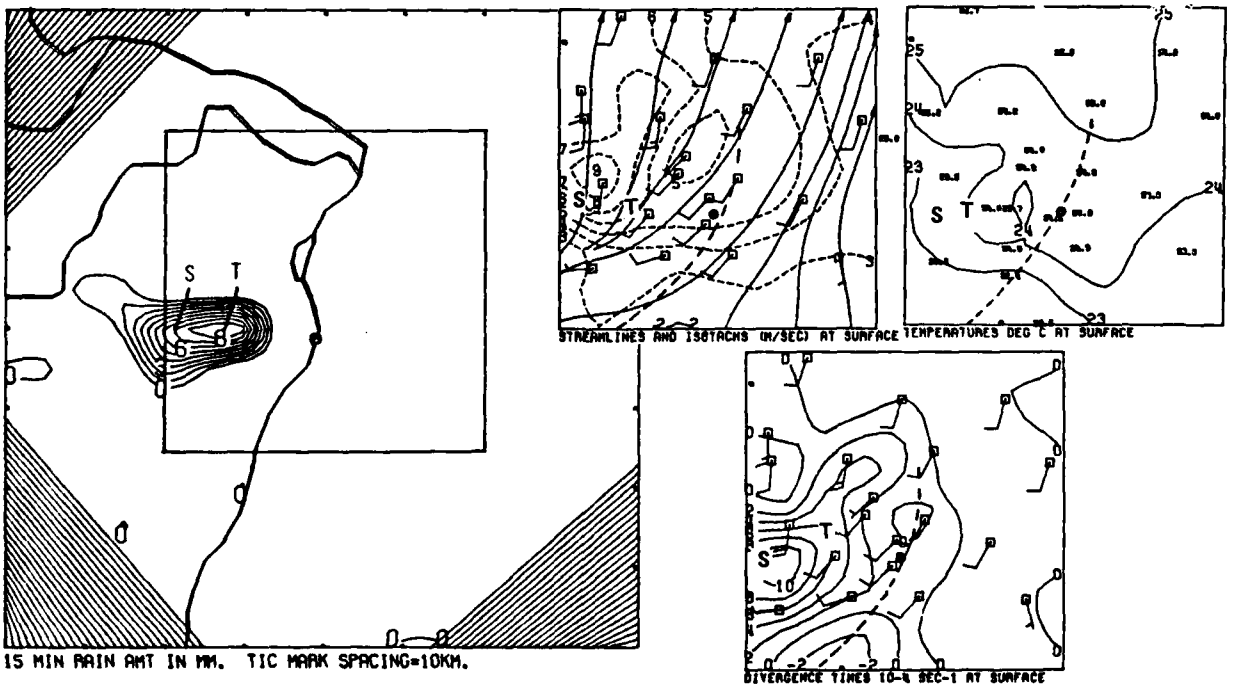

d. 1615 CST

Figure E8. Continued

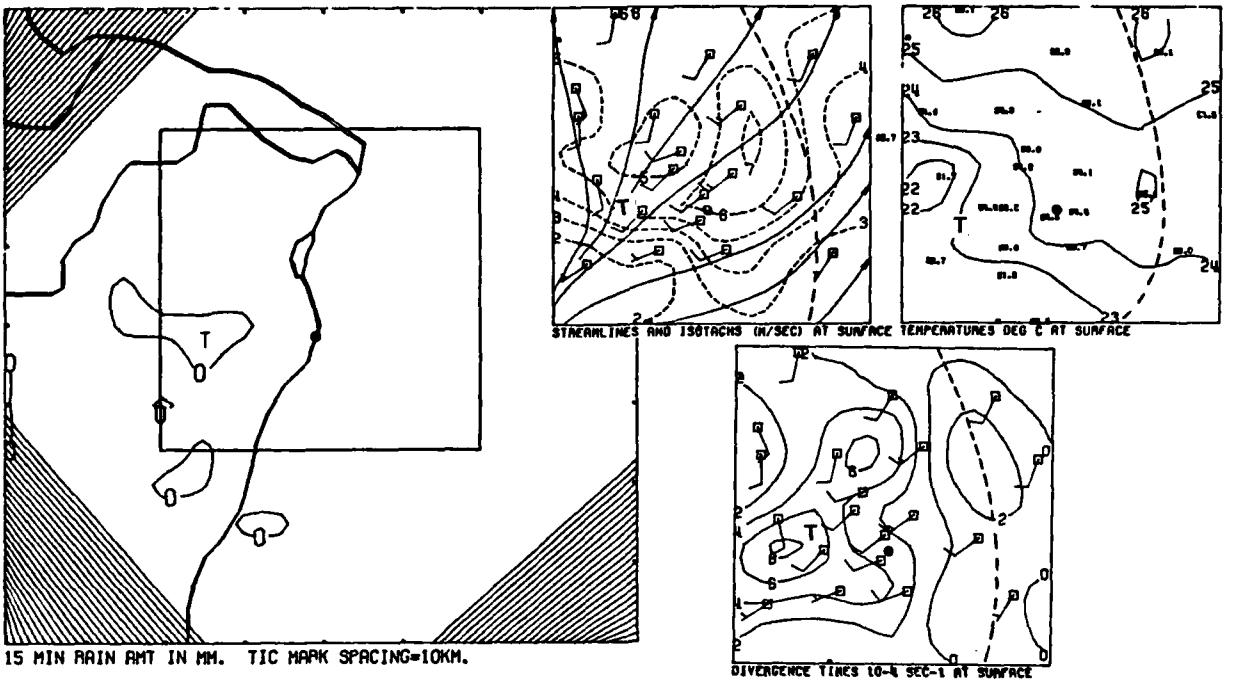

e. 1630 CST

Figure E8. Concluded

windshift line (dashed line, Fig. E8c) entered onto the network at 1600. Cells S and T formed along the windshift line in the vicinity of the 6U convergence center at 1545 (Fig. E8b). This complex developed strong outflow that pushed the convergence zone to the central part of the network (Fig. E8d) and then rapidly northeastward (Fig. E8e) with no new raincell development.

SUMMARY OF SHOWER DEVELOPMENTS ON 17 JULY

Rainshowers developed over southeastern Missouri in response to a regional scale convergence zone that developed at the interface between southerly flow out of Arkansas with southwesterly flow over central Missouri and to increasing convective instability as warm moist air at 850 mb was advected beneath a cold-core cyclone at mid-levels. Upward vertical displacement of these convectively unstable airmasses during the heated part of the day was sufficient to release the convective instability over parts of eastern Missouri including the St. Louis network.

The development of a mesoscale convergence zone over the St. Louis network caused inflow into the network to commence at 1030. The network scale convergence persisted for 1.5 hr until divergence was established by outflows from showers.

Raincell development over the St. Louis network was apparently highly dependent upon surface heating and surface convergence. Raincells formed persistently at the intersections of gust fronts or at gust front intersections with convergence zones. Twenty raincells developed over or sufficiently near the network to influence the wind field. Fifteen cells formed within the network making the 17th an ideal day for the study of the rainfall-convergence relationships.

Table E1 summarizes the cell strengths, convergence strengths, and convergence durations for the raincells that developed within the St. Louis network on 17 July. The majority of the cells ranked as moderate to strong in strength when compared with cell strengths for the other days in the case study. Convergence strengths were also moderate to strong.

Thirteen of the fifteen raincells that formed over the St. Louis network were preceded by convergence centers for periods up to 105-min. Cell strengths ranged from 0.5 to 38.0 mm. The average cell strength was 15.4 mm, the average convergence strength was 8.9U, and the average convergence duration was 36-min. Five convergence centers not associated with raincell development had strengths and durations of, respectively, 2U (15-min), 4U (15-min), 10U (45-min), and 22U (105-min).

The spatial relationship between the convergence centers and the raincells was quite good for the 17th. Convergence preceded raincells by 30-min or greater for 10 of the 15 raincells. This along with the finding of only five "false alarm" convergence centers is suggestive of a fairly good predictive relationship.

There was no apparent relationship between cell strength and convergence strength. Minor Cells H, O, R and Cells Q, T (developed after the network was covered with rain cooled airmasses) were the only cells with convergence

strengths less than 5U and convergence duration 15-min or less. A one-to-one correspondence between cell strength and convergence strength was not apparent for the remainder of the raincells.

Table E1. Cell Strengths, Convergence Strengths, and Convergence Durations for Raincells that formed within the St. Louis Network on 17 July.

Cell ID	Cell Strength	Convergence Strength	Convergence Duration
C	38.0mm	5U	45 min
D	9.5	22	105
F	27.0	17	90
G	38.0	8	30
H	0.5	2	15
I	8.0	20	45
J	19.0	8	30
K	28.0	8	30
L	19.0	14	45
M	12.5	12	30
N	4.5	12	45
O	0.5	4	15
Q	16.0	0	0
R	1.5	0	0
T	9.0	2	15

F. CASE STUDY: 18 JULY 1975

SYNOPTIC SITUATION

The synoptic situation on the 18th was a continuation of the slow eastward movement of the short wave trough out of the High Plains (Fig. F1). While the southern part of the trough remained stationary, the northern part and its associated surface frontal system had moved over Minnesota by 1800 CST (Fig. F 2). Showers accompanied the surface frontal system but remained over parts of Nebraska, Iowa, and Wisconsin far to the north and northwest of St. Louis.

The circulation aloft over the central Midwest was controlled by an anticyclone over the northern Gulf of Mexico. The flow from 850-500 mb was predominately anticyclonic over the St. Louis area. By 1800 CST (Fig. F2) the flow at 700-500 mb had shifted to westerly in advance of the High Plains short wave trough.

At 0600 CST (Fig. F1b) an 850 mb jet stream from Texas through Illinois (shaded area) curved around the periphery of the anticyclone. The St. Louis area was located on the anticyclonic shear side of this jet stream. Qualitatively, strong speed convergence was not compensated by directional difluence near the nose of the jet (arrow A) over eastern Illinois and Indiana. Further, warm relatively moist air (precipitable water at St. Louis at 1130 was 4.2 mm) was flowing beneath a cool airmass at 500 mb (shaded area, Fig. F1d). The combination of destabilization (K-index at St. Louis at 1130 was 35) by advection and convergence contributed to the development of showers over eastern Illinois and most of Indiana (shaded area A, Fig. F1a). The radar summary charts located a second area of showers over parts of Oklahoma, Kansas, and western Missouri (shaded area B, Fig. F1a).

The cloud masses associated with the two showery areas are identified in the satellite observations taken at 1100 and 1200 CST (Fig. F3). The sharp demarcation between cloudy and clear airmasses from central Kansas through northwest Missouri and into northwest Illinois (arrows C, in Fig. F3) identified the boundary of a stable airmass formed when drier and warmer air in advance of the High Plains trough had been drawn out over the moist air at the surface and acted to suppress deep convection. Some isolated showers formed with this airmass along the front where convergence and lifting was sufficient to release the convective instability. Numerous showers formed within fields of towering cumulus south of the demarcation line.

REGIONAL SCALE SITUATION

Figure F4 shows the development of an organized zone of convergence across southeastern Missouri from 0600-1500 CST on the 18th. As the depth of the mixing layer increased with daytime heating, westerly momentum from the low level jet stream seen at 850 mb (Fig. F1b) was brought to the surface and caused the winds over parts of northern and central Missouri to shift from southerly to southwesterly by 0900. Winds over southern Missouri remained southerly and an area of convergence developed between the two flow regimes.

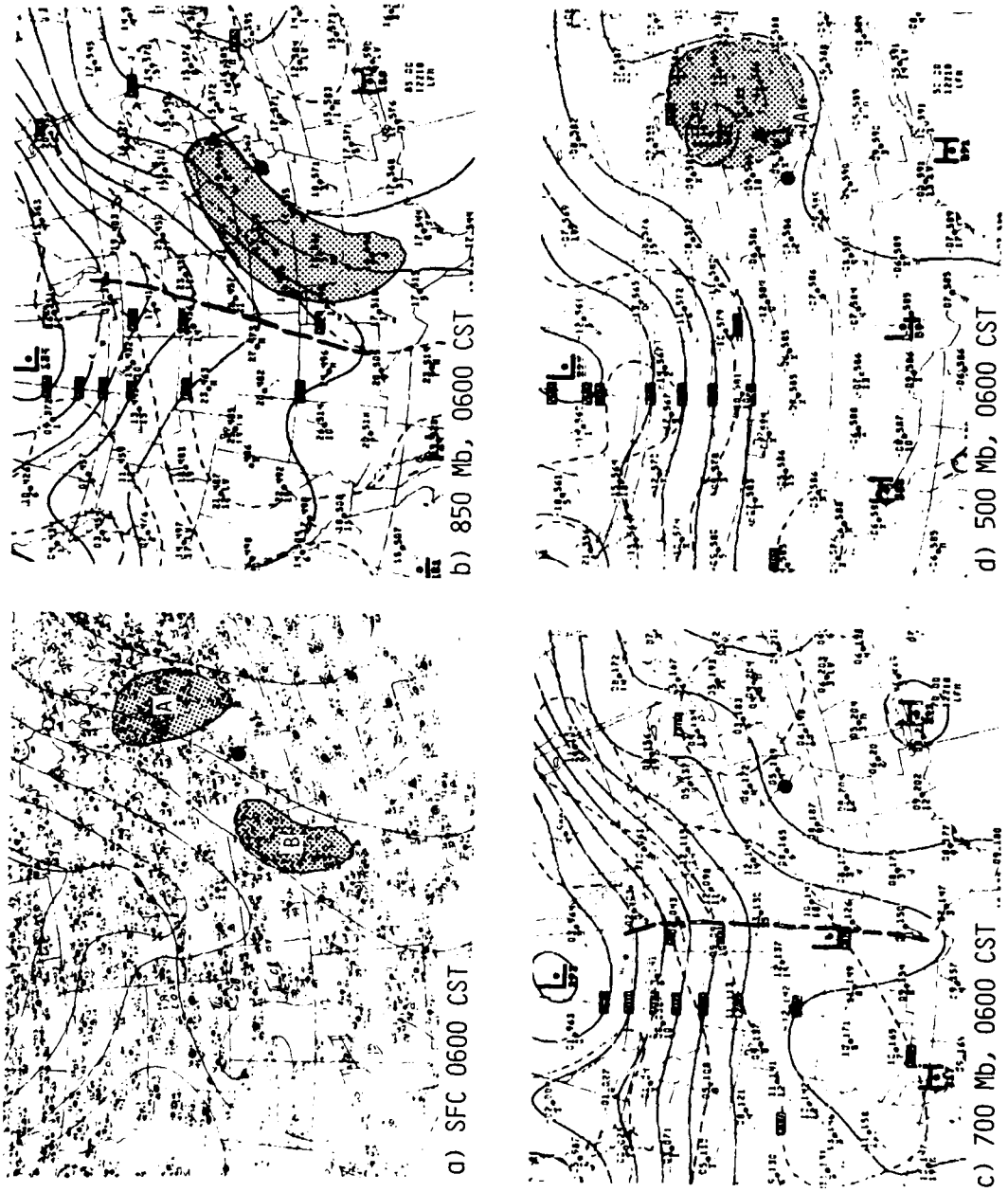

Figure F1. National Weather Service synoptic analyses for 0600 CST 18 July 1975. St. Louis area identified by black dot.

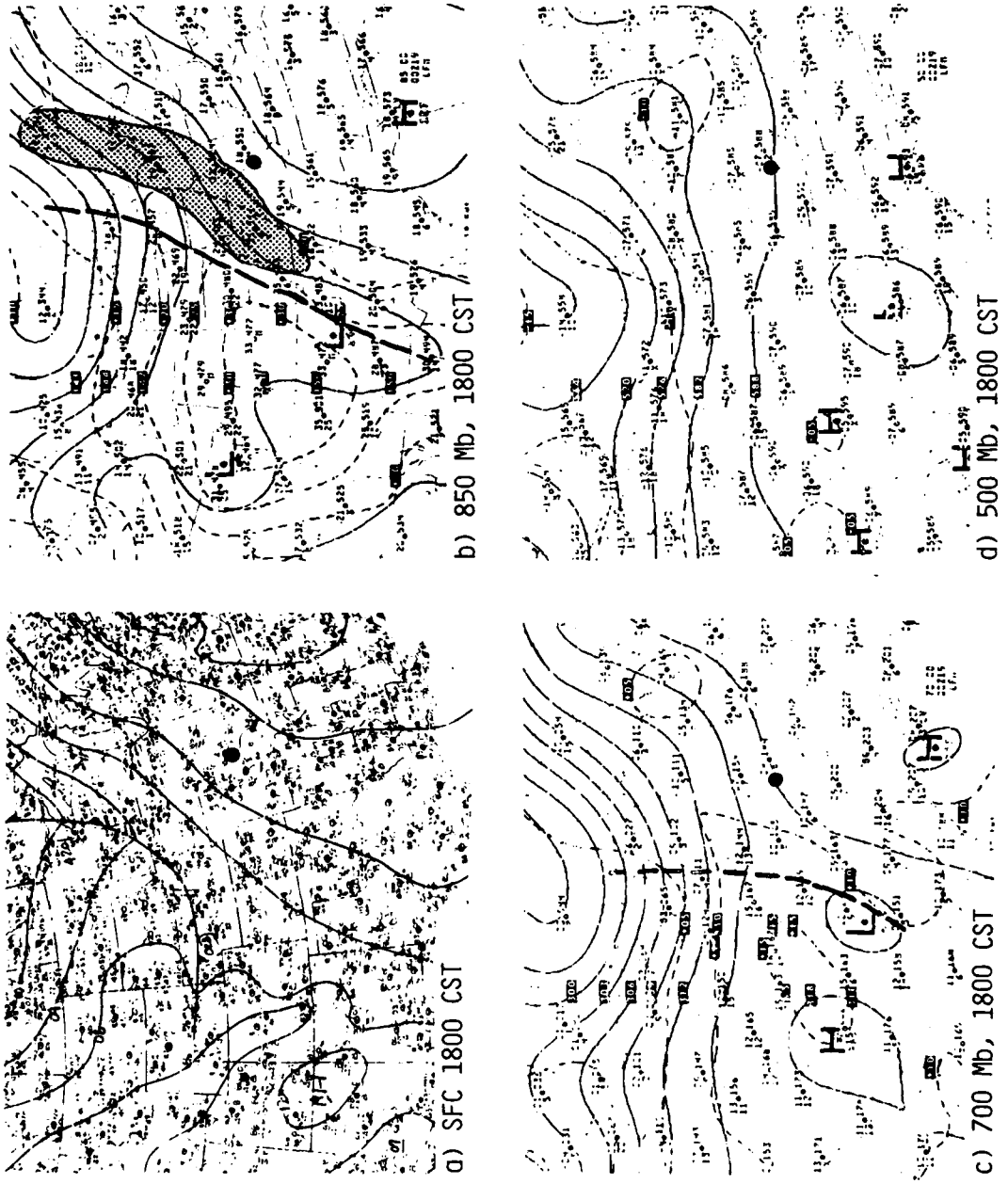

Figure F2. National Weather Service synoptic analyses for 1800 CST 18 July 1975.

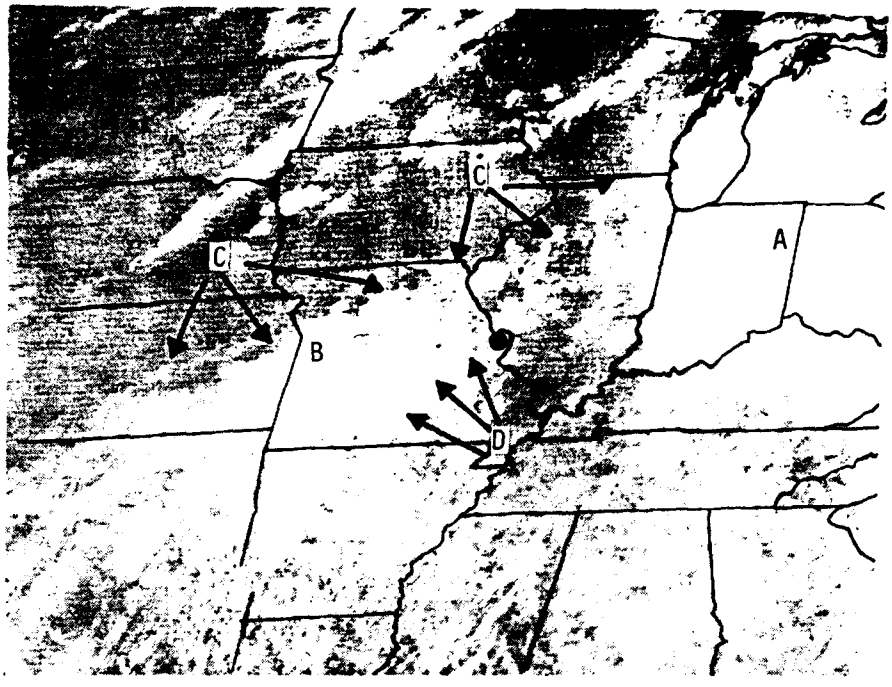

a. 1100 CST

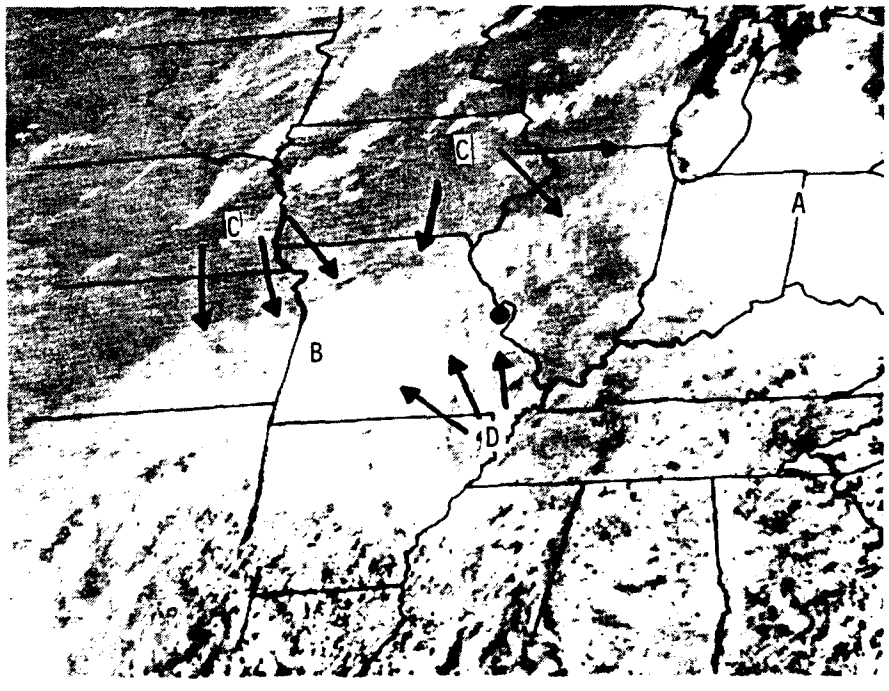

b. 1200 CST

Figure F3. GOES satellite photographs of the midwestern U.S. taken by satellite showing cloud systems associated with rainfall over the St. Louis area.

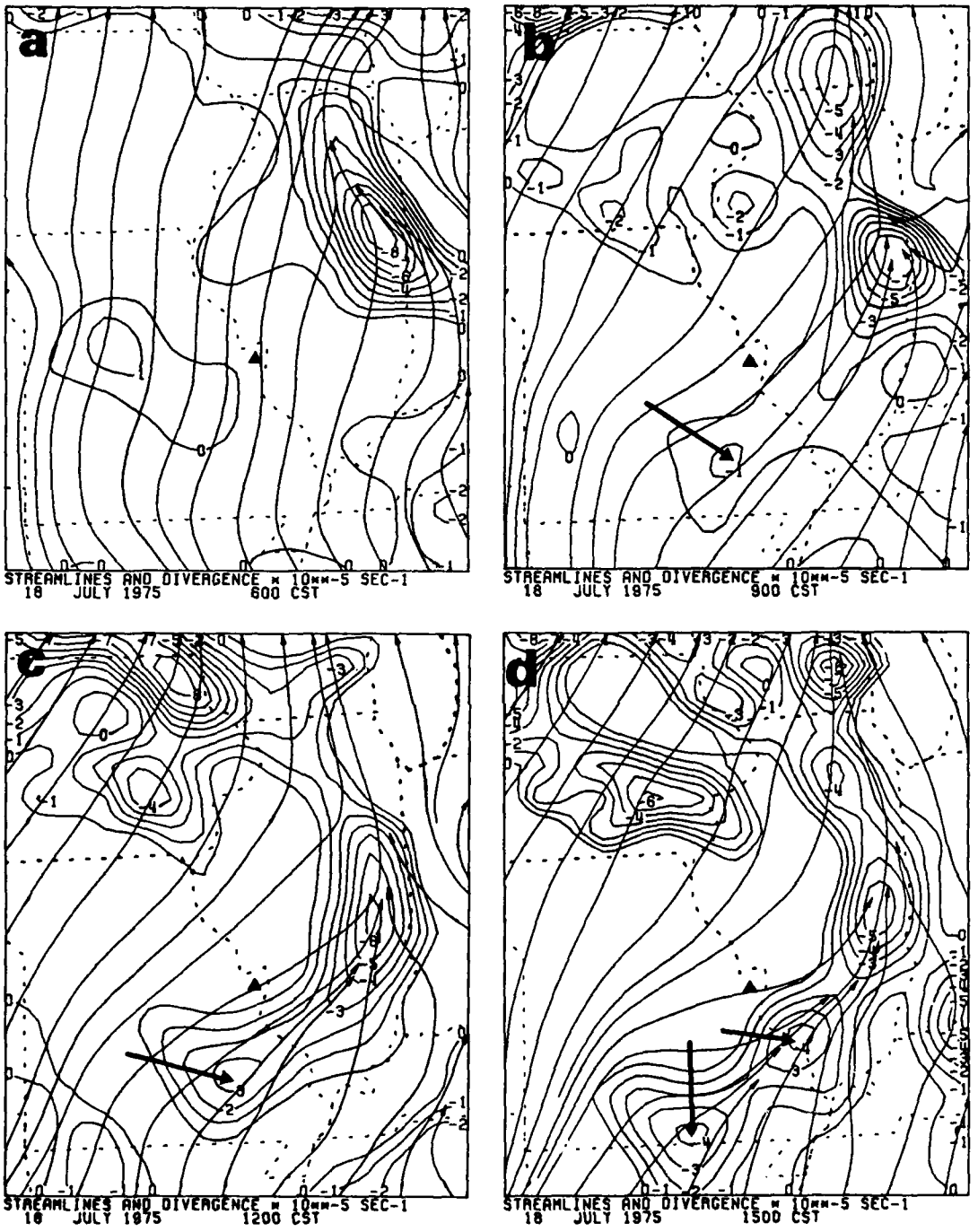

Figure F4. Regional scale analysis of surface wind field for 18 July 1975.

The convergence zone (arrows) developed from southeastern Missouri to eastern Illinois where it intersected the convergence area associated with the outflow from shower system A in Indiana (Fig. F3). The convergence area intensified and remained stationary through 1500 CST. Between 1100-1200 CST a line of towering cumulus (arrows D, in Fig. F3) developed into an area of showers. It was this area of showers that moved into the St. Louis network shortly after 1100 CST.

TIME SERIES OF DIVERGENCE AND RAINFALL

The time series for the number of gridpoints that reported rain, the average 15-min rainfall for the gridpoints reporting rain and the network mean divergence (Fig. F5a-c) shows that the flow into the network was weakly convergent for at least 2 hr prior to the beginning of rainfall. The stronger convergent regime from the beginning of the period until 0430 CST could have been coupled with the passage of the 850 mb jet stream convergence area (Fig. F1b) that produced showers over Illinois and Indiana at 0600 CST. The flow, convergent again from 0800-1200 CST (period A), produced network scale convergence to 0.4U at 1030 CST about 45-min before the rain began in the network.

Strong divergence occurred between 1200-1500 CST during the period when showers were present over the network. There was net inflow again at 1530 CST (B) just prior to a light shower beginning at 1600 CST.

The time series of the maximum 15-min rainfall, and the maximum and minimum point divergence show that rainfall began over the network shortly after 1100 CST. Convergence (negative divergence) that exceeded the background preceded the rainfall by about 45-min and lasted until 1400 CST (period A). The three convergence peaks exceeding 6U (arrows) preceded three rainfall peaks (arrows) by one half hour. The relationship between the convergence and the rainfall as seen in the surface convergence fields (see next section) was not found to be as apparent as implied by the peaks in Fig. F5e. However, it is possible that the establishment of organized strong convergence precedes rainfall even though the surface convergence patterns may not be easily related to the future locations of showers.

MESOSCALE SITUATION

Wind directions were generally from the southwest during the late morning of the 18th. Wind speeds were from 3-7 m sec^{-1}; variability that was sufficient to set up small convergence centers over the St. Louis network (see arrows, Fig. F6). At 1030, the wind field organized to develop a convergence zone (dashed line) from the southwest corner of the network to about 10 km north of the Arch. The convergence zone intensified to 4U between 1030 and 1100 but appeared as a local feature involving wind shifts to westerly at only 4 sites west and north of the Arch. Westerly winds became more widespread and the convergence zone had moved eastward by 1115.

Analyses of the pibal winds at levels from 250-1350 (Fig. F7) shows that the confluence extended above 350 m but was not found at the levels 550-1350 m. The vertical motion was upward along the confluence zone, at least within

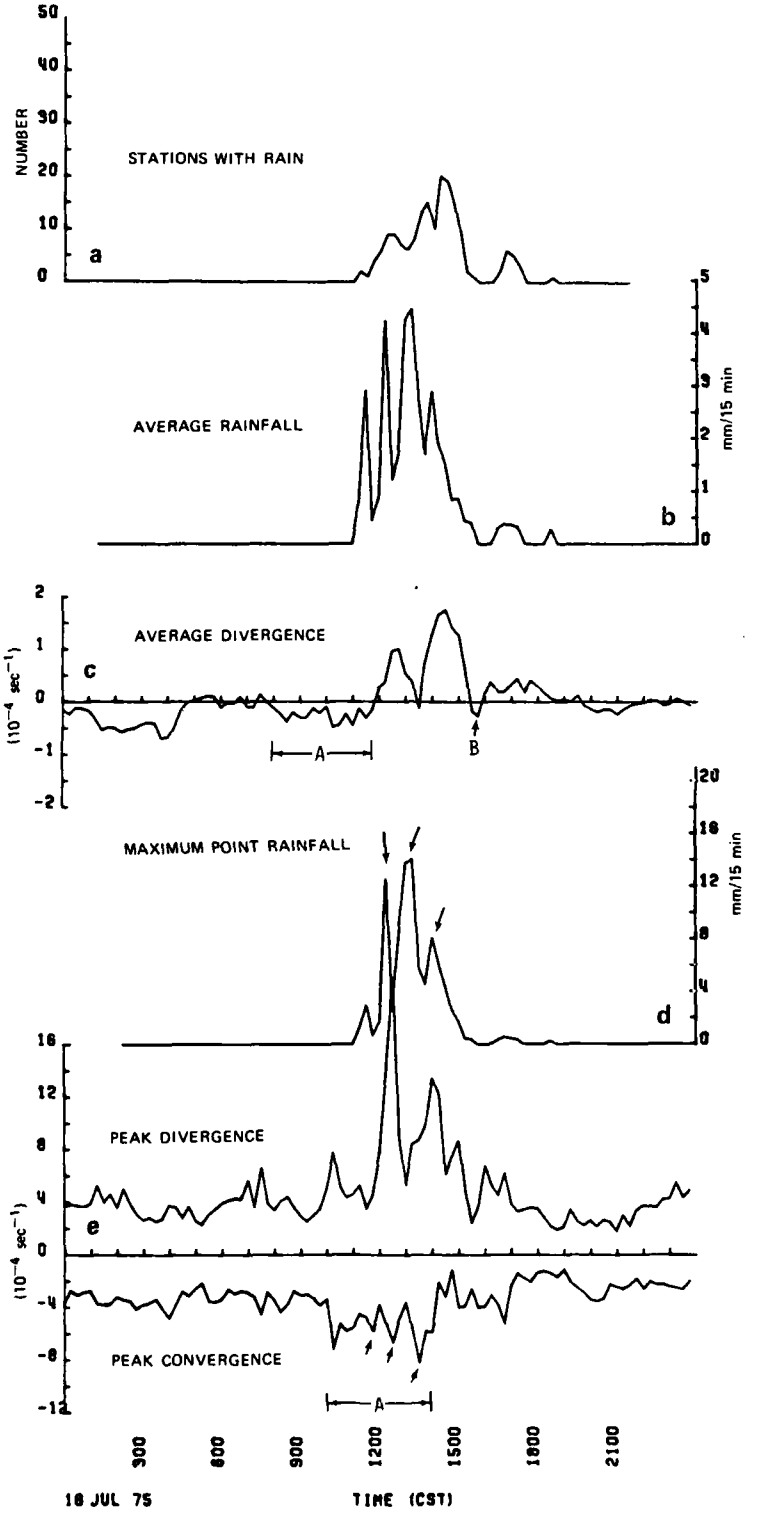

Figure F5. Time series of divergence and rainfall variables.

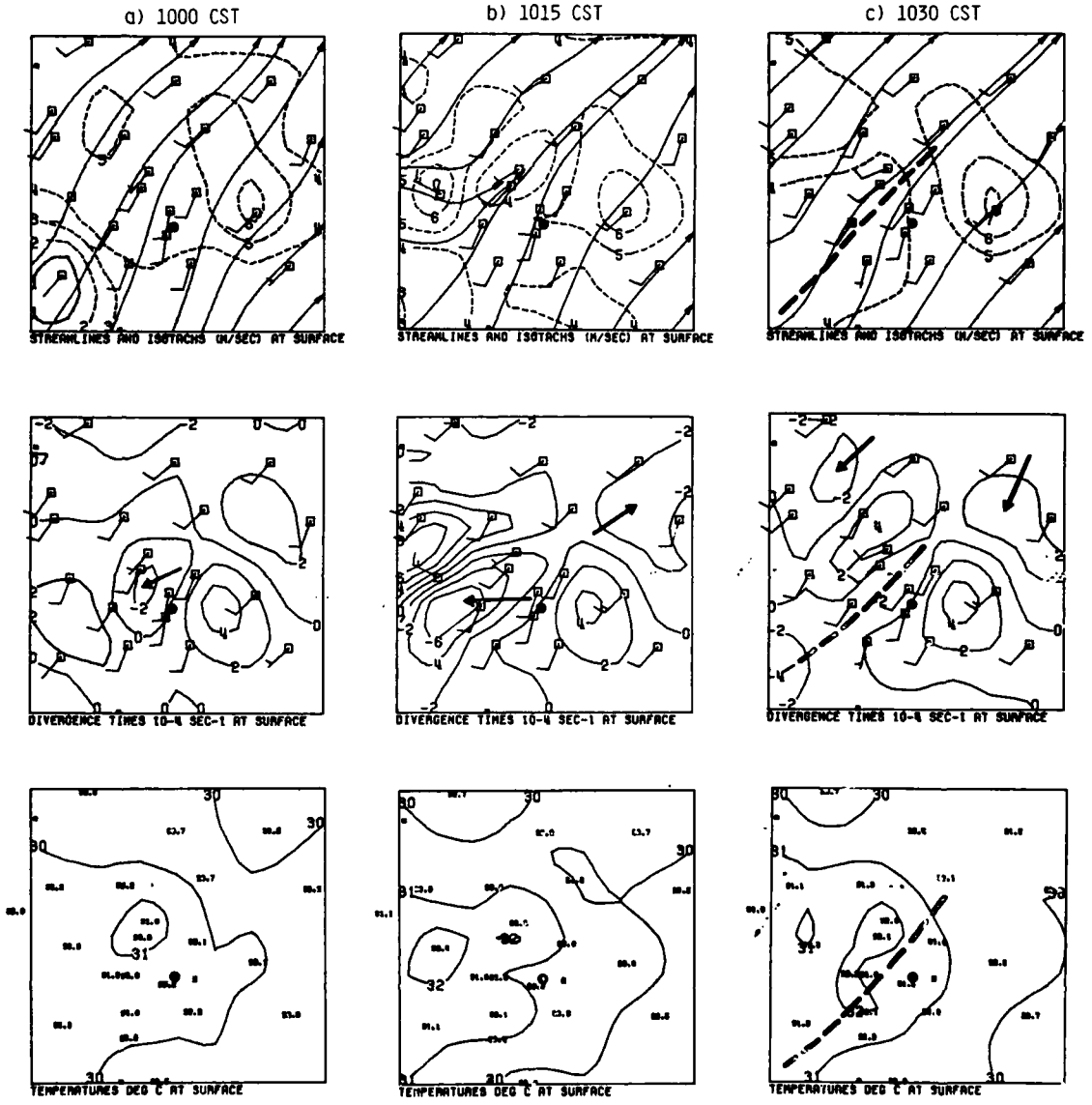

Figure F6. Composite of the objective isotachs and streamlines (upper map), divergence (middle map), and temperature (lower map) for the period 1000-1115 CST. St. Louis Arch identified by solid circle.

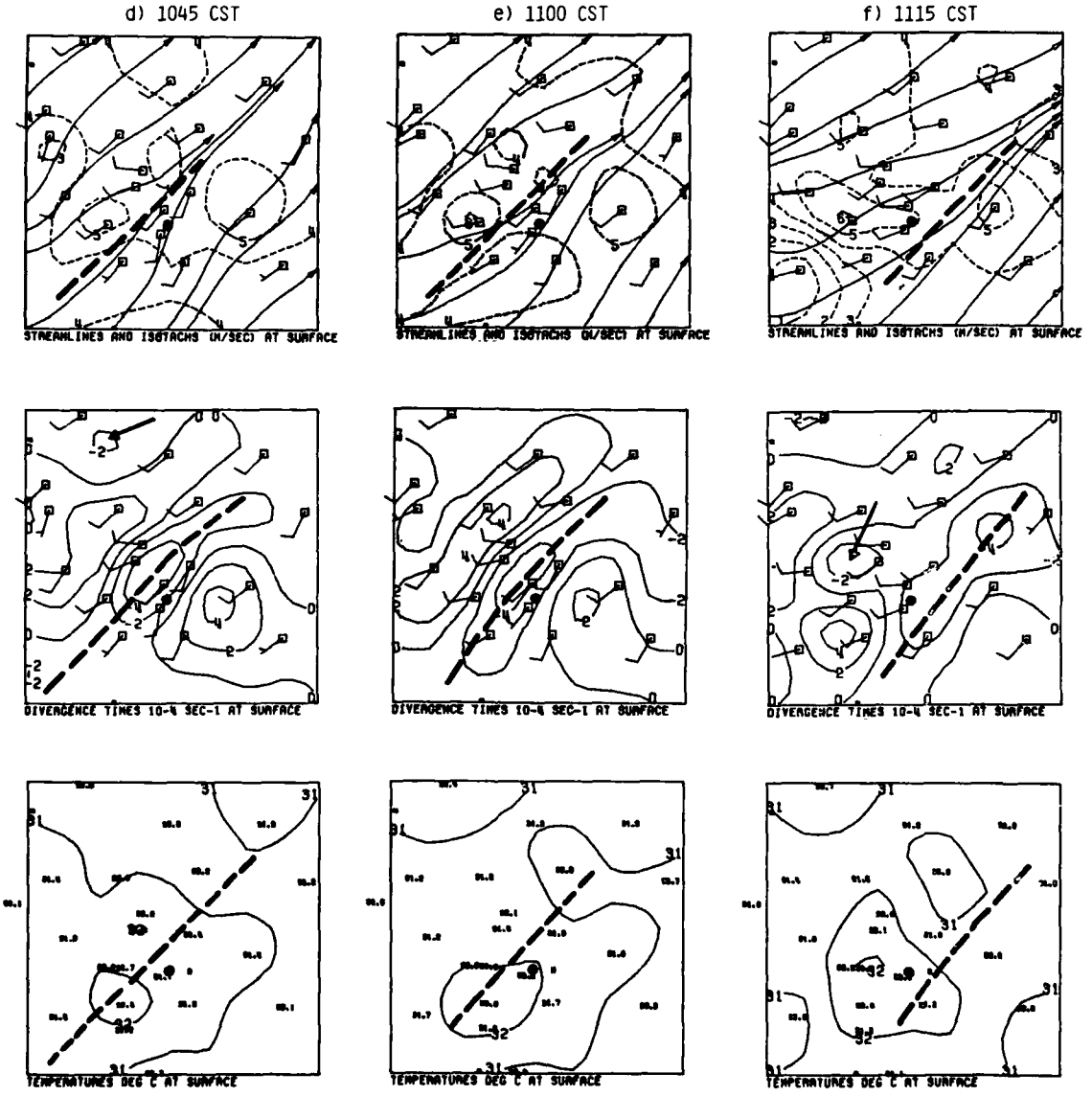

Figure F6. Concluded

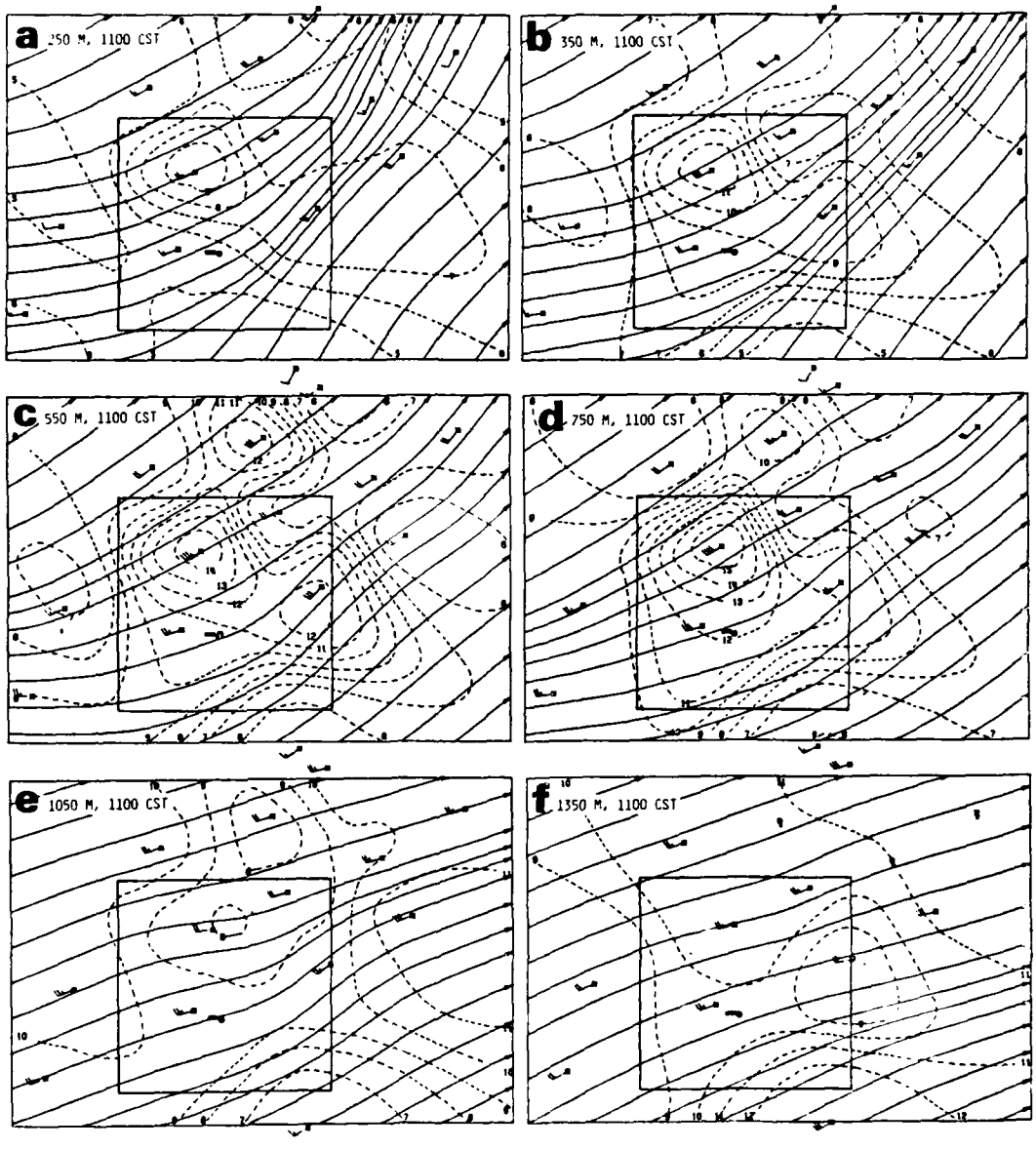

Figure F7. Objective streamlines and isotachs (m sec^{-1}) for 1100 CST at 6 heights msl.

the St. Louis network (Fig. F8). Two ascent centers at 550 m merged to form a zone of ascent (dashed line) over the same general area as the surface convergence zone. Maximum vertical velocities of 45 cm sec^{-1} were found 15 km northeast of the Arch at 1350 m.

An important aspect of the vertical wind structure on the 18th was the strong wind shear from the surface to 550 m. Winds increased from near 5 m sec^{-1} at the surface to almost 15 m sec^{-1} at 550 m. These winds were sufficiently strong to carry moisture displaced upward within the convergence zone near the Arch completely out of the St. Louis network in less than 30-min. This strong pluming may be the reason that the correspondence between areas of convergence and subsequent raincell development was not as good as was found for other case days.

Raincells began developing over the METROMEX raingage network shortly after 1115. Cell A appeared at the southwest corner of the St. Louis network at 1130 (Fig. F9a) in an area of convergent flow until 1100. Cell A's gust front pushed northeastward along the convergence zone but there was no observed increase in convergence (Fig. F9b). Cell A dissipated and Cells B and C were possibly triggered by A's gust front.

Rain cooled air spread over the southwestern third of the network by 1200 (Fig. F9c). Cell E formed ahead of the gust front in an area with little or no convergence during the previous hour. Cell F moved onto the network and merged with cell E west of the Arch at 1215 (Fig. F9d). Convergence centers to 4U along a zone from near the Arch northwestward to the grid boundary were produced when strong outflow from the E and F complex merged with the gust front from Cells A, B, C, and D. Meanwhile the convergence zone over the network east of the Arch had evolved into a 4U convergence center (arrow).

Wind fields at levels from 250-1350 m (Fig. F10) show the confluence zone over the St. Louis network to levels above 550 m. It was absent in the 750-1350 layer although strong convergence is implied by the decreasing wind speeds east of the Arch. A deep layer of upward vertical velocity persisted within this confluence zone (Fig. F11). Upward motions to 40 cm sec^{-1} were nearly collocated with the 4U surface convergence center (arrow, Fig. F9d) at 1215.

Strong outflow from the E and F complex pushed past the Arch at 1230 (Fig. F12a) developing an axis of convergence that connected with the old convergence center (arrow). Cells G, H, and J formed over the divergent outflow in close proximity to the location of dissipated cells E and F. Cell I pushed onto the south edge of the network. Its outflow reinforced the southern end of the gust front (Fig. F12b) which pushed rapidly out of the network by 1300 (Fig. F12c).

Cell K formed about 10 km northeast of Cell I where 2U convergence had appeared during the passage of the G, H, and J complex gust front at 1230 (Fig. F12a). Cell L appeared over a data void area near the southeast edge of the network at 1315 (Fig. F12d). Meanwhile a new raincell approached the network from the southwest. Its gust front pushed onto the network at 1330 (Fig. F12e) and developed an 8U convergence center (arrow). A 6U convergence center (arrow) appeared 10 km north of the location of a new rain area, Cell N.

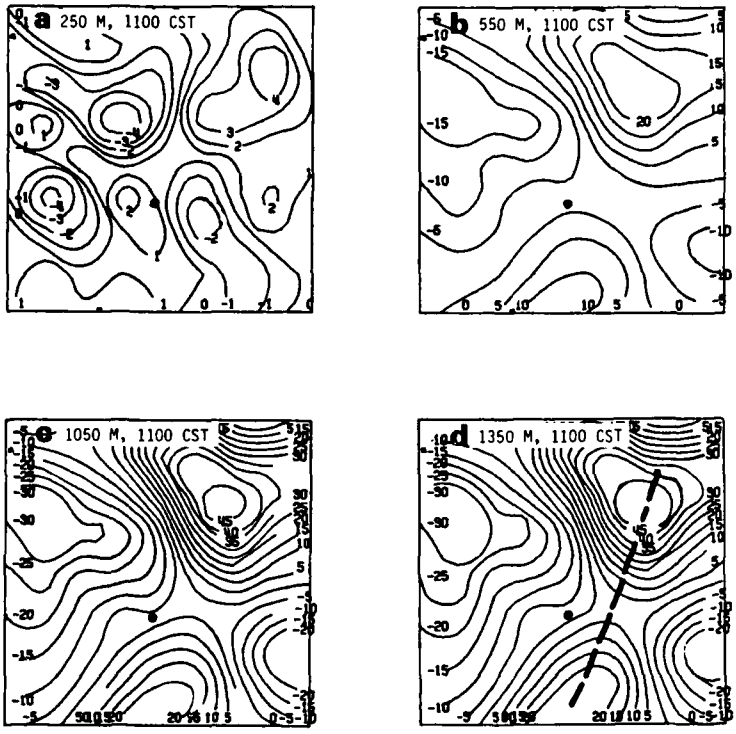

Figure F8. Vertical velocity maps (cm sec^{-1}) for 1100 CST.

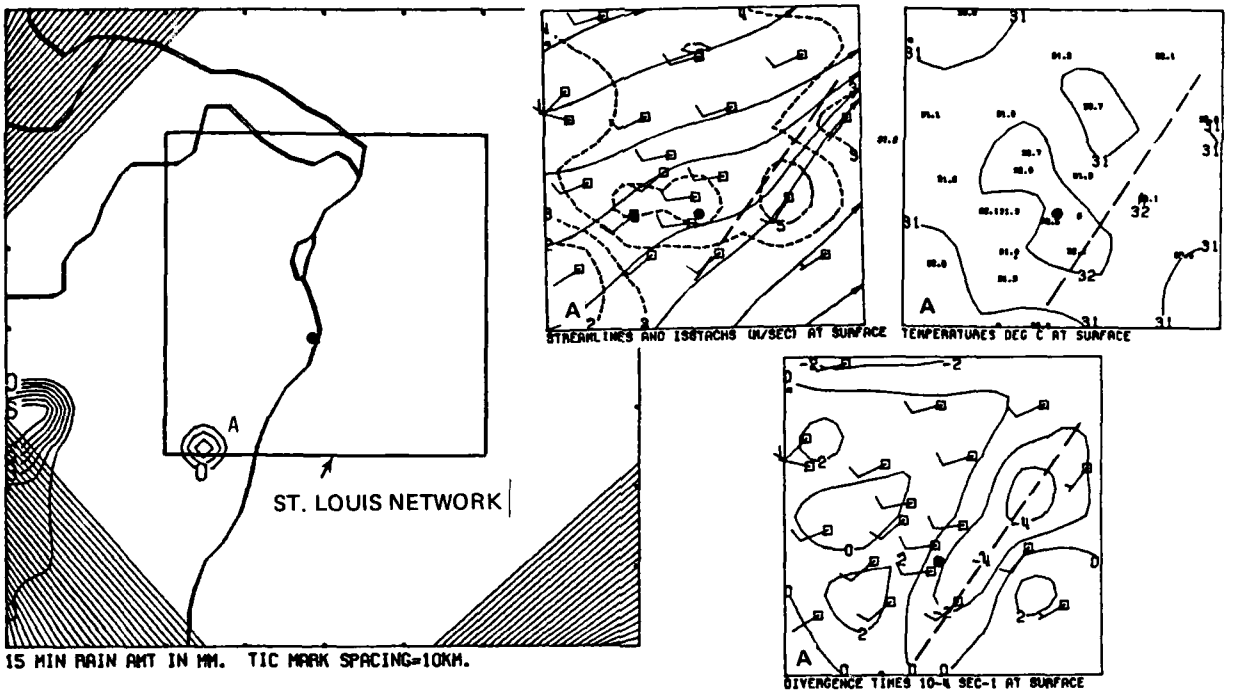

a. 1130 CST

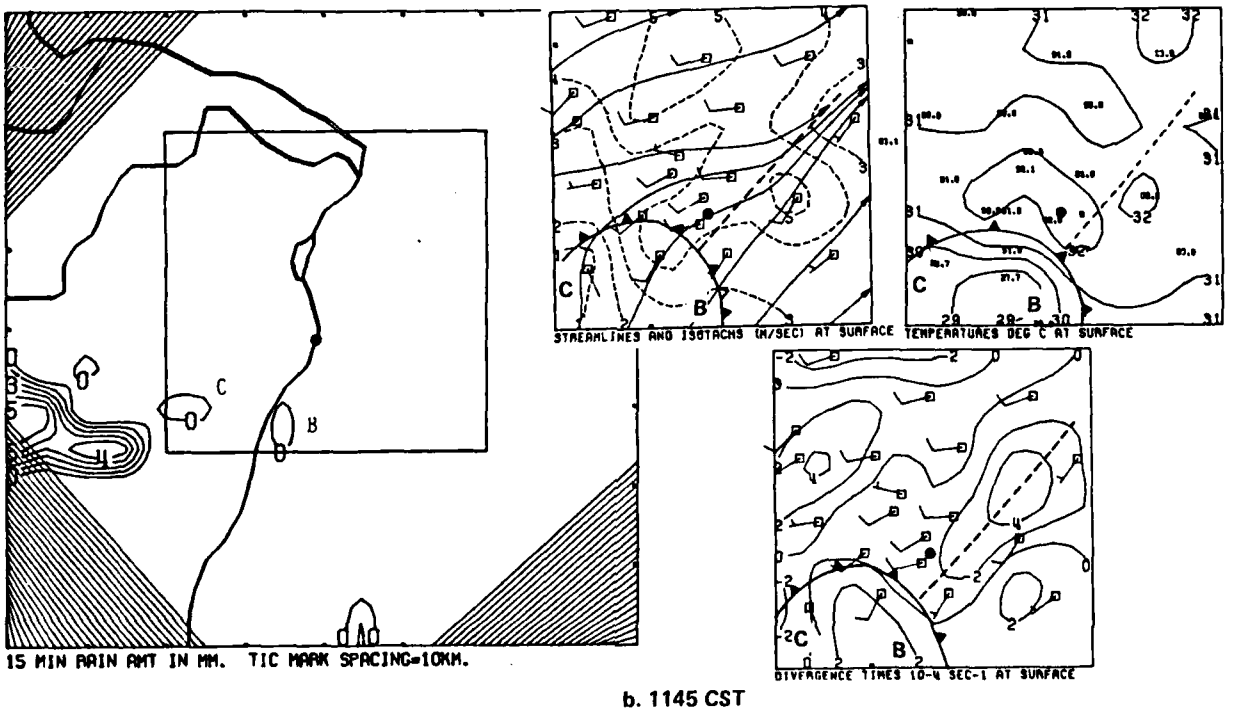

b. 1145 CST

Figure F9. Composite of the objective isotachs and streamlines, temperature, divergence, and rainfall for 1130-1215 CST.

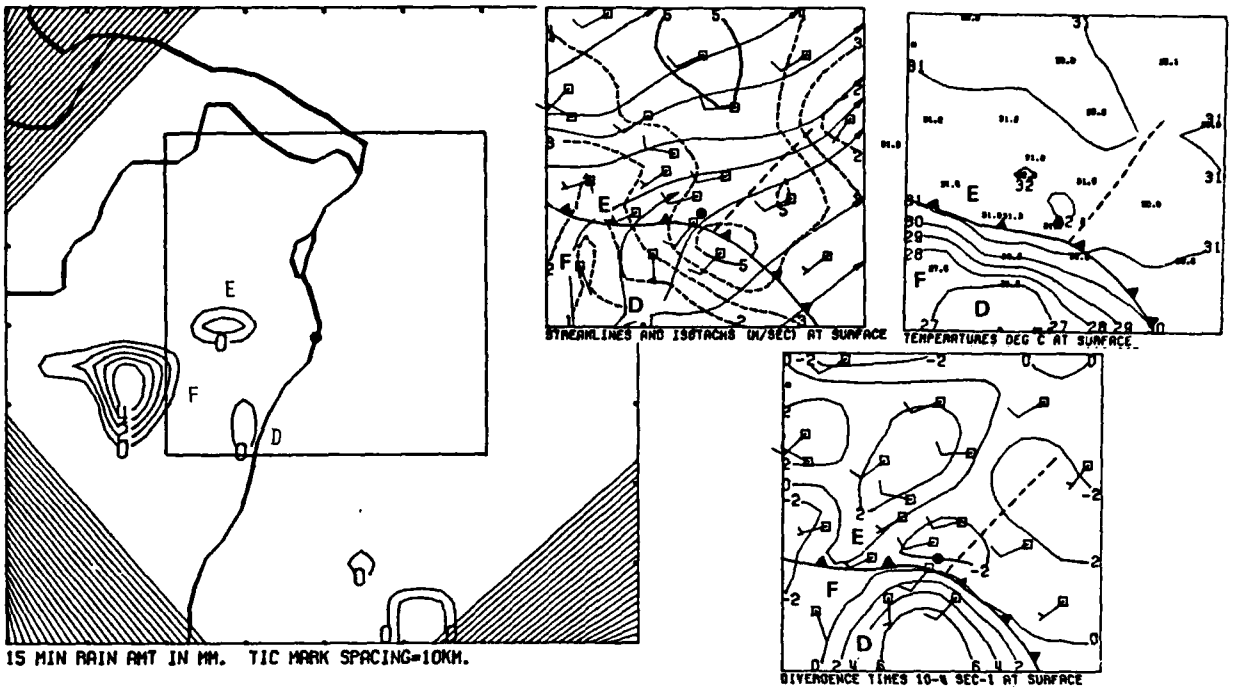

c. 1200 CST

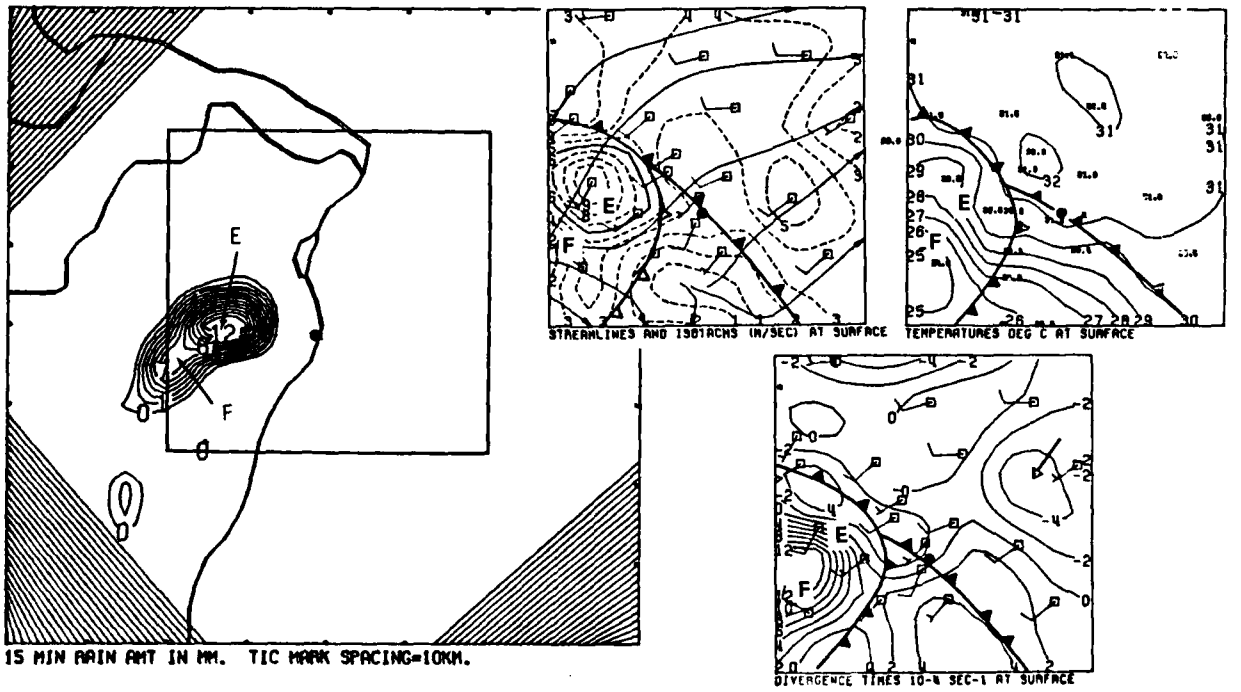

d. 1215 CST

Figure F9. Concluded

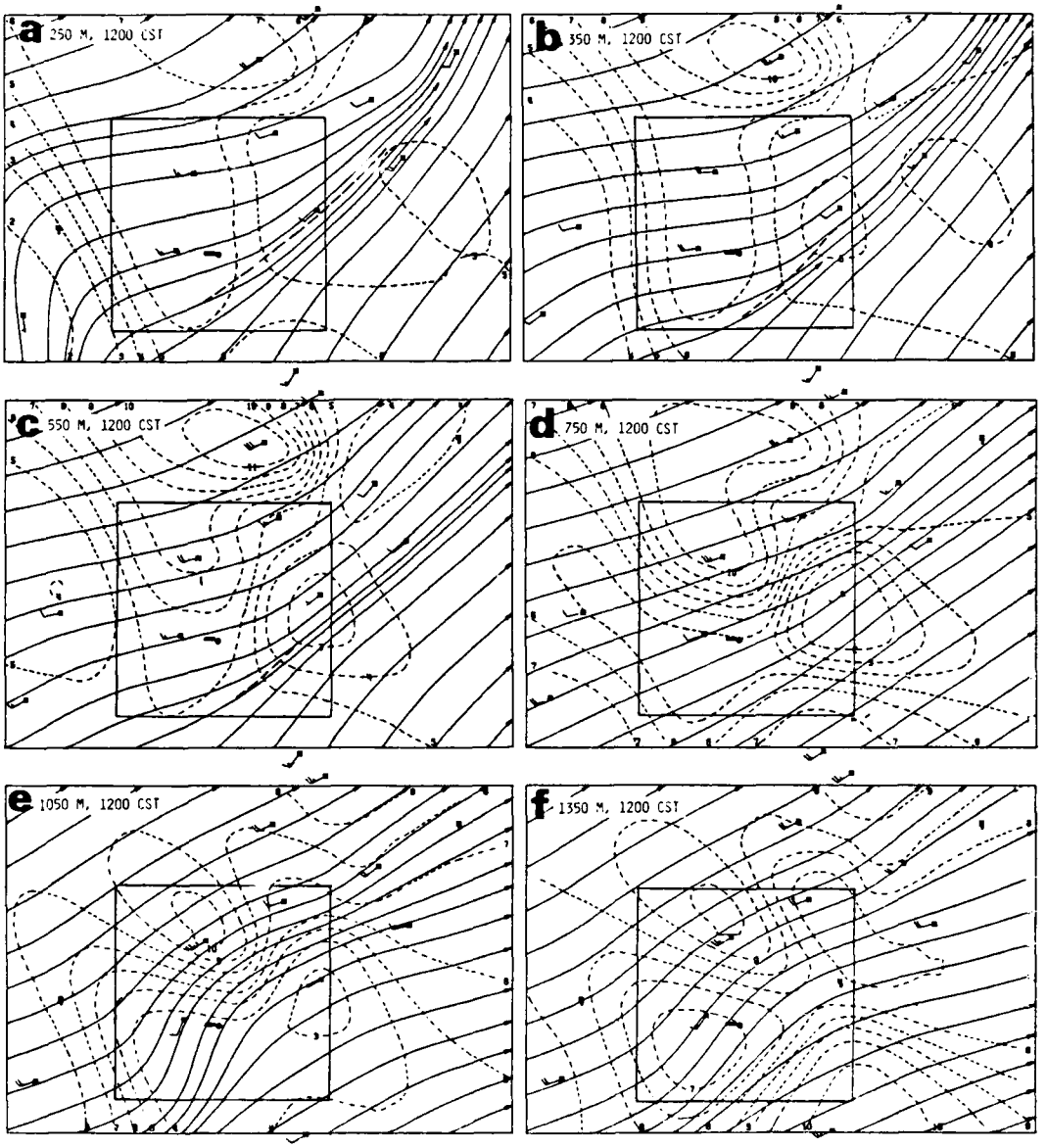

Figure F10. Objective streamlines and isotachs (m sec^{-1}) for 1200 CST at 6 heights msl.

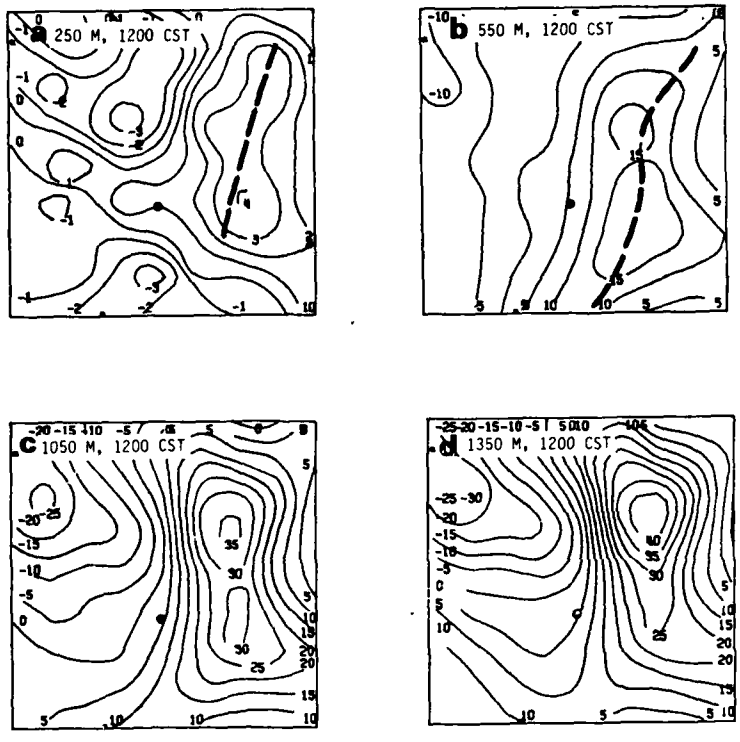

Figure F11. Vertical velocity maps (cm sec^{-1}) for 1200 CST.

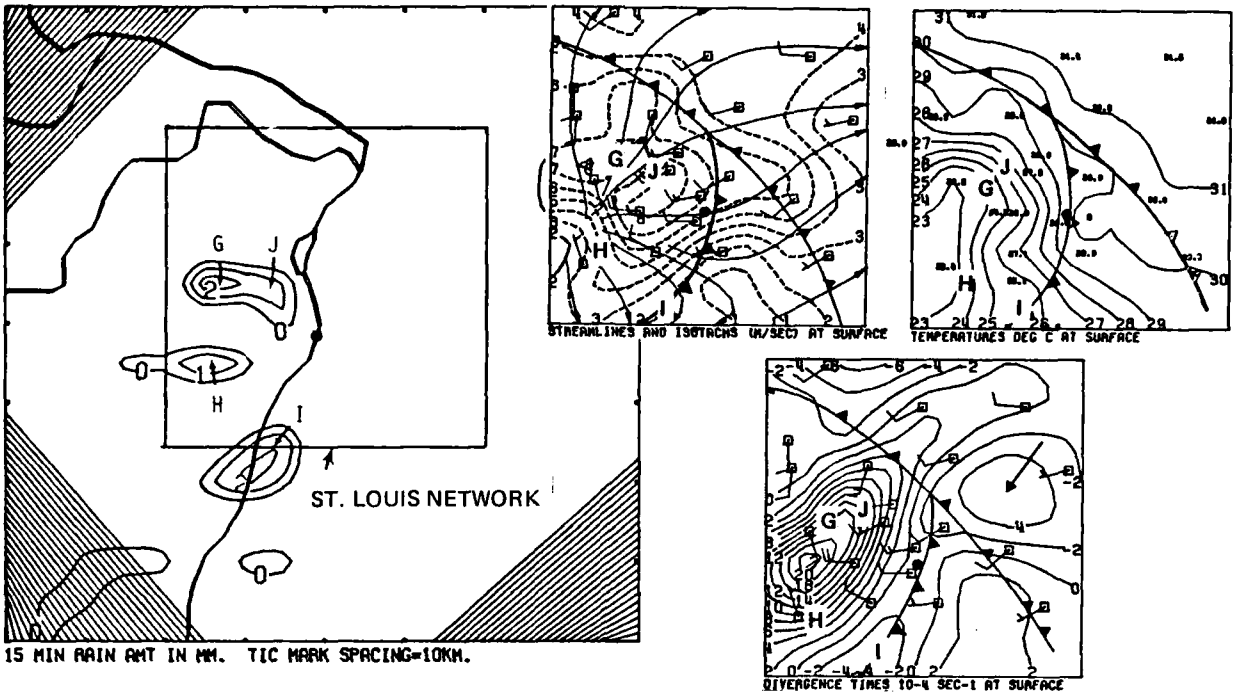

a. 1230 CST

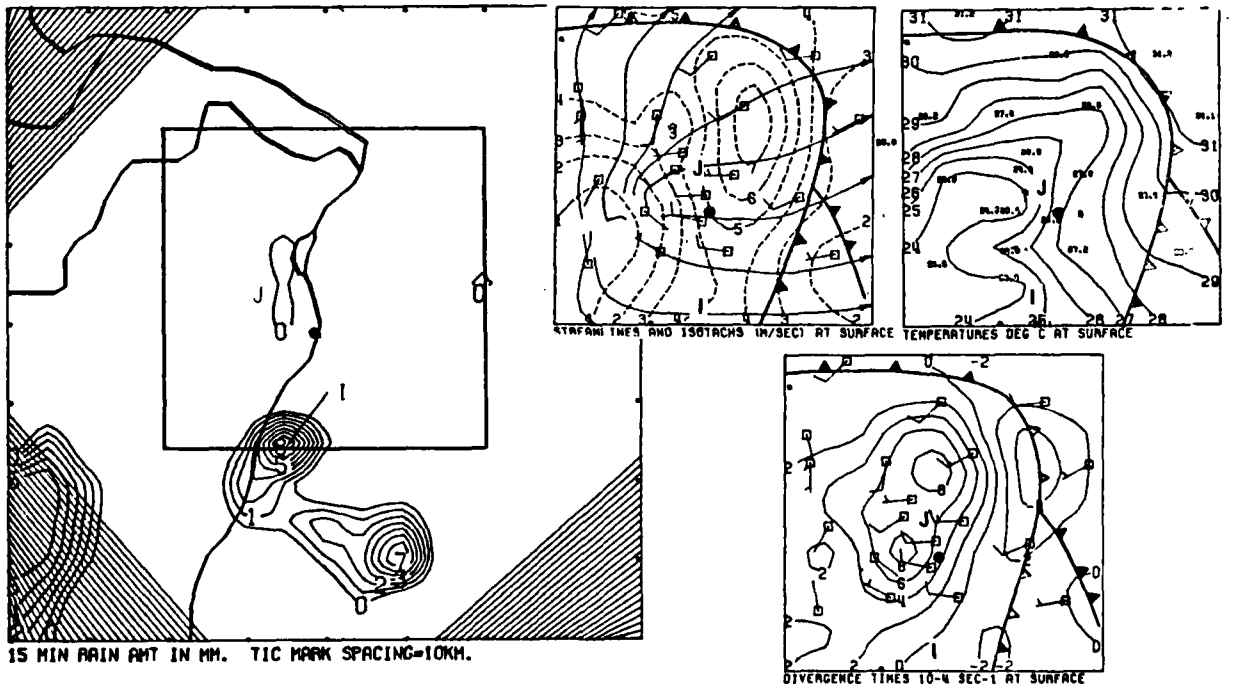

b. 1245 CST

Figure F12. Composite of the objective isotachs and streamlines, temperature, divergence, and rainfall for 1230-1515 CST.

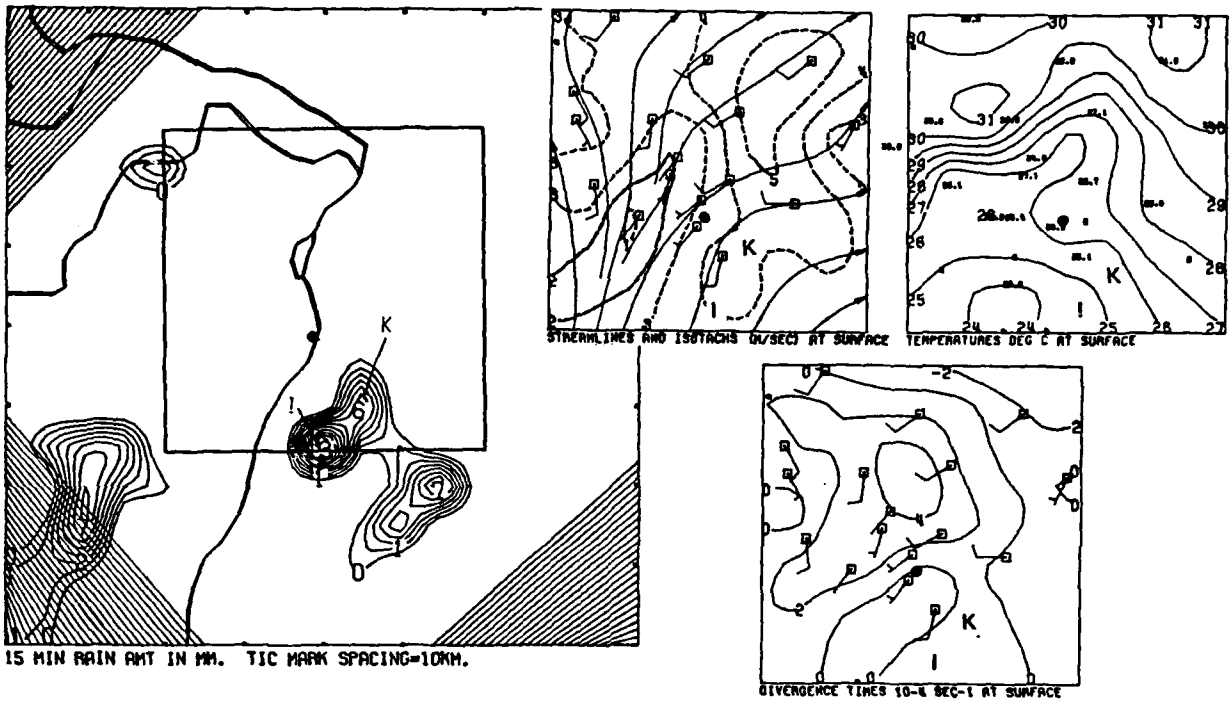

c. 1300 CST

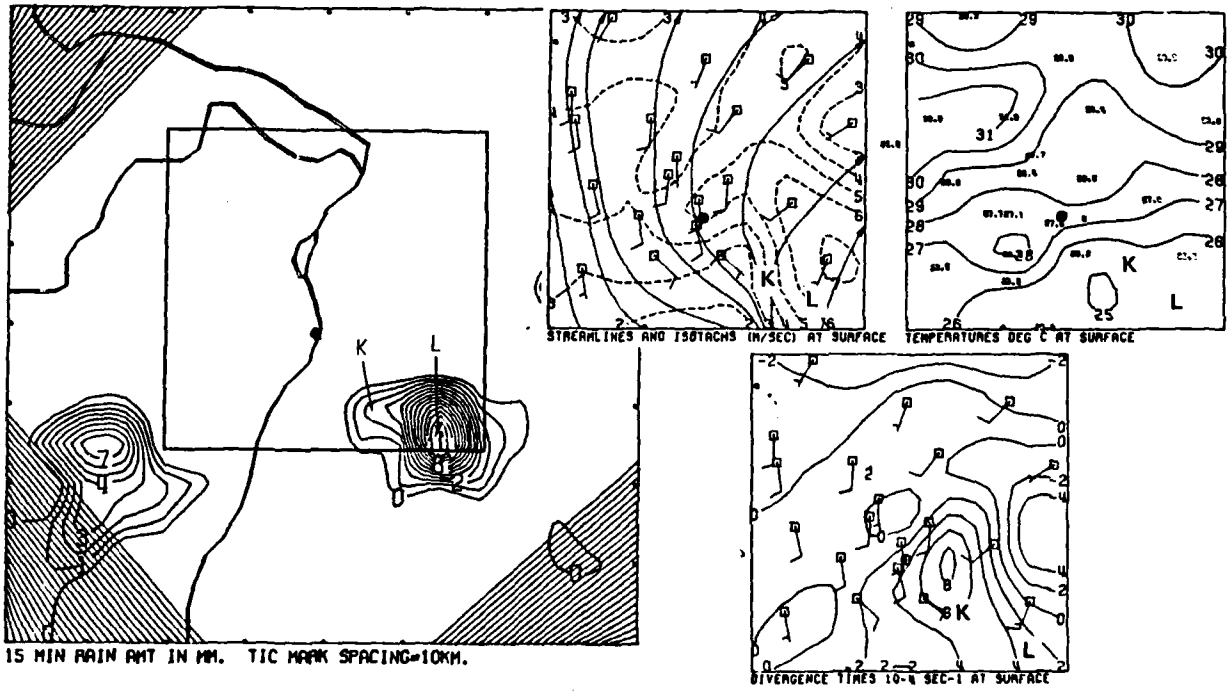

d. 1315 CST

Figure F12. Continued

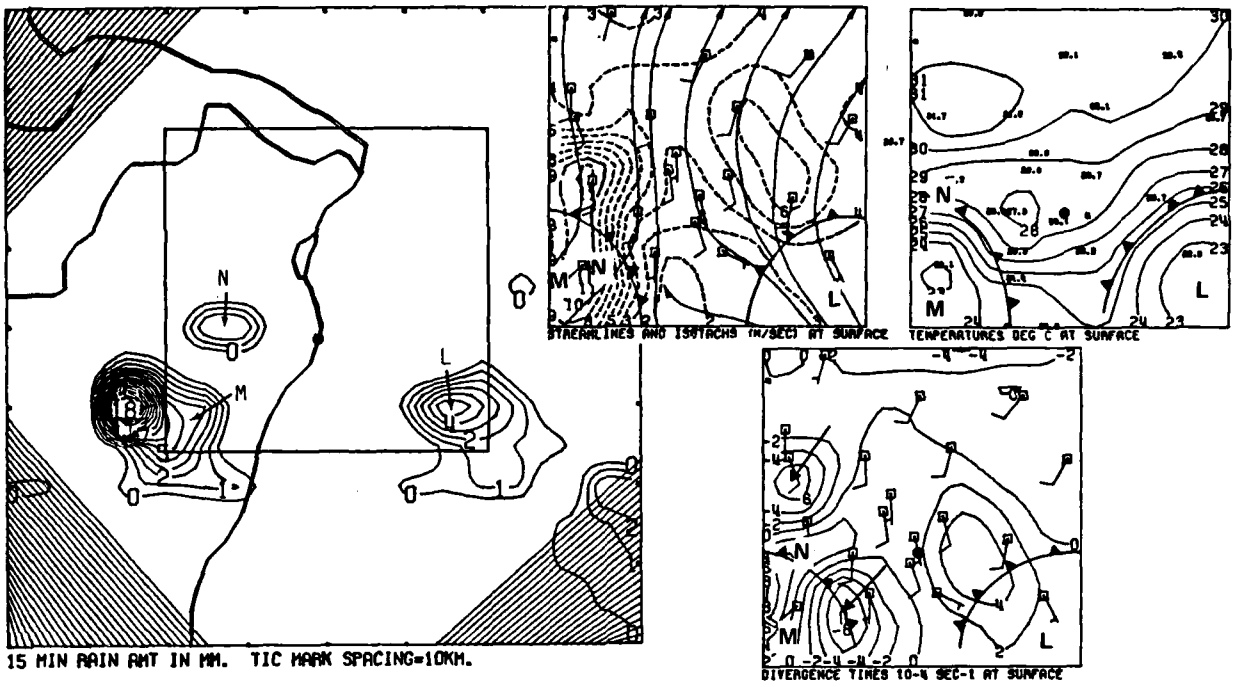

e. 1330 CST

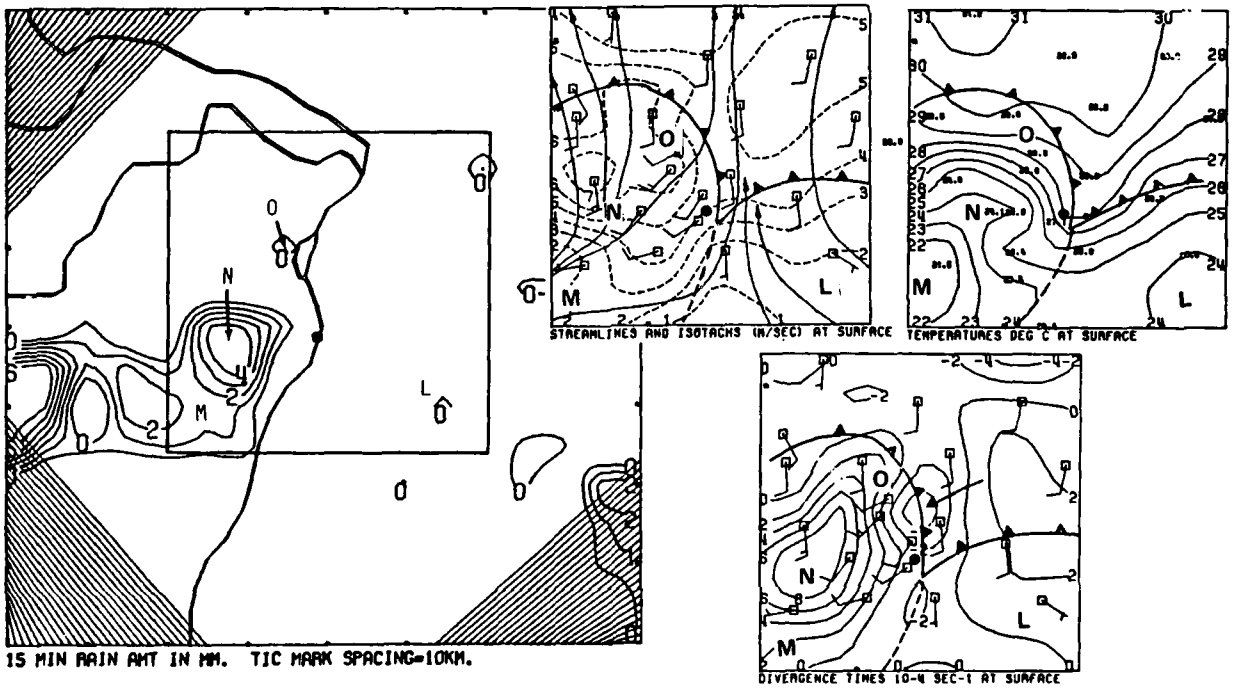

f. 1345 CST

Figure F12. Continued

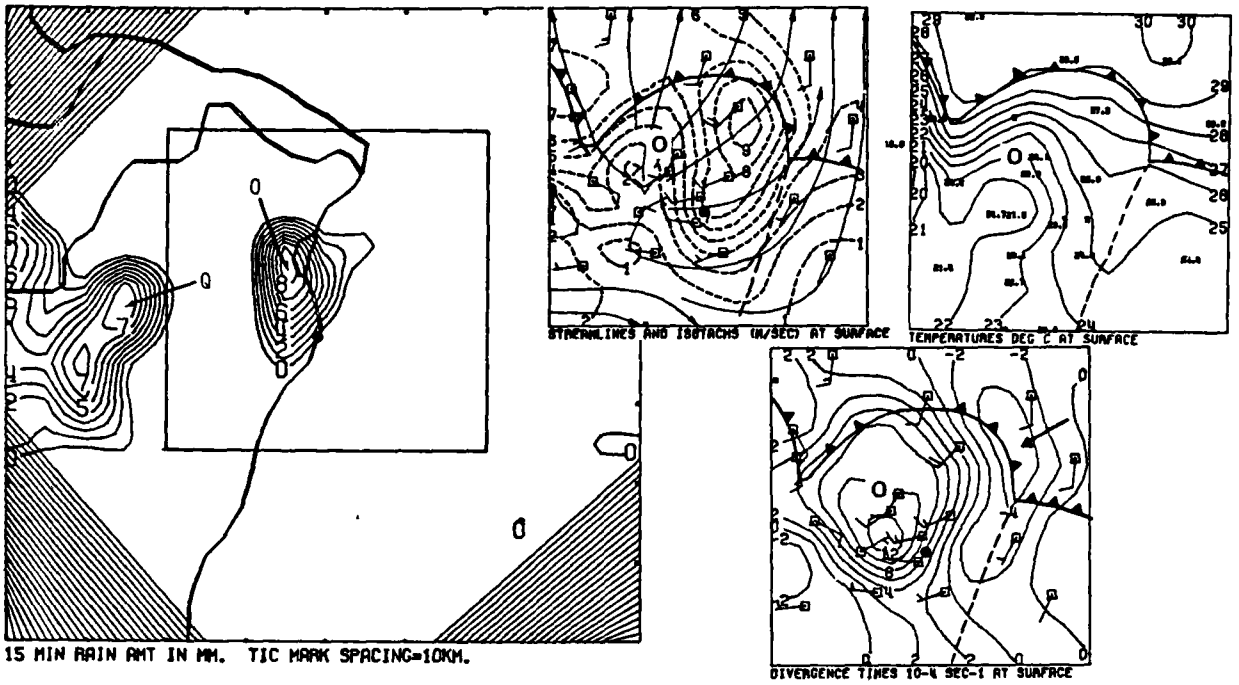

g. 1400 CST

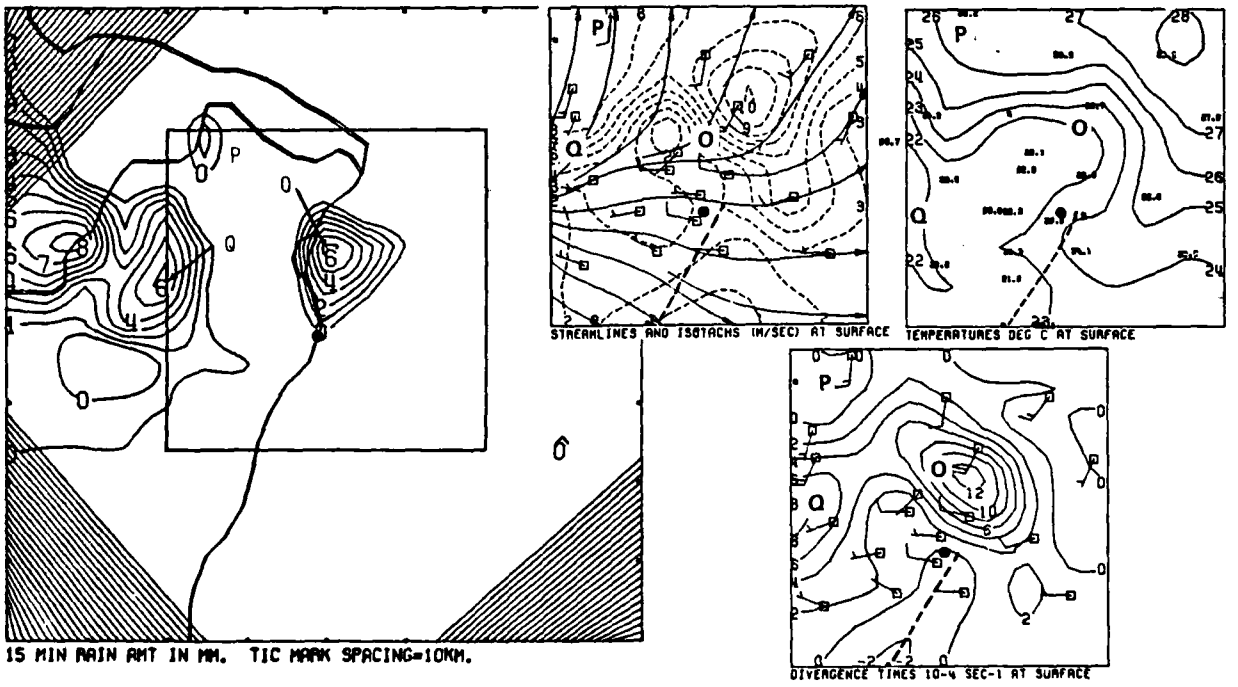

h. 1415 CST

Figure F12. Continued

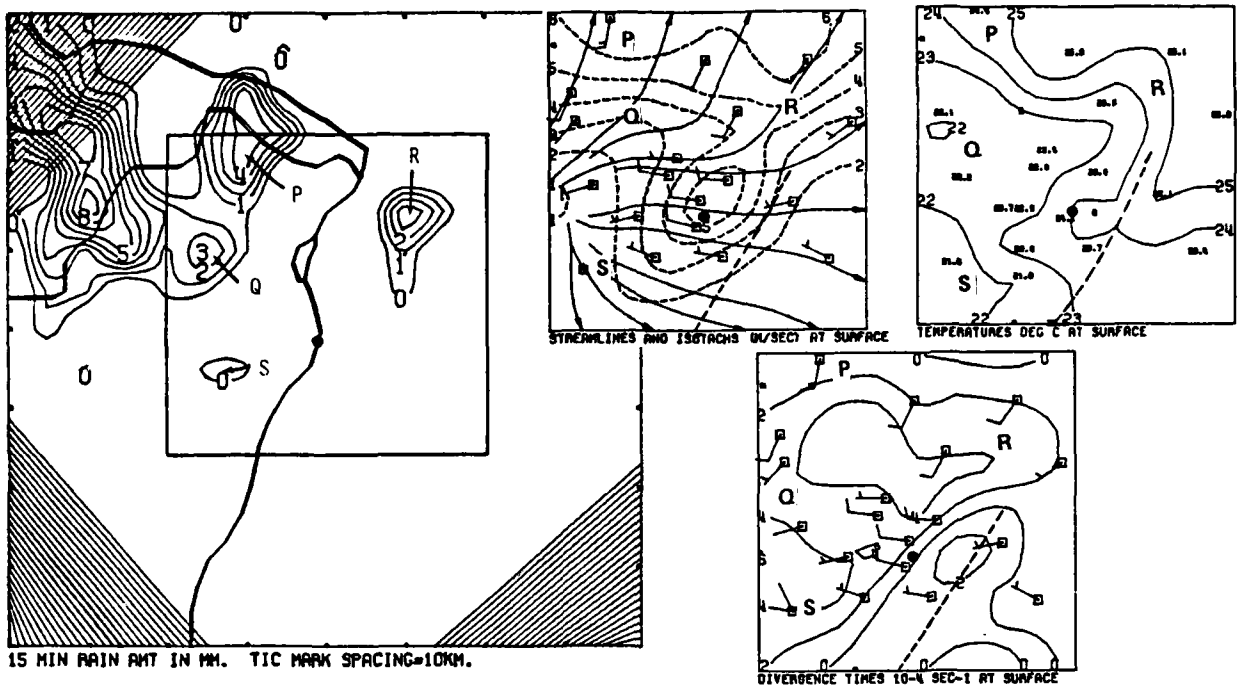

i. 1430 CST

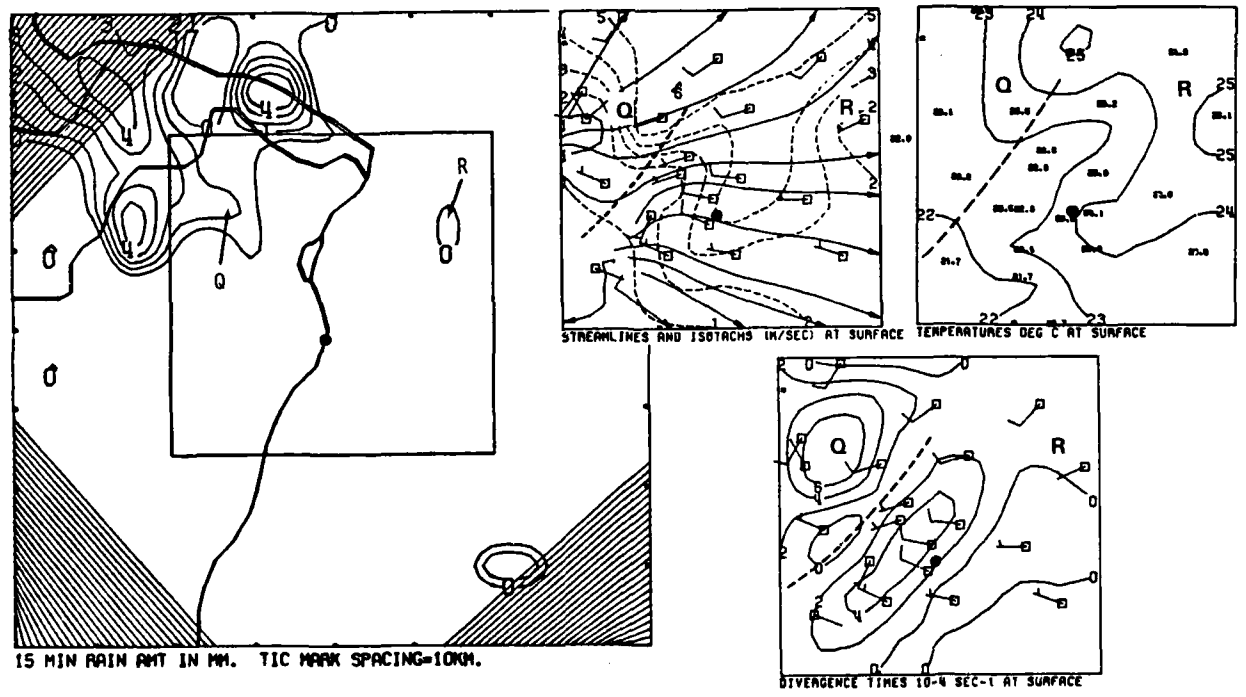

j. 1445 CST

Figure F12. Concluded

Cell M developed just behind the gust front. It merged with Cell N by 1345 (Fig. F12f) and the combined outflows accelerated the gust front eastward and northward to merge with the northwestward moving gust front from Cell L. Cell O formed along the gust front not far from a 4U convergence center (arrow) that appeared 5 km north of the Arch.

Cell O intensified to 8 mm/15-min rainfall by 1400 (Fig. F12g). Its outflow pushed the gust front northeastward to form an elongated 4U convergence center (arrow) near the junction with the gust front from Cell L. Meanwhile, outflow from Cell Q approaching from the west merged with the western edge of the Cell O outflow.

Cell P formed near the northwest corner of the network within an area of insufficient data to determine the convergence as outflow from Cells O and Q spread over the entire network (Fig. F12h). A weak convergence zone (dashed line) separated much cooler air pushing eastward from Cell O and Q from moderately cool outflow air from dissipated Cell L. Cells P and Q merged and Cells R and S formed over the rain cooled surface air at 1430 (Fig. F12i). Outflow from the P and Q complex pushed southeastward as a weak convergence zone after 1445 but there was no new raincell development.

SUMMARY OF SHOWER DEVELOPMENTS ON 18 JULY

Weather conditions became favorable for the development of convective showers over the St. Louis area on 18 July through the vertical displacement of an already convectively unstable airmass. The flow of warm moist air in the surface to 850 mb layer beneath a cold airmass in the middle troposphere combined with daytime surface heating to increase the instability of the airmass over the St. Louis area. Vertical mixing of horizontal momentum from a low level jet stream established a regional scale convergence zone over much of southeastern Missouri. The vertical displacement of the convectively unstable airmass were sufficient to release the convective instability over parts of southeastern Missouri.

Network scale convergence preceded the rainfall by approximately 2 hr. The maximum convergence persistently exceeded background as a mesoscale convergence zone developed across the network approximately 45-min before rain was reported.

An outbreak of showers 45-min after the appearance of a surface convergence zone during the heated part of the day leads to the expectation of a strong coupling between the kinematics of the surface airmass and the rainfall. However, the closer examination of the surface convergence fields with respect to the location of raincells shows that raincell development over the St. Louis network on the 18th was apparently not dependent upon surface heating and surface convergence. Showers frequently formed in areas with little or no persistent convergence and often seemed to show a preference for the divergent airmass with rain cooled temperatures.

Twenty raincells developed over or sufficiently near the network to influence the wind field. Of these, 10 raincells either moved onto the network or formed near the boundaries in areas where the data was not sufficient to define the convergence field with accuracy. Table F1 summarizes

cell strengths, convergence strengths, and convergence durations for the 10 raincells that formed within the network. The cell strengths ranged from 0.5 to 14.5 mm. The average cell strength was 5.3 mm, the average convergence strength was 1.20 and the average convergence duration was only 6 mm.

The surface wind field was convergent sometime during the hour before raincell formation for only 4 raincells. For all four instances, the convergence duration was 15-min - one analysis period. Eighteen convergence centers were not associated with rainfall over the network during the same period. There was no correlation between cell strength and convergence strength. No convergence was found in the area of Cells E and O which had strengths of 13.0 and 14.5 mm respectively.

Table F2 summarizes the convergence strengths and durations for all of the convergence centers that occurred over the St. Louis network during the period 1030-1515. Convergence persisted for 30-min or longer for 7 of the 22 convergence centers. The strongest center, 32U lasted for 150-min with no raincell formation. The asterisks indicate which convergence centers were nearly collocated with raincells and occurred within one hour prior to raincell formation. With ten raincells and 22 convergence centers during the same time period, it is likely that several raincells would be favorably located in space and time with convergence centers by chance.

Table F1. Cell Strengths, Convergence Strengths, and Convergence Durations for Raincells that formed within the St. Louis Network on 18 July.

Cell ID	Cell Strength	Convergence Strength	Convergence Duration
B	0.5mm	0U	0 min
E	13.0	0	0
G	2.0	4	15
H	1.5	0	0
J	2.0	2	15
K	8.0	2	15
N	7.0	0	0
O	14.5	0	0
R	3.5	4	15
S	0.5	0	0

Table F2. Convergence Strengths and Durations for all Convergence Centers that occurred over the St. Louis Network during the period 1030-1515 CST 18 July.

Number	Convergence Strength	Convergence Duration
1	4U	30 min
2	32	150
3	10	45
4	6	30
5	6	45
6	4	15
7	4	30
8*	2*	15*
9*	4*	15*
10	4	15
11*	2*	15*
12	4	15
13	6	15
14	8	15
15	4	15
16	2	15
17*	4*	15*
18	2	15
19	2	15
20	2	15
21	4	30
22	2	15

*Collocated with raincell development.

G. CASE STUDY: 19 JULY 1975

GENERAL OVERVIEW

Interactive regional scale and mesoscale weather systems were predominant on the 19 July. The synoptic scale circulations at middle tropospheric levels gave way to surface pressure fields with weak gradients. Several major mesosystems developed and interacted with surrounding airmasses to modify the regional scale circulation. Precipitation fell over the St. Louis network intermittently throughout the day. Three rain event periods selected for intensive study were 0000-0300, 0500-0700, and 1330-1500 CST. Because of the diversity of the weather systems, the regional scale discussions have been combined with the mesoscale discussion and each rain period presented separately.

SYNOPTIC SITUATION

Flow over Missouri shifted from southwesterly at the surface to westerly at 500 mb at 0600 (Fig. G1). The surface cold front from Colorado through Wisconsin remained north of Missouri (Fig. G2). An 850 mb jet stream of moderate strength (shaded area in Fig. G1) was a factor in the development of several convective mesosystems. The jet stream was within a deep layer of moist air drawn northeastward ahead of the frontal system and its associated weak trough aloft (dashed line). The trough, inferred in the 0600 CST 850 mb analysis as extending across Iowa, apparently intensified over Illinois as the intense thunderstorms developed into a squall line (dash-dot line, Fig. G2a) interacted with the environmental flow.

EVOLUTION OF DIVERGENCE AND RAINFALL

The time series for the number of gridpoints that reported rain (Fig. G3a), the average 15-min rainfall for the gridpoints reporting rain (Fig. G3b) and the network mean divergence (Fig. G3c) shows that flow into the network was mostly convergent throughout the 19th. The 3 rainfall periods selected for study are identified by number. The pre-rain convergence did not increase for the first two rain events. The increasing convergence from 1315-1400 (arrow A) precedes the rainfall, which began at 1330 and peaked at 1400, by only 15-min. A second convergence peak of the same duration and magnitude as the 1315-1400 peak occurred at 1800 (arrow B) but was not associated with rainfall. However, the surface temperatures were much cooler at 1800 than 1400.

Figures G3d through G3f give the time series of the maximum 15-min point rainfall and the maximum and minimum gridpoint divergence. Convergence peaks exceeding background are identified by the arrows. Rain event 1, which was mostly light rain from middle level clouds, had little impact upon the wind field. The convergence briefly increased at 0515 during convective rain event 2 and then again at 0715 after the rain had moved out of the network.

The strongest convergence preceded the peak in the rainfall of the third rain event by 15-min. The St. Louis network scale analyses show that the

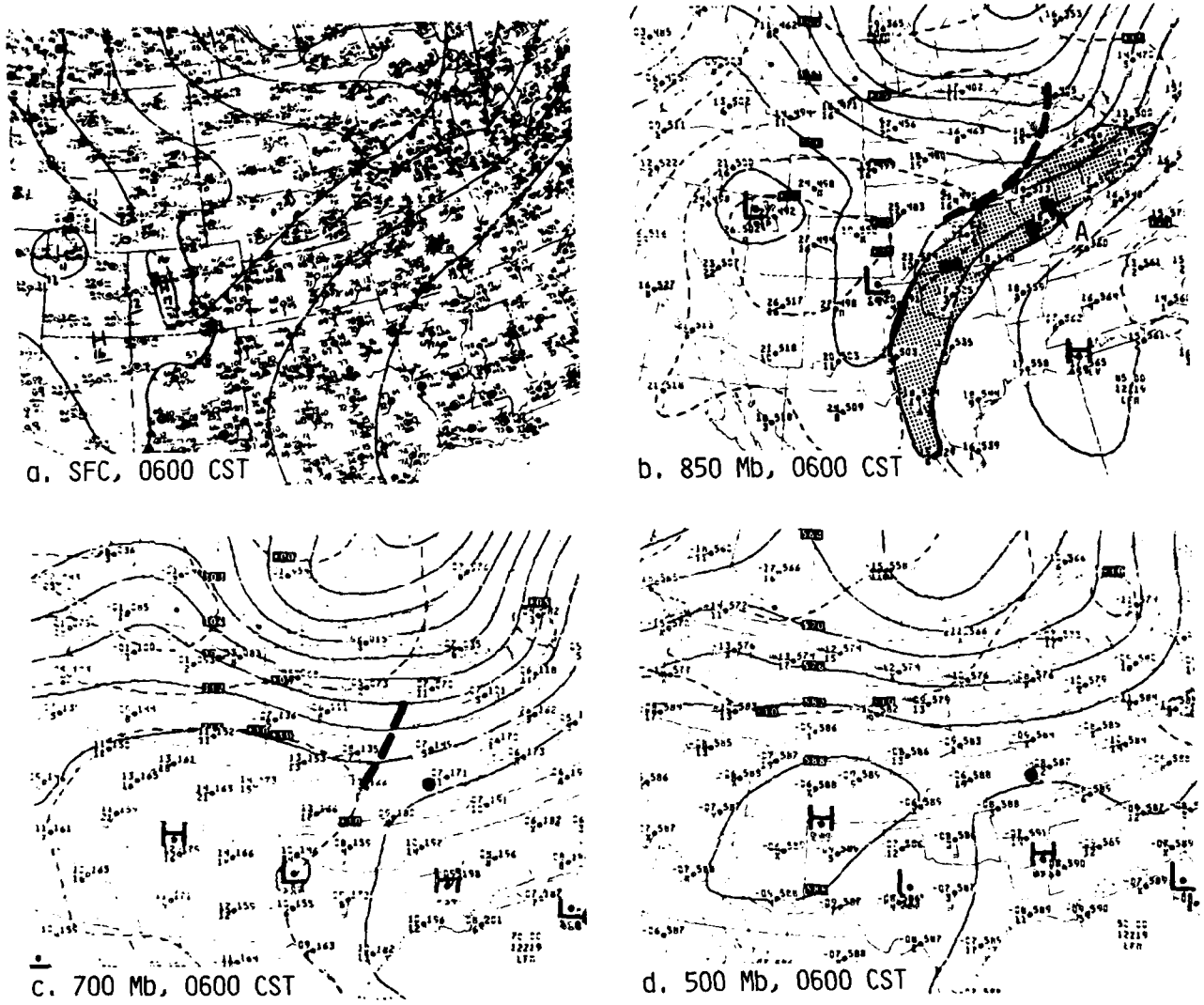

Figure G1. National Weather Service synoptic analyses for 0600 CST 19 July 1975. St. Louis area identified by black dot.

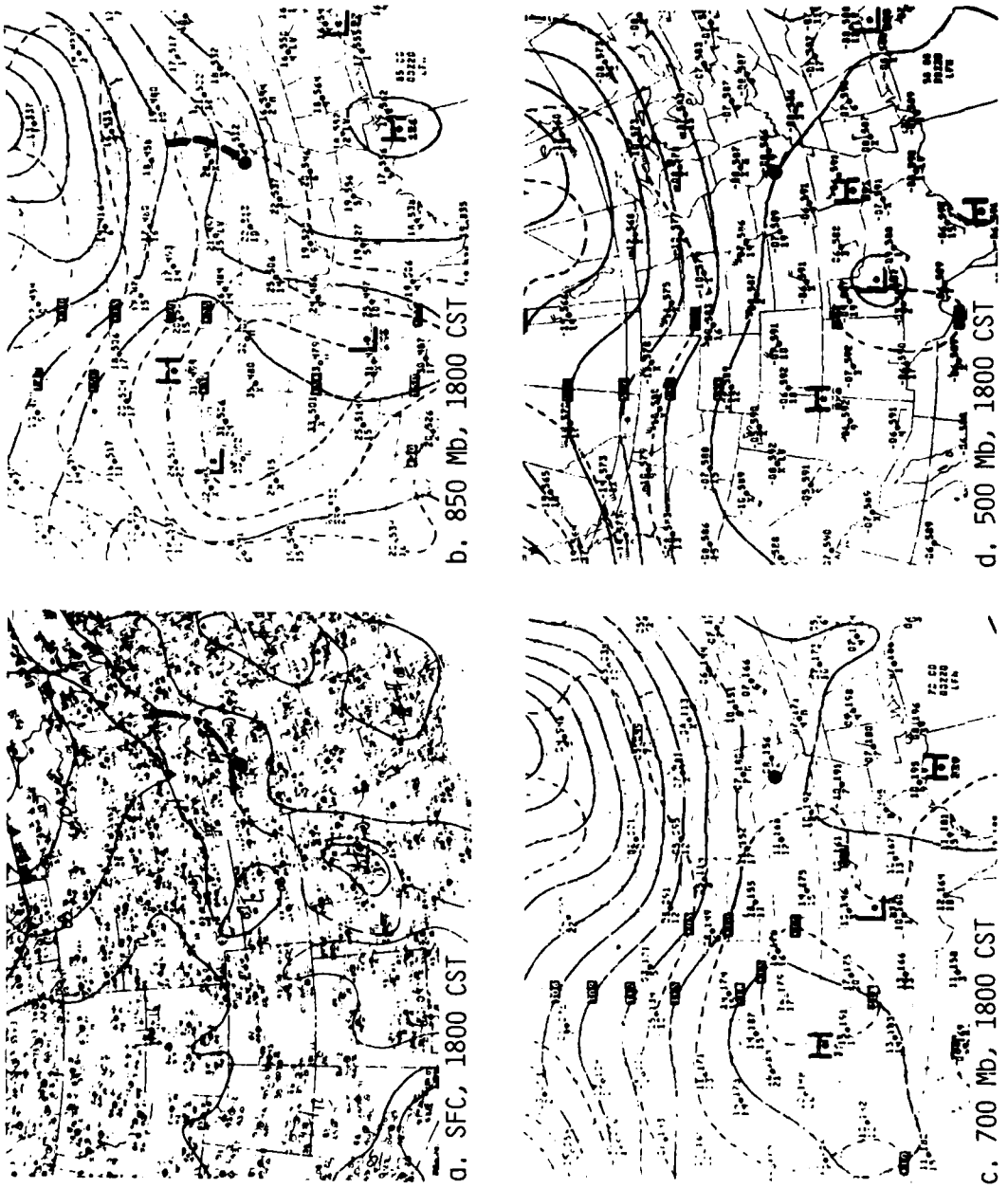

Figure G2. National Weather Service synoptic analyses for 1800 CST 19 July 1975.

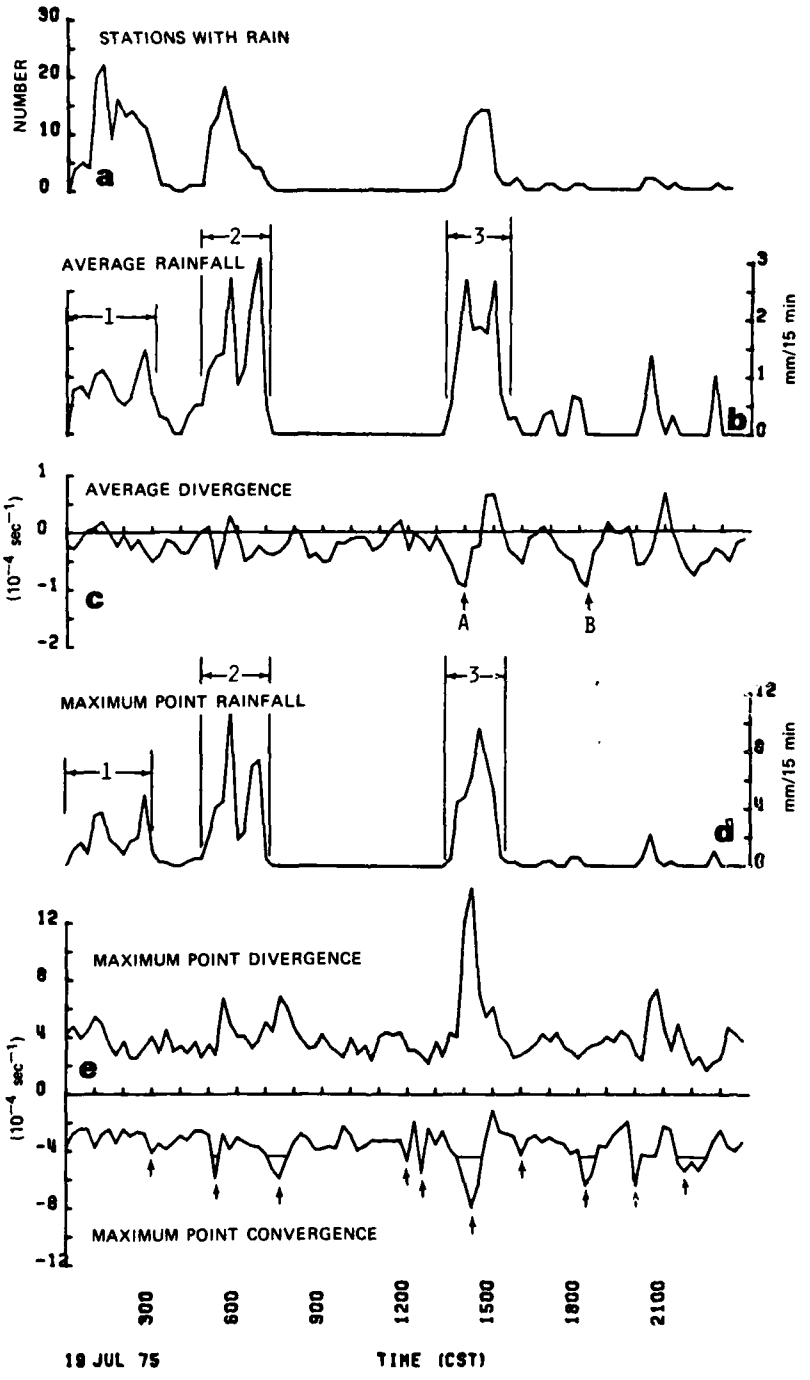

Figure G3. Time series of divergence and rainfall variables.

nearly simultaneous peak in the convergence was caused by local outflows that preceded showers moving onto the network. Otherwise, there was little or no increase in convergence in advance of rain event 3.

RAIN EVENT 1 0000-0300 CST 19 JULY

Regional Scale Situation

The shower activity over the St. Louis area from 0000-0300 was not accompanied by regional scale convergence that could be related to the rainfall. The wind field analysis for 0100 (Fig. G4) revealed mostly divergent flow over Missouri and Illinois. Diffluence was apparent within the southerly flow over parts of southeastern Missouri. The only significant convergence preceded a line of prefrontal thunderstorms approaching northeastern Iowa and southeastern Wisconsin.

Regional scale radar summary charts indicate that the St. Louis area was within an area of scattered light showers (see scalloped area in Fig. G4). This rain area began to increase in areal coverage and intensity shortly after 0000. Radar-echo tops increased from 20,000 feet at 0000 to 49,000 feet by 0300 with numerous echo tops exceeding 35,000 feet.

Mesoscale Situation

The first rain event on 19 July began as patches of light rain and a few light rain showers with rainfall amounts less than 5 mm. Individual cells moved eastward at 25 km hr^{-1} however, the rain areas seemed to propagate southeastward in long narrow bands. Figure G5 shows the development of one rain band during 0045-0130. At 0045, (Fig. G5a) Cell A formed near the northwest corner of the grid and Cell B formed about 5 km northwest of the Arch. Fifteen minutes later (Fig. G5b) a narrow band of light rain connected Cells A and B. Cell C appeared near the southeast corner of the network. At 0115 the light rain connected Cells B and C and extended southeastward to a new Cell D. The pattern had broken up by 0130 (Fig. G5d). Cell C had dissipated and Cells A, B, and D were diminishing in areal coverage and intensity.

According to the surface observations, a dense altocumulus layer covered much of central and eastern Missouri during the period of rain event 1. St. Louis reported towering cumulus capped by the altocumulus deck at 0300. This supportive information indicates that shower activity comprising the first rain event originated from middle level clouds with a few heavier showers developing from imbedded cumulus clouds.

A possible triggering mechanism for the rain bands could have been a series of southeastward propagating gravity waves. The southeastward propagation rate for the rain band in Fig. G5 and for other rain event 1 rain bands was estimated from the propagation of the interconnecting light rain areas to be 100 km h^{-1}.

The surface winds were light and southerly with a few gusts to 4 m sec^{-1}. These winds produced parallel bands of convergence and divergence that were oriented roughly 30 degrees to the rain bands. Figure G5 shows that a band of divergence with magnitudes up to 4U (dashed lines) persisted along a northwest

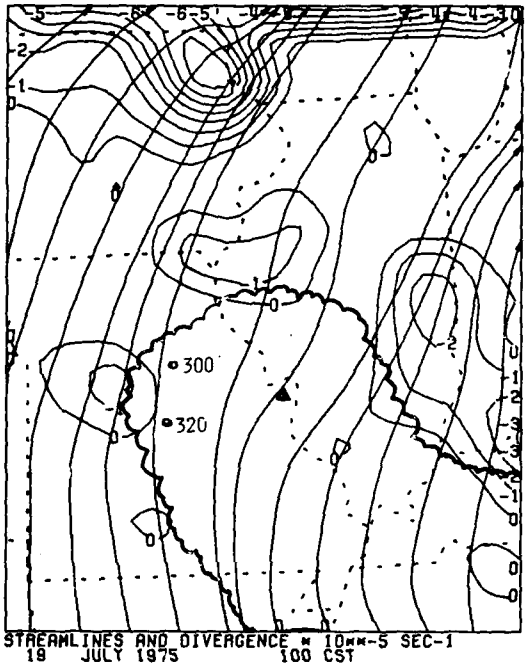

Figure G4. Regional scale analysis of surface wind field at 0100 CST. St. Louis area identified by triangle.

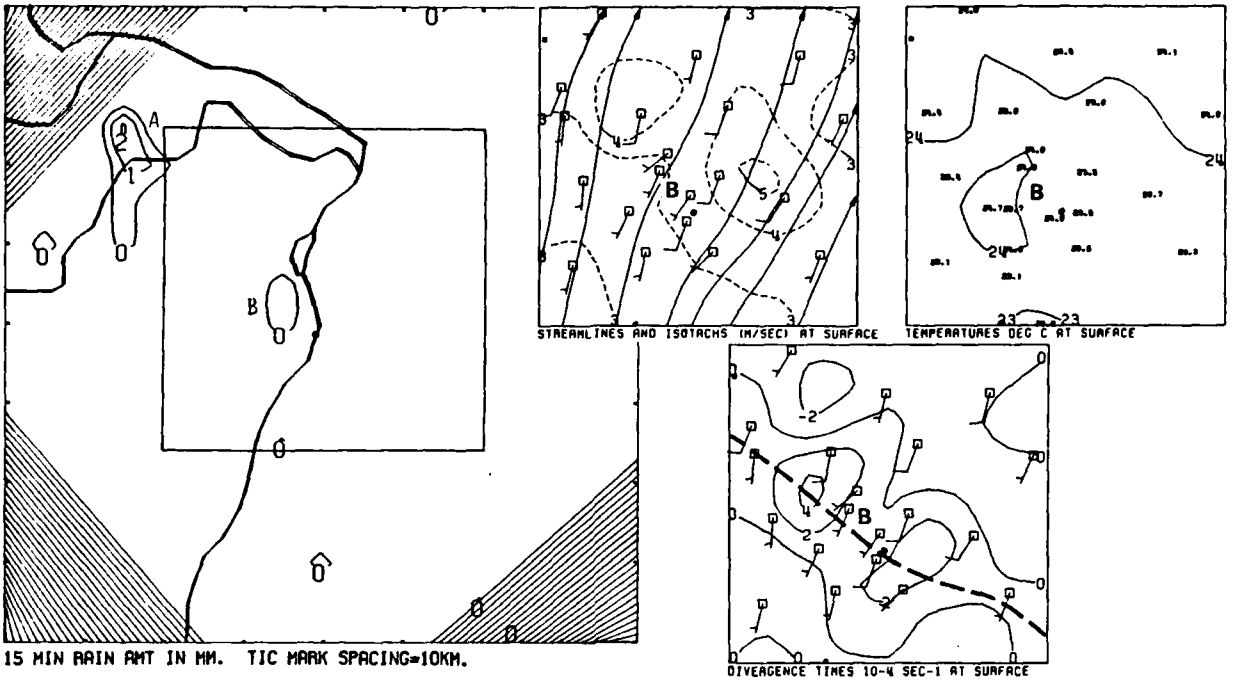

a. 0045 CST

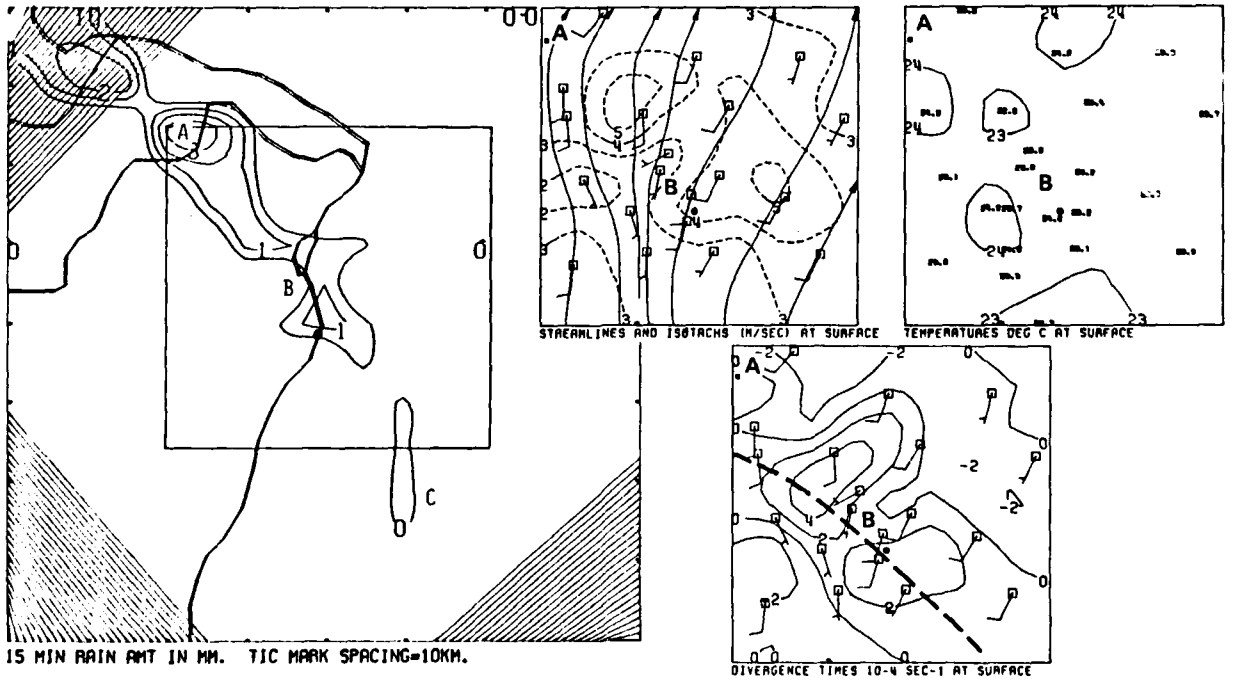

b. 0100 CST

Figure G5. Composite of the objective isotachs and streamlines, temperature, divergence, and rainfall for 0045-0130 CST. St. Louis Arch identified by black dot.

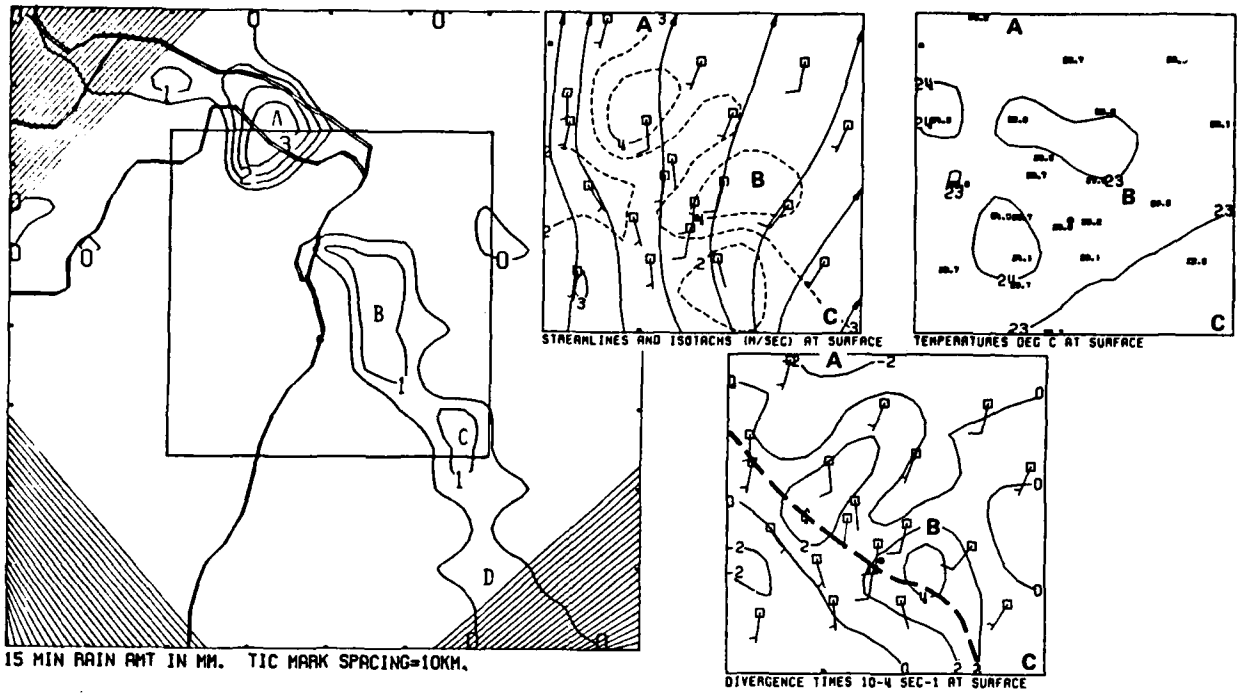

c. 0115 CST

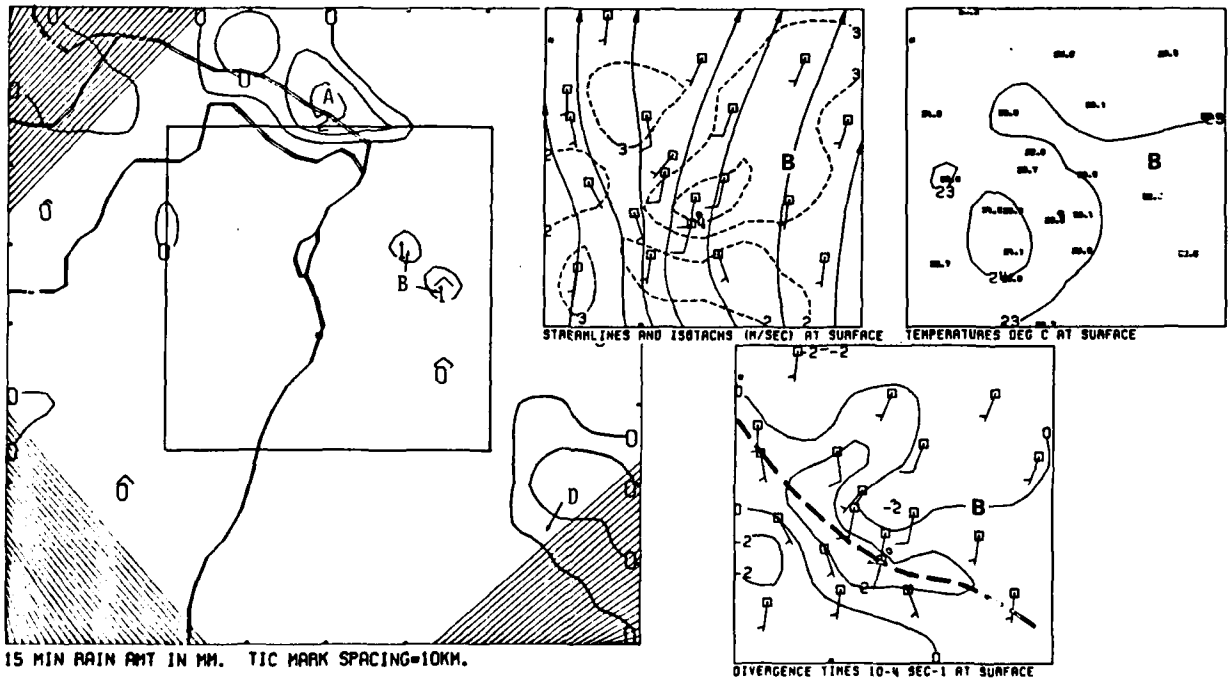

d. 0130 CST

Figure G5. Concluded

to southeast axis through the urban area. These bands had developed several hours prior to the rain within the network and persisted for several hours after the rain had moved away. Since a similar banded divergence structure had appeared on other case days, there was no reason to conclude that the bands were related to the development, movement or orientation of the rain areas.

RAIN EVENT 2 0500-0700 CST 19 JULY

Regional Scale Situation

Radar summary charts indicated that the area of scattered light rain showers that developed over eastern Missouri persisted although rain had ceased over the wind field network by 0300. Cells within this rain area intensified and at 0500 radar echoes extending to 42,000 feet were observed. The regional scale wind streamline and convergence analyses continued to show divergent flow over eastern Missouri and most of Illinois as in Fig. G4. Again it appears that the rain system was not coupled with the boundary layer flow.

Since there was no clearly defined pre-rain response in the mesoscale and the regional scale divergence fields, the synoptic charts were searched to find the intensification mechanism. The 0600 synoptic scale analysis at 850 mb (Fig. G1b) reveals a strong low level jet with wind speeds exceeding 17 m sec^{-1} over the St. Louis area. Both the height and wind analysis placed a small perturbation with strong convergence at 850 mb over eastern Illinois. Radar summary charts show that this convergence zone was located along the leading edge of the general area of strong thunderstorms that covered most of Illinois and eastern Missouri at 0600. There was no reflection of either the perturbation or the jet stream at 700 mb or above, nor as revealed by the surface regional analysis was there a reflection of the jet stream in the surface layers. It is possible that the passage of the perturbation through eastern Missouri prior to 0600 led to the intensification of showers there.

Mesoscale Situation

The banded divergence structure persisted from 0300 through 0445 (Fig. G6a) in essentially the same location but with diminished strength. Three raincells appeared on or near the network at 0500 (Fig. G6b). Cell B, about 15 km west of the Arch, had no reflection in the surface wind field. By 0515 (Fig. G6c) a wind shift north of the network near Cell C caused the appearance of a 4U convergence center (arrow). Meanwhile, Cells D and E formed with no reflection in the surface wind field.

Outflow from Cell D penetrated the boundary layer to form a 6U divergence center (arrow Fig. G6d) and a wind shift from south to southwest (indicated as a gust front). Cell D formed a complex with cell F which appeared 5 km west of the Arch and Cell G which appeared simultaneously with the passage of Cell D's gust front. Cell F dissipated by 0545 (Fig. G6e). The Cell D, G complex moved to the eastern edge of the network and intensified to produce 10 mm/15-min rainfall. Outflow from this complex pushed northeastward off the network.

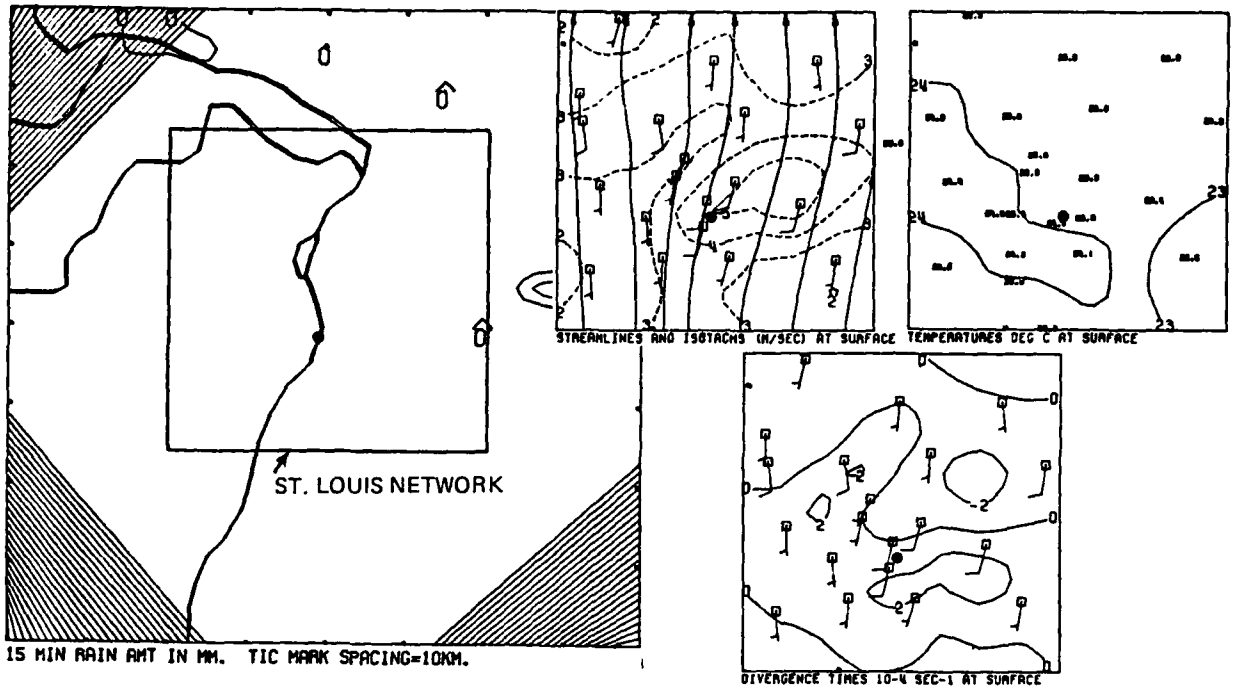

a. 0445 CST

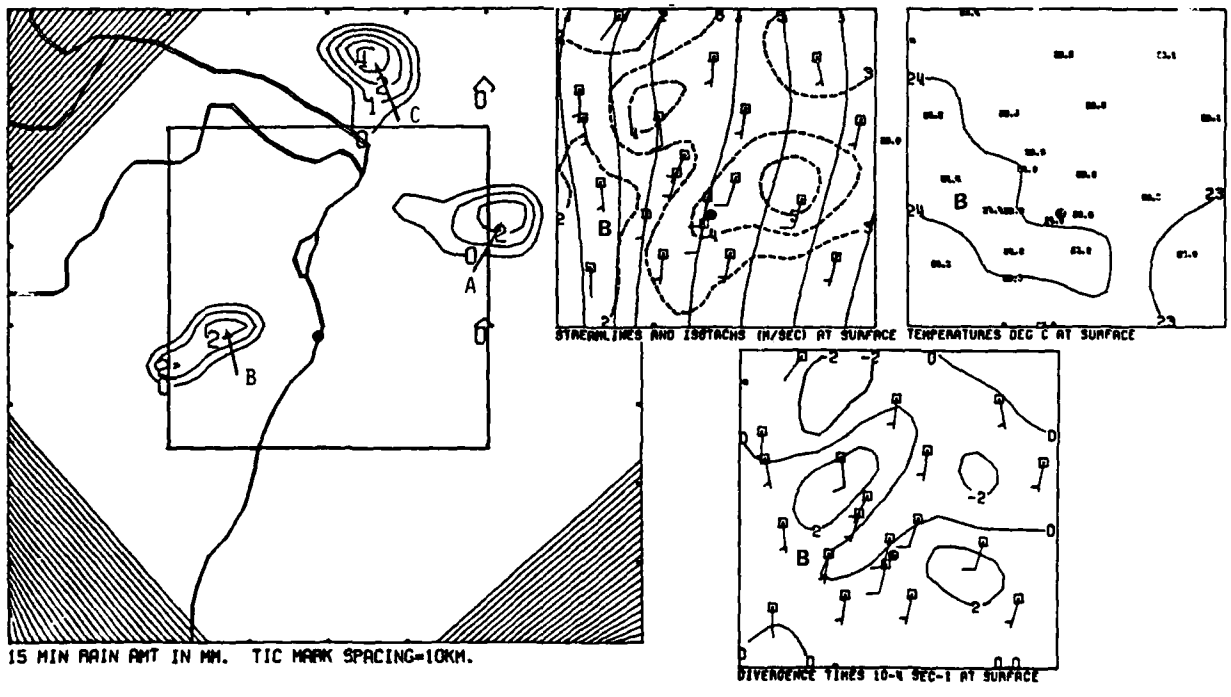

b. 0500 CST

Figure G6. Composite of the objective isotachs and streamlines, temperature, divergence, and rainfall for 0445-0600 CST.

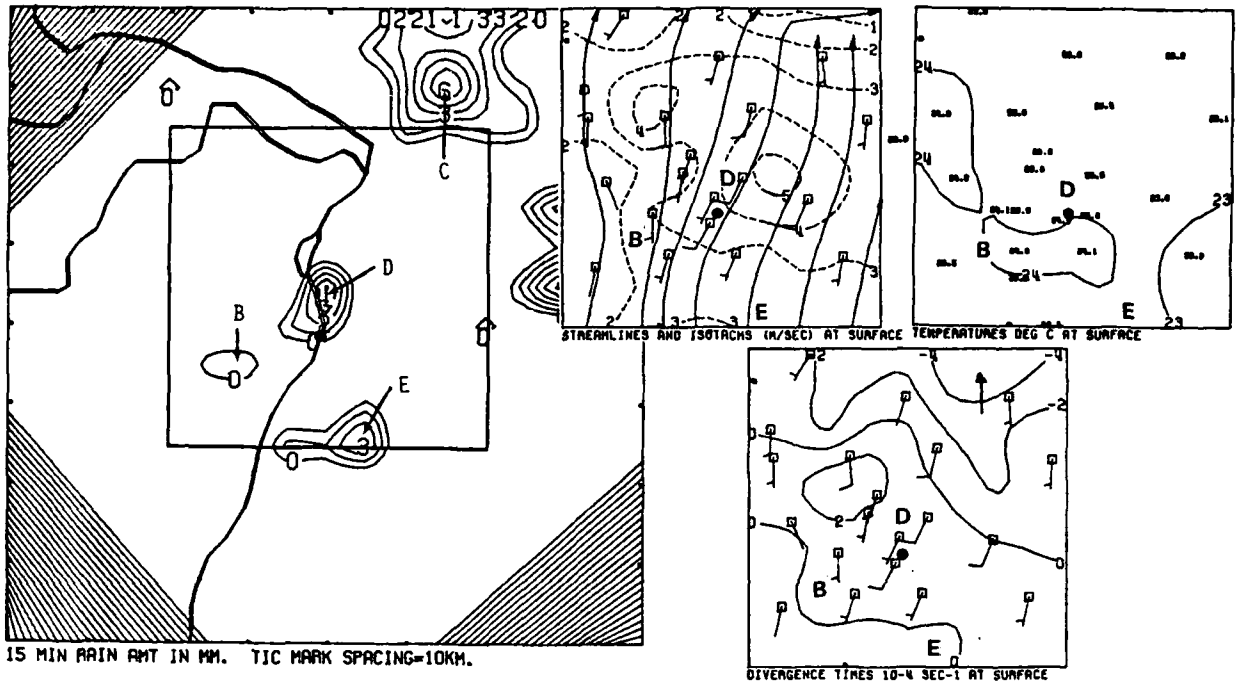

c. 0515 CST

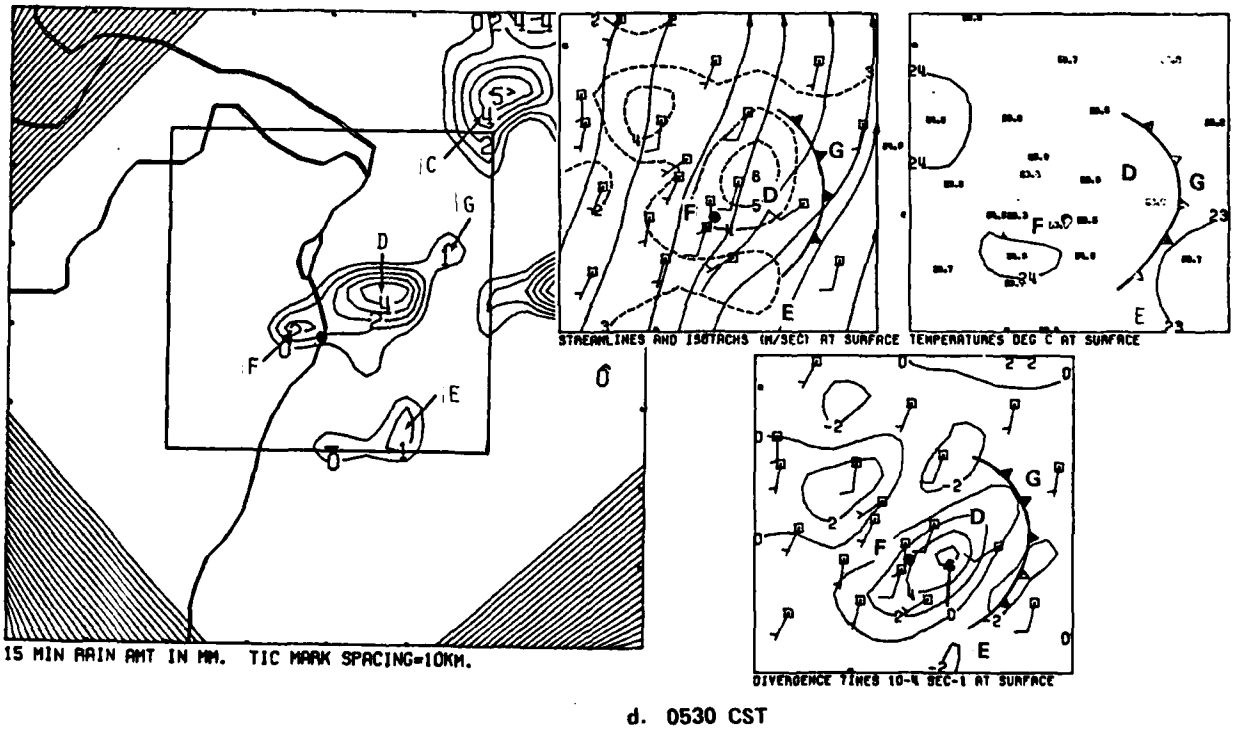

d. 0530 CST

Figure G6. Continued

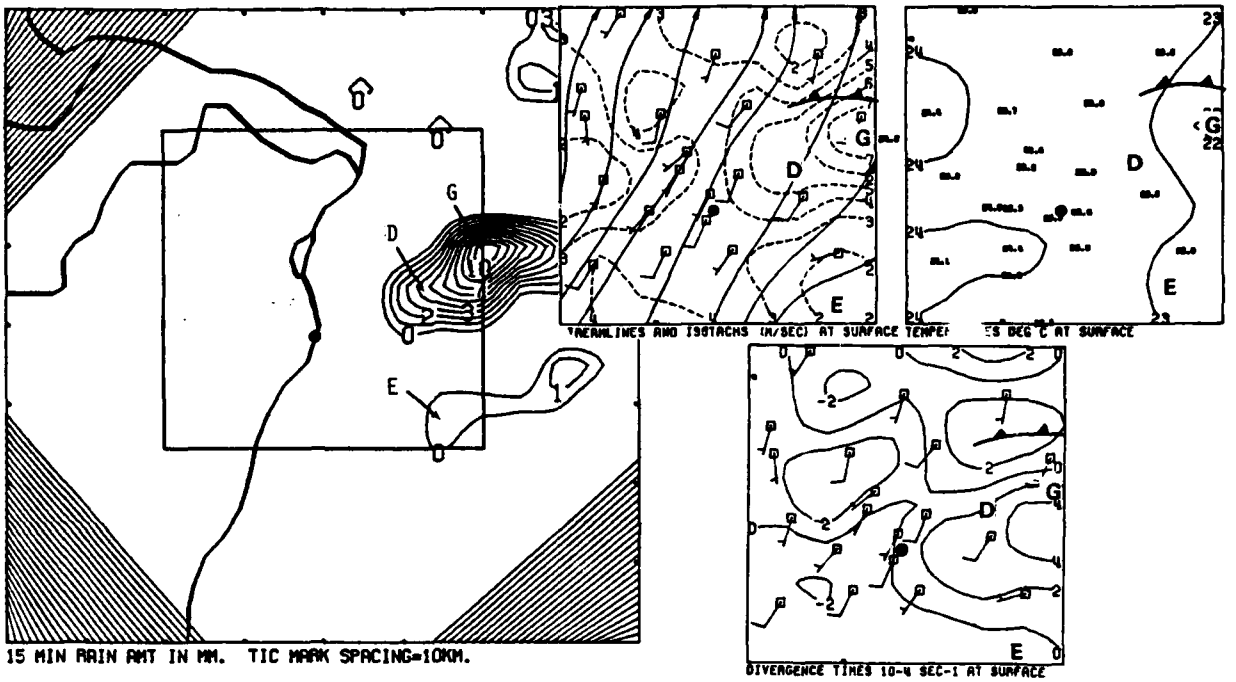

e. 0545 CST

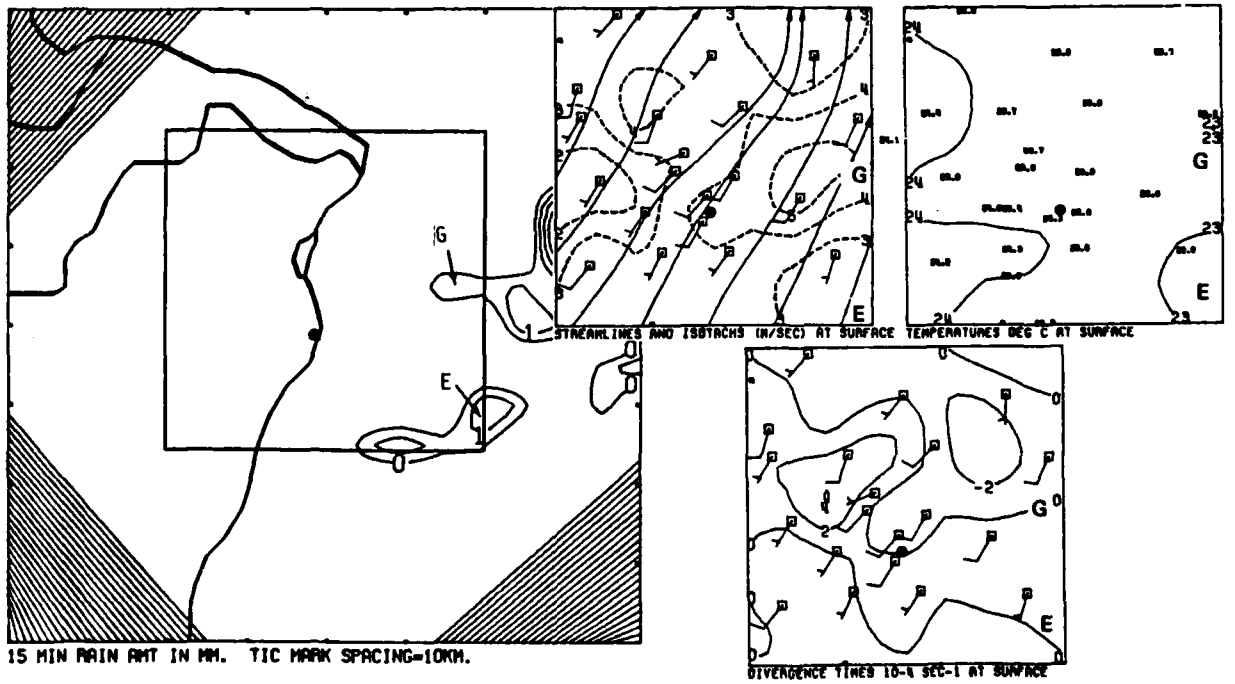

f. 0600 CST

Figure G6. Concluded

Cell G diminished rapidly after 0545 and Cell E moved off the network (Fig. G6f). Shower activity persisted along the southern edge of the network until 0700. Data in this area was insufficient to determine the character of the wind field.

RAIN EVENT 3 1330-1500 CST 19 JULY

Regional Scale

The weather system that triggered convective rainfall over the METROMEX rainfall network between 1345 to 1500 was present in the synoptic and mesoscale surface wind fields several hours prior to precipitation development. The wind field over most of Missouri including the St. Louis area gradually switched to westerly in apparent response to 1) the subsynoptic pressure field that developed troughing to the east and ridging to the west of St. Louis and 2) mixing with strong westerly flow within the 850 mb low level jet stream as the mixing layer deepened in response to surface heating during the mid-morning. Over Arkansas and southern Missouri there were northward moving airmasses that were subject to neither of the above forcings. The persistence of the momentum imbalance led to increasing convergence and by 1200 a well developed subsynoptic convergence zone covered most of the southern one-half of Missouri.

Figure G7 shows the regional scale streamline and divergence fields for 1100 and 1200. The subsynoptic scale convergence zone that developed south and west of the St. Louis network is identified by the arrows. This convergence zone corresponds well with an area of deep cumulus clouds over Missouri south of St. Louis at 1100 (Fig. G8a). Cloud line A was not within the convergence zone at 1100 but was located near the westward extension of the zone at 1200 (arrows).

Cloud line B appeared parallel to and about 50 km south of cloud line A at 1200 (Fig. G8b). Showers along both cloud lines developed eastward to influence the St. Louis network wind field by 1400. These showers were small in areal extent, but extended to great depths as indicated by radar summary charts. Tops ranged from 46,000 ft at 1135 to 55,000 ft by 1335.

Mesoscale Situation

At 1300, wind flow over the St. Louis network from 250-1350 m was generally westerly (Fig. G9). Within this general flow was considerable variation in speed and direction - gustiness that might be expected in a situation of strong vertical momentum exchange between the surface flow and the 850 mb jet stream (Fig. G1b). The vertical motions over the network (Fig. G10) were mostly subsident. A center of -30 cm sec^{-1} subsidence about 15 km southeast of the Arch was located above a 2U surface convergence center (arrow, Fig. G11a), an indication that surface kinematic fields were not representative of the kinematic fields in the boundary layer. Rising motions were confined to the extreme southwest and near the northeastern corner of the network.

The wind field at 1300 (Fig. G11a) was generally westsouthwesterly and the divergences were within the background levels. The 2U convergence center east of the Arch (arrow) was beneath an area of strong subsidence aloft. A

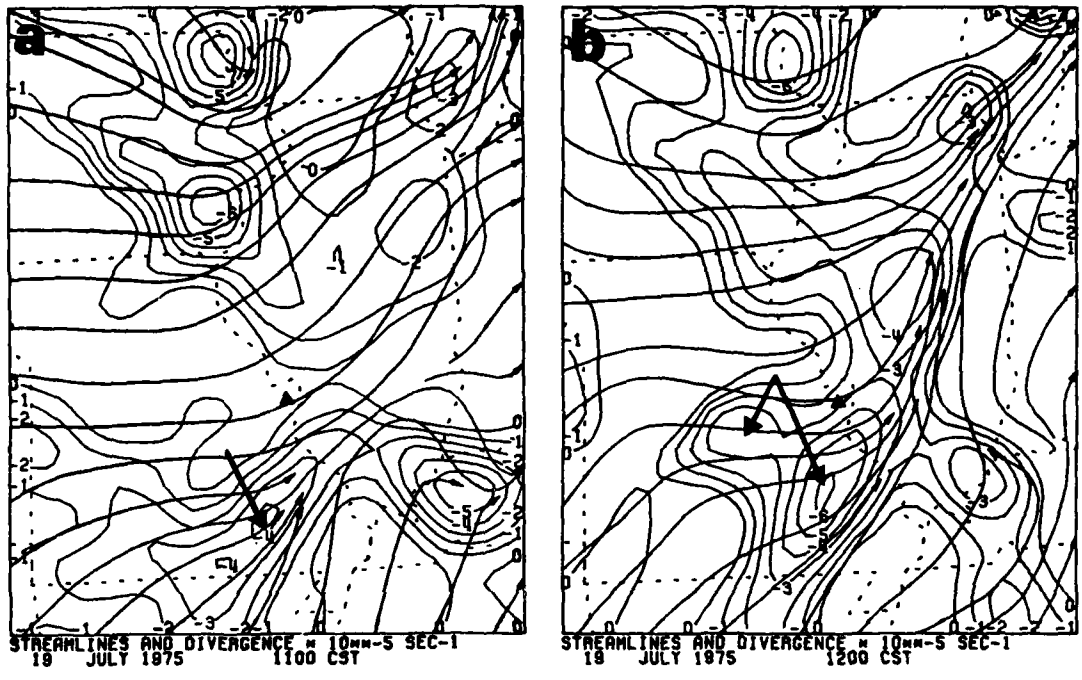

FIGURE 8

Figure G7. Regional scale analysis of surface wind field at 1100-1200 CST.

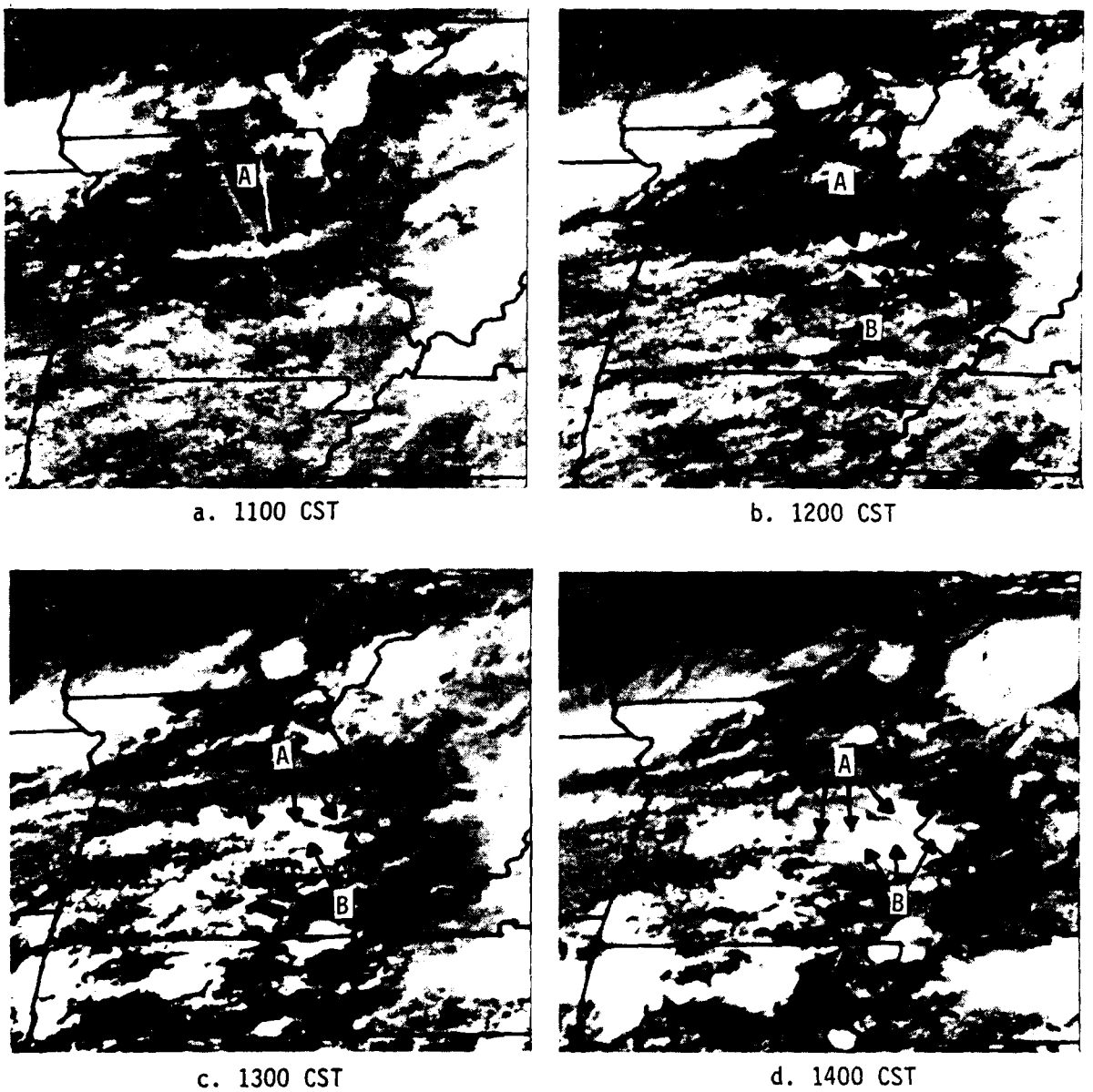

a. 1100 CST

b. 1200 CST

c. 1300 CST

d. 1400 CST

Figure G8. GOES satellite photographs of the Midwest for 1100-1400 CST showing the evolution of convective showers along two parallel cloud lines. St. Louis identified by black dot.

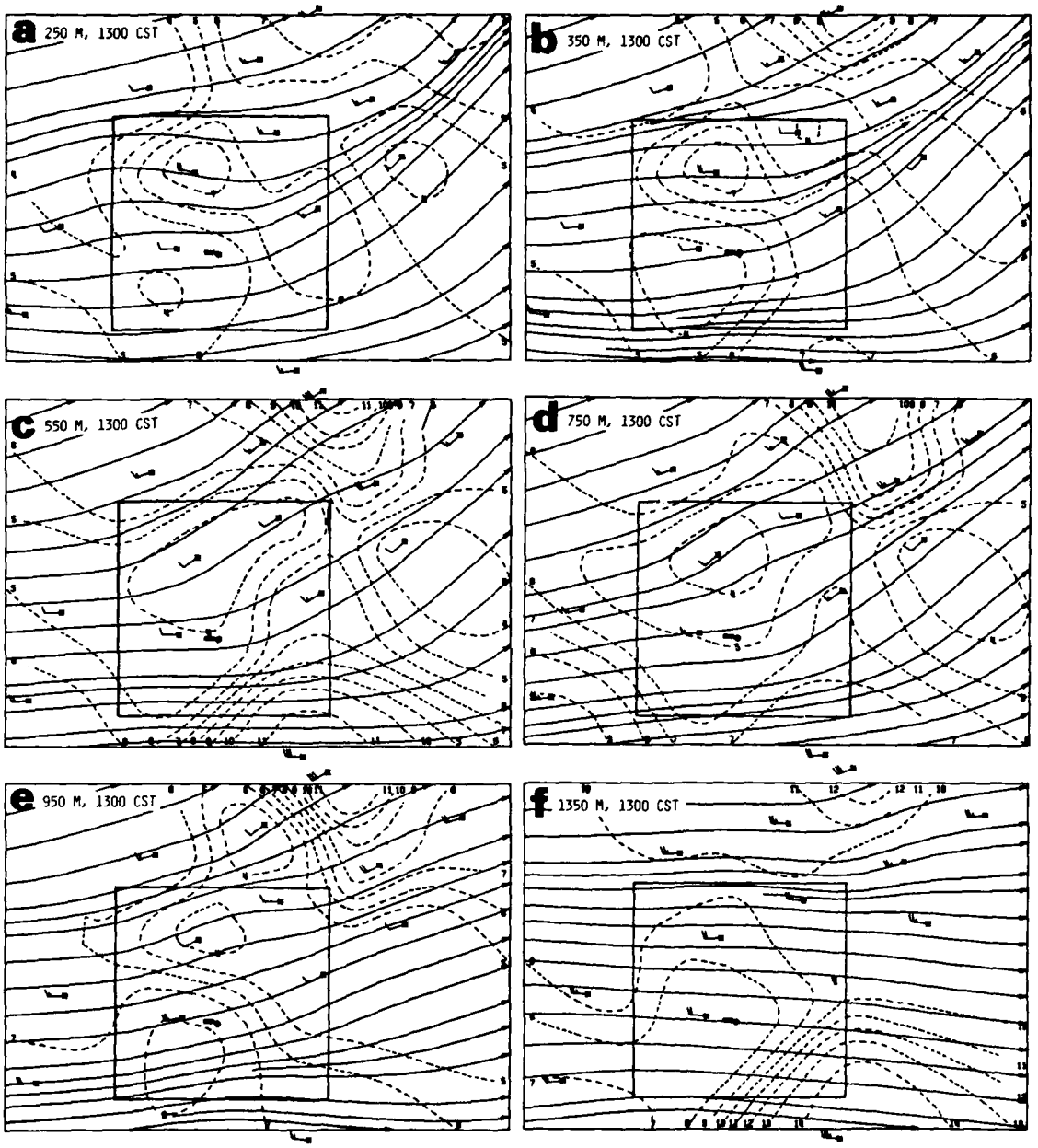

Figure G9. Objective streamlines and isotachs (m sec^{-1}) for 1300 CST at 6 heights msl.

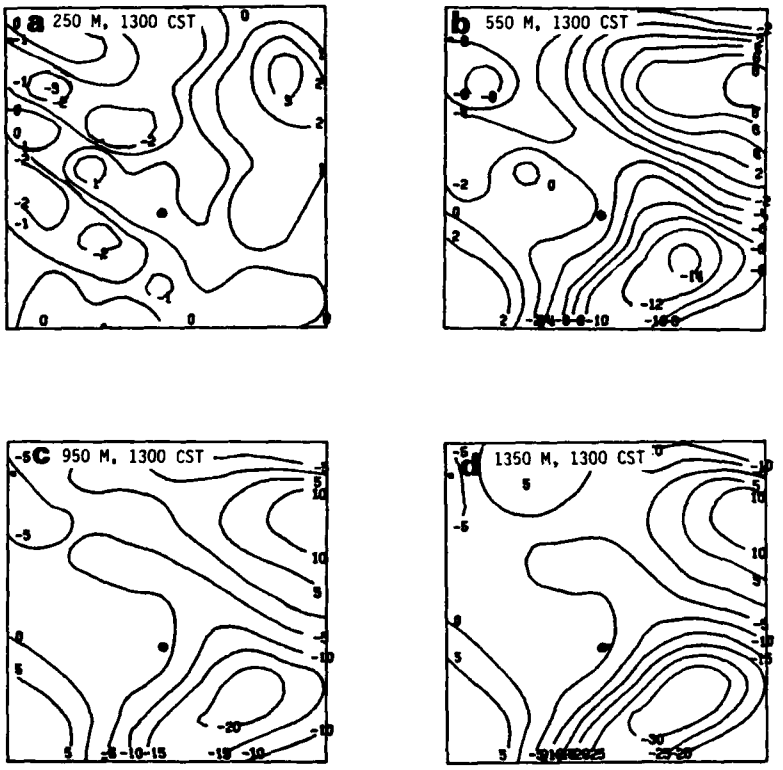

Figure G10. Vertical velocity maps (cm sec^{-1}) for 1300 CST.

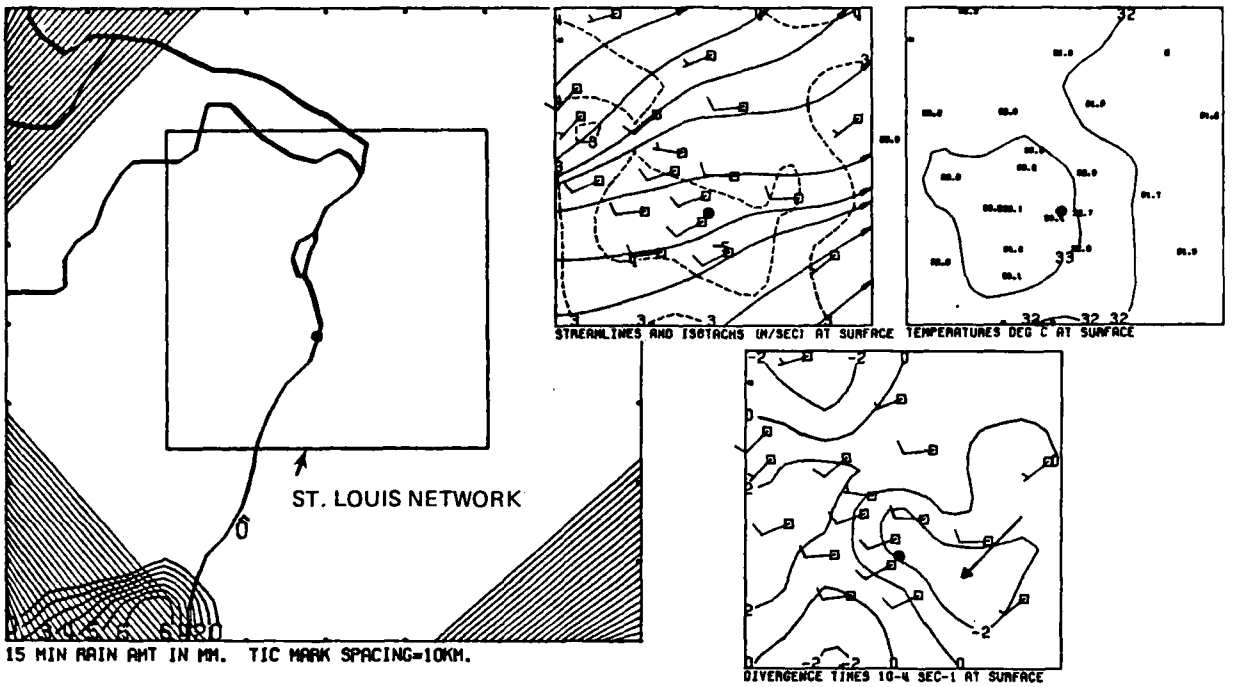

a. 1300 CST

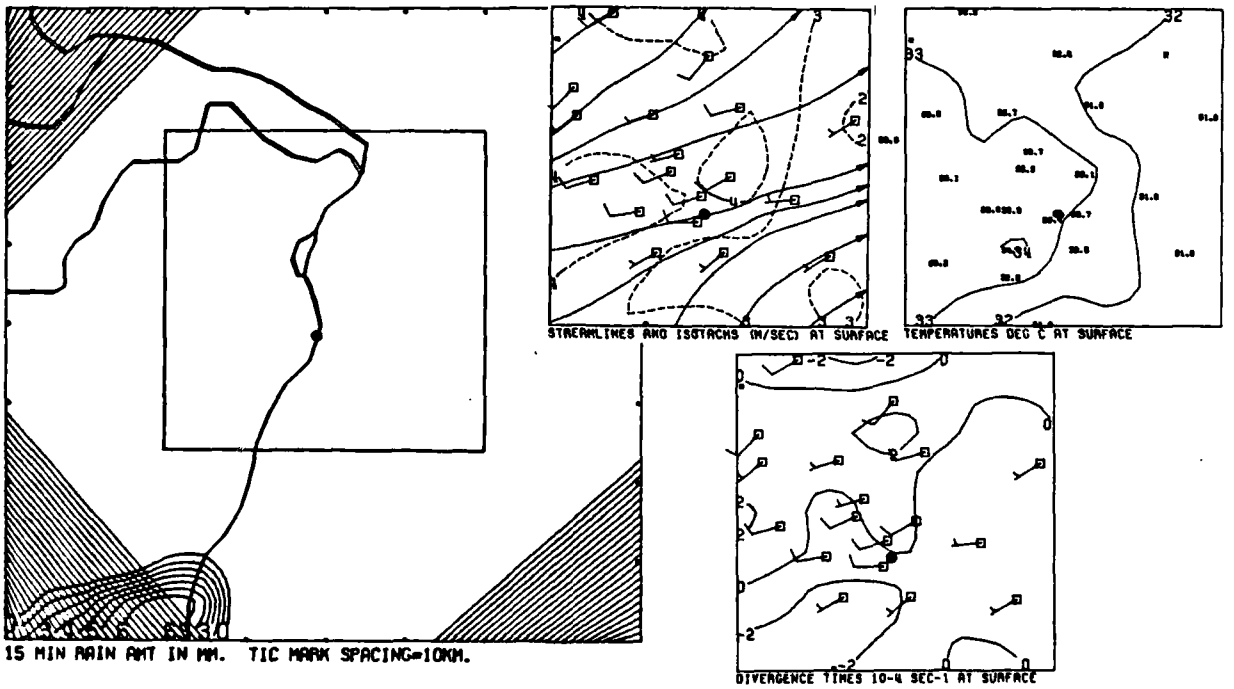

b. 1315 CST

Figure G11. Composite of the objective isotachs and streamlines, temperature, divergence, and rainfall for 1300-1500 CST.

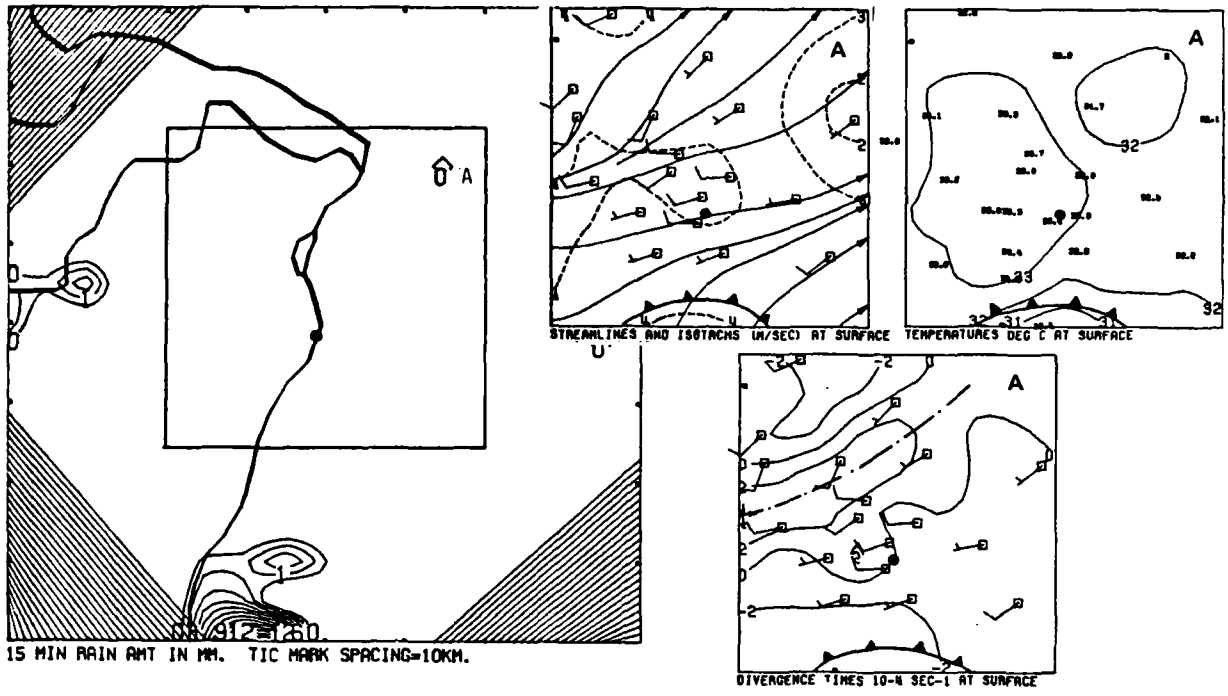

c. 1330 CST

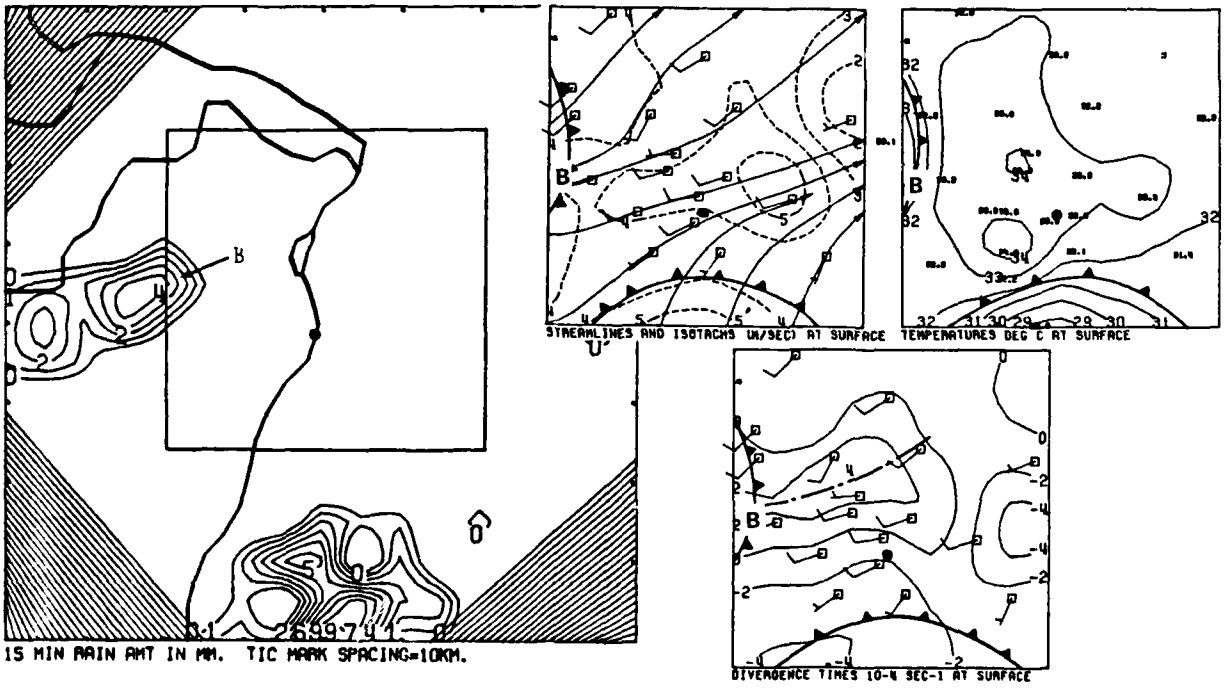

d. 1345 CST

Figure G11. Continued

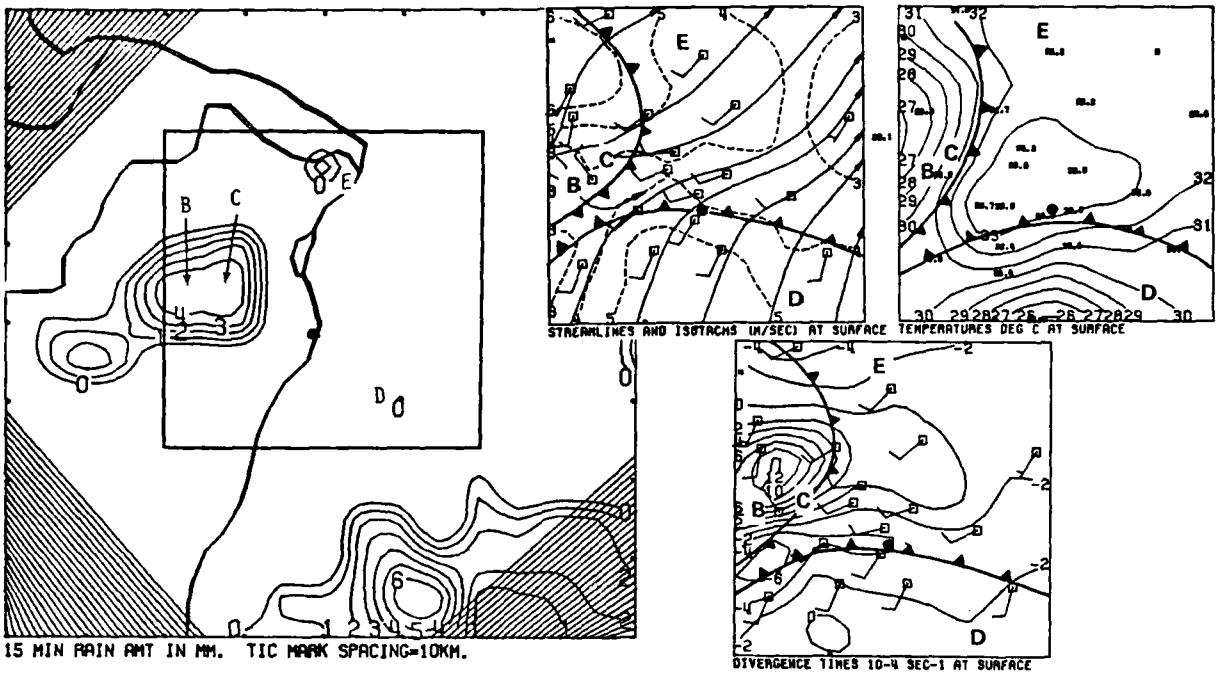

e. 1400 CST

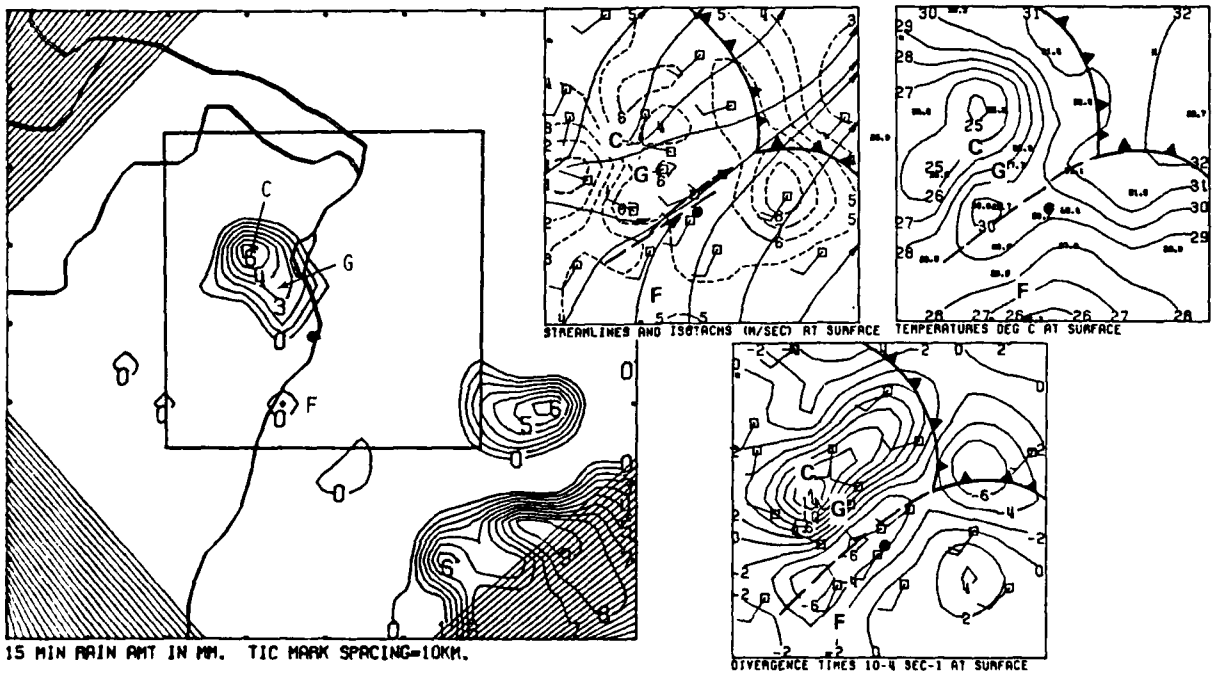

f. 1415 CST

Figure G11. Continued

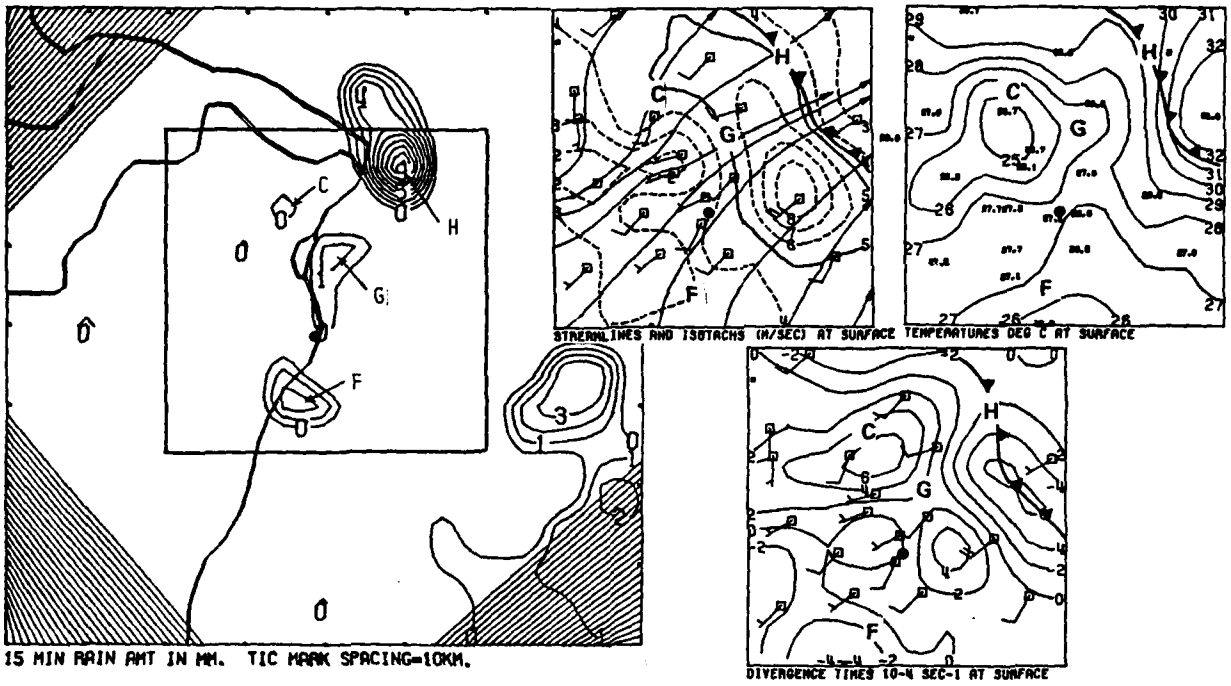

g. 1430 CST

Figure G11. Concluded

raincell associated with cloud line B (Fig. G8c) drifted onto the southern part of the METROMEX raingage network. Temperatures ranged from near 31C to 34C with the warmest readings located over the urban area. Two other convergence areas located at the north and south network boundaries persisted at 1315 (Fig. G11b) as the southeastern convergence area dissipated.

The wind field organized into parallel convergence and divergence zones at 1330 (Fig. G11c). Cell A appeared near the northeastern end of the divergence zone (dash-dot line) which was better organized than the convergence areas. This divergence increased to 4U (Fig. G11d) as gust fronts from raincells within cloud lines A and B moved onto the network.

Raincells B and C moved directly down the divergence zone (Fig. G11e). Their gust front increased the convergence along the northern part of the network to 4U. Cell E formed ahead of this gust front within an area of little or no convergence. Meanwhile, Cell D formed behind the gust front from cloud line B as it pushed northward to near the Arch. The convergence zone accompanying this gust front included a 6U center near the junction with the gust front from complex B, C.

Strong 6U convergence persisted along the intersection of the two gust fronts (Fig. G11f) and Cell F formed immediately downwind from one of these centers. Cell H formed at the eastern end of the pre-storm divergence area (Fig. G11g) as the combined gust front passed. Some time must elapse from between the ascent of a moist airmass from the surface and rain at the ground. The simultaneous appearance of Cell H with the gust front passage suggests that the gust front did not trigger the raincell.

SUMMARY OF SHOWER DEVELOPMENTS ON 19 JULY

Weather systems on different motion scales combined to produce favorable conditions for precipitation over the St. Louis area on 19 July. Showers occurred intermittently throughout the day. Three major rain systems 0000-0300, 0500-0700, and 1330-1500 were selected for study.

The synoptic scale circulation was generally anticyclonic from the surface to 500 mb. No frontal systems were present in the St. Louis area. Regional and mesoscale weather systems were the predominant precipitation producers.

The rain event from 0000-0300, possibly triggered by gravity waves, consisted of numerous small patches of light rain. Rainfall was apparently from a dense altocumulus cloud deck that had embedded cumulus elements. There was little or no relationship between the precipitation and the surface convergence centers.

The second rain event from 0500-0700 began in an apparent response to the passage of a convergent disturbance within the 850 mb low level jet stream that was located over the St. Louis area. The formation of these raincells was not directly related to surface convergence centers. Seven raincells developed over or sufficiently near the network to potentially influence the wind field. Five of these cells formed within the network.

Table G1 summarizes the cell strengths, convergence strengths, and convergence durations for the raincells that formed within the St. Louis

network during rain event 2. The lower half of the table summarizes the convergence strengths and durations for the convergence centers that existed during the same period. Cell strengths ranged from 2.0 mm to 12.0 mm. The average cell strength was 6.8 mm. None of the raincells formed within the convergence areas although seven convergence centers were present during the period. The convergence areas were weak; only one (No. 5) exceeded 4U and this was in response to a shower outflow.

The third rain event began at 1330 and lasted for 1.5 hours. Although there was evidence for coupling with the surface airmasses (no raincells developed after the network was occupied by rain cooled airmasses), there was almost no relationship between the raincell location and timing and the surface convergence. Eight raincells formed over or sufficiently near the network to influence the wind field. Seven cells formed within the network. Table G2 summarizes the convergence and rainfall strengths for these seven cells and for eight convergence centers that occurred during the same period. The strongest raincells (11.0 mm and 21.0 mm) were not preceded by convergence. Only two raincells formed within the convergent areas (asterisks). These produced light rainfall amounts. Since heavier raincells formed over divergent areas, the convergence-rainfall relationship for rain event 3 was negative.

During this same period there appeared 8 convergence centers with strengths ranging from 2U to 18U and durations ranging from 15-min to 120-min. Only 2 of the 8 convergence centers were near raincells. These were a 2U 15-min center (Cell D) and an 18U 120-min center (Cell F). Cell F formed just downwind of the center after it had persisted for one hour. Cell F dissipated but the convergence center continued for an additional hour with no new cell development. Thus there was no apparent spatial relationship between the convergence centers and rainfall and the convergence centers were not predictive of raincell formation.

Table G1. Cell Strengths, Convergence Strengths, and Convergence Durations for Raincells that formed within the St. Louis Network between 0500-0700 19 July. Also, Convergence Strengths and Durations for all Convergence Centers that Occurred During the Same Period.

Cell ID	Cell Strength	Convergence Strength	Convergence Duration
B	3.0mm	0U	0 min
D	12.0	0	0
E	5.5	0	0
F	2.0	0	0
G	11.5	0	0
Number			
1		6	45
2		8	60
3		2	15
4		2	15
5		2	15
6		4	15
7		4	30

Table G2. Cell Strengths, Convergence Strengths, and Convergence Durations for Raincells that formed within the St. Louis Network between 1330-1500 19 July. Also, Convergence Strengths and Durations for all Convergence Centers that Occurred During the Same Period.

Cell ID	Cell Strength	Convergence Strength	Convergence Duration
A	0.5mm	0U	0 min
C	11.0	0	0
D	0.5	2	15
E	1.0	0	0
F	3.5	10	60
G	4.5	0	0
H	21.0	0	0
Number			
1		2	15
2		6	45
3*		18*	120*
4		18	60
5		12	60
6		10	30
7		12	60
8*		2*	15*

*Convergence centers were associated with raincells.

H. CASE STUDY: 30 JULY 1975

SYNOPTIC SCALE SITUATION

A tropical low moved into Mississippi from the Gulf of Mexico on 29 July and pushed copious amounts of moisture through a deep layer to 500 mb into the southern states (Fig. H1). The circulation of the tropical low coupled with the circulation around a large middle tropospheric anticyclone located over the Great Lakes produced southeasterly flow from the surface to 500 mb over the St. Louis network. This pattern had changed little by 1800 CST (Fig. H2).

Anticyclonic circulation prevailed at the surface in the vicinity of St. Louis throughout the day. A cold front associated with an upper level trough moving through the northwestern U.S. was held to the west over the northern plains (Fig. H2a). A weak stationary front located over the Ohio River valley at 0600 CST was dropped from the 1800 CST analysis, but a weak trough in the surface pressure field remained. There were no significant temperature and/or dewpoint contrasts across the western end of the front at either 0600 or 1800 CST.

The winds over Missouri and Illinois above 700 mb became light and variable as the pressure pattern became a series of minor highs and lows embedded within a large high pressure ridge that covered much of the eastern two-thirds of the U.S. At 300 mb, a low pressure center over northeastern Kansas at 0600 CST (arrow Fig. H1d) moved to southwest Missouri by 1800 CST (arrow Fig. H2d). The wind field around this low pressure center implied rising motions favorable for assisting deep convection over roughly the southern half of Missouri. It was within this area that thunderstorms broke out during the afternoon of 30 July.

Although the standard surface data gave no support for a frontal system in the St. Louis vicinity during 30 July, the satellite observations for 0846 CST (Fig. H3a) showed airmass differences in the amount of haze. Cloudiness associated with the tropical disturbance (L) covered much of the Gulf Coast area and most of Arkansas. Most of the central and west, including Illinois and Missouri, was cloud free and this gave a clear view of the contrast in haze between the tropical airmass brought northward with the tropical disturbance and a tropical airmass with a long residence time over the industrial areas of the central and eastern states. The boundary (arrows) extended along the stationary front from near West Virginia to southern Indiana and turned northwestward up the Mississippi valley through the St. Louis area. Then it curved southwestward toward Oklahoma as the hazy air was drawn into the tropical disturbance.

REGIONAL SCALE SITUATION

The regional scale surface streamline and convergence analyses for 1000-1300 CST (Fig. H4a-d) show the development of a convergence zone over southern Illinois and parts of Missouri and Iowa. The convergence zone over Illinois and Missouri formed along the approximate boundary between the clear

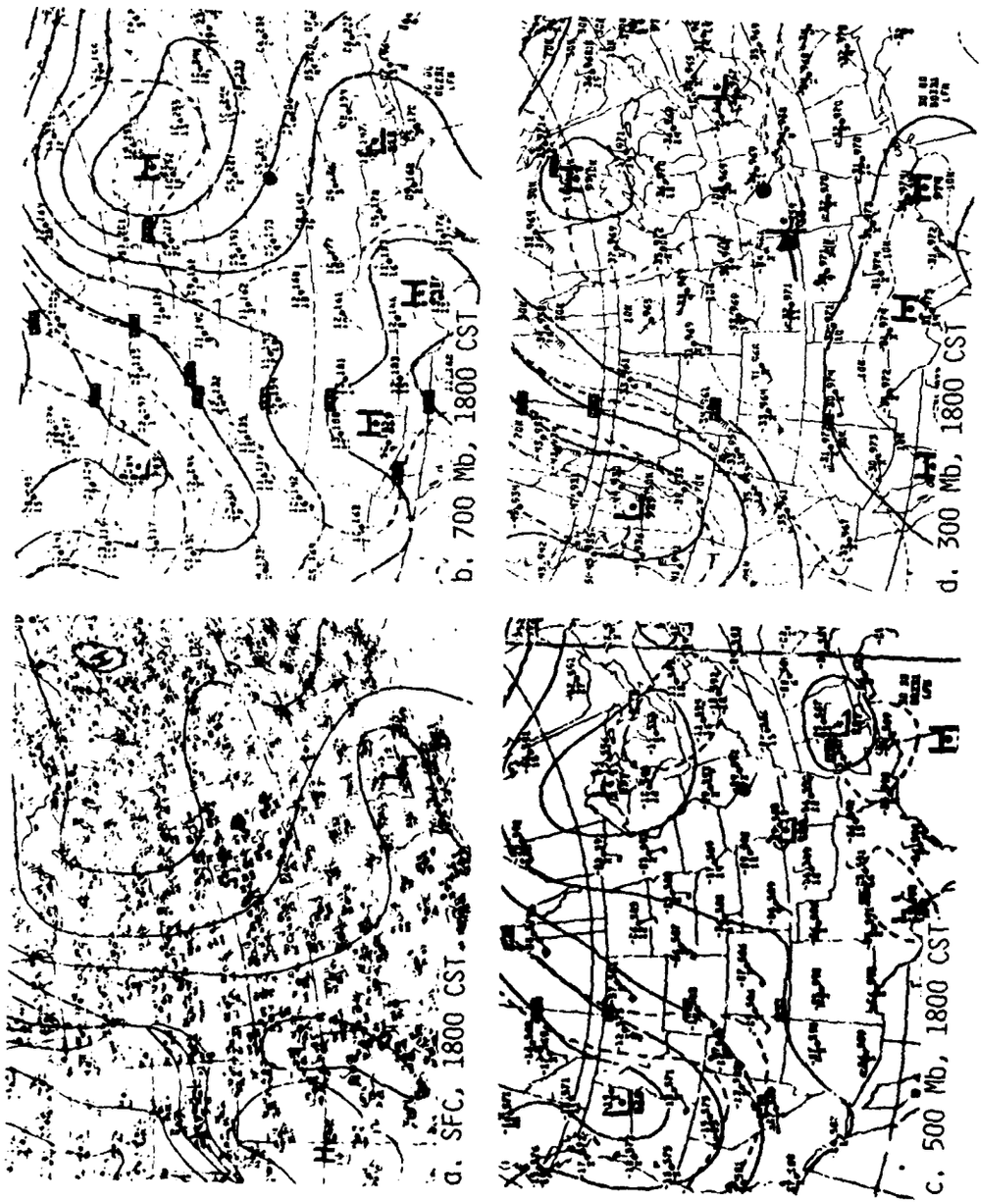

Figure H1. National Weather Service synoptic analyses for 0600 CST 30 July 1975. St. Louis area identified by black dot.

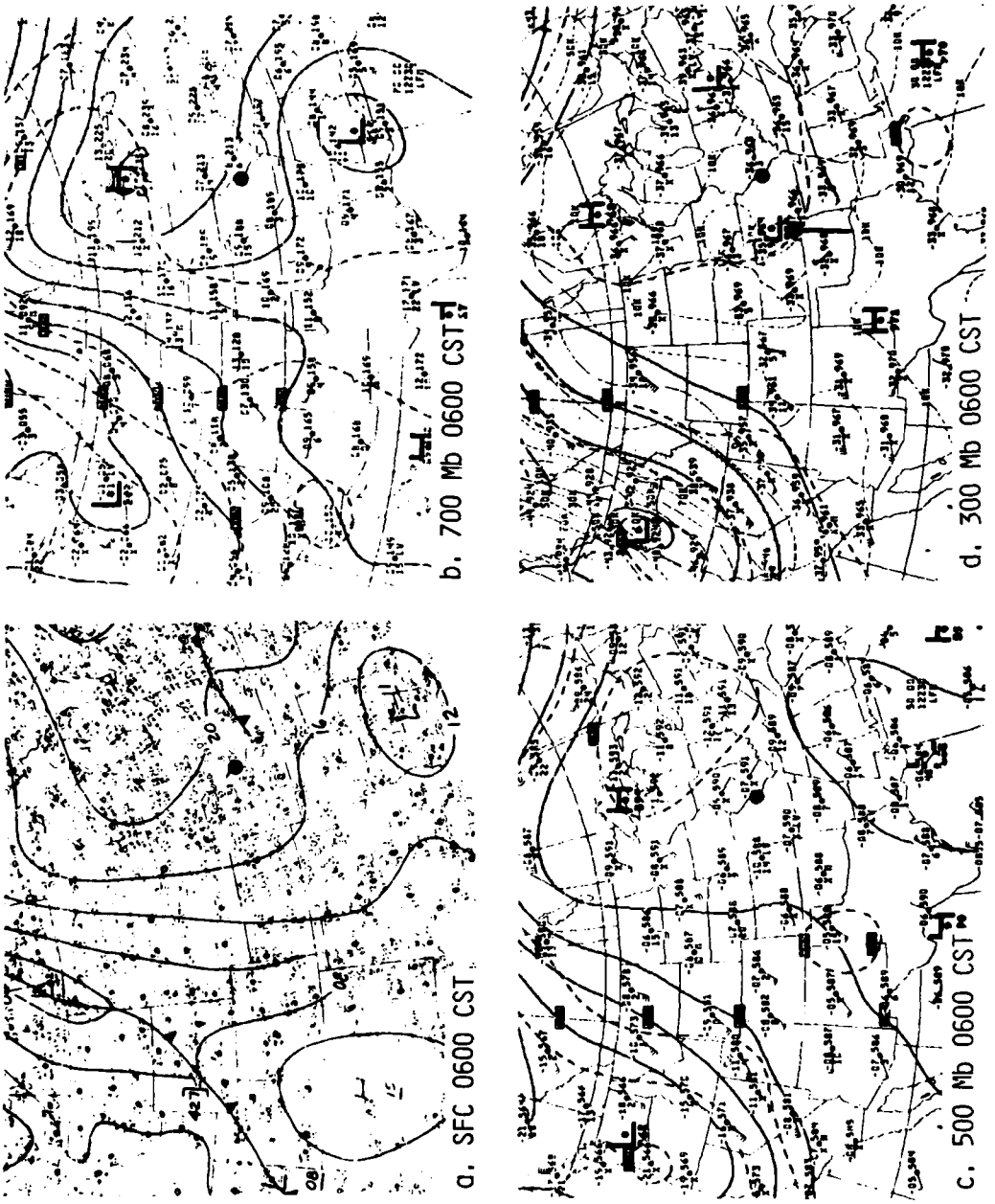

Figure H2. National Weather Service synoptic analyses for 1800 CST 30 July 1975.

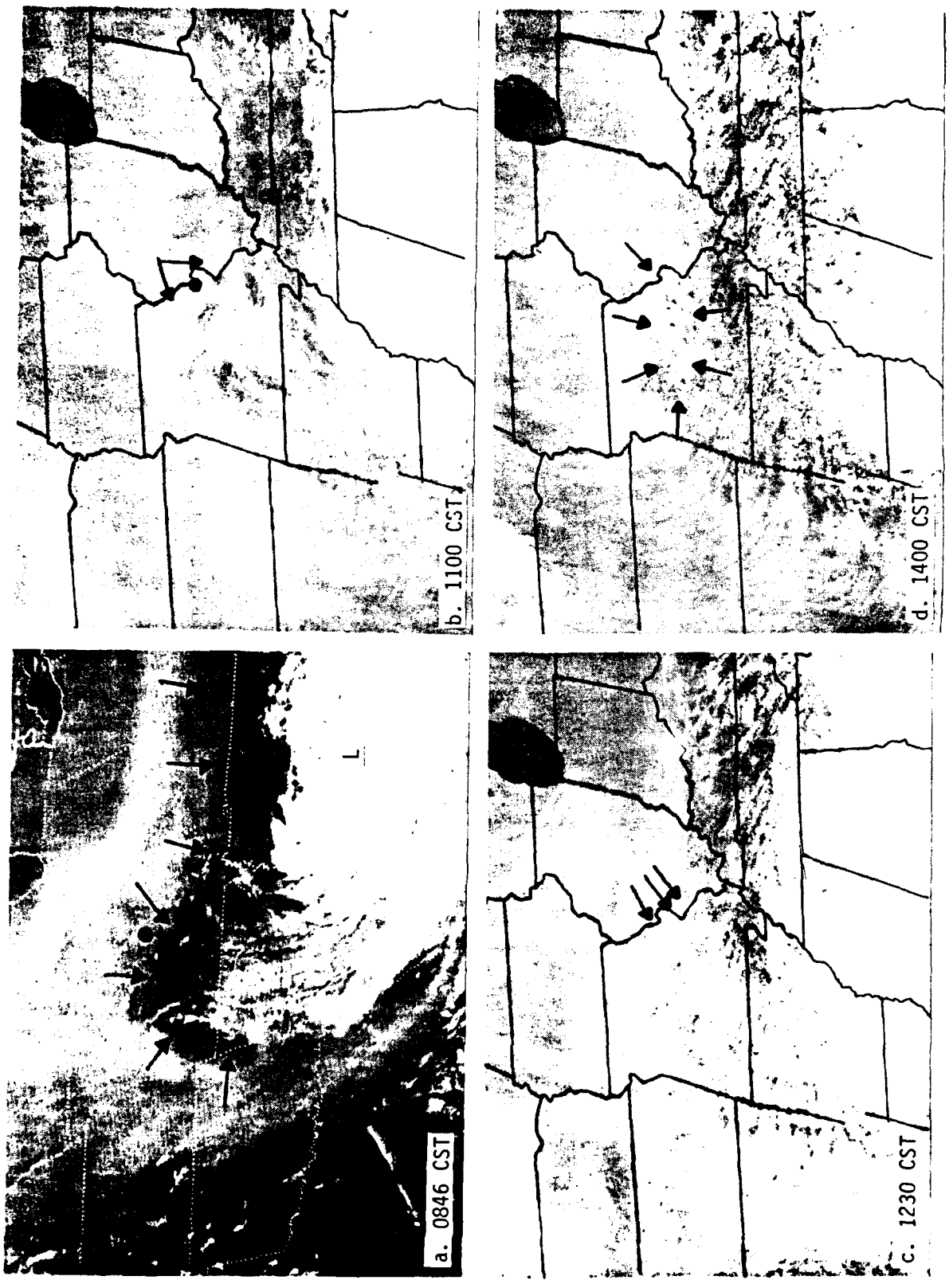

Figure H3. GOES satellite photographs of Midwest on 30 July.

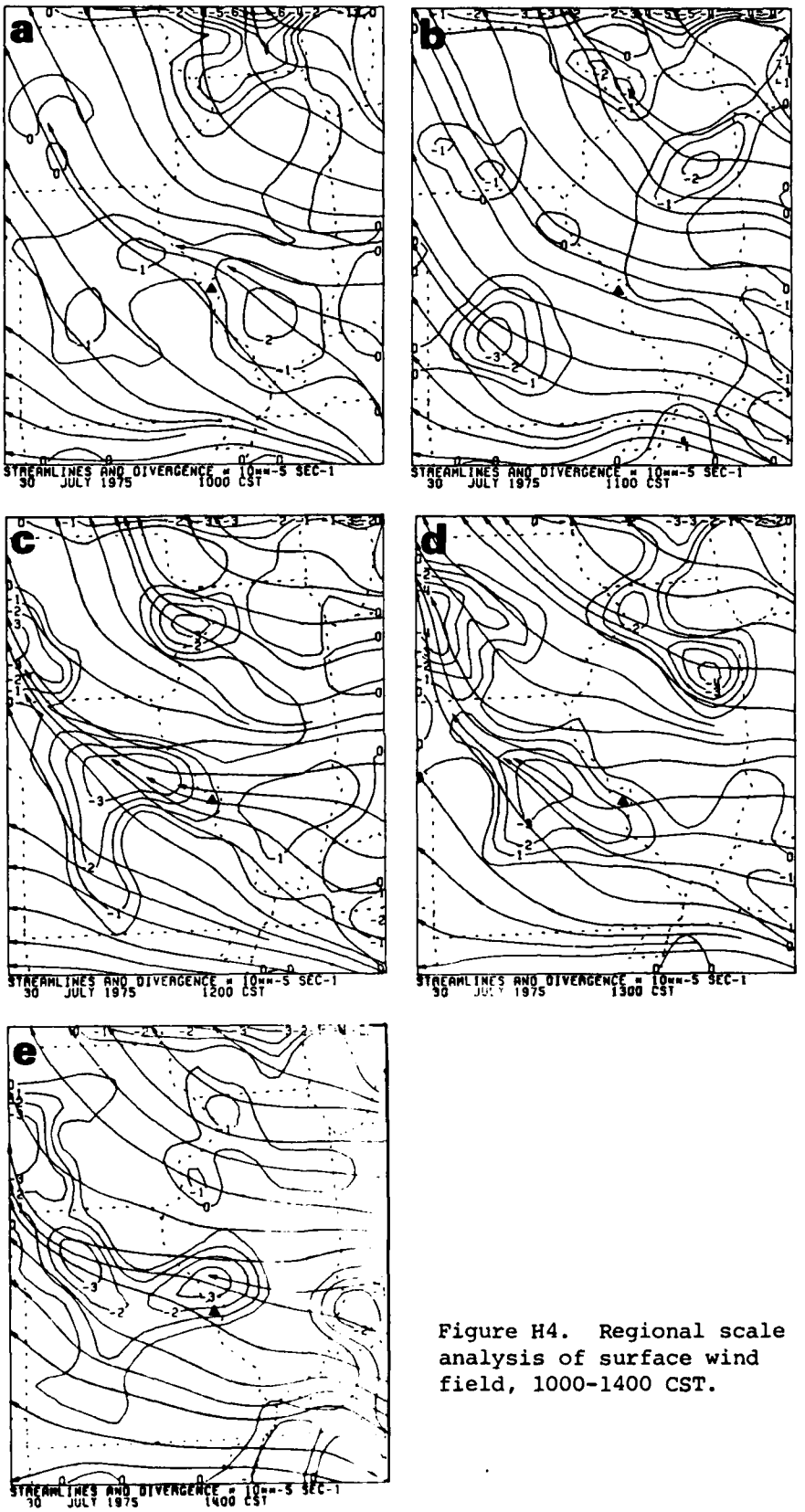

Figure H4. Regional scale analysis of surface wind field, 1000-1400 CST.

and hazy airmasses discussed above. It appeared over southern Illinois at 1000 CST, vanished at 1100 CST and reappeared at 1200 CST as a persistent and stronger convergence area over Missouri. Rain fell within the network shortly after 1200 CST.

The satellite observed numerous lines of cumulus oriented along the wind direction at 1100 CST (Fig. H3b). One line of towering cumulus (arrows) extended through the St. Louis area near the convergence zone. By 1230, the appearance of anvils (arrows Fig. H3c) identified three storms within the METROMEX raingage network. These were an isolated cloud field; there were no clouds of comparable development anywhere in the Midwest, save for the extensive cloudiness associated with the tropical disturbance.

By 1400 (Fig. H3d) the showery area had expanded westward from St. Louis to include much of central Missouri. The regional analysis for 1400 CST (Fig. H4e) indicated close correspondence between the convergence and the area of showers. Further, the showery area was within the area of possible upward vertical motion with the upper 300 mb low (Fig. H2d). The surface convergence may have been reinforced by the circulation within the low aloft.

TIME SERIES OF DIVERGENCE AND RAINFALL

Figure H5a-c gives the time series for the number of gridpoints at which rain fell, the average 15-min rainfall, and the network mean divergence. The showers were brief in duration and small in areal coverage. Fewer than 10 gridpoints "reported" rainfall at any one time and the sharp rainfall peaks indicate brief shower lifetimes. (The satellite views in Fig. H3 also show that the showers were small in areal coverage.)

The winds over the network were convergent, in the mean, from midnight until 0830 CST and again for two brief periods from 1015-1200 CST (arrow, Fig. H5c). The field became divergent at 1215 CST as showers began within the network. There was net convergence (inflow) over the network again between 1230-1300 CST (arrow B) when the wind field became dominated by shower outflows. Net convergence occurred again shortly after 1600 CST (arrow C), just before a second period of brief showers from 1645-1800 CST.

The time series for the maximum 15-min rainfall and the maximum and minimum divergence (convergence), (Fig. H5d, e) also show that the showers were brief. The background divergence (+/- 2.5U) was less on the 30th than on some of the other case days. The peak convergence exceeded background briefly several times prior to 0900 CST. Beginning at 1030 CST (arrow A) about 1.5 hr before rainfall, and except at 1445 CST, it remained above background. As will be shown in the section to follow, gust fronts and a mesoscale convergence zone developed the persistently strong convergence.

MESOSCALE SITUATION

The mesoscale convergence zone located in the regional scale surface wind field at 1000 CST (Fig. H4a) may have formed over the St. Louis area. Before 0945 CST, winds were light and variable and no significant patterns persisted.

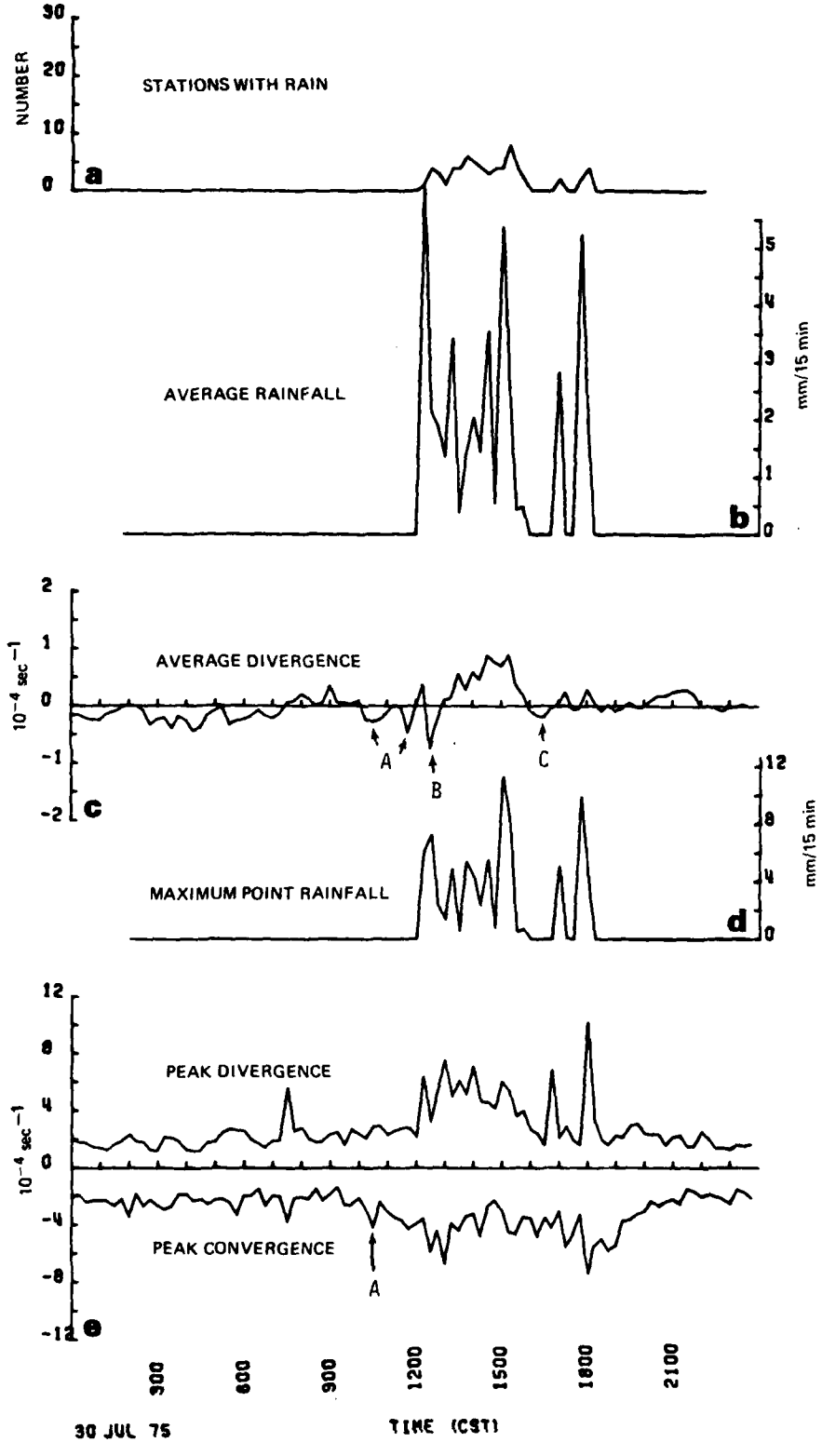

Figure H5. Time series of divergence and rainfall variables.

A weak convergence zone (heavy dashed line) that developed at 0945 CST (Fig. H6a), persisted and strengthened to 4U at 1030 CST, but became diffuse after 1030 CST. The peak convergence (Fig. H5e) persistently exceeded the background throughout this period.

Temperatures increased slowly through the 0945-1145 CST period. Maximum temperatures of near 34C at 1145 CST were found west of the Arch (solid circle) over a suburban area downwind of the central city (Fig. H6f).

The mesoscale convergence zone in the surface wind field was found aloft as a confluence zone. Well defined at 1100 CST at 250 m (heavy dashed lines Fig. H7a) it weakened with height. Although present at 550 m, it largely vanished above. A general confluence area was found up to 550 m at 1200 CST also, but again was not present above (Fig. H7e-h).

The vertical motions calculated from the surface and pibal convergences show an axis of ascent exceeding 10 cm sec^{-1} at 550 m and exceeding 25 cm sec^{-1} at 1350 m at 1100 CST (Fig. H8a-d); the ascent axis was located in the same position as was the surface convergence zone. Strong ascent was confined to the areas roughly west of the Arch at 1200 CST (Fig. H8e-h). Ascent exceeding 35 cm sec^{-1} at 1350 m (Fig. H8h) resulted mostly from convergence within a speed maximum (see Fig. H7g) observed about 15 km west of the Arch. Strong subsidence was found over the network south of the Arch at both 1100 and 1200 CST.

Showers began developing over the larger METROMEX raingage network at 1200 CST. One raincell was located about 40 km northwest of the Arch along the western extension of the mesoscale convergence zone, and a second raincell had developed about 40 km southeast of the Arch (Fig. H9a). Both raincells were found far outside but were near the logical extension of the lower boundary layer confluence zone (Fig. H7e).

The convergence remained through the center of the surface network at 1215. Raincell A (Fig. H9b) developed south of the Arch at the south edge of the network within an area where strong subsidence was found aloft at 1200 (Fig. H8g, h). By 1230 (Fig. H9c) a gust front, accompanied by a well-defined temperature drop and a wind shift from easterly to southerly, had pushed over the southwest part of the network ahead of the westward moving Cell A. The gust front continued to expand northward and westward at 1245 (Fig. H9d).

Meanwhile, Cell B developed about 10 km south of the network (Fig. H9b). Its cold outflow expanded onto the southeastern part of the network at 1300 (Fig. H9e). Cell A had dissipated by 1300 but a new raincell C developed near the southwest corner of the network. Outflow from this cell reinforced that from Cell A and helped drive the gust front northward into the mesoscale convergence zone west of the Arch and convergence increased to 6U there.

Figure H10 shows the vertical structure of the motion field at 1300. The confluence zone (dashed line) at 250 m is the boundary between the mesoscale convergence zone and the gust fronts from raincells A, B, and C. The confluence zone is diffuse at 550 m and is similar in appearance to the confluence zone observed earlier in the afternoon (Fig. H7f). The confluence zone is not apparent above 550 m.

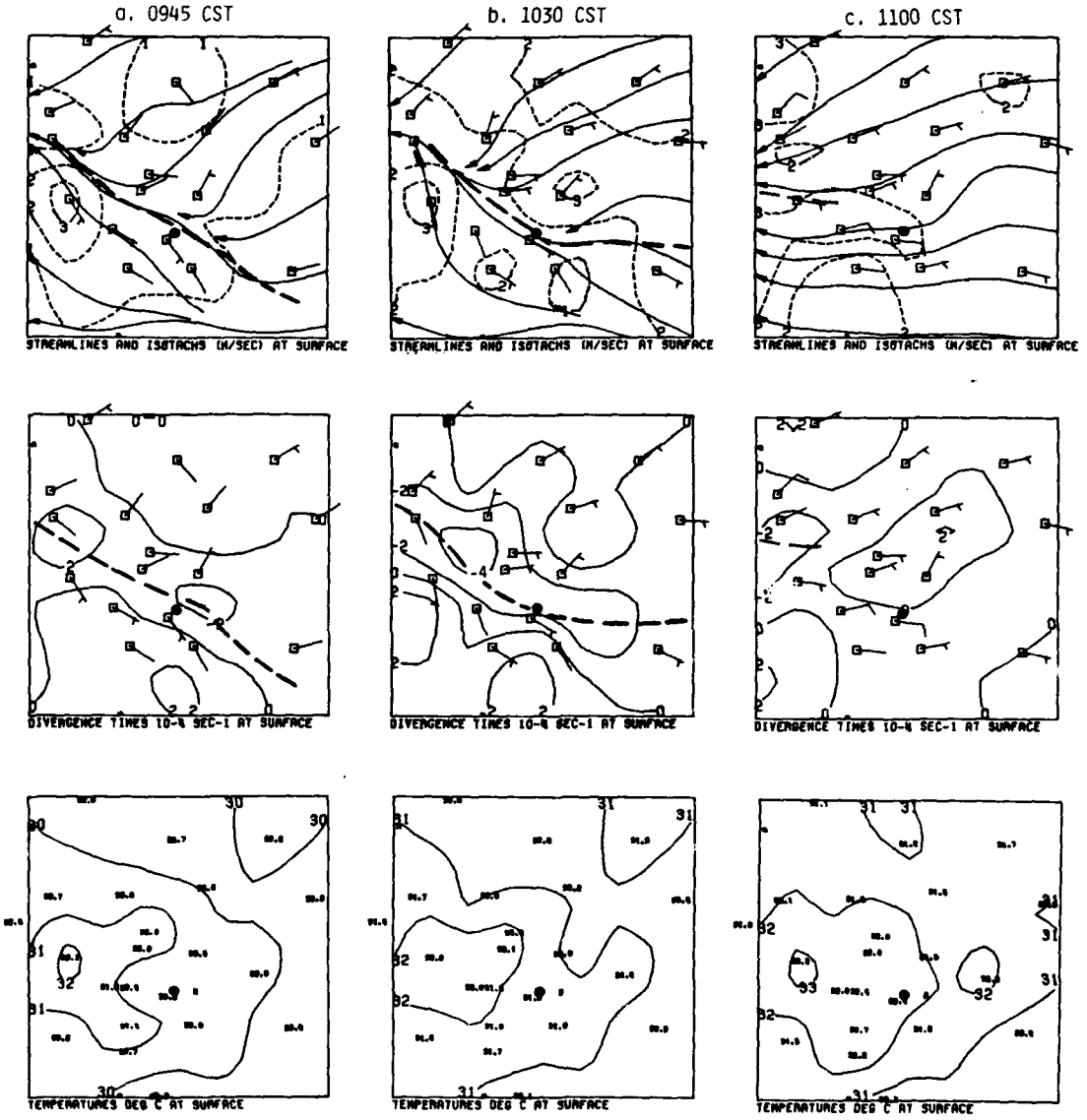

Figure H6. Composite of the objective wind field isotachs and streamlines (upper maps), divergence (middle maps), and temperature (lower maps) for 0945-1145 CST. St. Louis Arch identified by black dot.

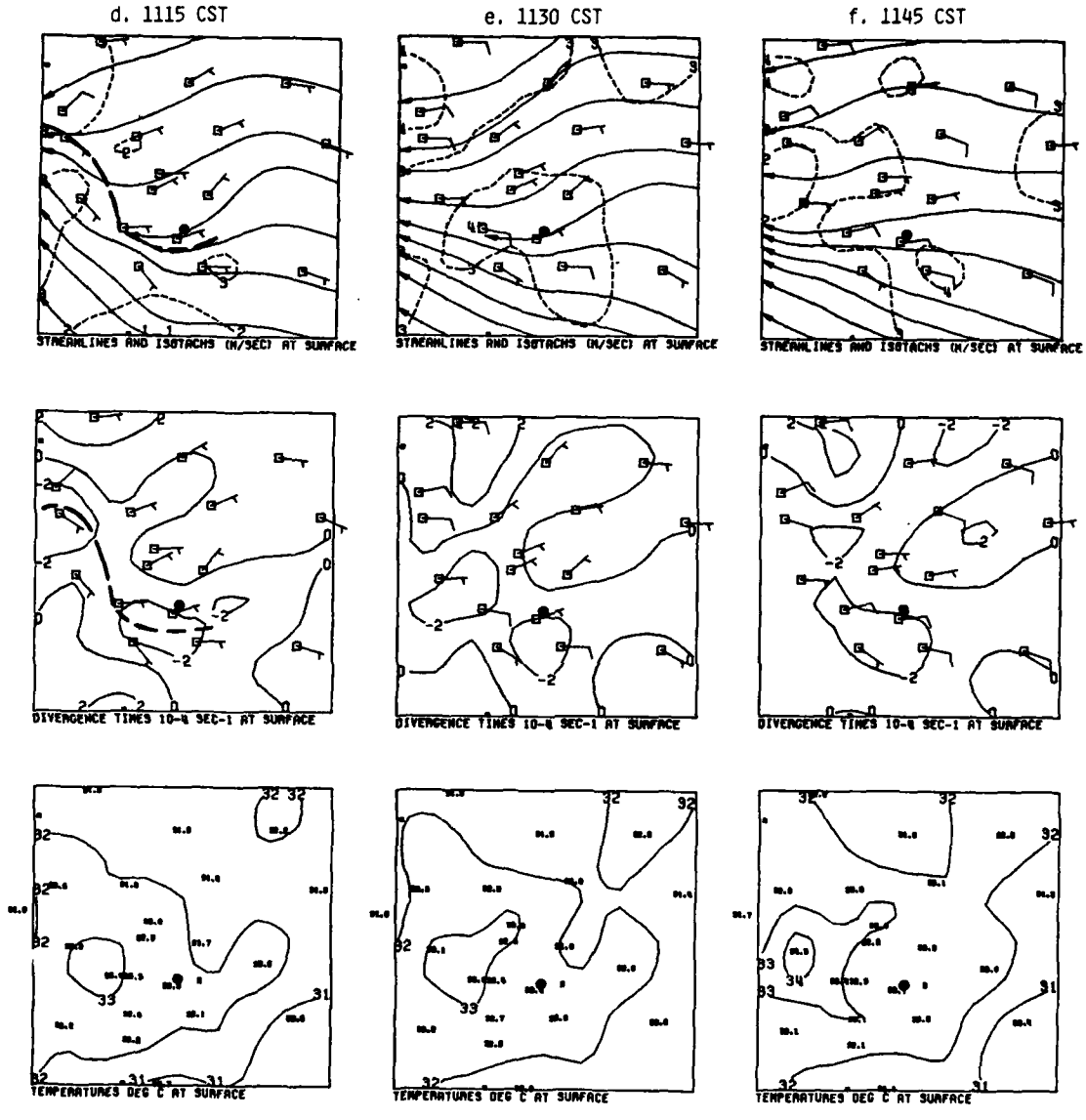

Figure H6. Concluded

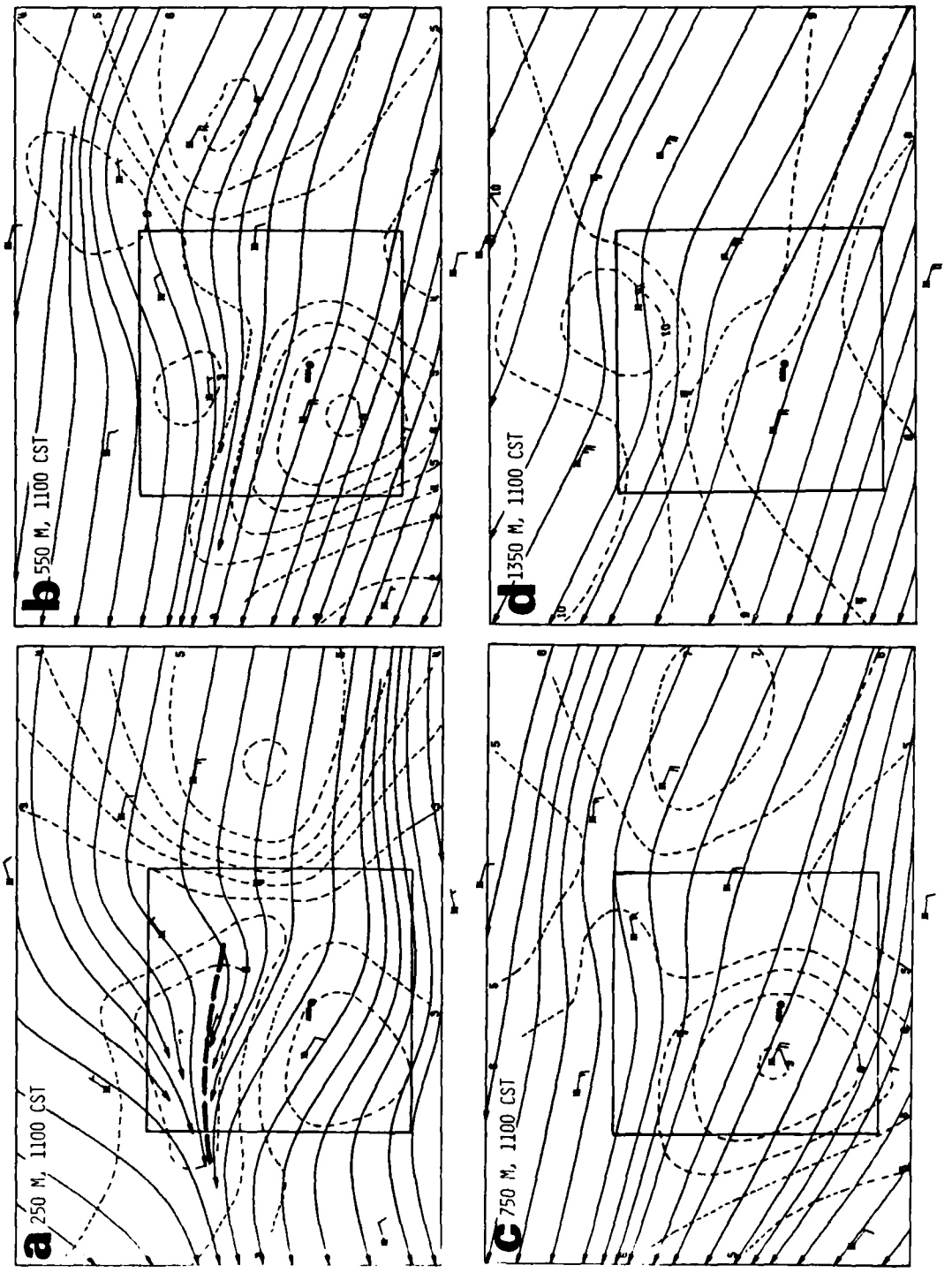

Figure H7. Objective streamlines and isotachs (m sec^{-1}) for 1100 and 1200 CST at four heights (msl).

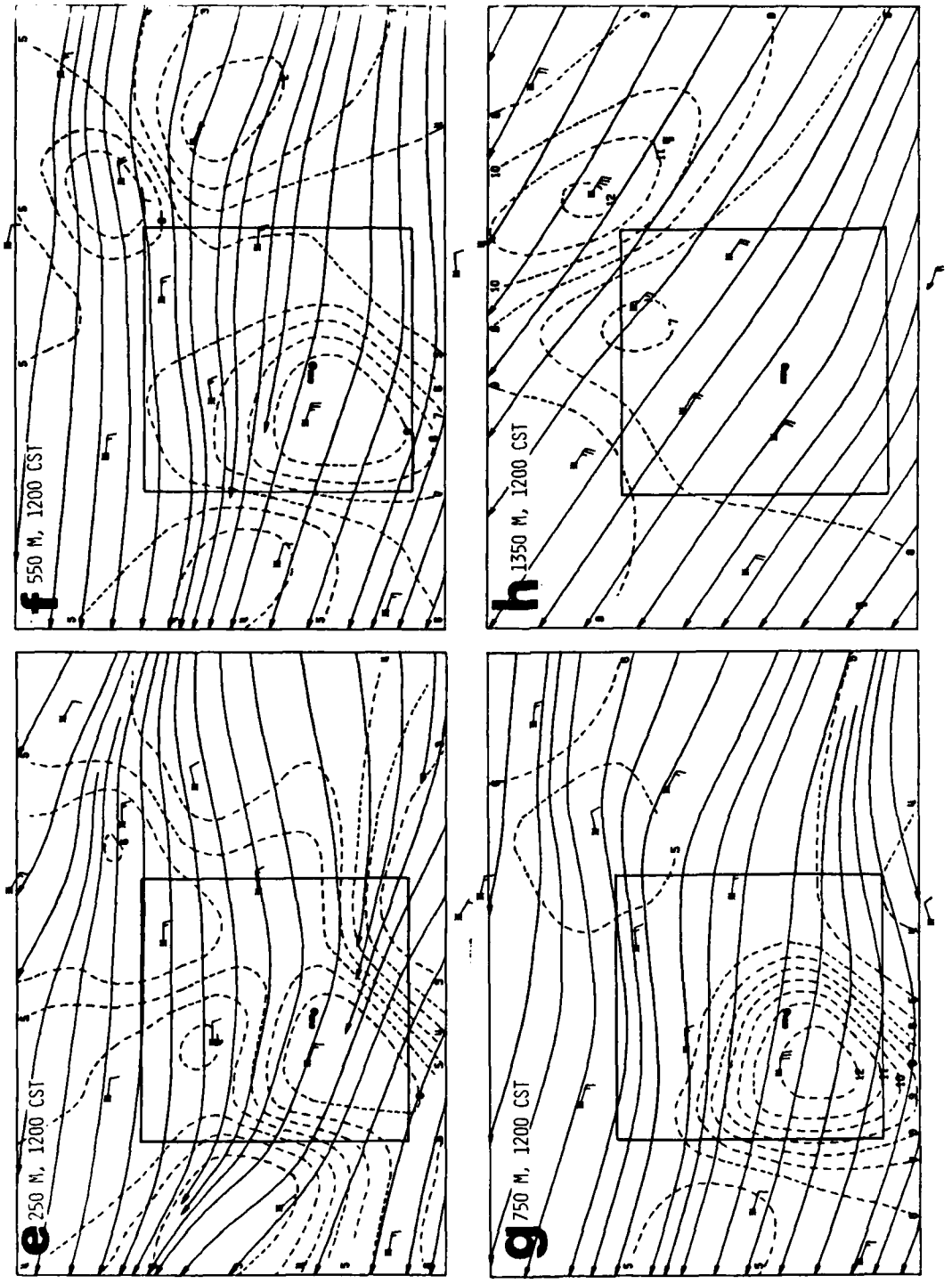

Figure H7. Concluded

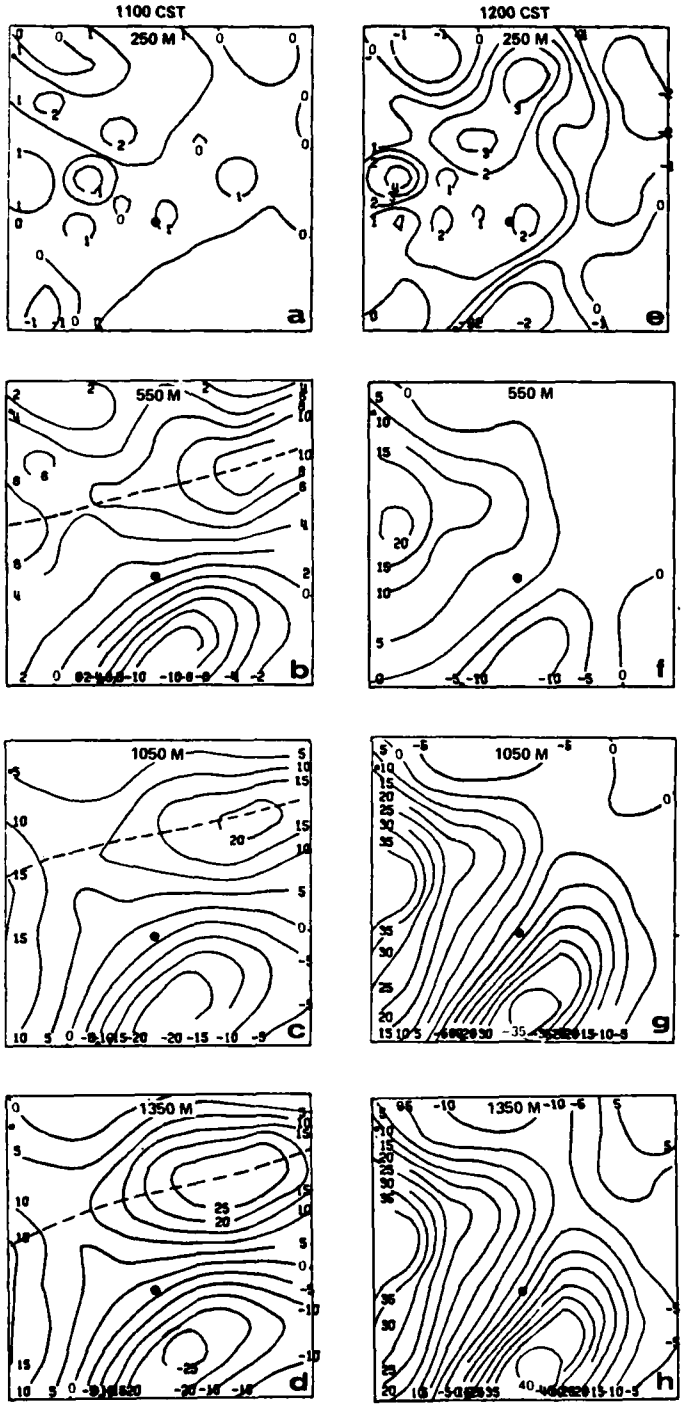

Figure H8. Vertical velocity maps (cm sec^{-1}) for 1100 (a-d) and 1200 (e-h) CST.

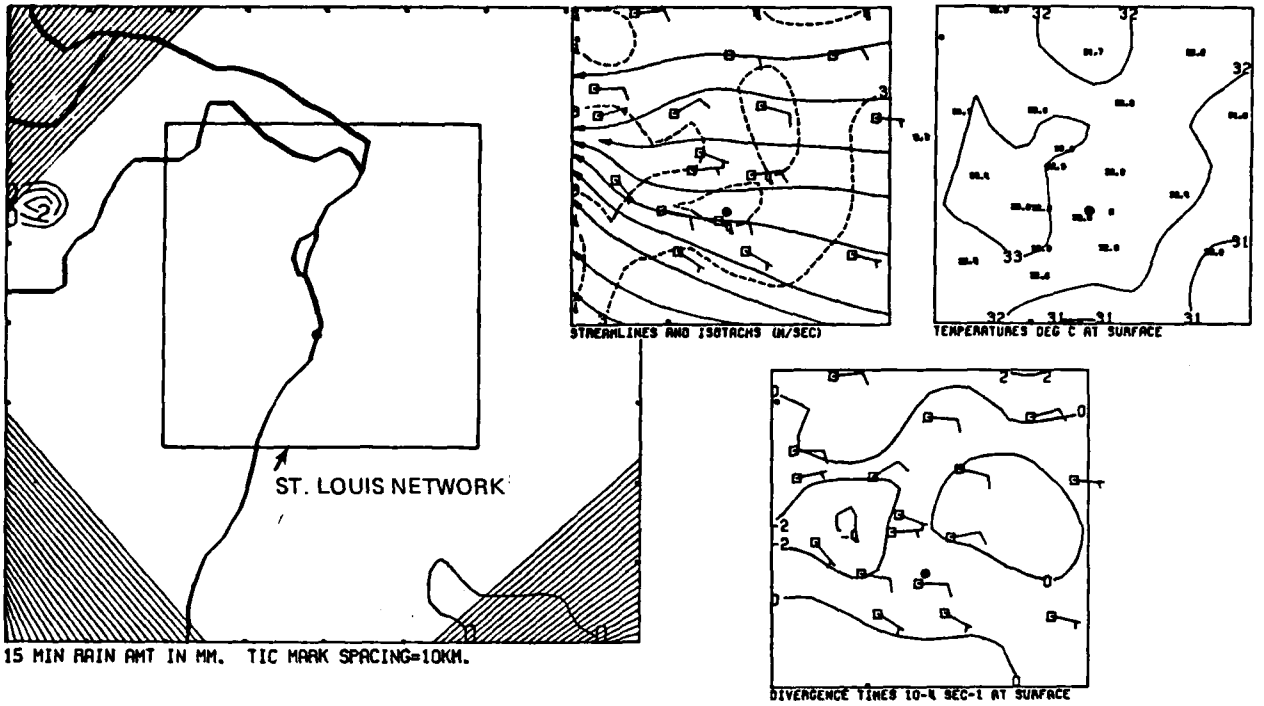

a. 1200 CST

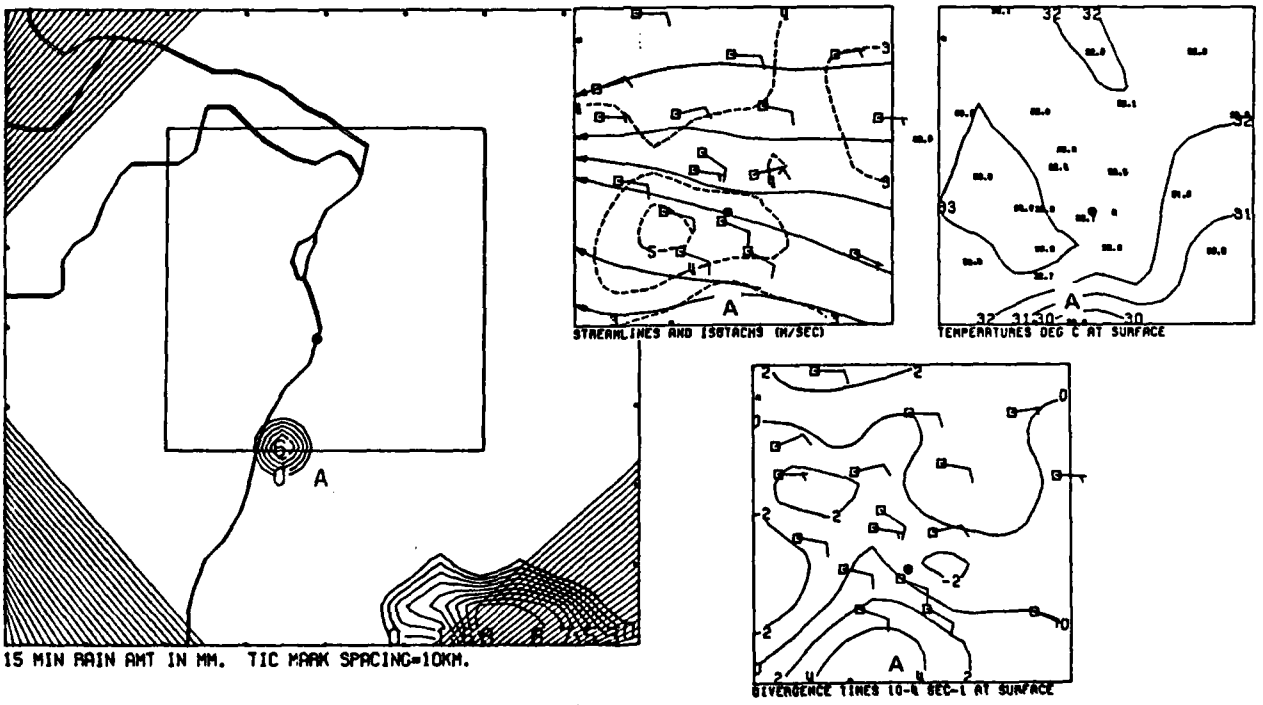

b. 1215 CST

Figure H9. Composite of the objective wind field isotachs and streamlines, temperature, divergence, and rainfall for 1200-1300 CST.

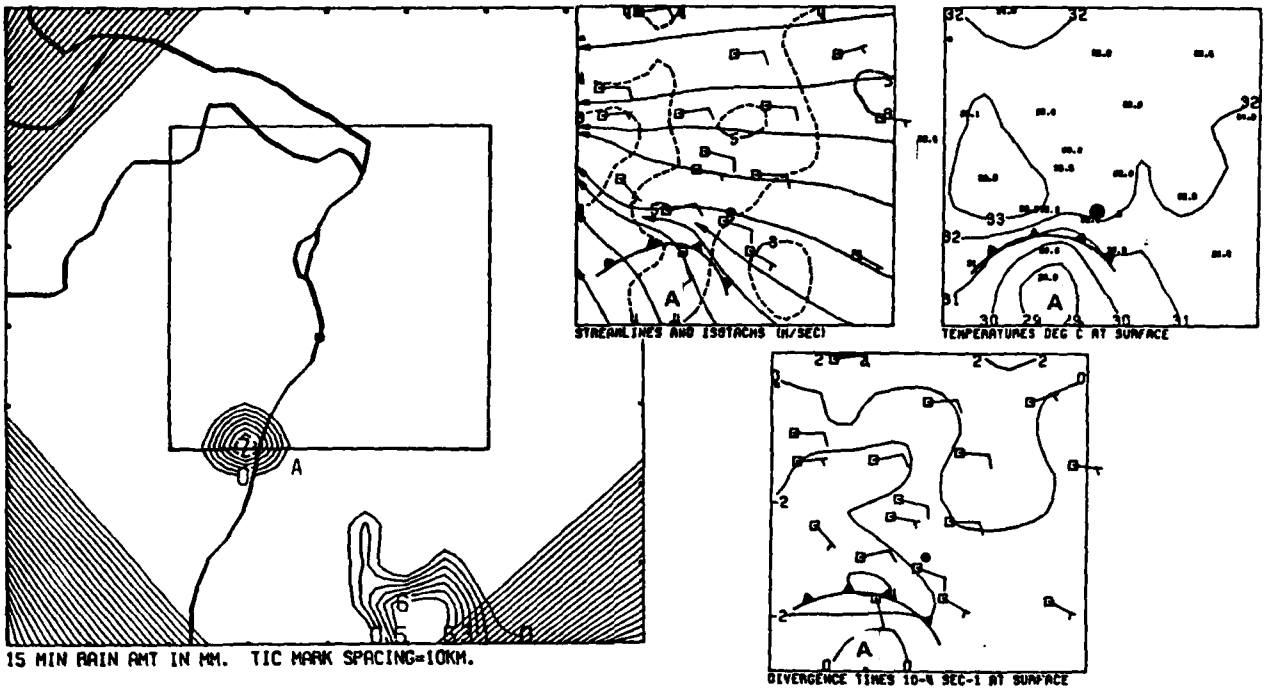

c. 1230 CST

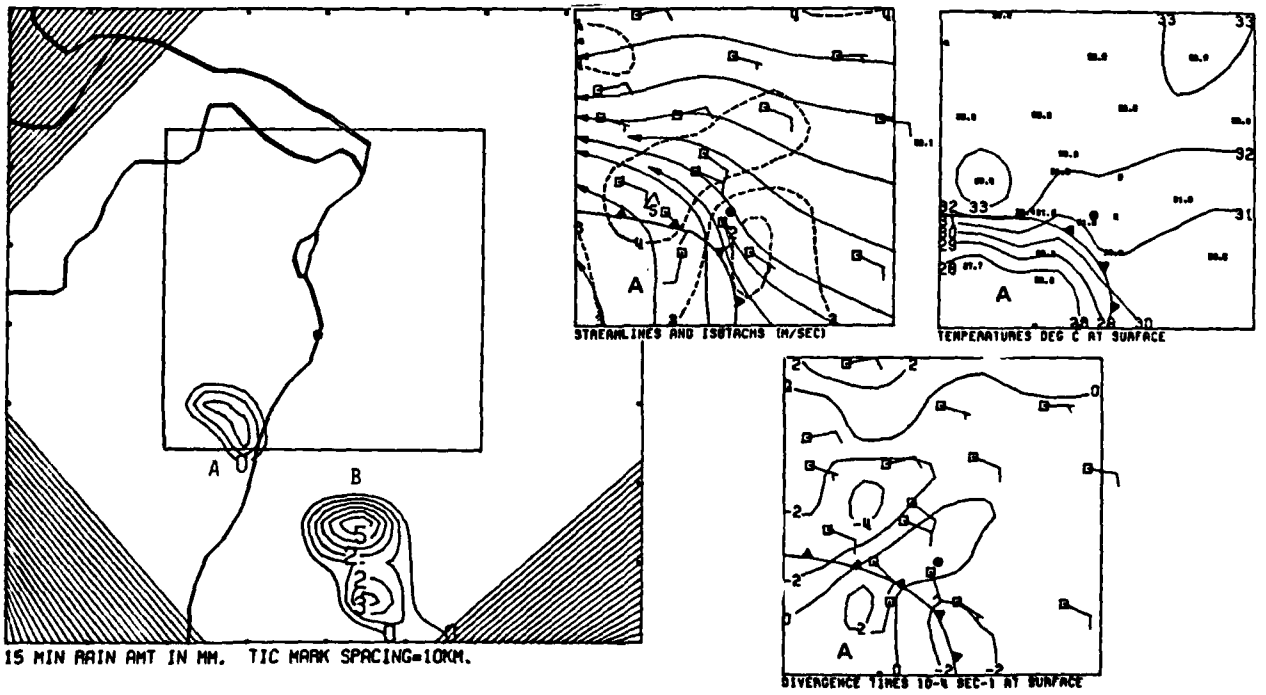

d. 1245 CST

Figure H9. Continued

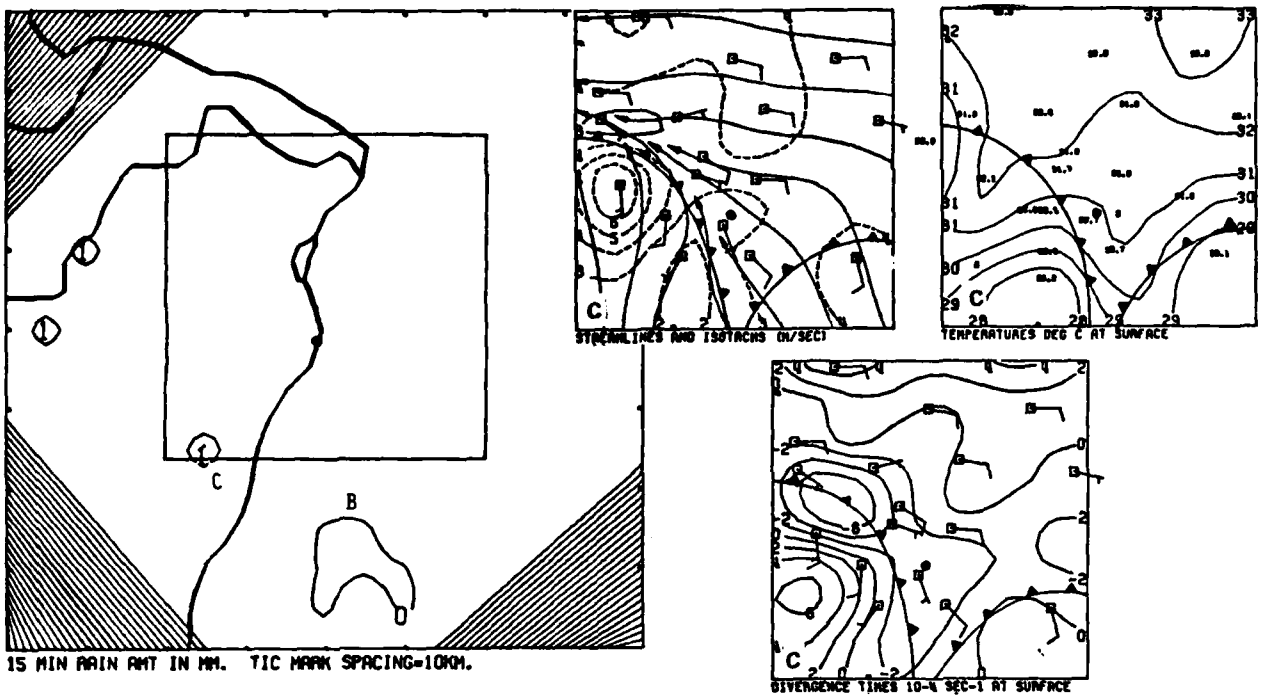

e. 1300 CST

Figure H9. Concluded

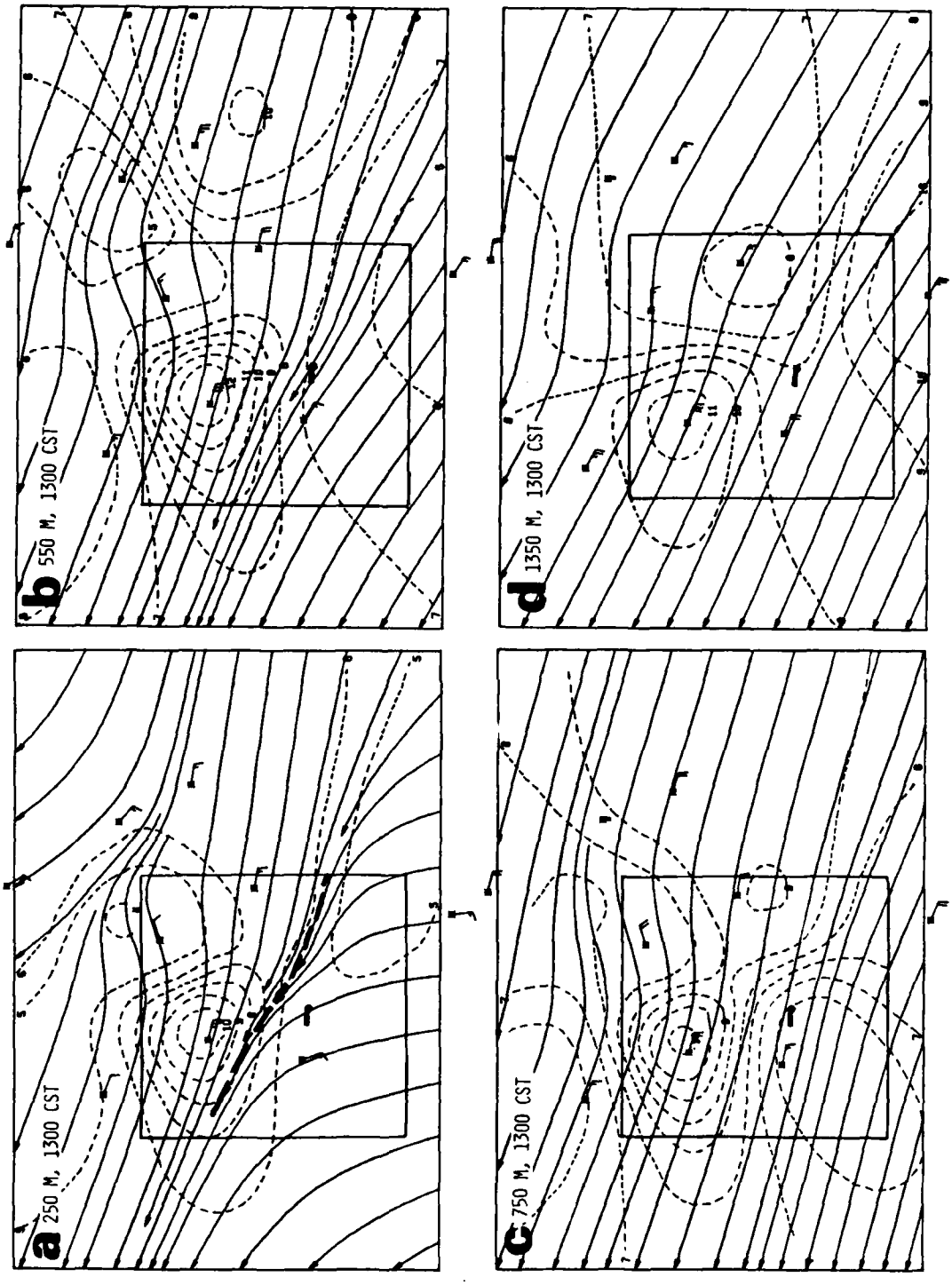

Figure H10. Objective streamlines and isotachs (m sec^{-1}) for 1300 CST at four heights (msl).

As might be expected from examination of the wind speeds in Fig. H10, the sign and magnitude of the convergence was determined more by the wind speed perturbations than by the general direction confluence. The horizontal axis of ascent along the convergence zone and gust fronts (dashed lines, Fig. H11) at 250-550 m gave way to centers of ascent and descent by 1350 m. Subsidence west of the Arch (arrow) was located within the diverging, outflow from cell A. Subsidence north of the Arch existed because speed divergence exceeded directional convergence over that area (Fig. H10).

The outflows from Cells A, B, and C had merged by 1315 (Fig. H12a) to produce a continuous front of northward moving cold air with the leading edge through roughly the center of the network. Raincell D appeared about 5 km behind the surface position of the gust front but was short-lived. It occurred within an area of 25 cm sec^{-1} ascent at 1300 (Fig. H11d).

The area of strongest convergence remained about 20 km northwest of the Arch (arrow Fig. H12a). Its magnitude decreased from 6U at 1300 to 4U at 1315. Raincell E appeared within this persistent convergence at 1330 (Fig. H12b). It was about 10 km behind the surface position of the gust front which had moved the convergence zone farther north. Maximum convergence exceeding 4U was located 10 km north of the Arch at 1330 (arrow Fig. H12b).

Cell E, moving northwestward, developed a gust front that reinforced the western end of the initial gust front (Fig. H12c). The mesoscale convergence zone, identified by the streamline confluence over the northern part of the network, was located about 10 km north of the gust fronts. Two weak 2U convergence centers (arrows) remained, one ahead of Cell E and the second about 15 km northeast of the Arch. Meanwhile, Cell F had developed near the eastern edge of the study area, about 10 km behind the gust front in an area of sparse data coverage.

Outflow from Cell E pushed the gust front and the convergence areas (arrows) to the northern part of the network at 1400 (Fig. H12d). Cell G developed about 10 km behind the gust front in an area where the convergence had been persistently weak. However, convergence on a smaller scale undoubtedly occurred with the passage of the gust front.

The combined confluence of the mesoscale convergence zone and the gust front at 250 m (Fig. H13a) was shifted to the northern part of the network and remained nearly collocated with the surface gust front location. The mesoscale confluence zone remained at 550 m. Above 550 m, the flow was nearly parallel.

The vertical velocities for the study area south of the Arch (Fig. H14) are unreliable because wind data from a pibal station south of the network was missing at levels below 1350 m. Ascending air was found along the northern border of the network in roughly the position of the mesoscale convergence zone. A 25 cm sec^{-1} ascent center 20 km north of the Arch was near the location of a 2U convergence center at the surface.

The outflows from Cells E and G continued to push the gust front toward the boundary of the network. Cell H appeared at 1415 about 18 km north of the Arch (Fig. H15a). The convergence history for the area of Cell H began at 1330 when a 4U center appeared (Fig. H12b). This location remained convergent

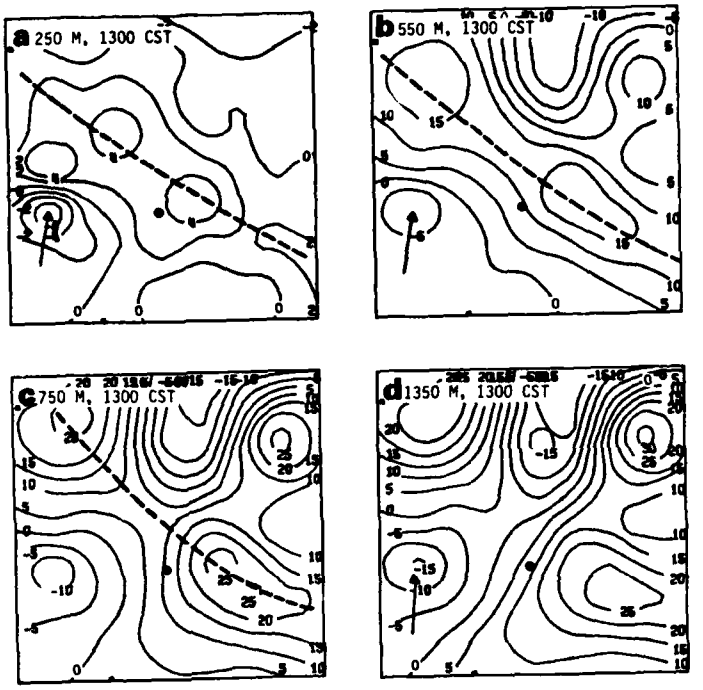

Figure H11. Vertical velocity fields (cm sec^{-1}) for 1300 CST.

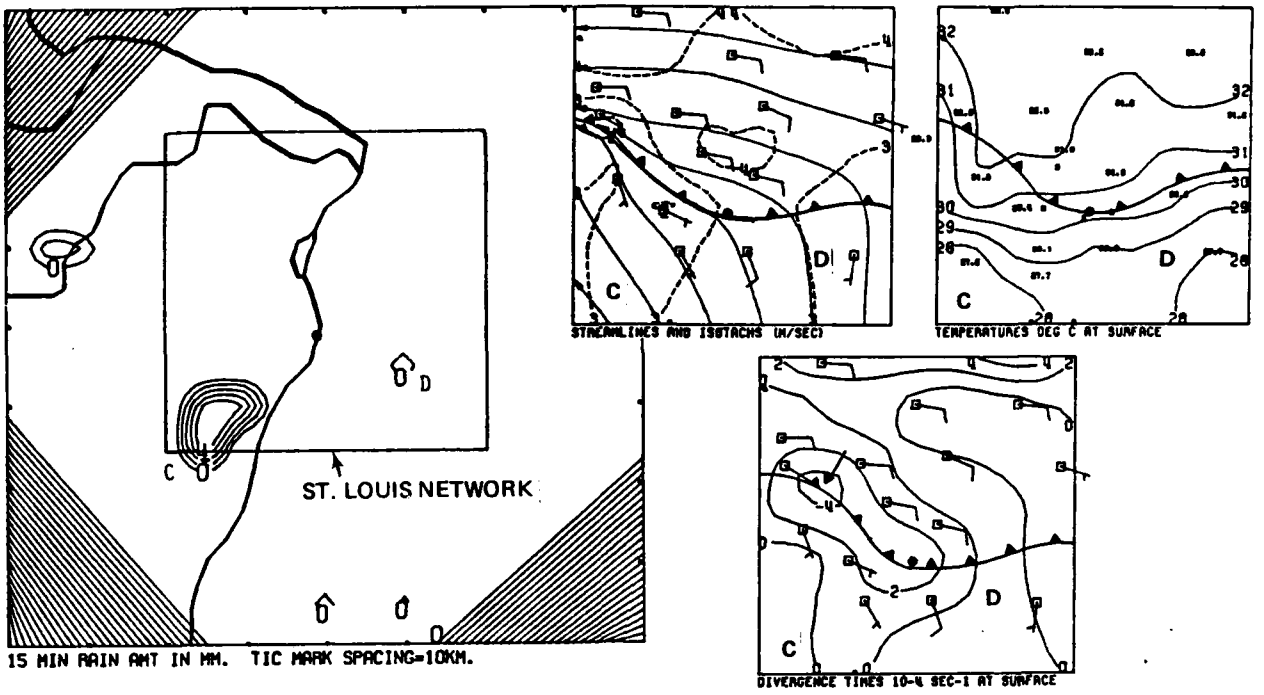

a. 1315 CST

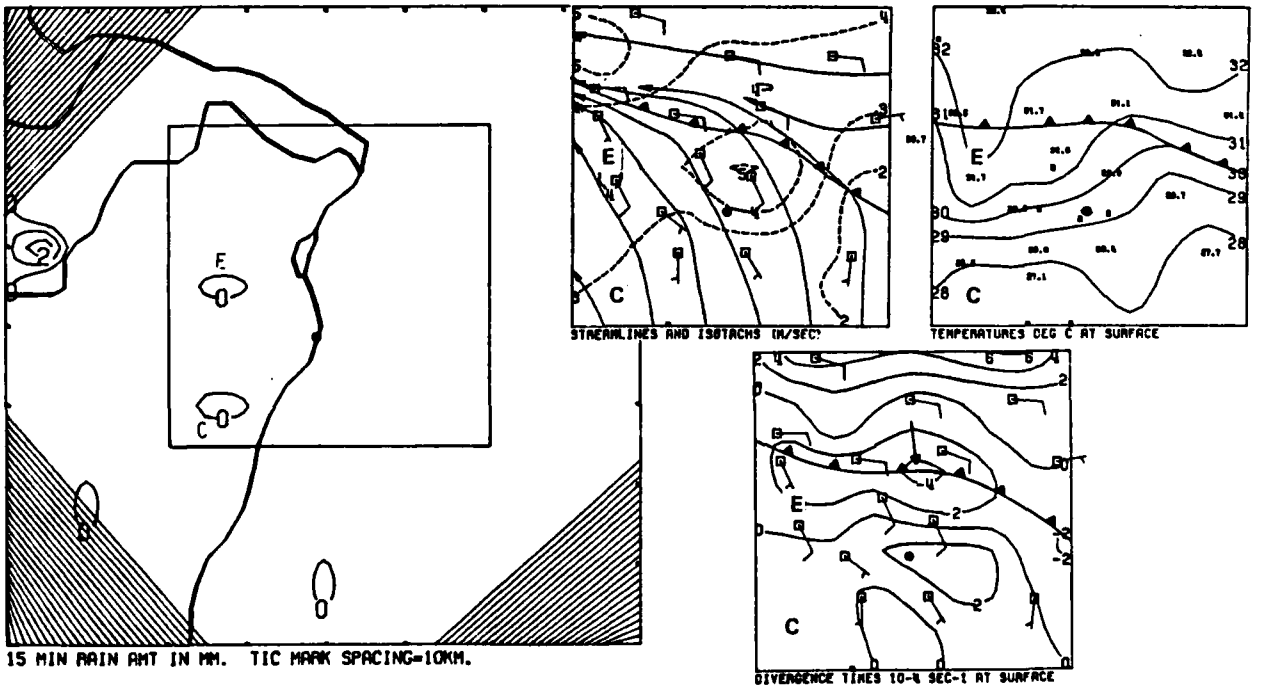

b. 1330 CST

Figure H12. Composite of the objective wind field isotachs and streamlines, temperature, divergence, and rainfall for 1315-1400 CST.

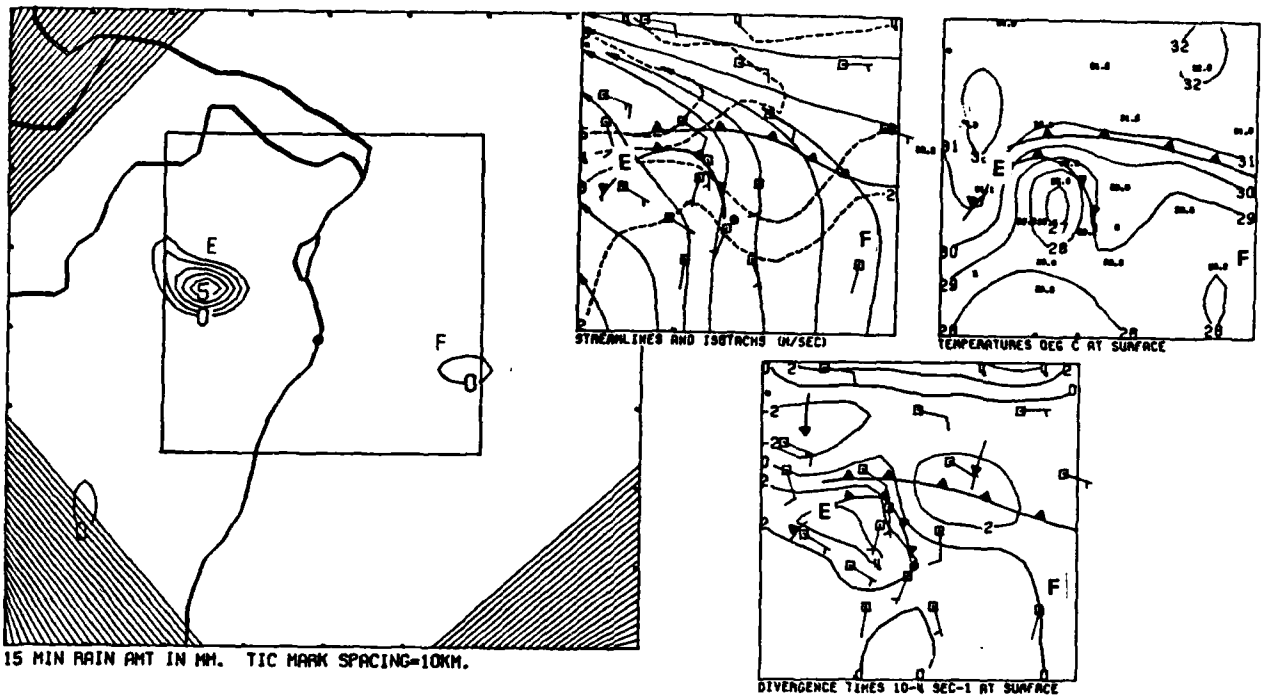

c. 1345 CST

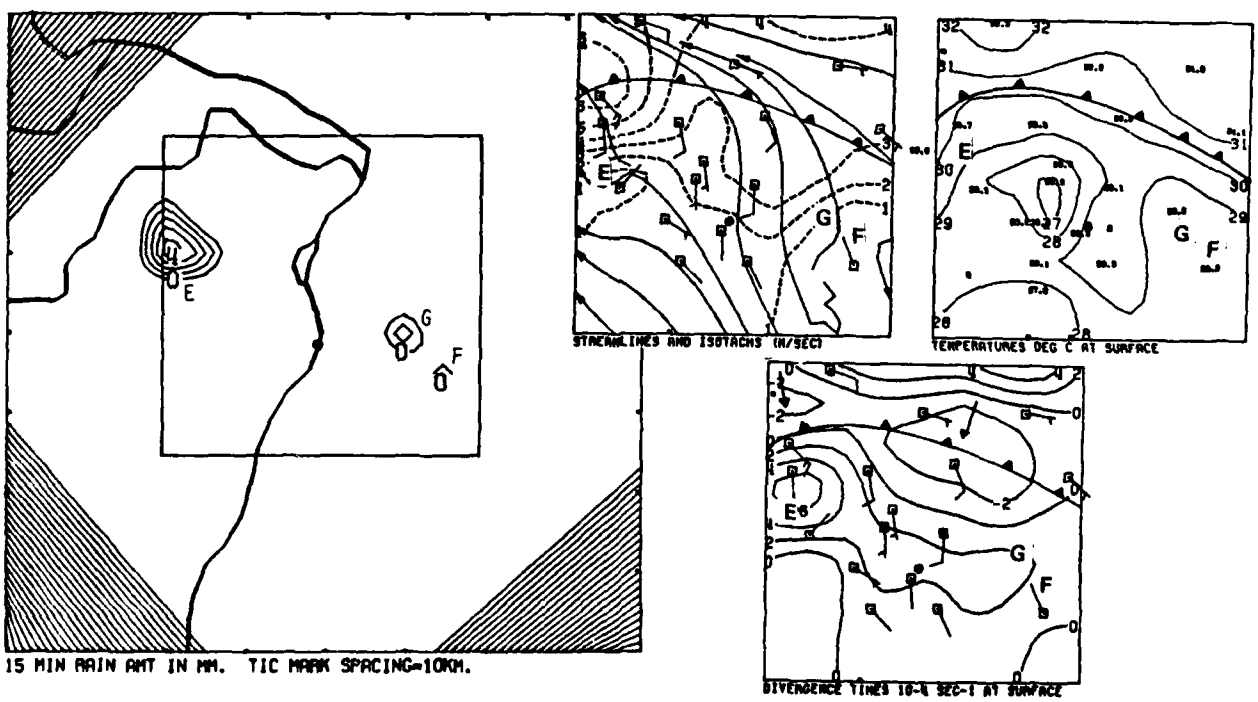

d. 1400 CST

Figure H12. Concluded

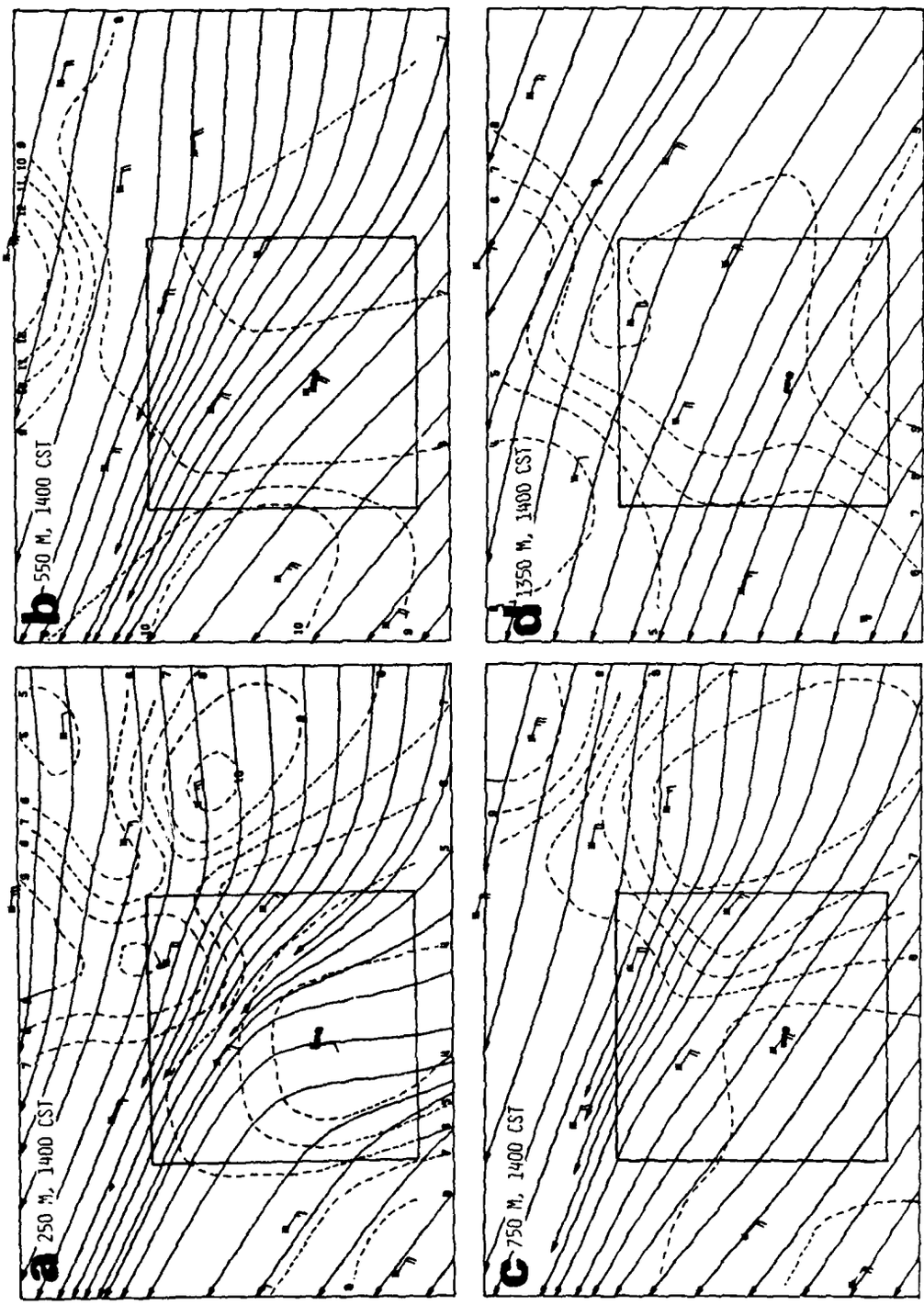

Figure H13. Objective streamlines and isotachs (m sec^{-1}) for 1400 CST at four heights (msl).

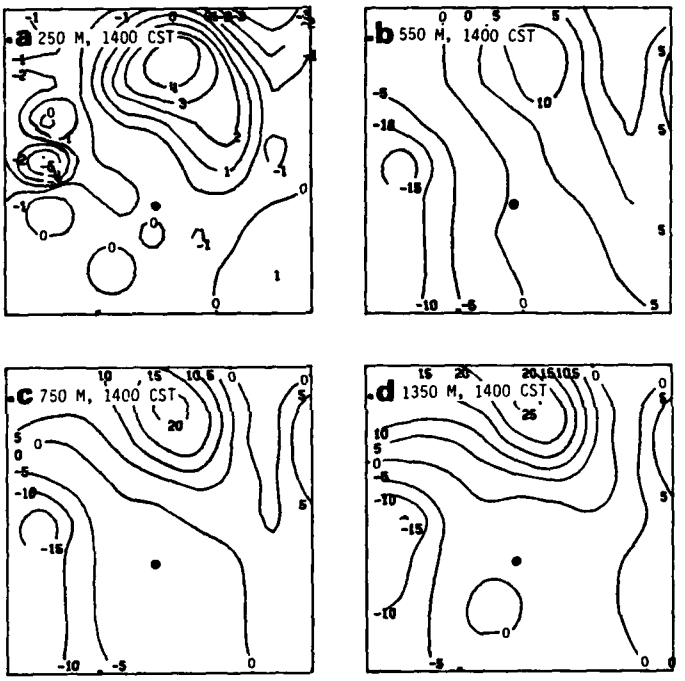

Figure H14. Vertical velocity fields (cm sec^{-1}) for 1400 CST.

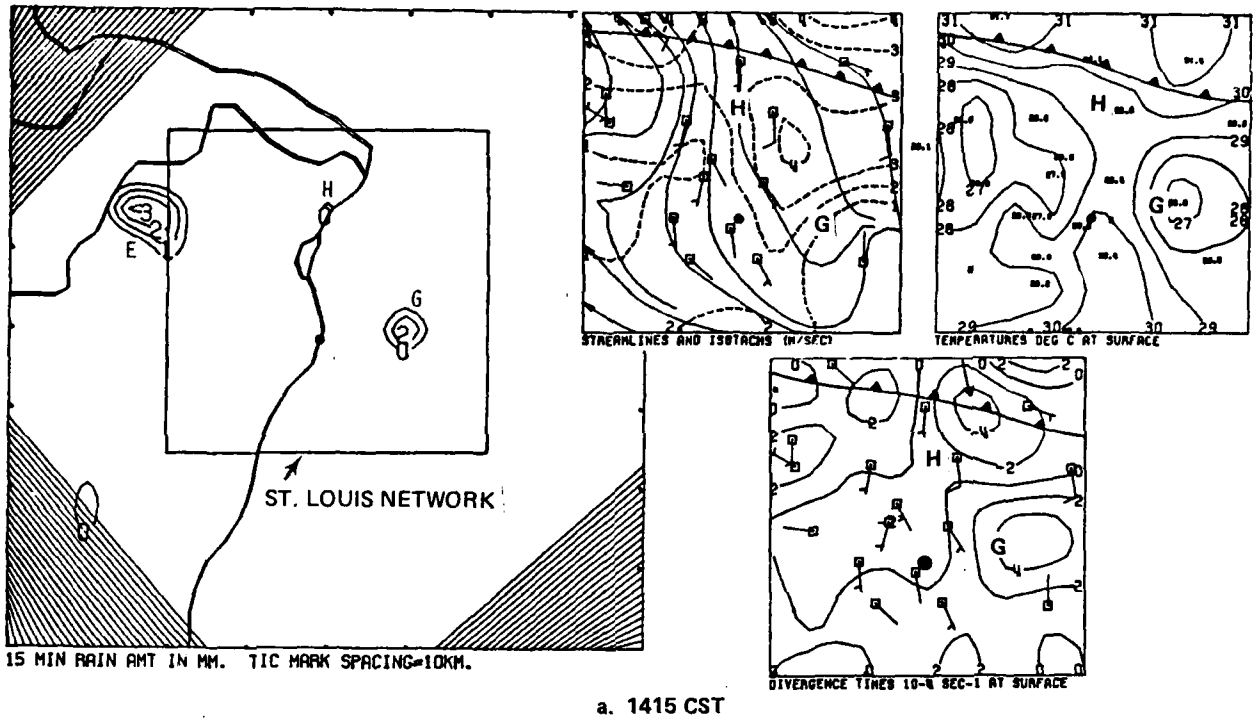

a. 1415 CST

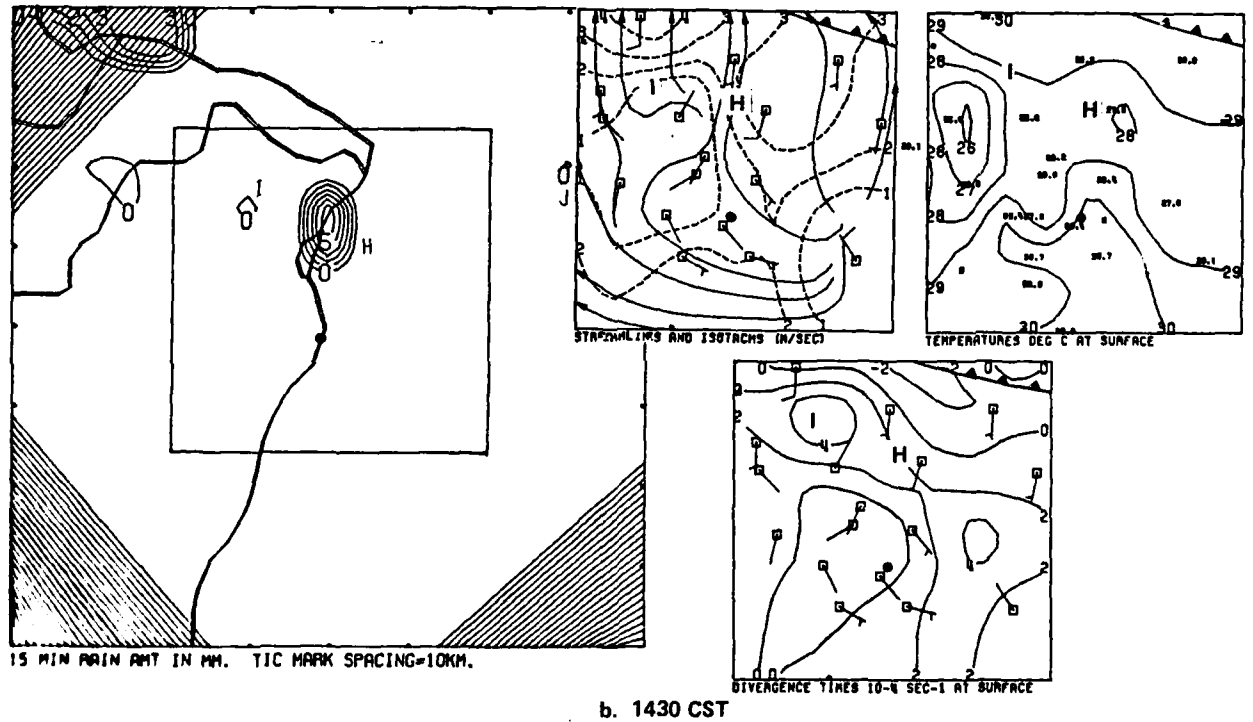

b. 1430 CST

Figure H15. Composite of the objective wind field isotachs and streamlines, temperature, divergence, and rainfall for 1415-1500 CST.

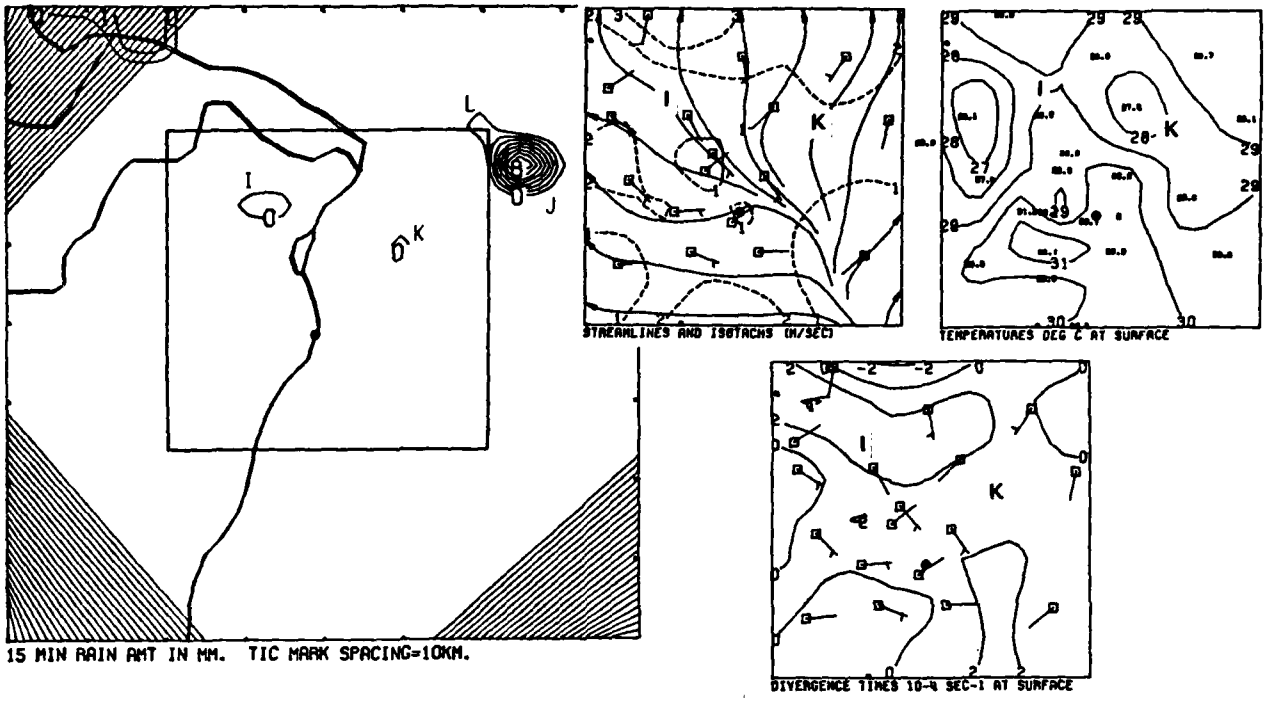

c. 1445 CST

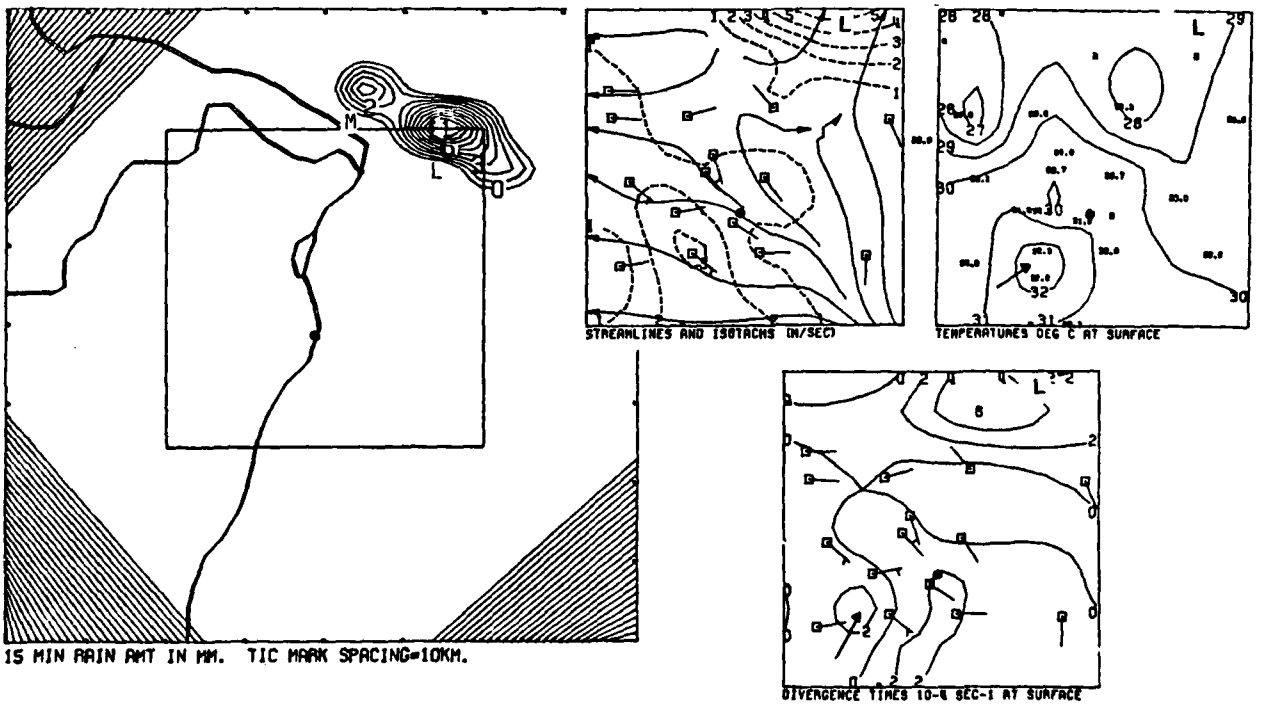

d. 1500 CST

Figure H15. Concluded

until the gust front passed at 1415 (arrow Fig. H15a). Cell H intensified to 5 mm/15-min at 1430 (Fig. H15b) and its outflow pushed the gust front out of the wind field network. Raincell I appeared briefly at 1430, in an area that had been weakly convergent during the past one half hour. It was located about 10 km behind the 1430 position of the gust front.

As the raincells developed progressively further north, the cloudiness apparently decreased over the southern part of the network. Temperatures at several sites increased 2C in 15-min to exceed 30C (Figs. H12d and H15a). The warming area, which continued to expand by 1430 (Fig. H15b), increased the instability locally and prepared the area for a new outbreak of showers later in the day.

Winds within the shower outflow area became light and variable by 1445 (Fig. H15c). The major convective development, Cell J, occurred off the network in the location of the surface gust front inferred by continuity of its motion while within the network. Cell J combined with Cells L and M at 1500 (Fig. H15d) to produce the strongest showers observed for the 30th of July. During this same period, temperatures over parts of the network south of the Arch had warmed to pre-rain readings and a weak 2U convergence center (arrows Fig. H15d) had appeared in close proximity to the warmest temperatures.

The vertical structure of the wind field at 1500 (Fig. H16) was one of transition from a regime of shower outflows below 500 m to the mesoscale confluence zone above 1000 m. Speed and direction divergence at 250 and 350 m gave way to speed divergence at 550 m. The speed divergence weakened at 750 and 1050 m and weak directional convergence was also found at 1050 m. Directional convergence was the salient feature of the 1350 m wind field.

The pibal wind analyses at 1100-1400 (Figs. H7, H10, H13) all showed the mesoscale confluence zone to be most prominent in the layer from the surface to 550 m. It is apparent from the 1500 analyses that the mesoscale convergence zone was not destroyed by the surface outflow but rather was lifted above the surface by it. This transition was also apparent in the network-average vertical velocity (Fig. H17) as a reversal in the slope of the vertical velocity profile. Divergence within the outflow layer below 750 m caused the subsidence to increase in magnitude with height. The 750-1050 m layer was nondivergent as the subsidence remained constant at -7.0 cm sec^{-1}. Convergence within the mesoscale confluence zone in the 1050-1350 m layer caused the vertical velocity to increase to -5.5 cm sec^{-1}.

The transition with height from subsidence to ascent was greatest along the northern part of the wind field network (Fig. H18) where the confluence zone was apparent at 1350 m (Fig. H16f). Subsidence was present over the network from the surface to 550 m. Convergence within the mesoscale confluence zone reversed the sign of the vertical motion over the northern sections, and upward motion of 5.0 cm sec^{-1} was found at 1350 m. A small area of (relatively) weaker subsidence at 550 m in the southwest (arrow Fig. H18b, c) appeared near the location of raincells N and O which developed at 1515.

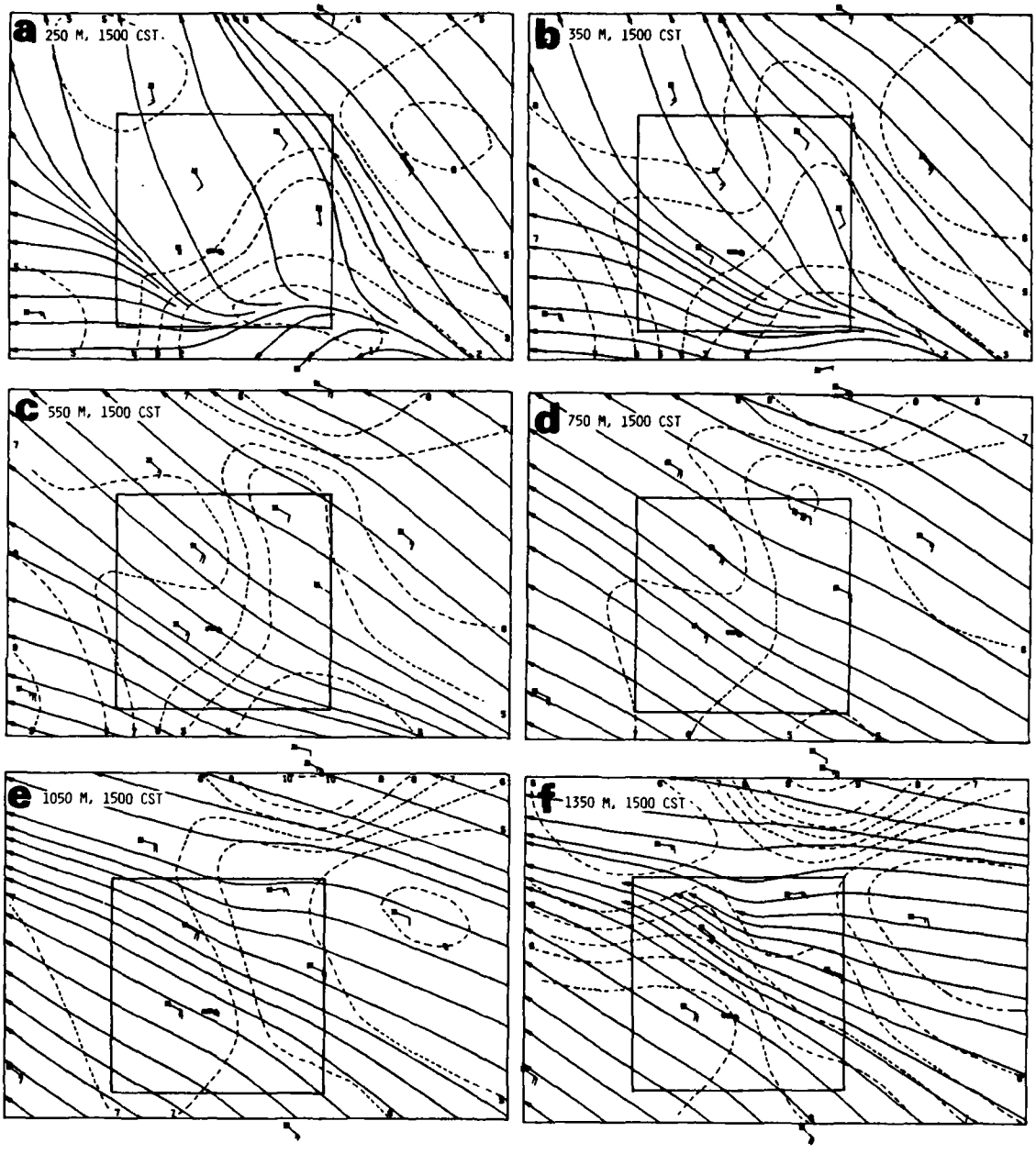

Figure H16. Objective streamlines and isotachs (m sec^{-1}) for 1500 CST at six heights (msl).

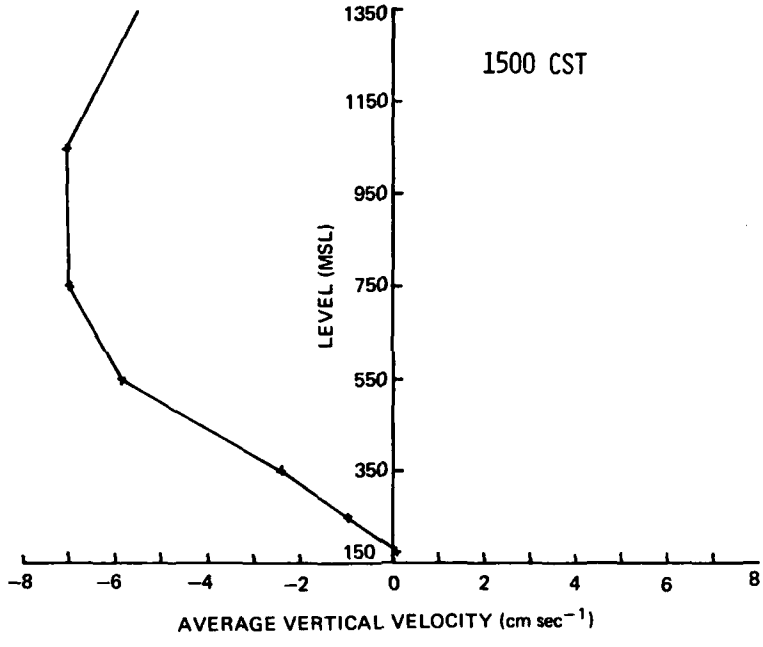

Figure H17. Vertical profile of network average vertical velocity, 1500 CST.

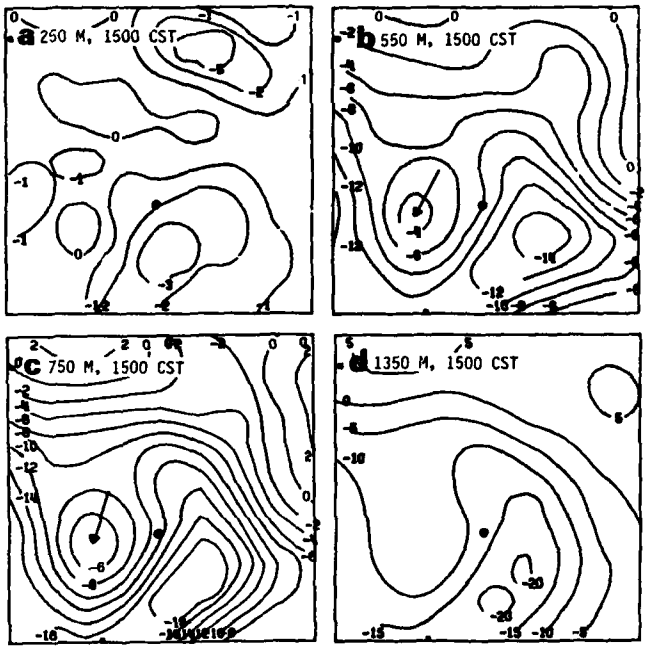

Figure H18. Vertical velocity fields (cm sec^{-1}) for 1500 CST.

Raincells N and O developed 5-15 km west of the Arch at 1515 (Fig. H19a). They were near the area of weak convergence and warmer temperature shown in Fig. H15d and within the area of weaker subsidence discussed in the previous paragraph. Outflow from Cell N caused an increase in the convergence in the vicinity of Cell O to 4U at 1530 (arrow Fig. H19b); however, Cell O was dissipating and no new cell development occurred in this area.

The rapid temperature recovery to pre-rain values increased the low level instability over the network and allowed the pre-rain mesoscale convergence zone in the area to be re-established in the surface wind field (Fig. H19b). The initial wind shift to northeasterly over the northeast part of the study area could have been associated with outflow from Cells J, L, and M. A weak convergence zone was extended E-W across the area at 1530 and remained at 1545 (Fig. H19c).

No rain occurred from 1600-1630 when a more pronounced convergence zone became established across the center of the network (Fig. H20). A well defined axis of convergence with a center up to 4U moved slowly southward and had pushed into the area of warmer temperatures by 1645 (Fig. H21a). Raincell P formed at the southern edge of the network at 1700 in a data-sparse area south of the major convergence zone. Its outflow pushed northwestward and interacted with the mesoscale convergence zone to increase convergence to 4U about 15 km west of the Arch at 1715 (Fig. H21c).

Strong convergence persisted south of the Arch at 1730 (Fig. H21d). Raincell Q developed at 1745 (Fig. H21e) in an area of 4U convergence at 1715 associated with the intersection of the gust front from Cell P the mesoscale convergence zone, immediately downwind from the expanded 4U convergence center found southwest of the Arch at 1730 (Fig. H21d). Its strong outflow, reversed the wind direction, and caused the formation of a zone of strong 6U convergence at 1800 (Fig. H21f) that was maintained at 1815 after the termination of the rain in the same location (Fig. H21g).

No new raincell development occurred after Cell Q. Surface temperatures had begun to cool off after 1730 as the period of maximum daytime heating was well past. The destabilization by lifting along the gust front was apparently insufficient to overcome the stabilization brought on by low-level cooling on this evening.

SUMMARY OF SHOWER DEVELOPMENTS ON 30 JULY

Weather systems on different scales of motion combined to produce conditions favorable for precipitation over the St. Louis network on 30 July. The synoptic-scale circulation from the surface to 500 mb was anticyclonic over the area, a situation not considered favorable for deep convection. However, a subsynoptic scale cyclone above 500 mb over southwest Missouri was in a location favorable for producing high level ascent over St. Louis.

No surface frontal systems were present in the St. Louis area on the 30th as there were no discernible temperature or moisture contrasts. However, the satellite observation revealed significant airmass contrasts in the amount of haze over the St. Louis area. Regional scale analyses of the surface wind field showed the formation of a convergence zone in the same area beginning by

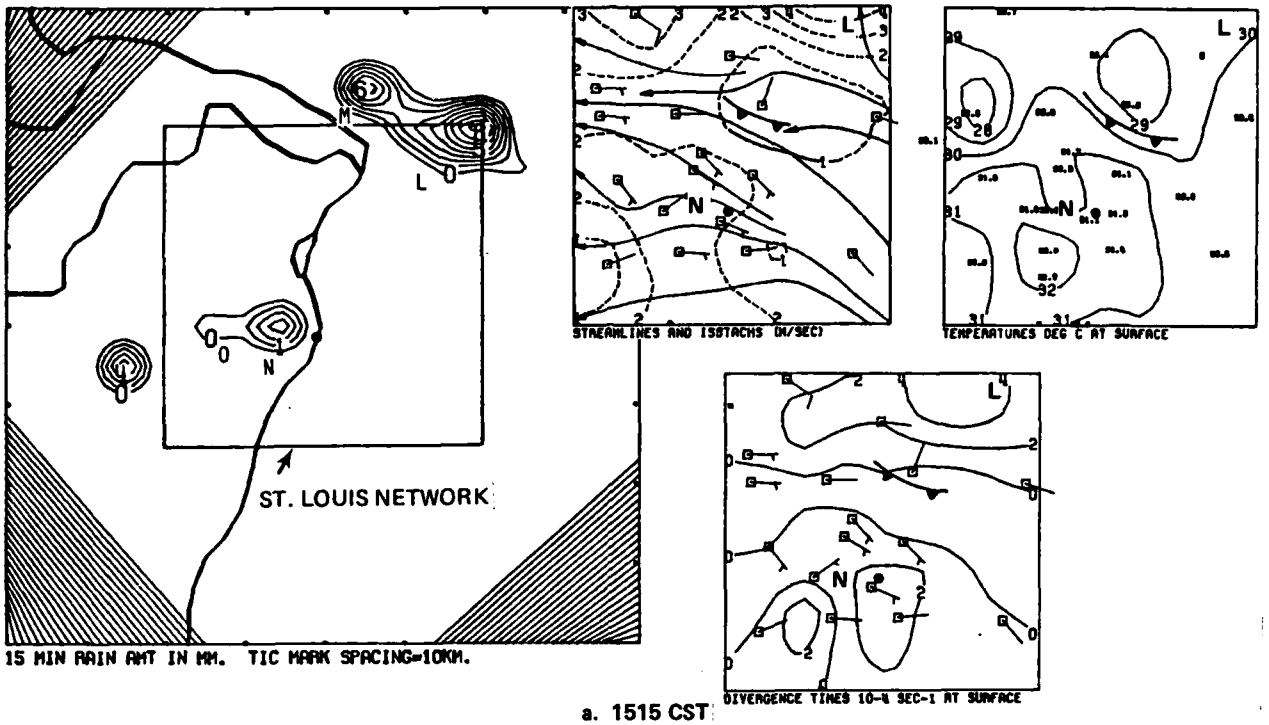

a. 1515 CST

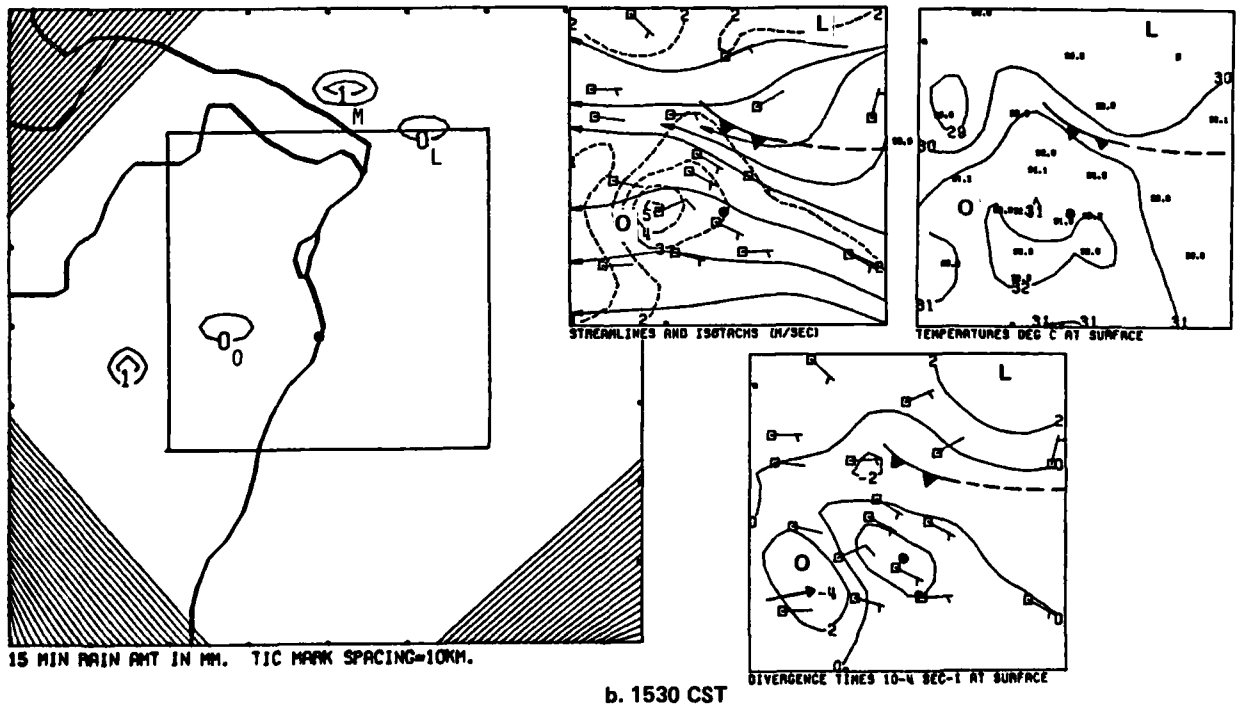

b. 1530 CST

Figure H19. Composite of the objective wind field isotachs and streamlines, temperature, divergence, and rainfall for 1515-1545 CST.

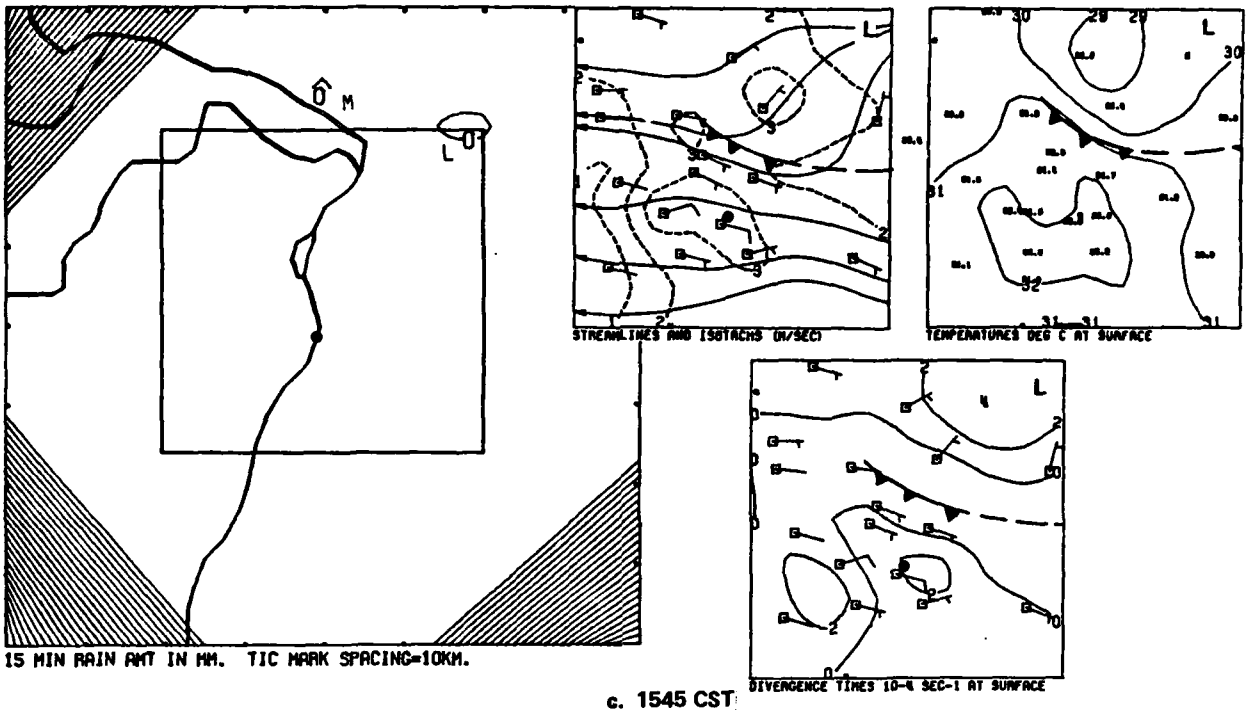

c. 1545 CST

Figure H19. Concluded

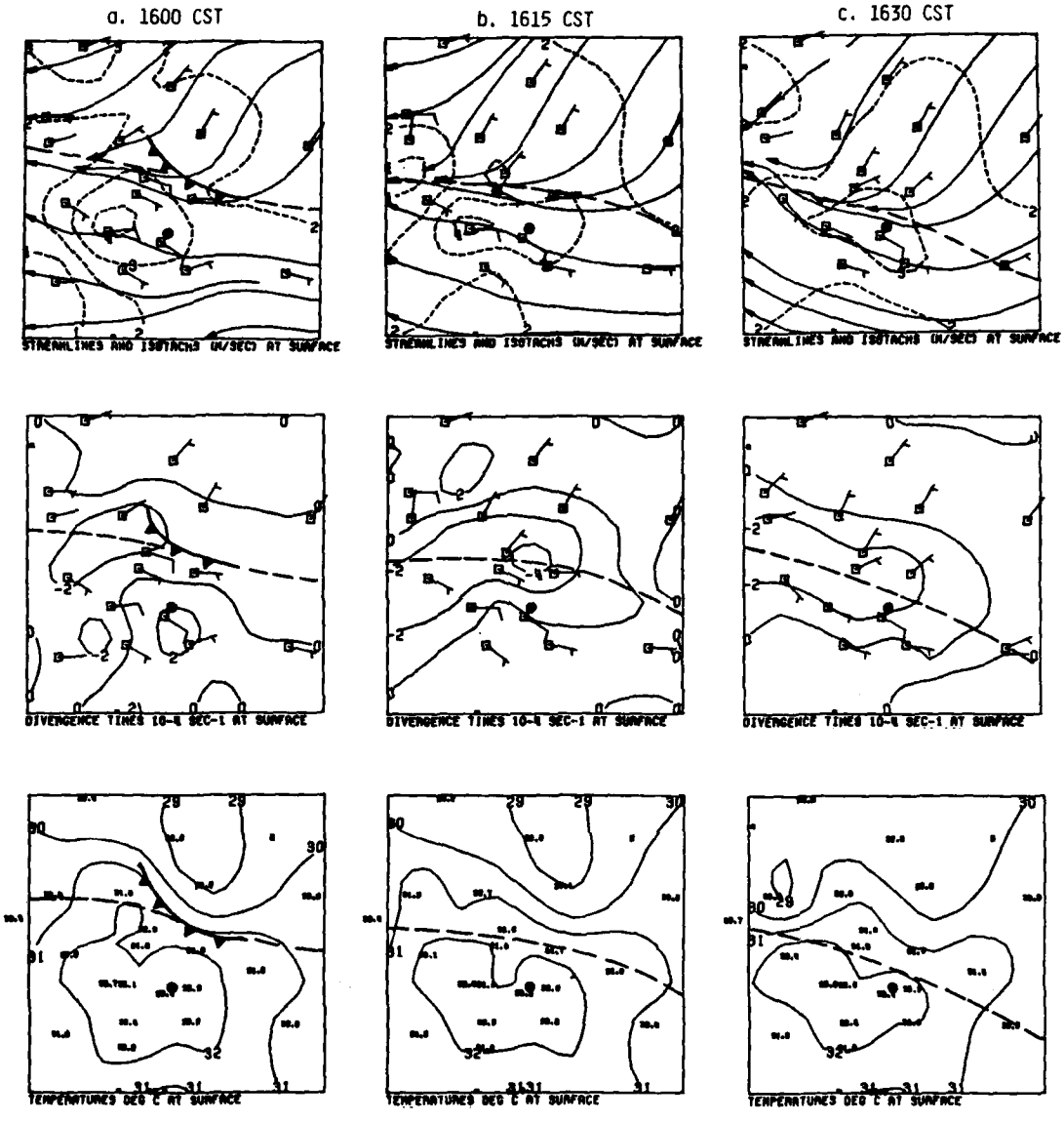

Figure H20. Composite of the objective wind field isotachs and streamlines, divergence, and temperature, 1600-1630 CST.

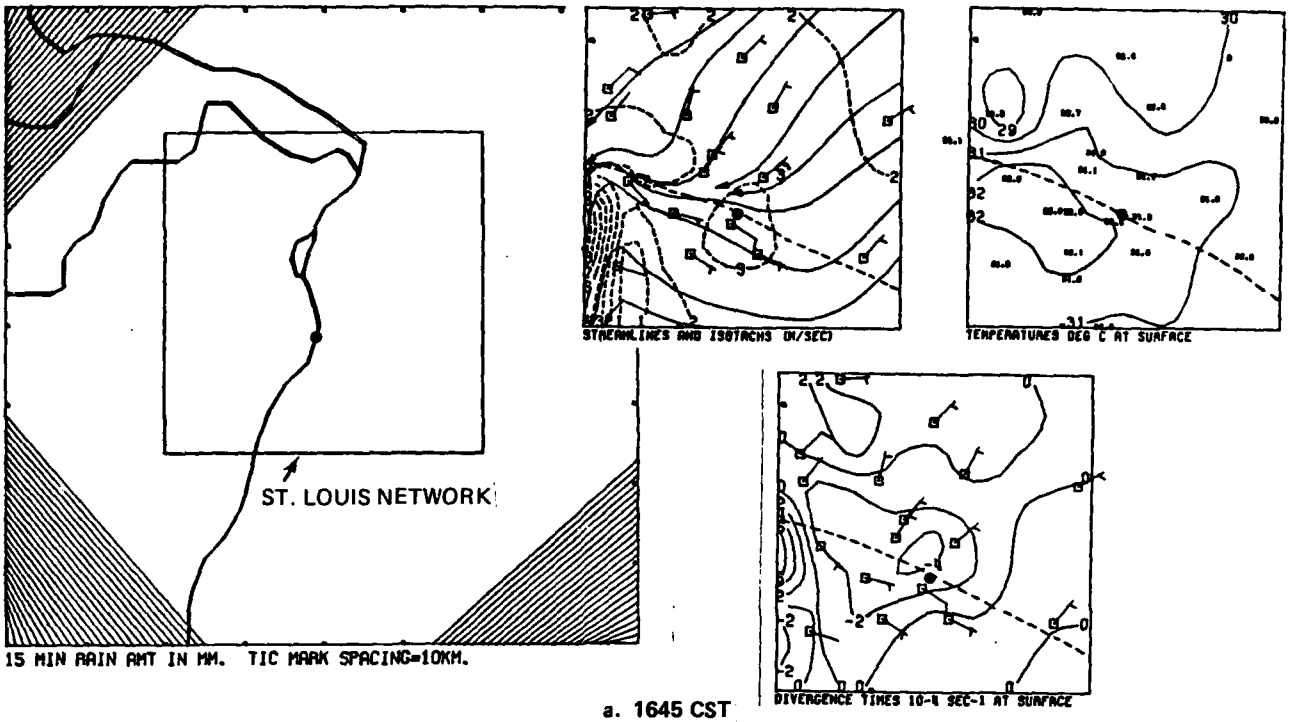

a. 1645 CST

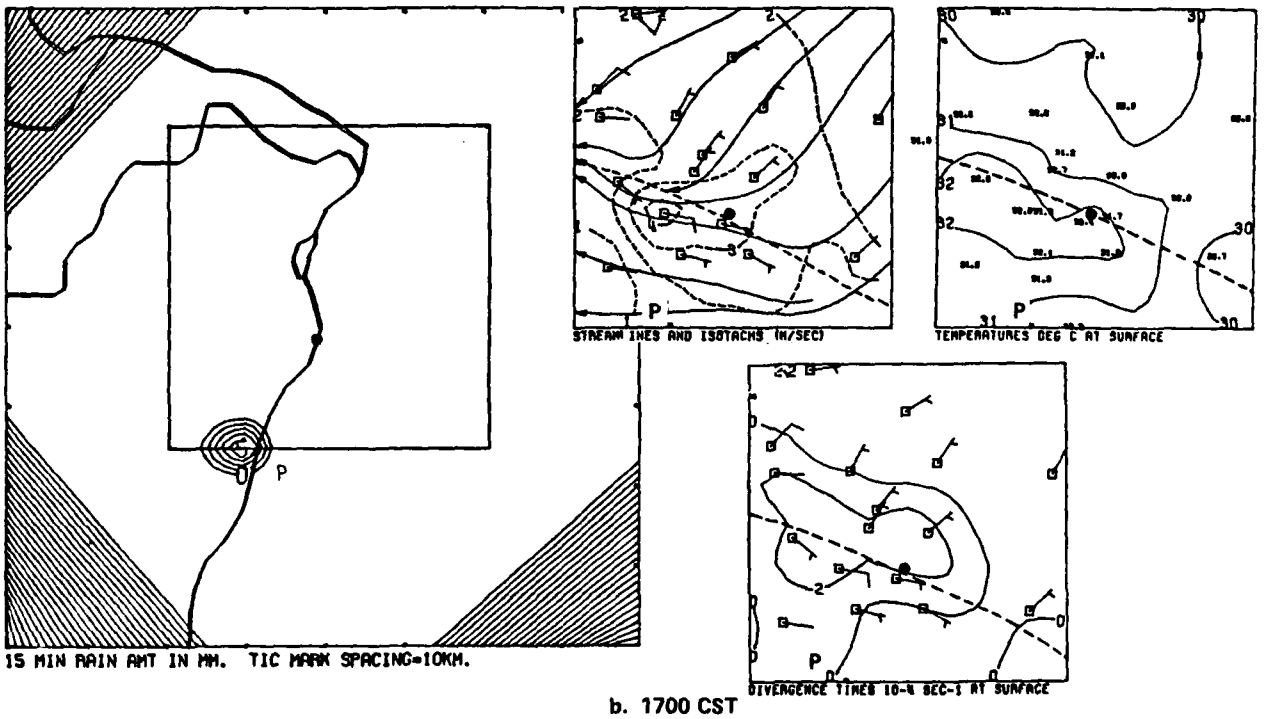

b. 1700 CST

Figure H21. Composite of the objective wind field isotachs and streamlines, temperature, divergence, and rainfall for 1645-1815 CST.

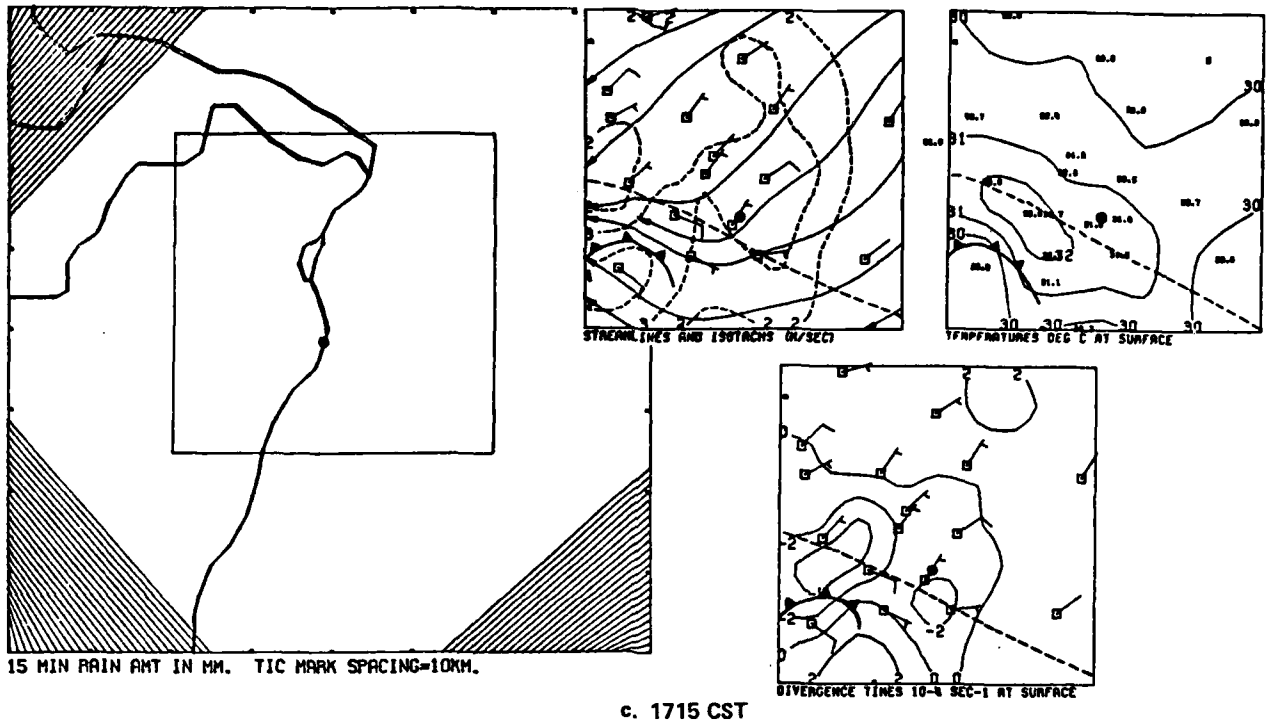

c. 1715 CST

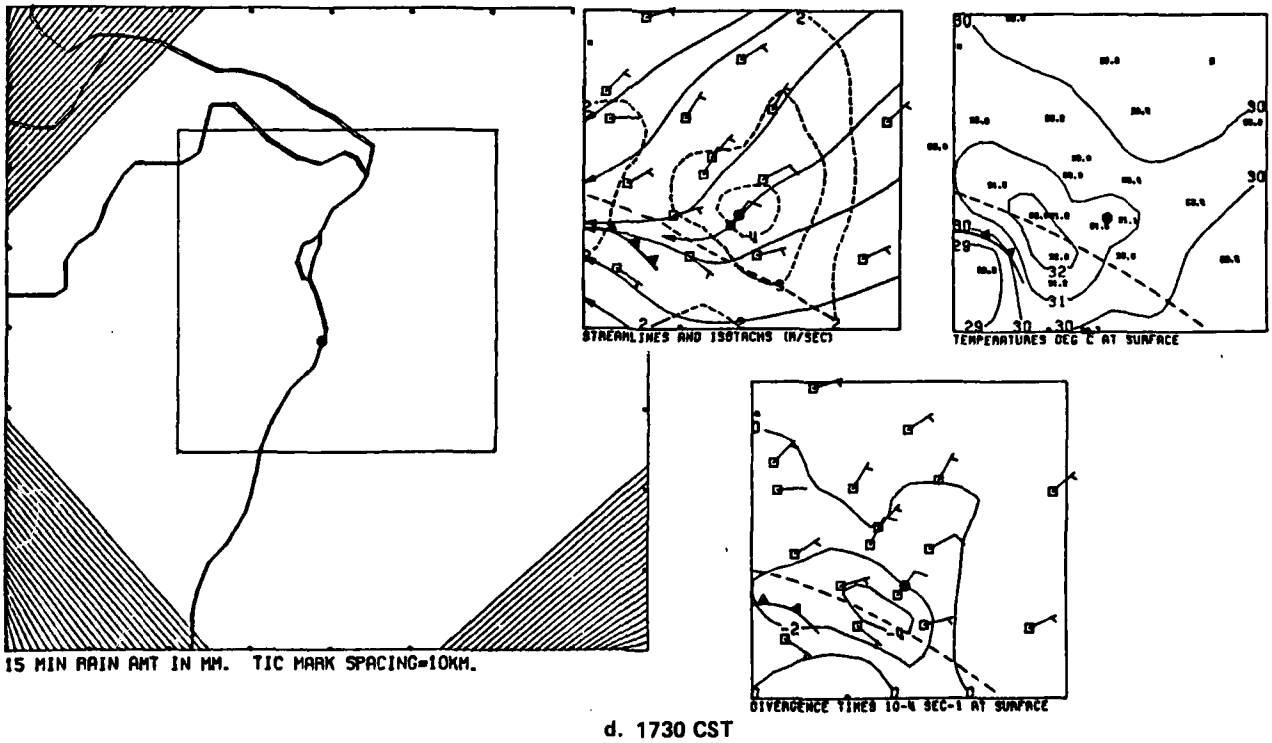

d. 1730 CST

Figure H21. Continued

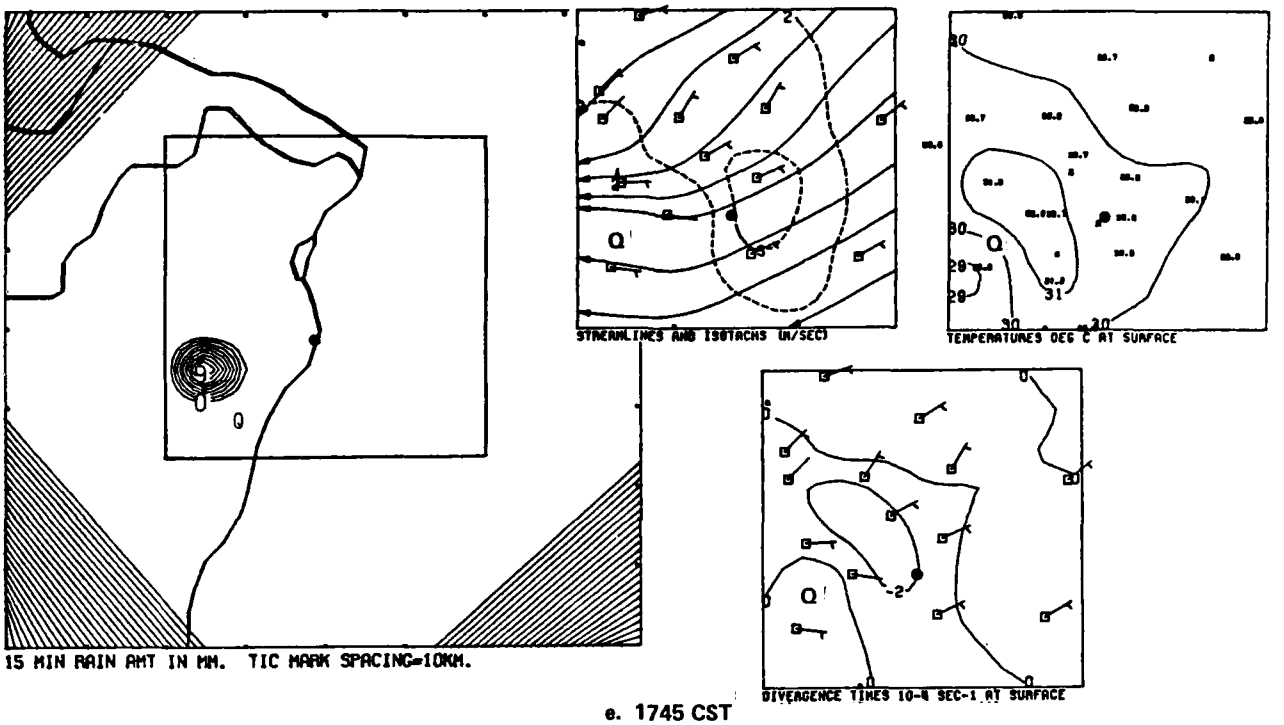

e. 1745 CST

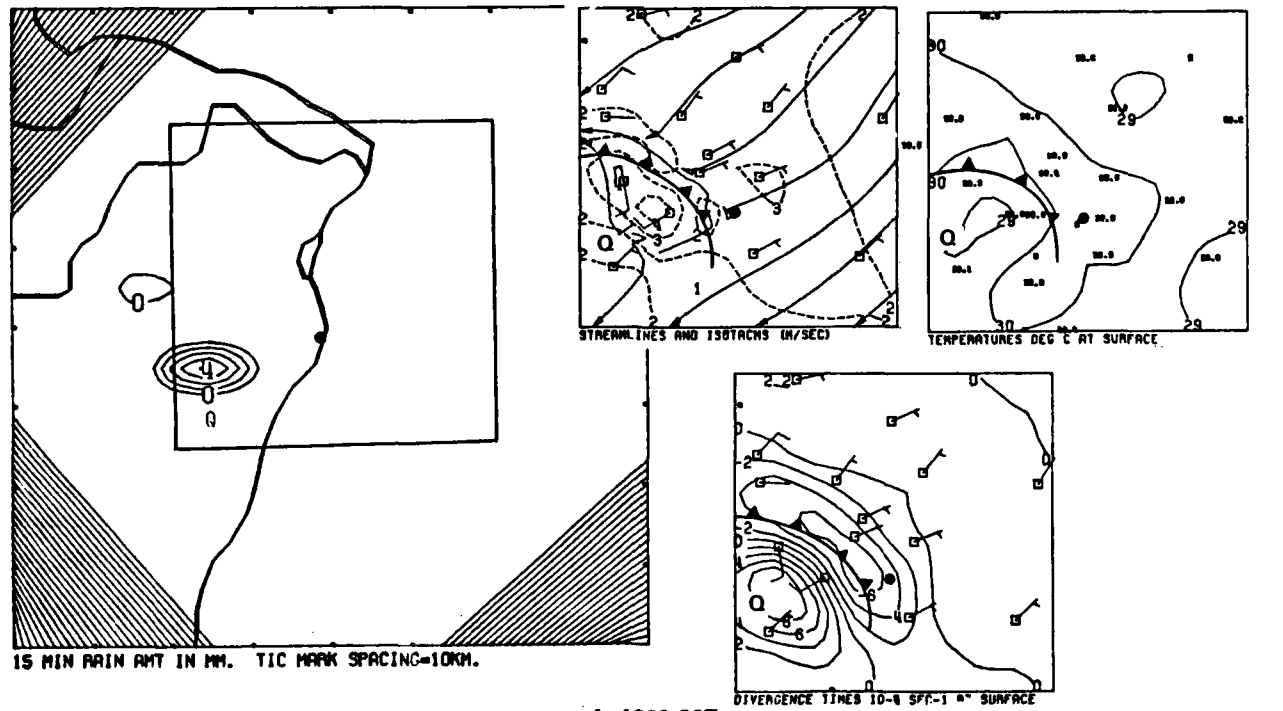

f. 1800 CST

Figure H21. Continued

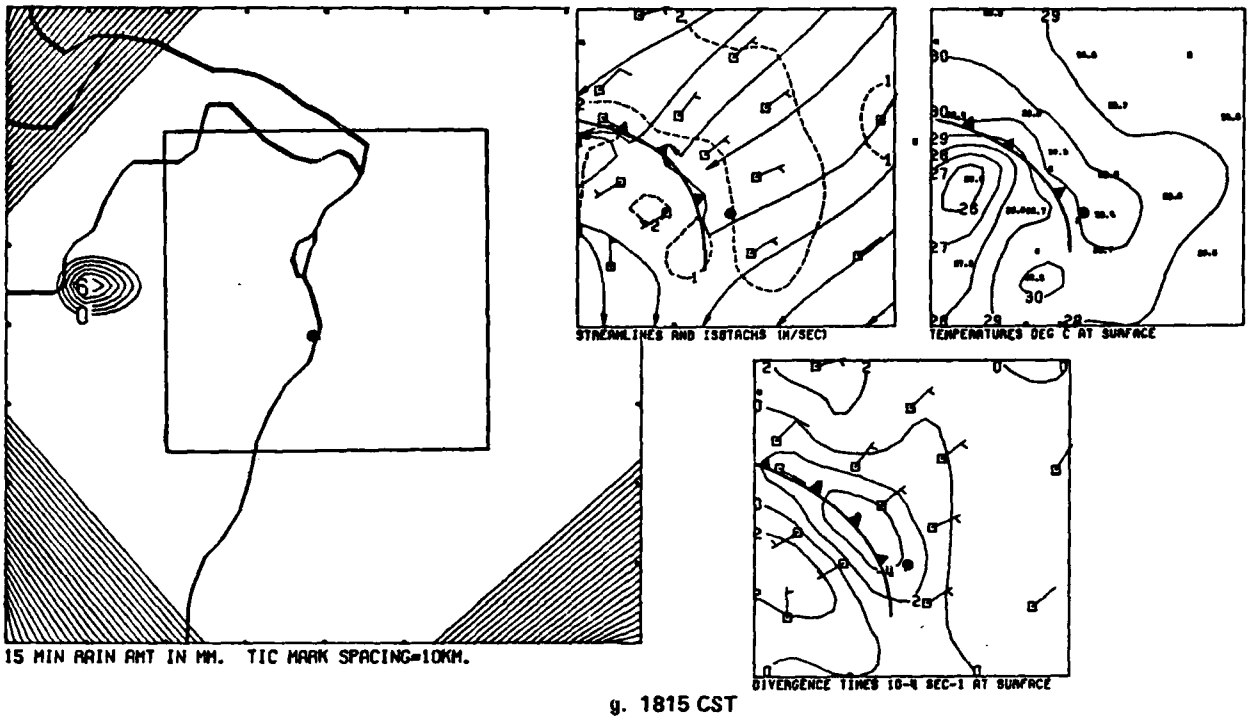

g. 1815 CST

Figure H21. Concluded

AD-A093 795 ILLINOIS STATE WATER SURVEY URBANA F/G 4/2
BOUNDARY LAYER STRUCTURE AND ITS RELATION TO PRECIPITATION OVER--ETC(U)
OCT 80 G L ACHTEMEIER NSF-ATM78-08865
UNCLASSIFIED SWS-CR-241 ARO-15529.4-GS NL

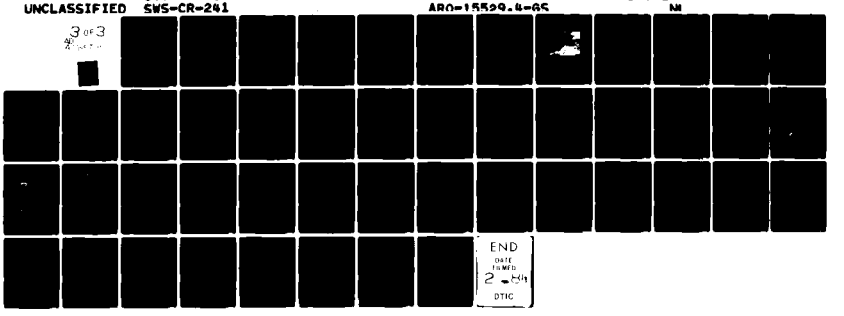

mid-morning. Vertical motions along the convergence zone, possibly coupled with vertical motions within the upper tropospheric cyclone, were apparently sufficient to release the convective instability over parts of eastern Missouri.

The development of the mesoscale convergence zone over the St. Louis network about mid-morning, caused a mean inflow of air into the area to commence at 1030, approximately 1.5 hours before rain began. Point maximum convergence persistently exceeded the background during this same period.

Raincell development over the St. Louis network was apparently highly dependent upon surface heating and local surface convergence. Seventeen raincells developed over or sufficiently near the network to influence the wind field. Cells A, B, and C formed near the boundary or outside the network and were apparently not directly associated with the convergence zone found over the network. Cells J, L, and M also formed along the boundary or outside the network but were associated with the mesoscale convergence zone and the gust front established by earlier storms within the area.

The remainder of the raincells formed within the network. Cells D, F, G, I, and K formed in areas of little or no convergence as determined from the 15-min average winds but were likely triggered by the passage of gust fronts. Cells N and O also formed in an area of little or no surface convergence and with no evidence of a surface trigger. They also formed within an area of weak subsidence aloft that was embedded within a larger area of strong subsidence. Cells E, H, and Q formed within areas of persistent strong convergence along the intersections of gust fronts and the mesoscale convergence zone that appeared to be a fairly persistent feature of the ambient (non-storm) wind field.

All raincells within the network formed over areas with warm surface temperatures. Significant convergence was found in areas cooled by shower outflows or by evening cooling established after the passage of the period of maximum heating. No shower activity was associated with these convergence areas.

The cell strengths, convergence strengths, and convergence durations for the raincells within the network are summarized in Table H1. The much stronger Cells E, H, and Q were found to be associated with much stronger and longer duration convergence than the other cells. Taken as a class, those raincells that formed in areas of little or no convergence had an average strength of 1.3 mm and an average convergence strength of 2U. The cells that formed in areas of persistent convergence had an average strength of 9.2 mm and an average convergence strength of 11.2U.

The spatial relationship between raincells and centers of convergence was excellent. The pre-rain centers persisted for 30-min or longer for 7 of the 10 storms. Thus, on this day, the convergence centers were fairly predictive of the future location of raincells and there were only 4 convergence centers not associated with rainfall.

There appeared to be a qualitative relationship between convergence strength and raincell strength for the 30th. Convergence strengths for the lighter raincells (strengths equal to or less than 3.0 mm) did not exceed 4U.

Raincell strengths and convergence strengths for the heavier raincells were, respectively, 5.5 mm (8U), 9.0 mm (18U), and 13.0 mm (9U). The relationship was also apparent in the convergence durations which ranged from 45-min to 75-min for the stronger storms and ranged from 15- to 30-min for the lighter storms.

Table H1. Cell Strengths, Convergence Strengths, and Convergence Durations for Raincells that formed within the St. Louis Network on 30 July, 1975.

Cell ID	Cell Strength	Convergence Strength	Convergence Duration
D	0.5mm	1U	15 min
F	1.0	1	15
G	3.0	1	15
I	1.0	3	30
K	0.5	4	30
N	2.0	2	30
O	1.0	2	30
E	9.0	18	75
H	5.5	8	45
Q	13.0	9	45

I. CASE STUDY: 14 AUGUST 1975

INTRODUCTION

Three rain events occurred on 14 August 1975. The first began on 0115 and ended at 0200 CST. Raincells formed along the southern boundary of the St. Louis network within an area with insufficient data to resolve the character of the wind field. Therefore, this rain event was not studied. The second rain event, from 0730 CST to 1000 CST, produced moderate amounts of precipitation from an aged squall line that died out in the network.

The third rain event began at 1530 and lasted through 1700 CST as the squall line redeveloped over the eastern part of the network. Its rainfalls, of cloudburst proportions, were the heaviest rainfalls observed on any of the 7 case study days. Data collection at 3 RAMS surface wind stations was disrupted during the course of these storms.

Unfortunately, much of the surface data for the regional scale analyses were missing for 14 August. Large numbers of key surface stations were missing at 0400, 0800, 1000-1200, and 1400-1700 CST.

SYNOPTIC SITUATION

A short wave trough with two embedded minor troughs at 700 mb (dashed lines A and B Fig. I1) had penetrated a high pressure ridge over the Mississippi valley and had shifted the winds from westerly to southwesterly over the St. Louis network. During the day, the trough split with minor trough A moving to western Illinois by 1800 CST (Fig. I2). The remainder of the trough remained stationary over the High Plains. Qualitative pattern analysis would place most of Missouri within a regime of weak positive vorticity advection and upward vertical motion at 700 mb. Only a weak trough was present at 500 mb.

Copious amounts of moisture at 850 mb at both 0600 CST and 1800 CST over the St. Louis area were indicated by temperature - dewpoint spreads of 6C or less.

At the surface, (Fig. I1) a stationary front extended from a weak low pressure center over eastern Kansas across northern Missouri and through Illinois and Indiana. The St. Louis area remained within the warm moist air south of the front throughout the day (Fig. I2). The northern edge of a squall line (of which rain event 3 was a part) extended from eastern Arkansas into the St. Louis area at 1800 CST. The combination of mid-level ascending motion, copious moisture, and the convergence along the squall line led to an ideal situation for heavy rainfall.

REGIONAL SCALE SITUATION

Figure I3 shows the regional scale streamline and convergence fields for times leading up to the second and third rain events for 14 August. The confluence zone along the stationary front north of St. Louis is evident in

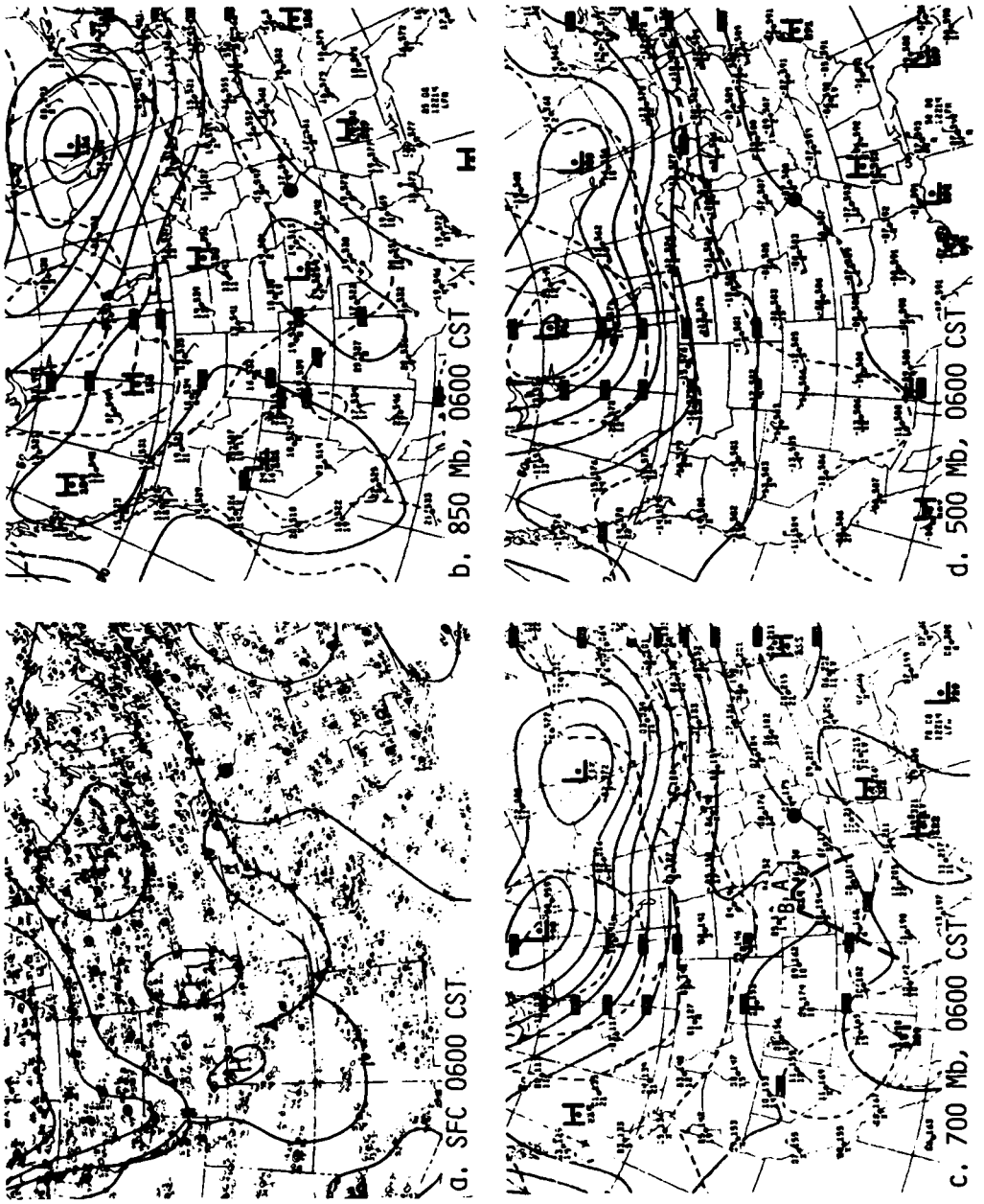

Figure 11. National Weather Service synoptic analyses for 0600 CST 14 August 1975. St. Louis area identified by black dot.

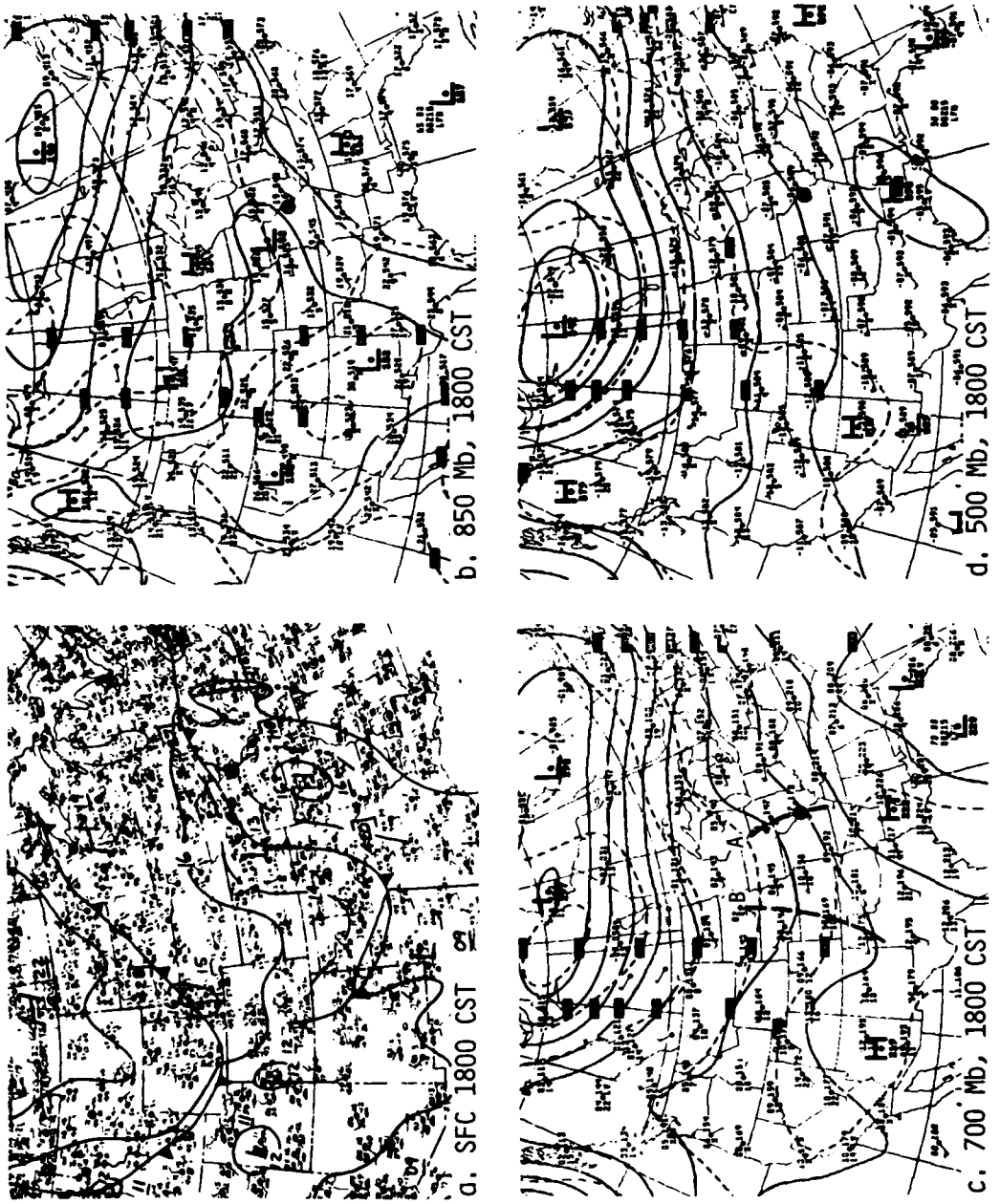

Figure I2. National Weather Service synoptic analyses for 1800 CST 14 August 1975.

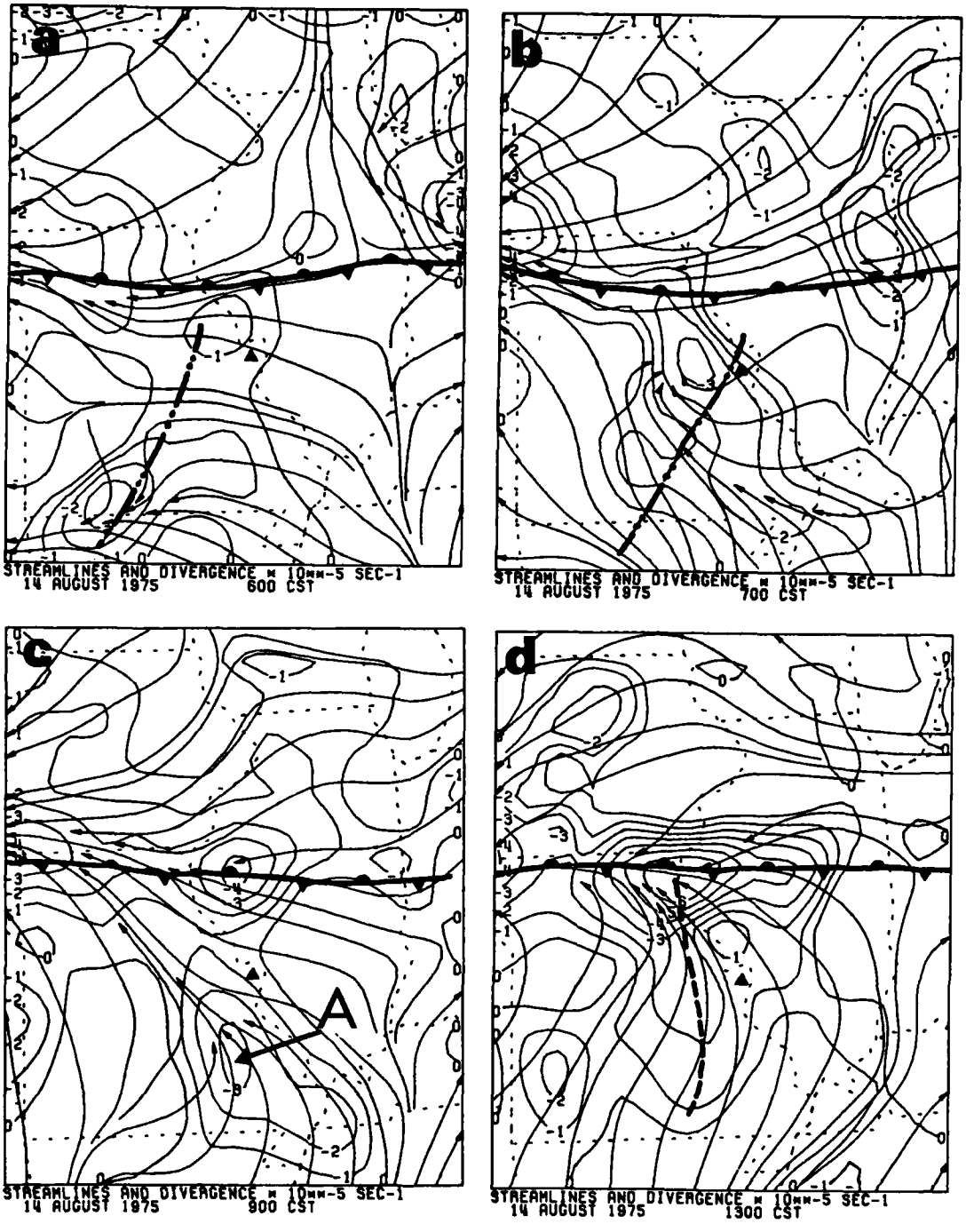

Figure I3. Regional scale analysis of surface wind field.

all analyses. The squall line that produced the second rain event is shown in Figs. I3a, b; its position deduced from surface reports, satellite images, and by extrapolation from the time and movement of raincells through the St. Louis network. The squall line was found within an area of convergence at 0600 and 0700 CST. Convergence increased to 0.3U west of St. Louis as showers moved into the network. The satellite photo of the Midwest (Fig. I4) shows the cloud mass associated with the squall line (arrows) at 0830 CST during the second rain event.

An area of moderate convergence (arrow A) remained southwest of St. Louis at 0900 CST after the squall line had dissipated. By 1300 CST, about 2.5 hr before the start of the third rain event, a zone of convergence (dashed line Fig. I3d) extended from the stationary front to near the Missouri-Arkansas border; the zone passing about 100 km west of St. Louis. Rain event three began as the squall line redeveloped along or near the convergence zone. (Note that the objective analysis can be in error up to one half the local station separation in locating convergence zones.)

EVOLUTION OF DIVERGENCE AND RAINFALL

The time series for the number of gridpoints with rain, the average 15-min rainfall for the gridpoints with rain and the network mean divergence, (Fig. I5a-I5c) show that flow in the network was convergent prior to and during parts of all three rain events. Persistent convergence began shortly before 0600 CST, about one hour before the second rain event (A Fig. I5c). Strong convergence began at 1500 CST about one half hour before rain event three (B Fig. I5c). This convergence was associated with the redevelopmeent of the squall line.

The time series of the maximum 15-min rainfall and the maximum and minimum divergence are given in Figs. I5d-I5f. The background convergence was about 3U. Convergence persistently exceeded background beginning at 0430 CST during the period identified as A (Fig. I5f). This was more than 2.5 hr prior to the second rain event. Convergence persistently exceeded background again beginning at 1430 CST, about 1 hr prior to rain event three. Outflow from the heavy rainstorms produced the strong convergences up to 10U.

The increase in the maximum convergence during the 0530-0800 CST period (Fig. I5f) was not as prominent as the increase in the network mean convergence during the same period (Fig. I5c). This means that the increase in the network scale convergence came about because of an increase in the areal coverage of the convergent flow; the increase in the magnitude was small. This is an additional indicator that the second rain period was preceded by mesoscale rather than by raincell-scale circulations.

MESOSCALE SITUATION RAIN EVENT 2: 0730-1000 CST

Shortly before 0600 CST, a mesoscale convergence zone developed when light northeasterly winds merged with light southeasterly winds over the northern part of the network. This convergence zone was not associated with the stationary front located across northern Missouri (Figs. I1 and I2). The axis of the convergence zone intersected the leading edge of an approaching squall line at a large angle.

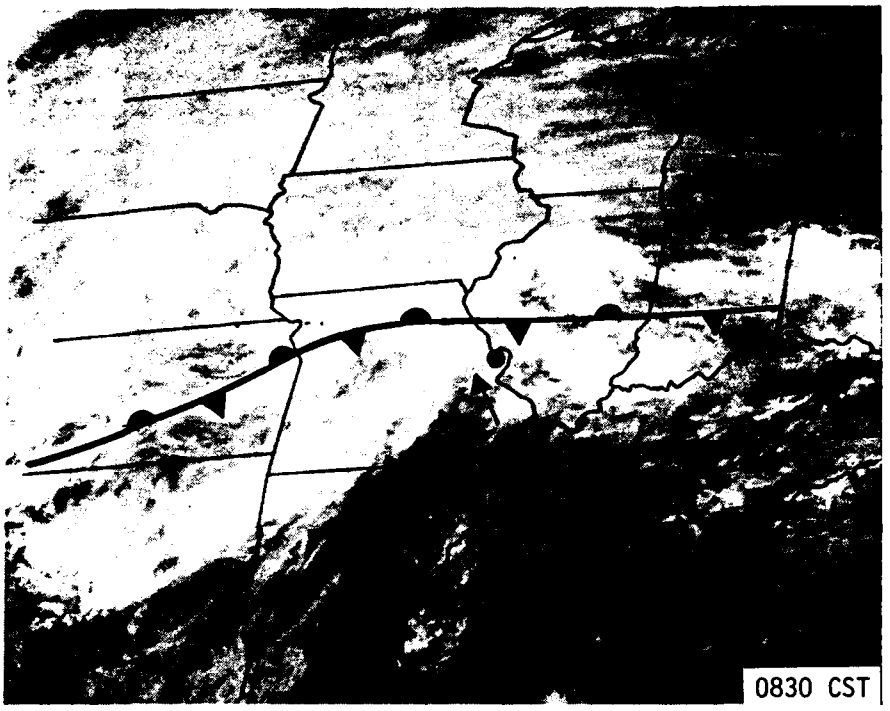

Figure I4. GOES satellite photograph of the Midwest for 0830 CST showing location of surface frontal system and cloud masses associated with middle troposphere trough. St. Louis area identified by black dot.

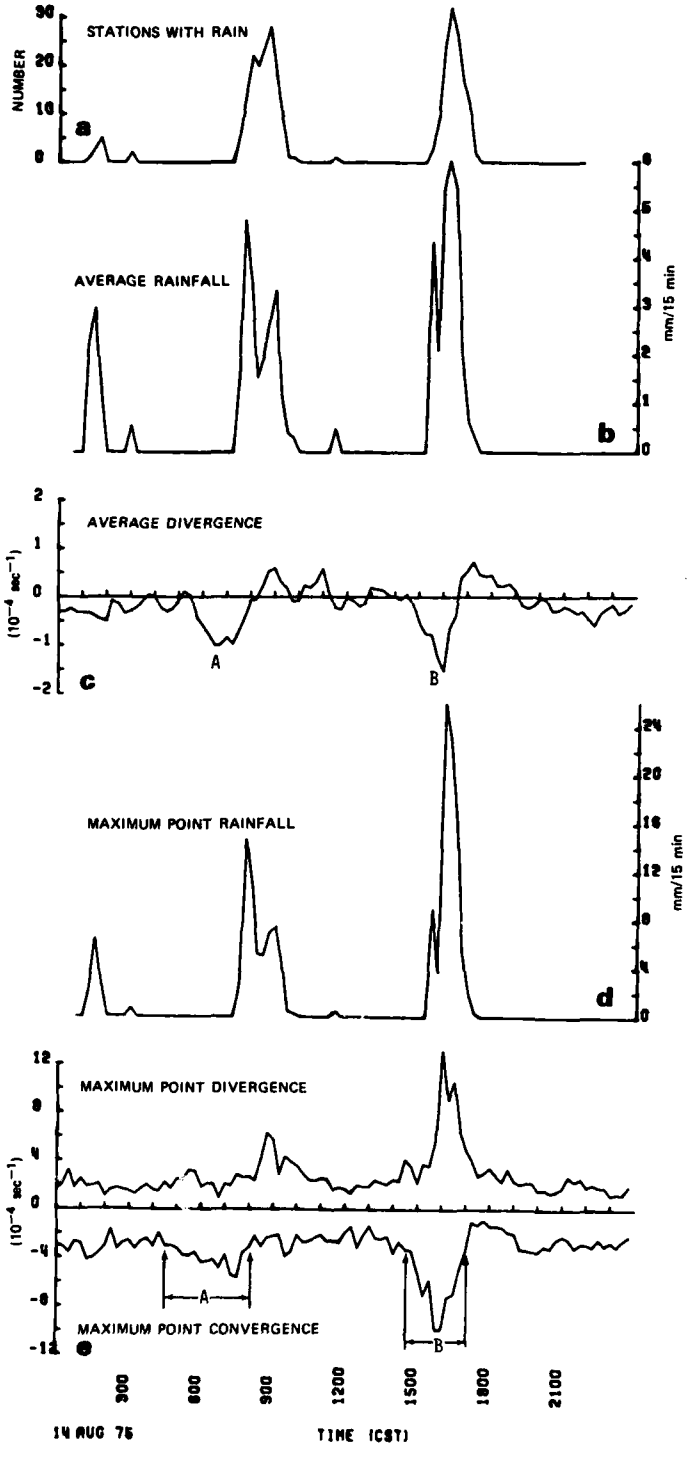

Figure I5. Time series of divergence and rainfall variables.

During the period from 0615-0645, the convergence zone (dashed lines Fig. I6) developed several 4U centers. It was during this same period that the network scale convergence approached 1U (see A Fig. I5c), and the point maximum convergence persistently exceeded background (see A Fig. I5f).

The first of several large raincells entered the METROMEX raingage network at 0700 (Fig. I7a). The squall line moved toward the St. Louis network (Fig. I7b) and a weak wind shift along its leading edge penetrated the network at 0730 (Fig. I7c). The wind shift line, which separated southerly winds from southwesterly winds, pushed ahead of raincells A and C which were within the network at 0745 (Fig. I7d). A 2U convergence center (arrow) formed near the intersection of the wind shift line with the mesoscale convergence zone. The temperture field remained essentially undisturbed.

By 0800, Cells A, B, and C covered the northwestern one quarter of the network in an area north of the mesoscale convergence zone. Outflow from these storms caused little or no response in the surface wind field north of the convergence zone. South of the convergence zone, the winds became light and variable but generally northeasterly to the west of the wind shift line that had moved to near the Arch to a 2U convergence center over the southern part of the network.

Cell B dissipated and the Cell A, C complex weakened and moved to the northern part of the network by 0815 (Fig. I7f). Both the mesoscale convergence zone and the wind shift line dissipated. A new Cell D was developing near the grid boundary about 20 km west of the Arch. A small 2U convergence center (arrow) formed northwest of the Arch within the weakly perturbed flow. Cell D moved onto the network at 0830 (Fig. I7g) with no apparent response in the wind field. Cell E formed in the location of the convergence center at 0815. The convergence center had expanded and moved to the central part of the network by 0830.

Cell F formed between Cells D, E and in the location of the convergence center as the complex moved rapidly to the center of the network (Fig. I7h). Meanwhile, the 2U convergence center (arrow) had moved eastward to where the mesoscale convergence zone had redeveloped (dashed line).

Weak outflow from Cells D, F, which moved to the northeast part of the network at 0900 (Fig. I7i), shifted the winds to the north and northeast and strenghtened the convergent area through the center of the network (arrow). Cell G, which had followed the larger complex onto the network at 0845, passed near the convergence area without intensification. By 0915 (Fig. I7j) raincells D, F had moved out of the wind field network. Cell G continued northeastward with no apparent response in the generally southeasterly flow. No new raincells developed after 0915 until mid-afternoon.

MESOSCALE SITUATION RAIN EVENT 3: 1530-1700 CST

Rain event 3 began as the squall line redeveloped over roughly the southeastern one half of the St. Louis network. Winds west and southwest of the Arch shifted to southwesterly shortly after 1300 and a convergence zone extended from the network's southern boundary through St. Louis passing about 5 km west of the Arch (see dashed lines Fig. I8). This mesoscale convergence

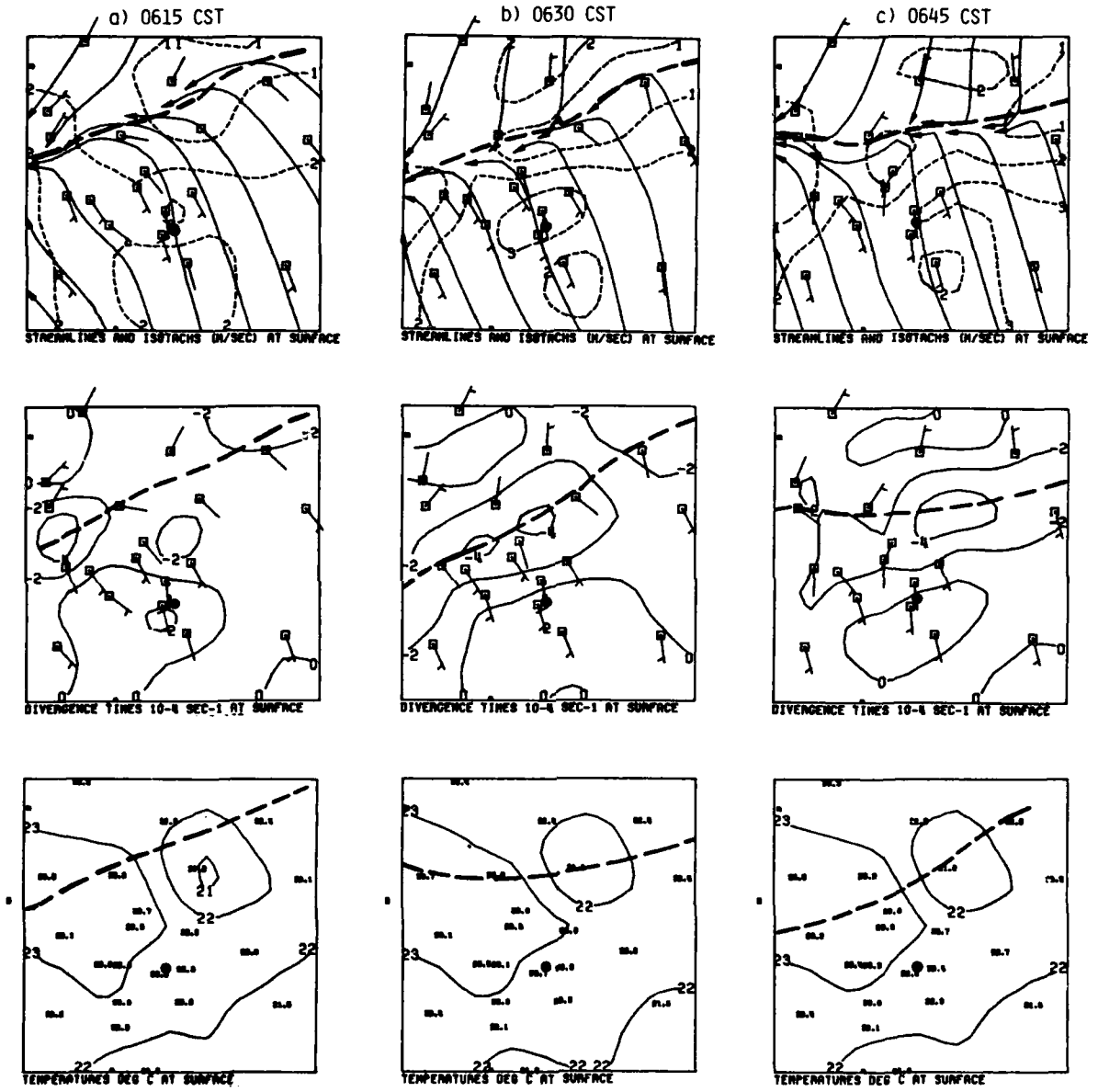

Figure I6. Composite of the objective isotachs and streamlines (upper maps), divergence (middle maps), and temperature (lower maps) for 0615-0645 CST. St. Louis Arch identified by black dot.

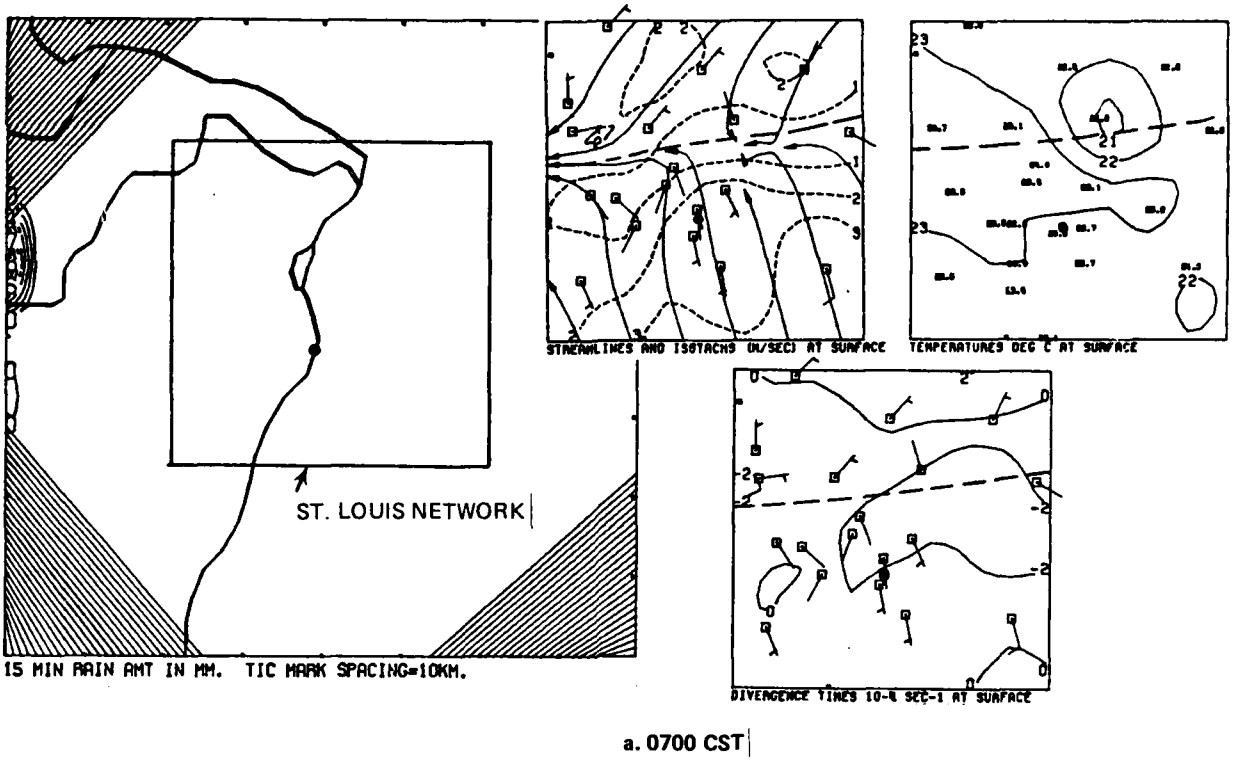

a. 0700 CST

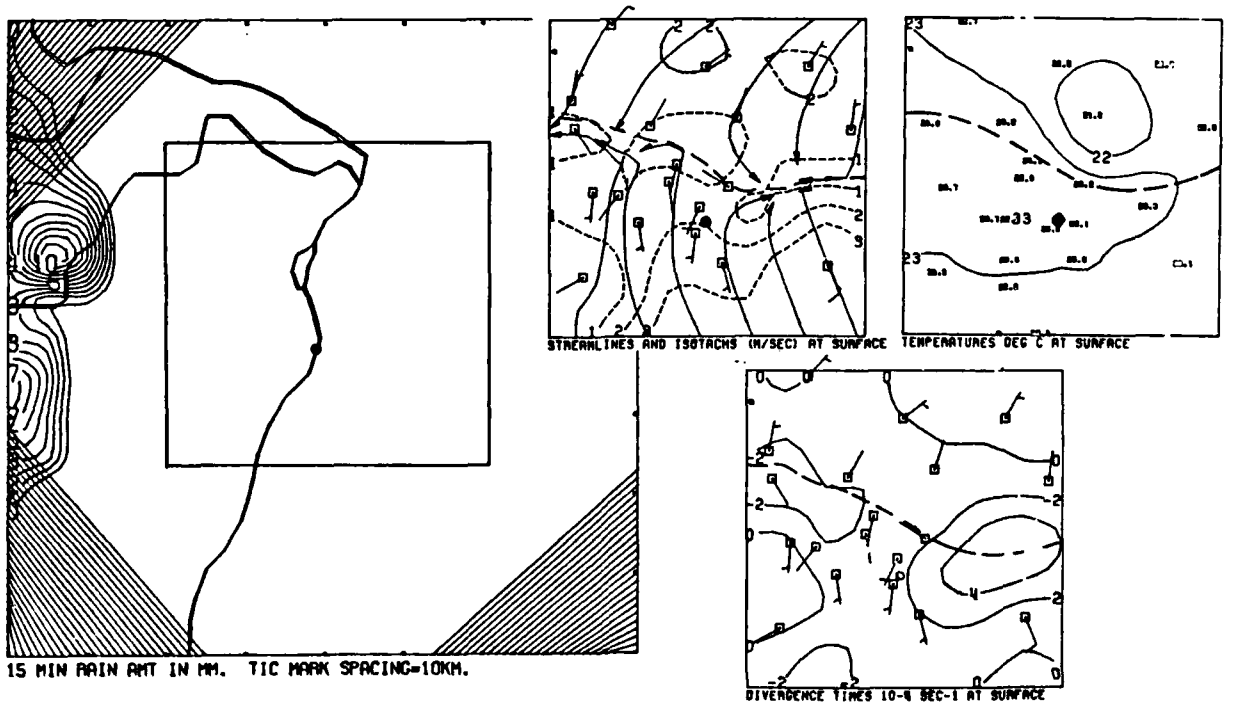

b. 0715 CST

Figure I7. Composite of the objective isotachs and streamlines, temperature, divergence, and rainfall for 0700-0915 CST.

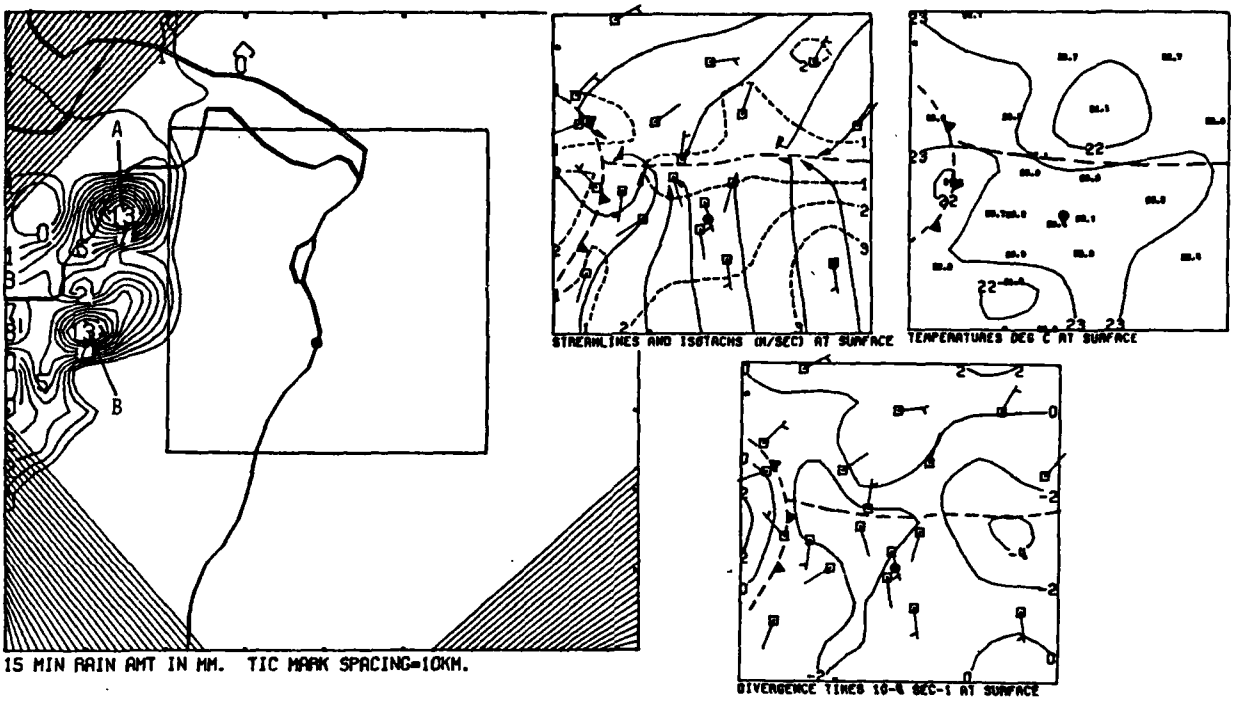

c. 0730 CST

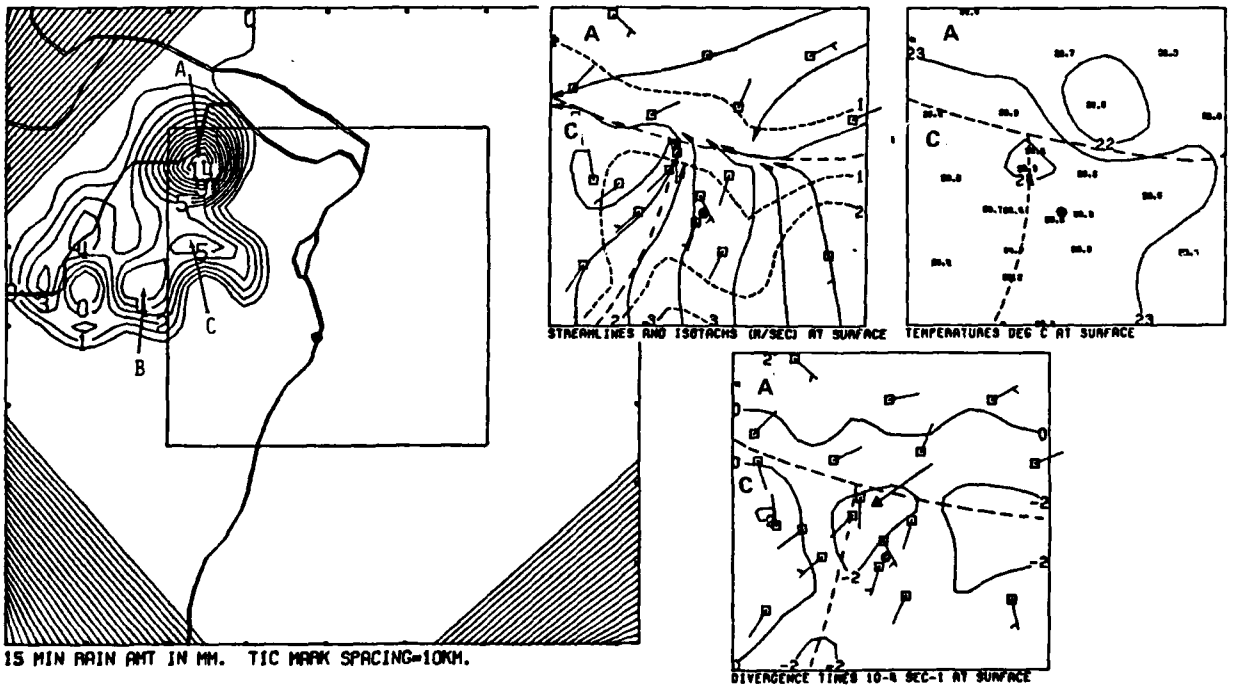

d. 0745 CST

Figure I7. Continued

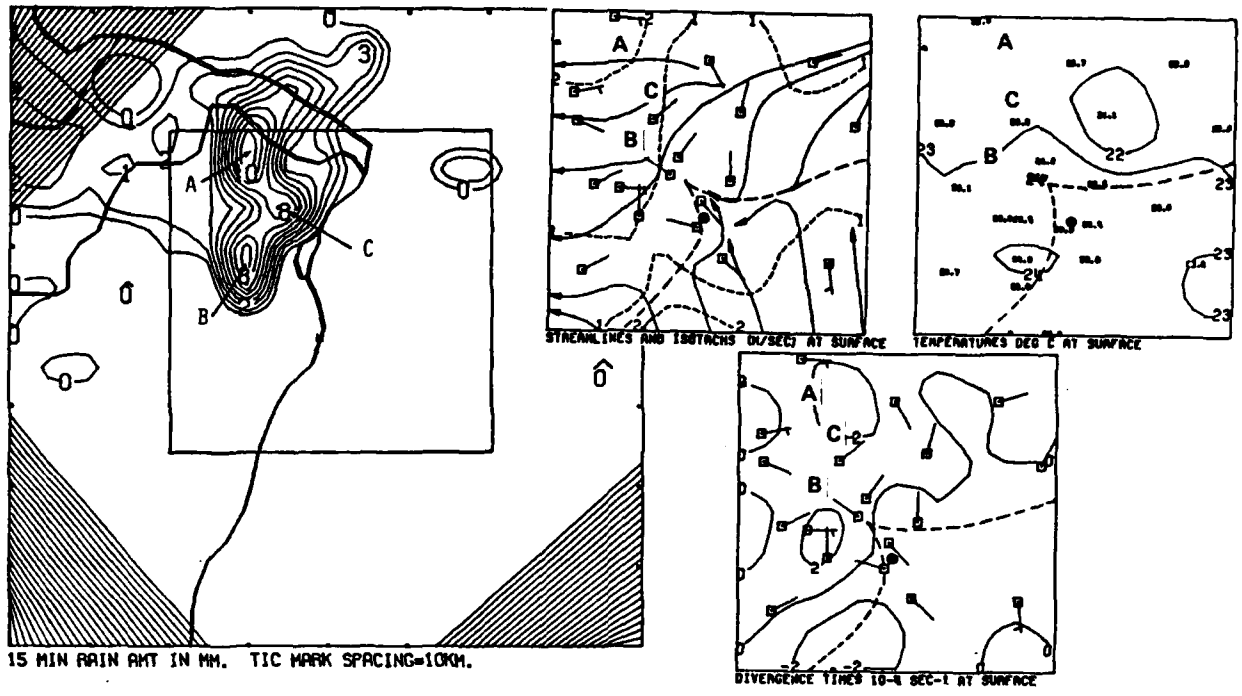

e. 0800 CST

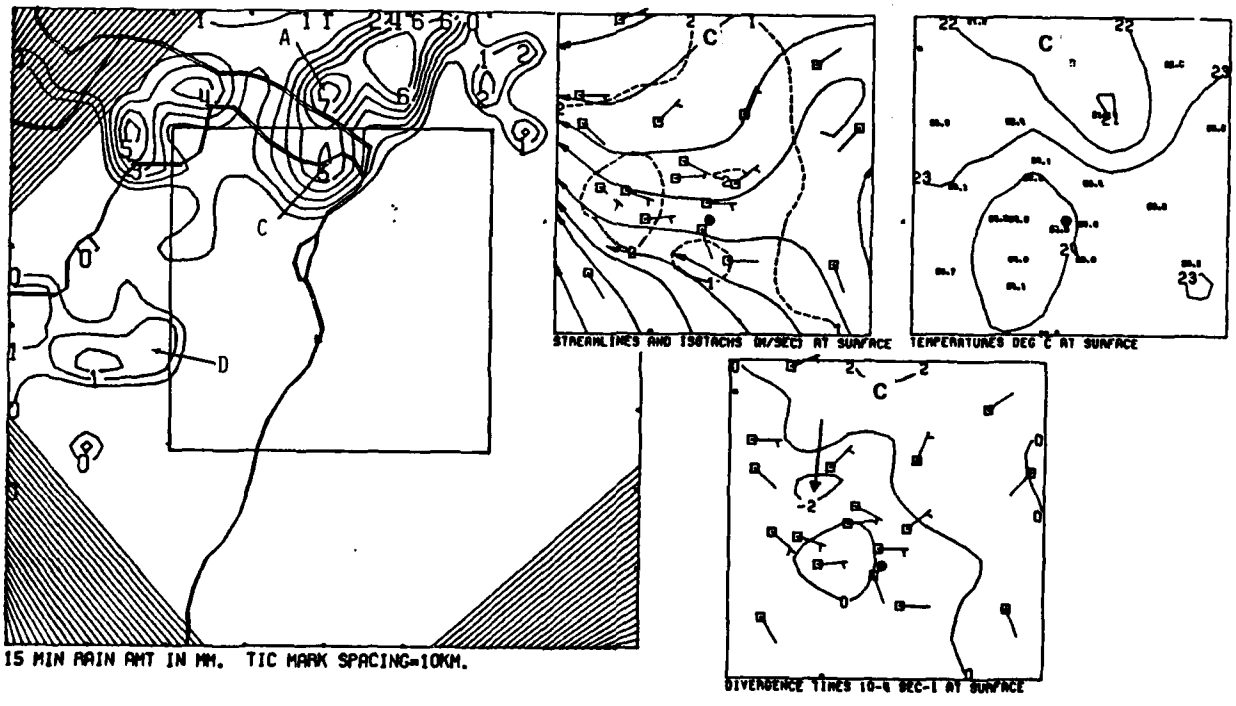

f. 0815 CST

Figure I7. Continued

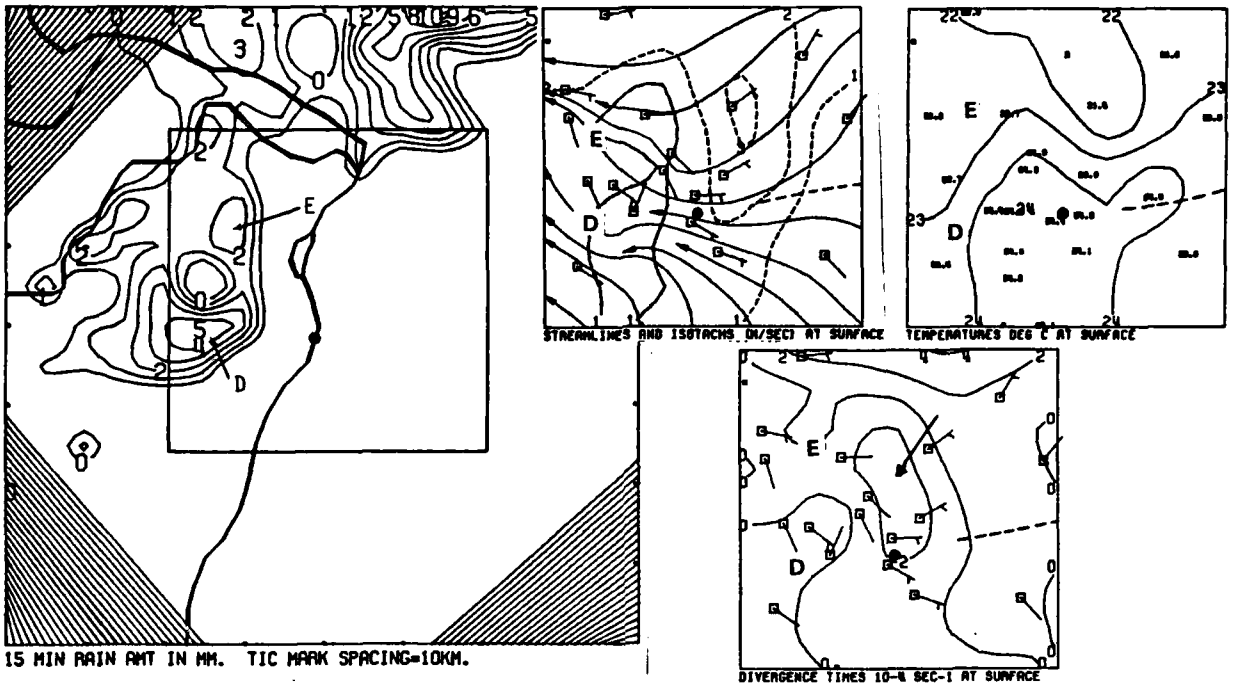

g. 0830 CST

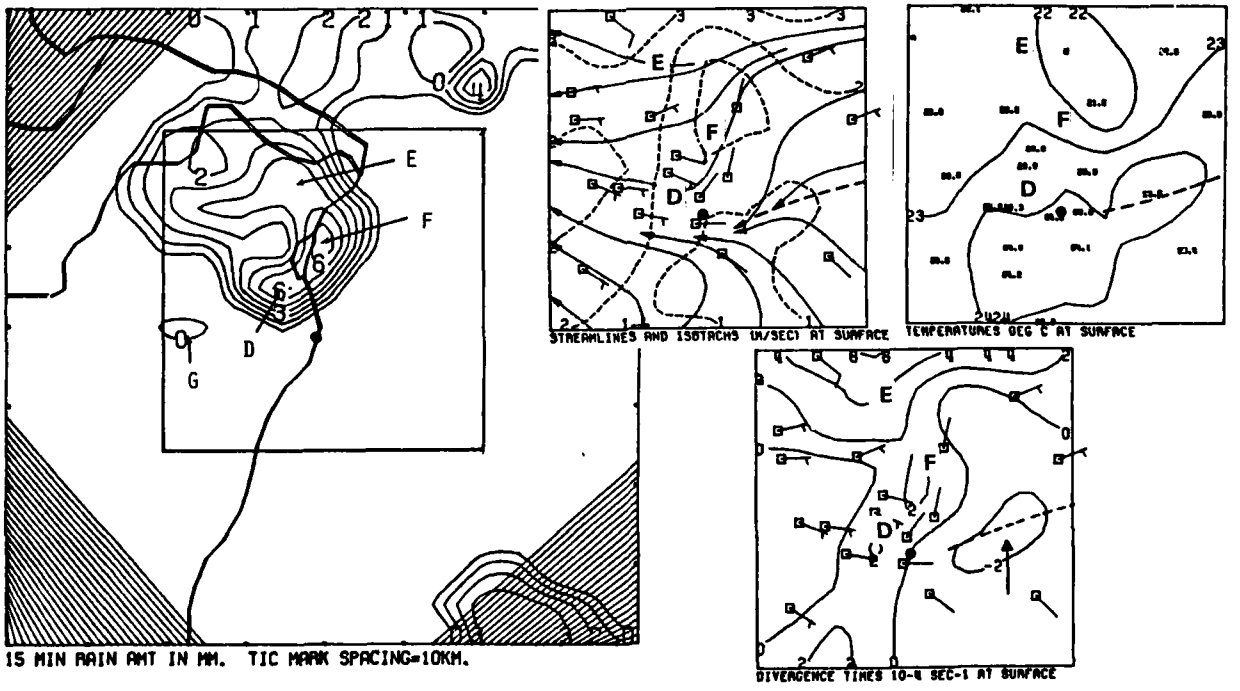

h. 0845 CST

Figure I7. Continued

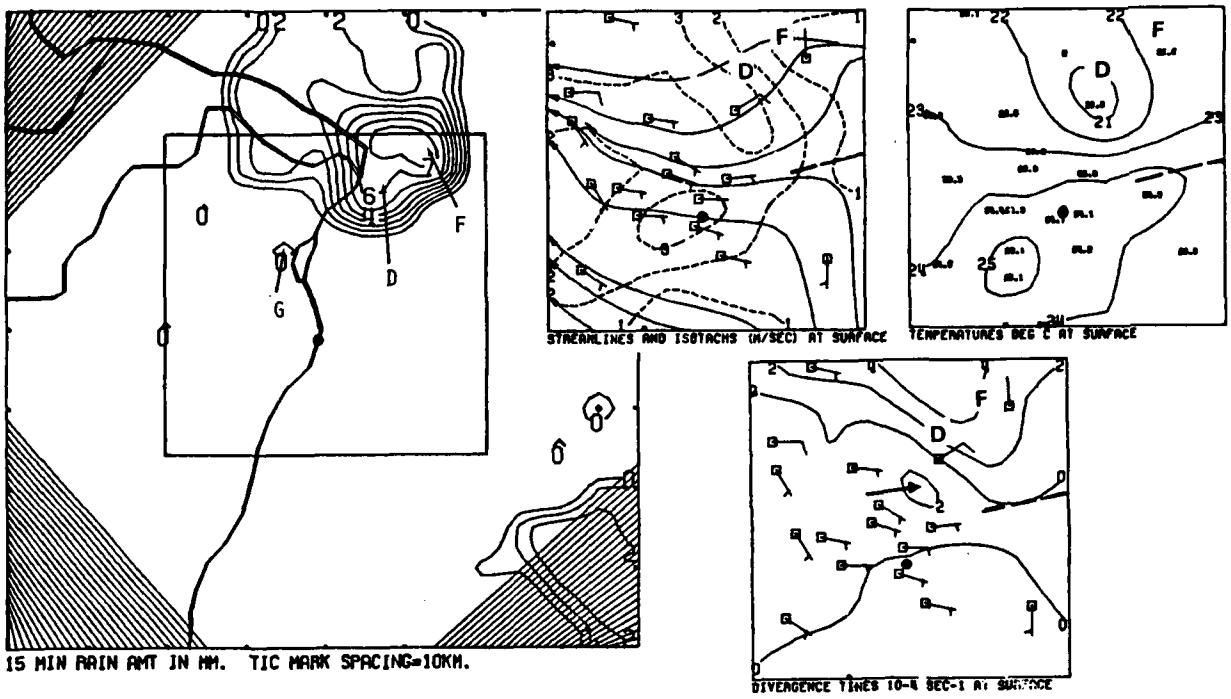

i. 0900 CST

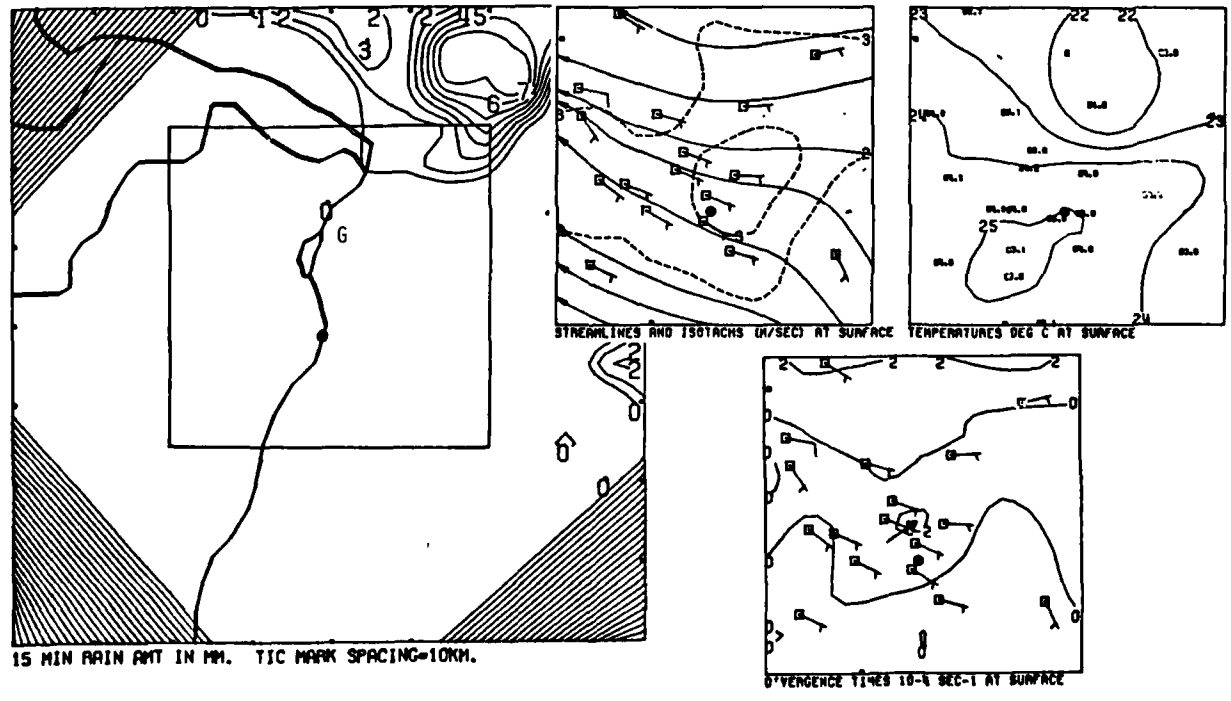

j. 0915 CST

Figure I7. Concluded

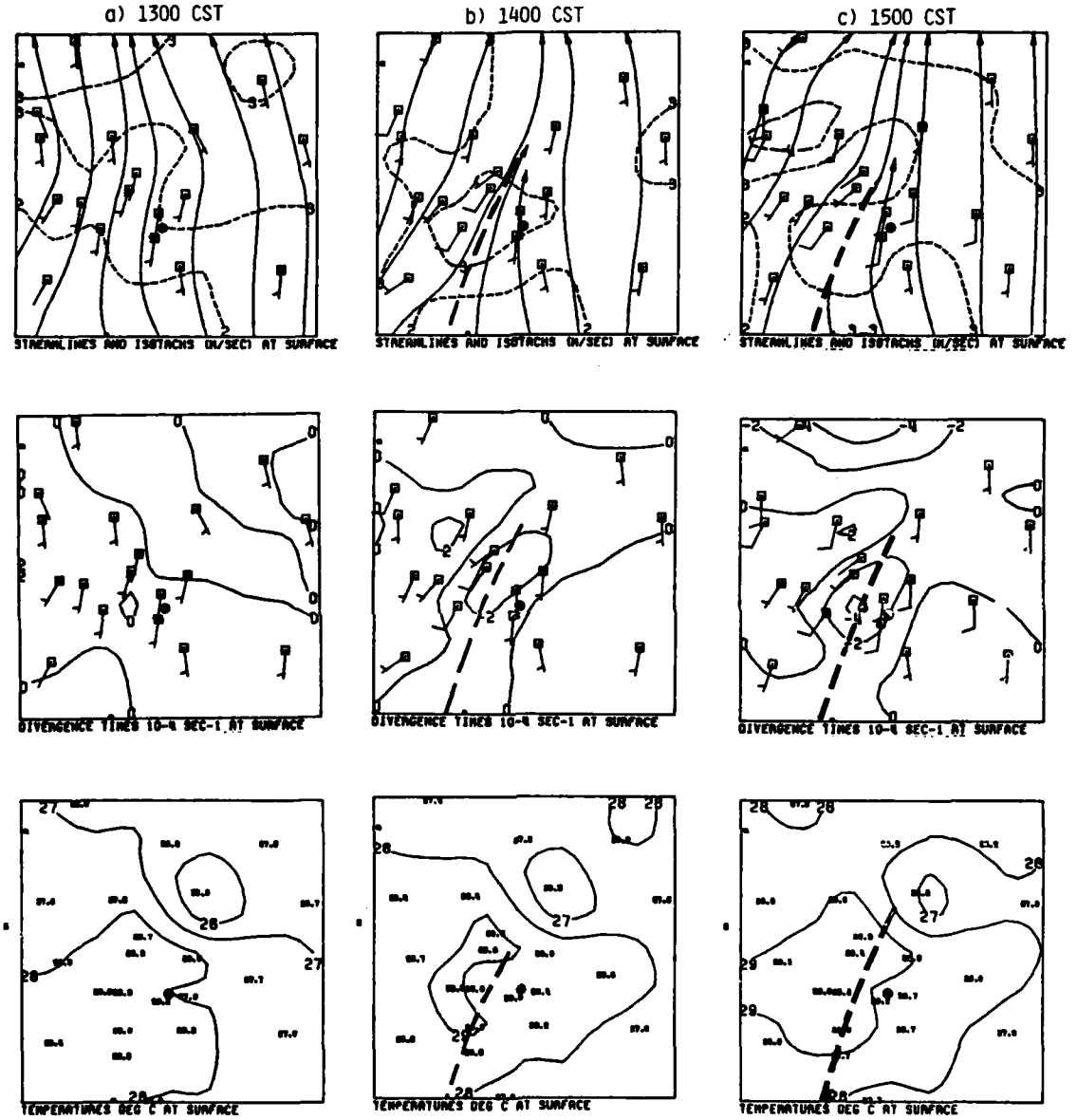

Figure I8. Composite of the objective isotachs and streamlines, temperature, and divergence for 1300-1500 CST.

zone persisted in the same location through 1500, a 2 hr period free of precipitation. Convergences exceeding 2U appeared locally at various times until 1500 when convergence increased to 4U west of the Arch.

The flow on the scale of the network (Fig. I5c) was slightly divergent at the beginning of the period but became increasingly convergent shortly before 1500 as the mesoscale convergence zone intensified. Convergence persistently exceeded background beginning at 1400 (B Fig. I5f).

The boundary layer flow at 1300 (Fig. I9) was southerly from 250-550 m with a transition to southwesterly within the 550-950 m layer. Slight streamline confluence over the surface wind network is indicative of the incipient mesoscale convergence zone. Flow west of the network was southwesterly from 250-550 m. The confluence did not appear in the southwesterly flow above 550 m. A zone of ascent with vertical motions exceeding 10 cm sec^{-1} (dashed lines Fig. I10) appeared across the network in roughly the position of the developing convergence zone.

Southwesterly winds intensified the mesoscale convergence zone below 550 m at 1400 CST (Fig. I11). The confluence was not apparent above 550 m. The vertical velocity analyses (Fig. I12) did not reveal a clearly defined axis of ascent at 1400 because gustiness below 350 m developed large magnitude divergence centers which determined the magnitudes and signs of the vertical velocity fields. The ascent axis at 250 m (dashed line, Fig. I12a) gave way to vertical velocity centers of varying sign by 350 m.

The mesoscale confluence zone remained stationary over the network at 1500 CST (Fig. I13) and its persistence is an excellant example of coupling between the surface wind fields (Fig. I8) and the winds aloft in an area of strong thunderstorm development. The confluence zone was not present above 550 m; this mesoscale disturbance had a depth of approximately 500 m for the 2 hrs prior to the onset of precipitation.

The ascent axis passing near the Arch (dashed lines Fig. I14) shifted eastward about 10 km in the flow above 250 m. Largest vertical motions at 1350 m were along the convergence zone south of the Arch and along the western part of the network. The westernmost ascent center was a shallow feature not found below 950 m.

The thunderstorms first developed in the area of the strongest and deepest ascent near the mesoscale convergence zone. Raincell A appeared 10 km west of the network at 1515 (Fig. I15a) and propagated eastward to the network boundary at 1530 (Fig. I15b). It was not directly linked to the mesoscale convergence zone (dashed lines) but was located within the ascent area at 1350 m (Fig. I14d). Cell B developed within the convergence zone 10 km southwest of the Arch. Cell C appeared 20 km east of the Arch in an area with little or no surface convergence. Figure I14 shows that there was little or no ascent at 1350 m in the same area at 1500 CST. However, the winds at 1350 m were from the southwest and Cell C was directly downwind from the area of 20 cm sec^{-1} rising motion. It is likely that the moisture within the layer deepened by vertical displacements within the convergence zone was carried downwind and that Cell C drew from this moisture source.

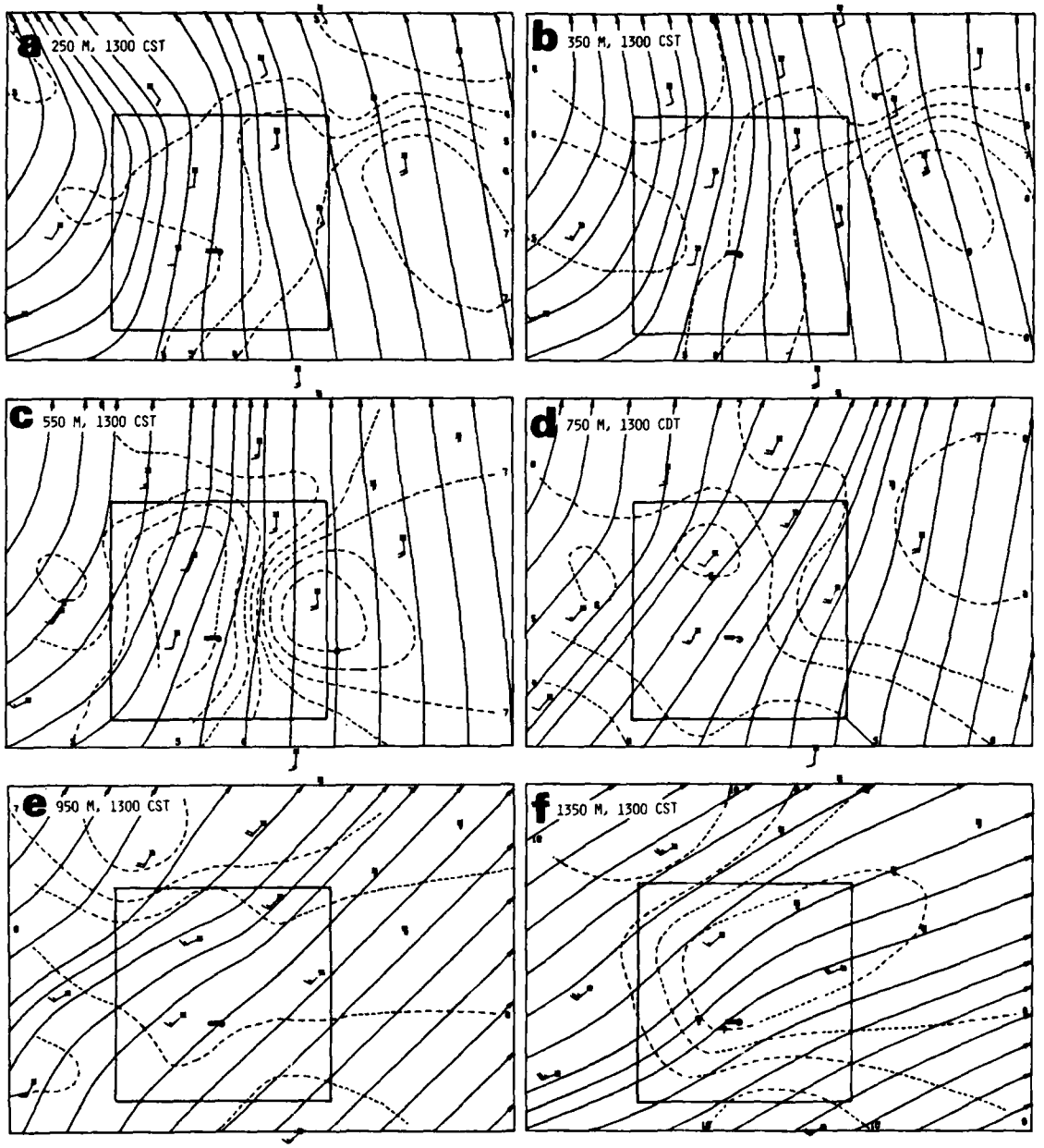

Figure I9. Objective streamlines and isotachs (m sec^{-1}) for 1300 CST at six heights (msl).

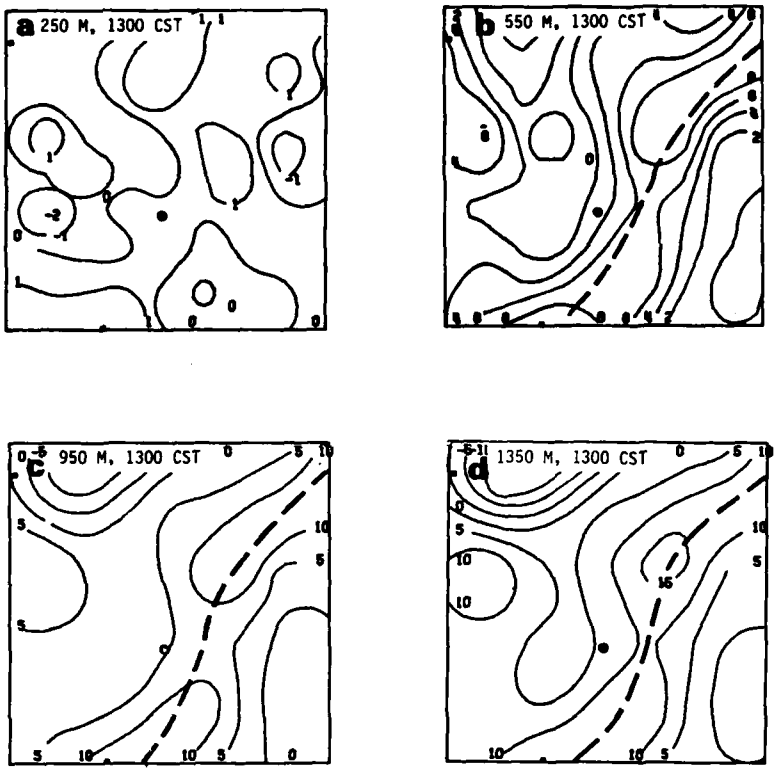

Figure I10. Vertical velocity maps (cm sec^{-1}) for 1300 CST.

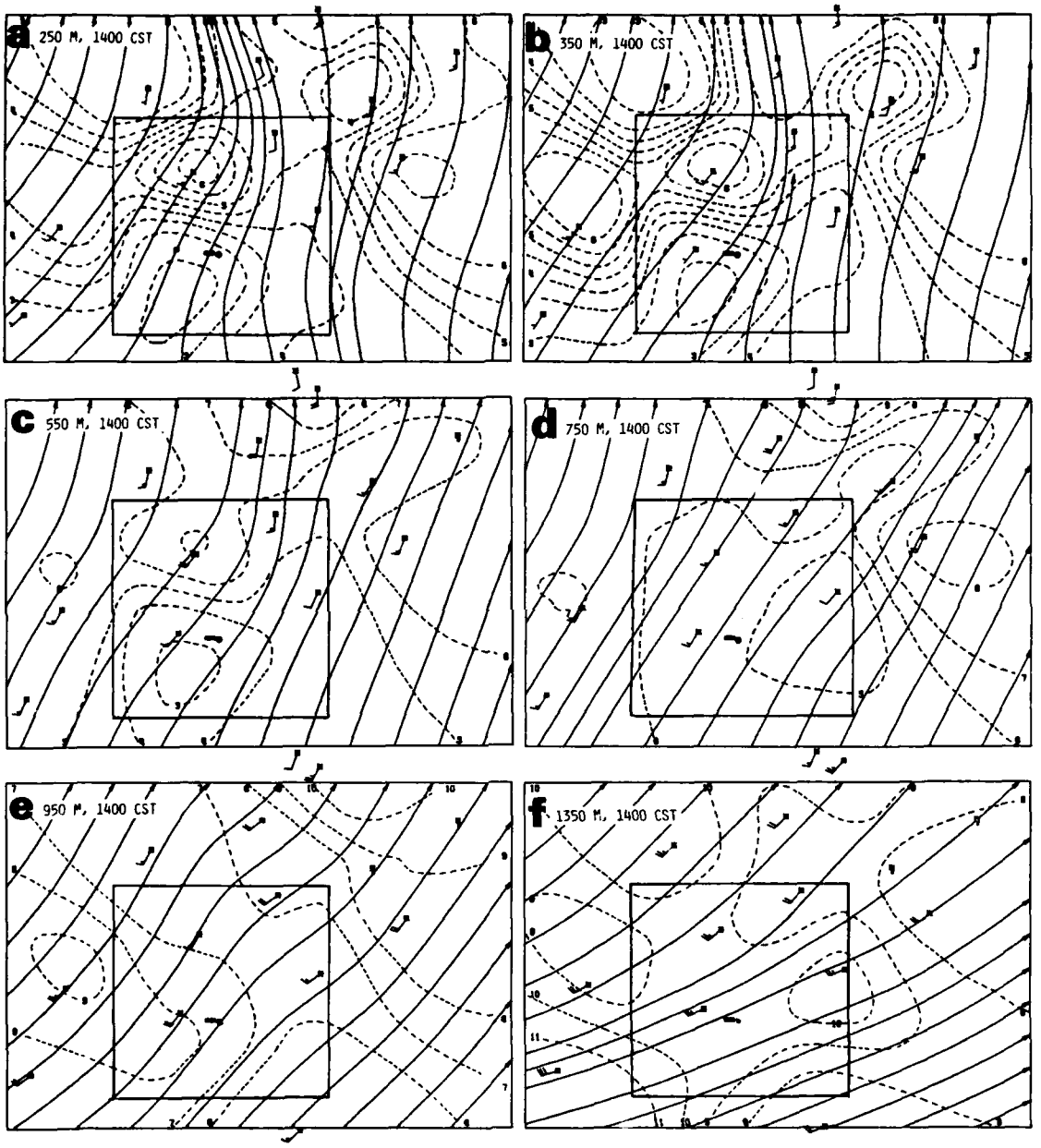

Figure I11. Objective streamlines and isotachs (m sec^{-1}) for 1400 CST at six heights (msl).

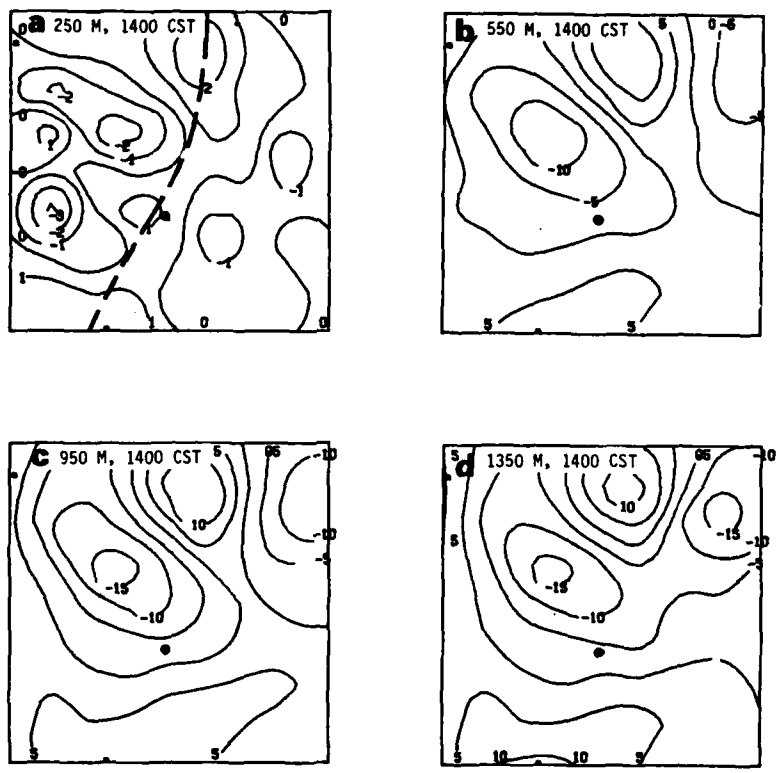

Figure I12. Vertical velocity maps (cm sec^{-1}) for 1400 CST.

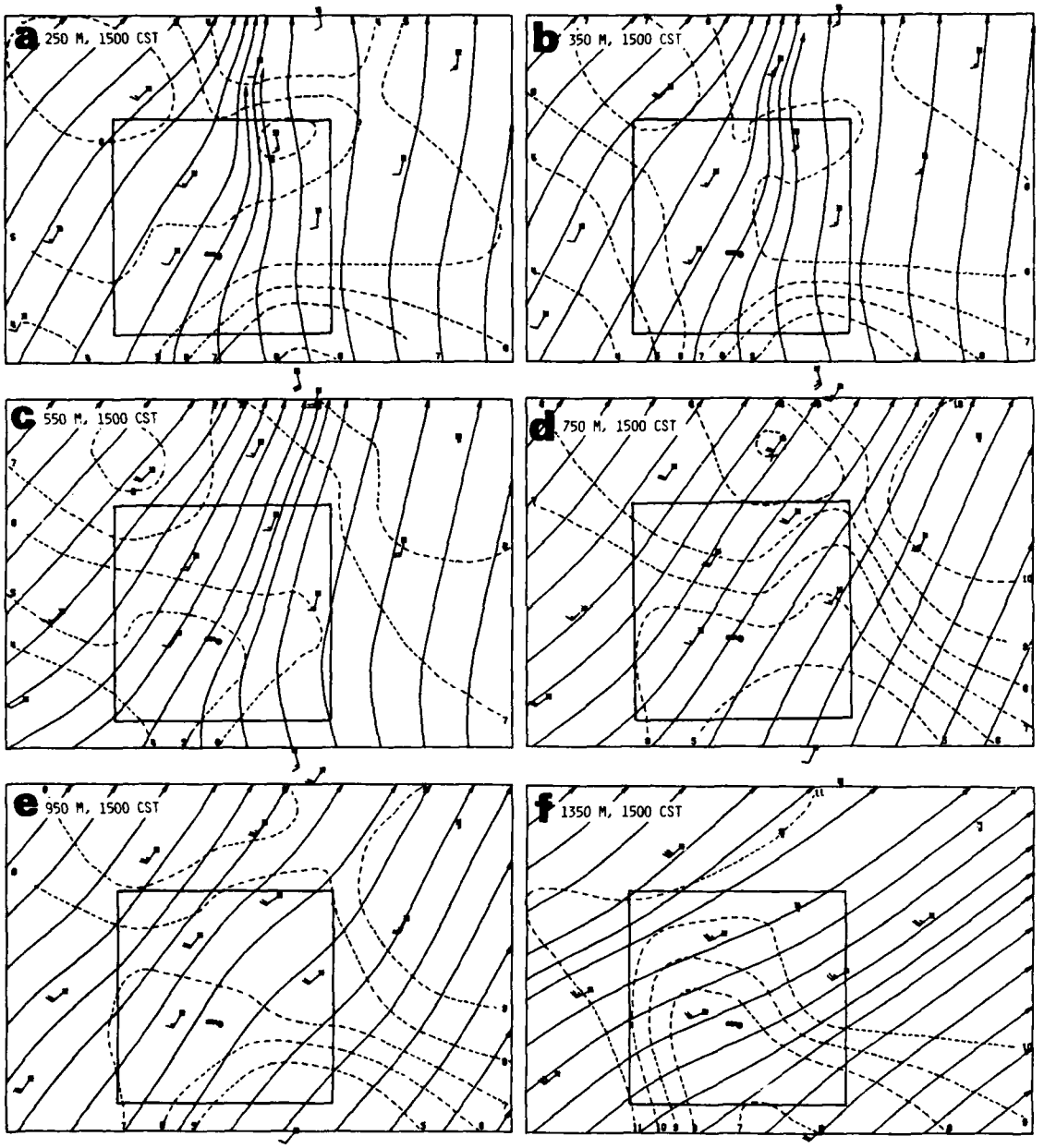

Figure I13. Objective streamlines and isotachs (m sec^{-1}) for 1500 CST at six heights (msl).

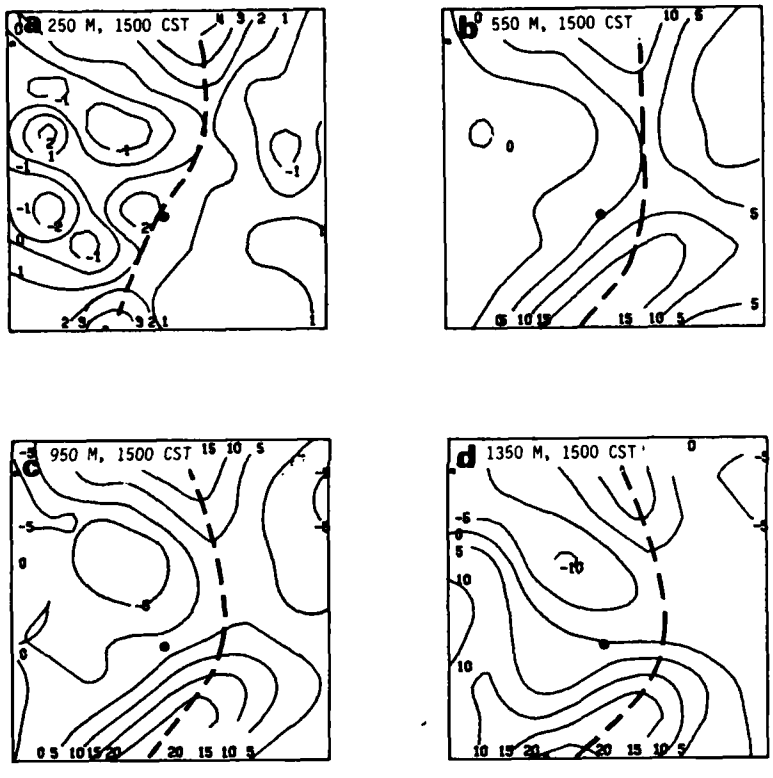

Figure I14. Vertical velocity maps (cm sec^{-1}) for 250, 550, 950, and 1350 m for 1500 CST.

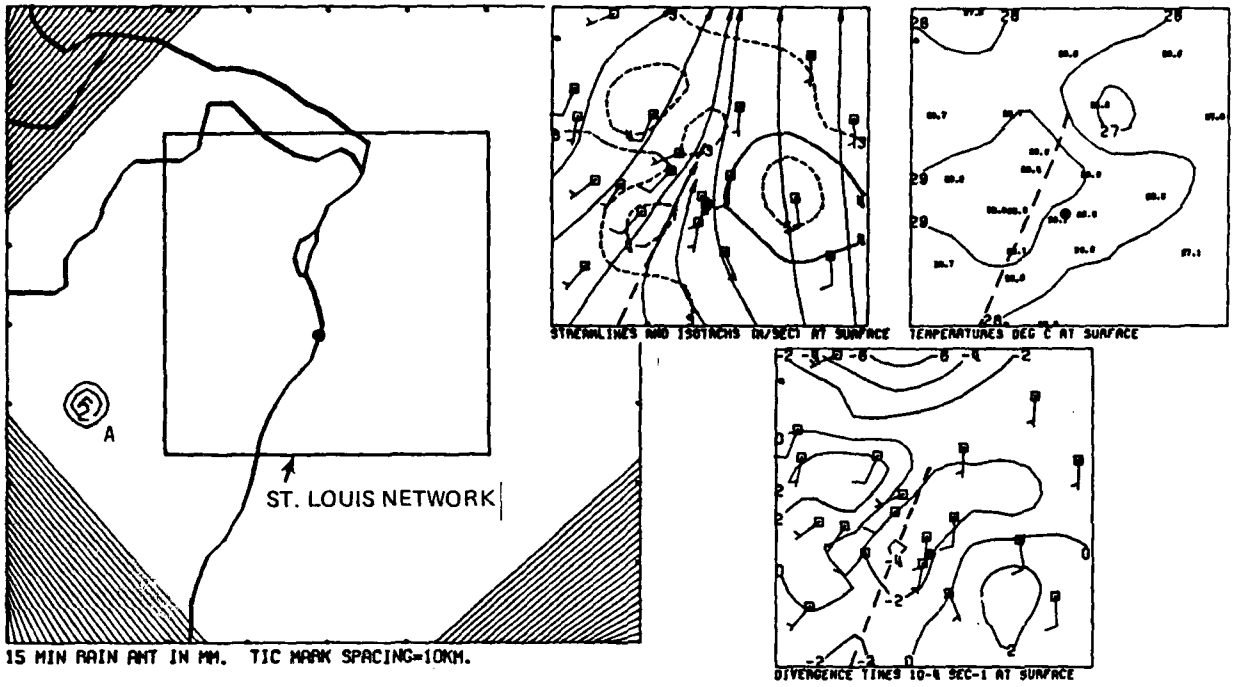

a. 1515 CST

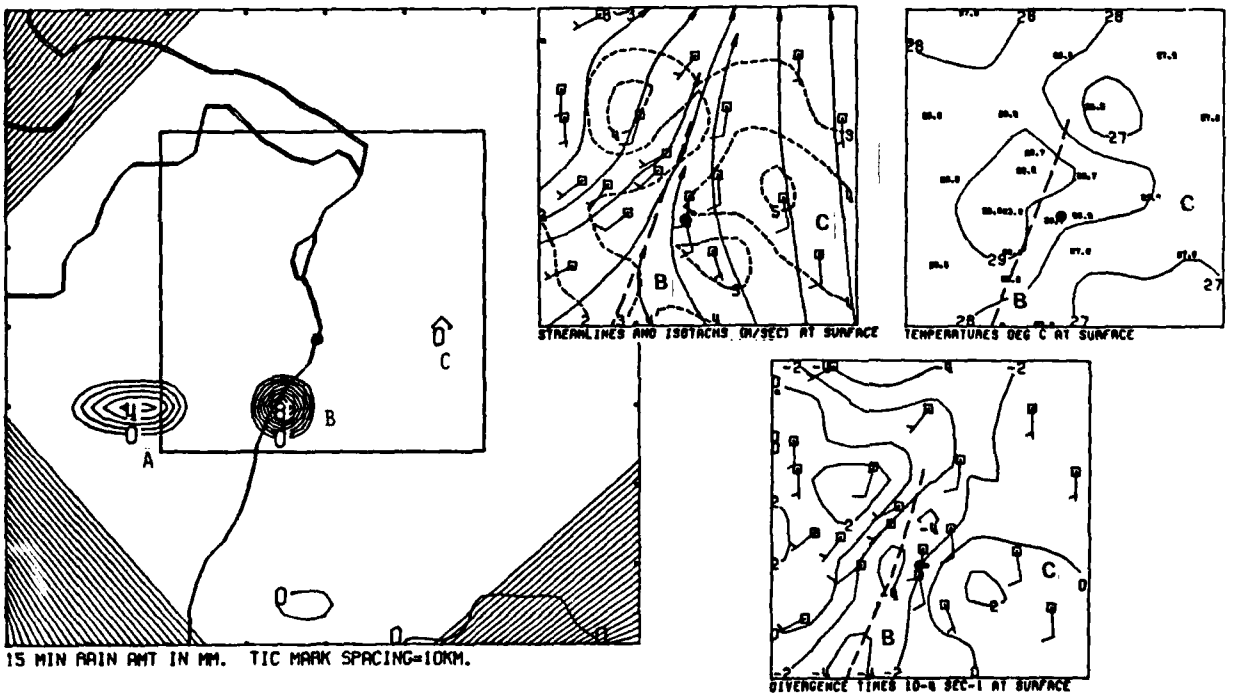

b. 1530 CST

Figure I15. Composite of the objective isotachs and streamlines, temperature, divergence, and rainfall for 1515-1700 CST.

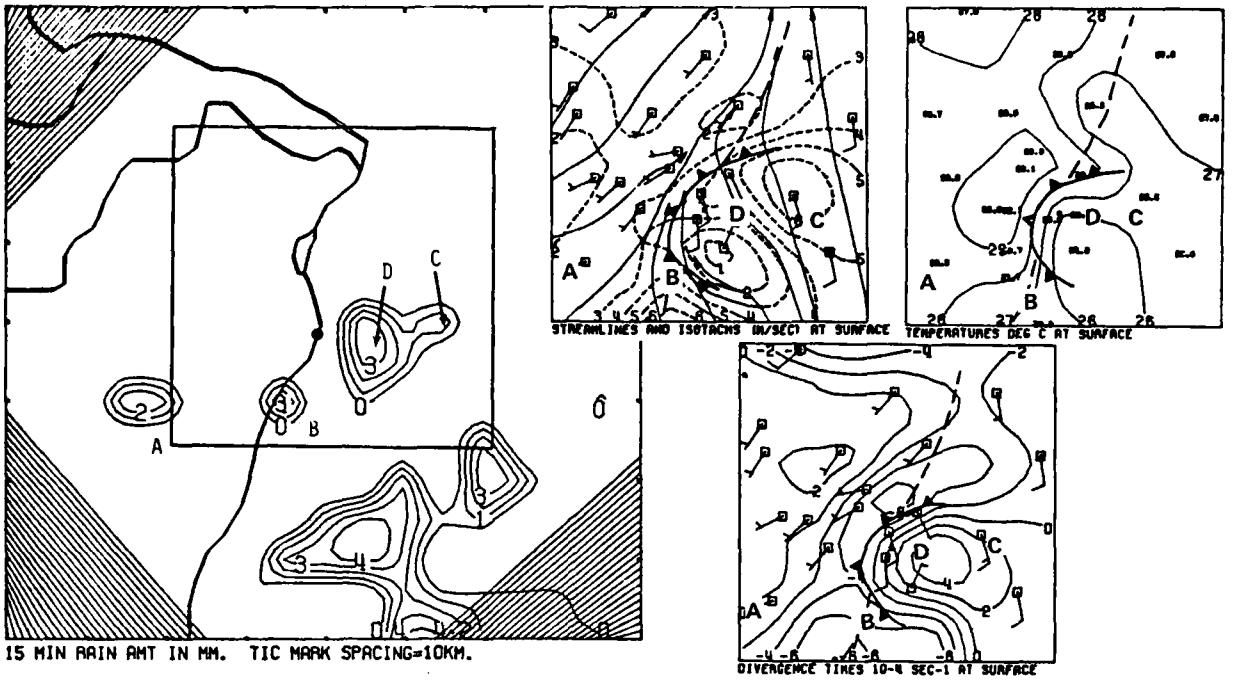

c. 1545 CST

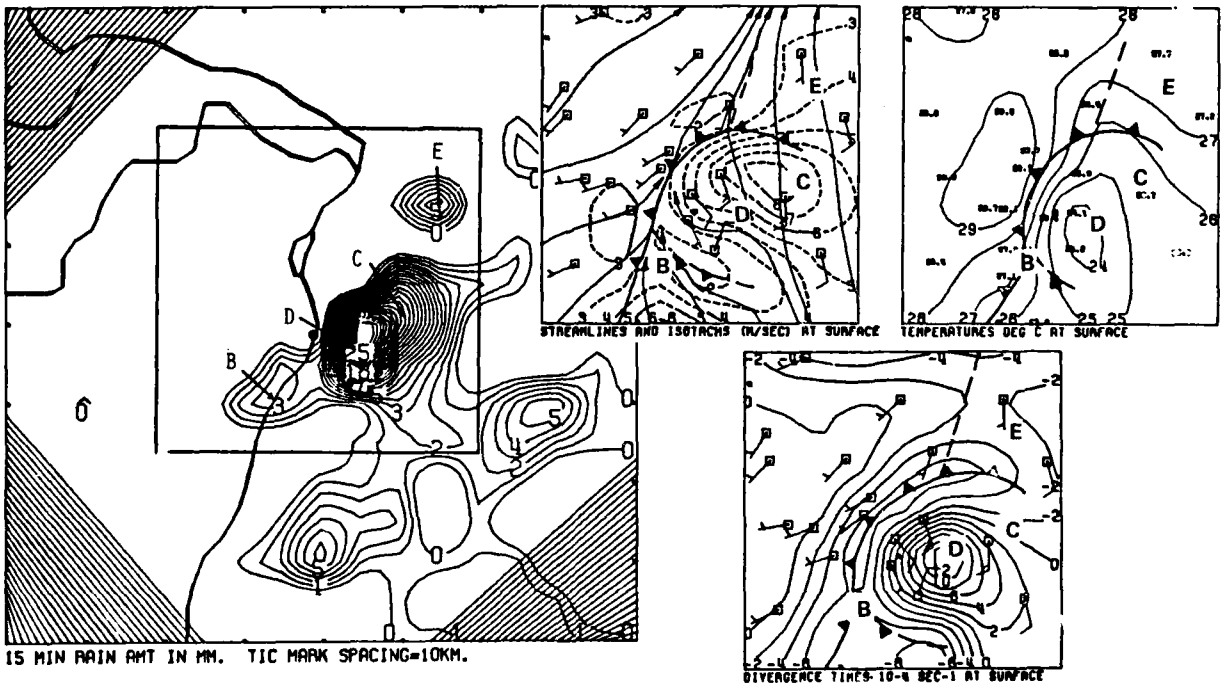

d. 1600 CST

Figure I15. Continued

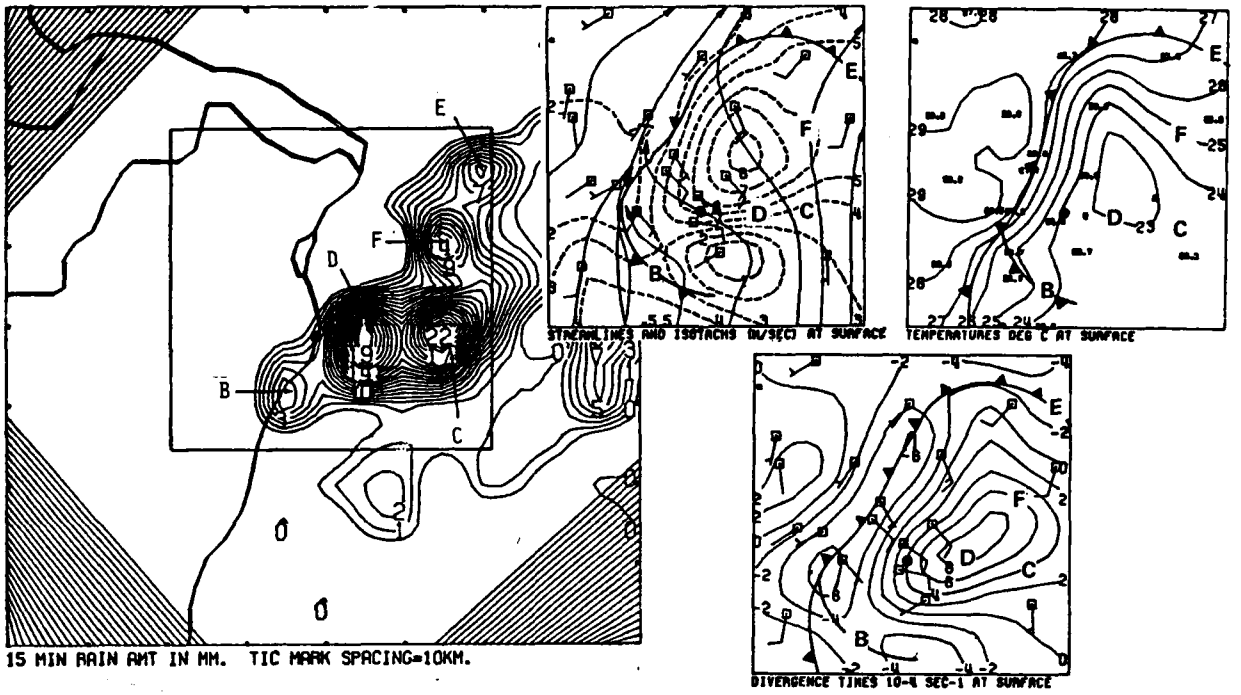

e. 1615 CST

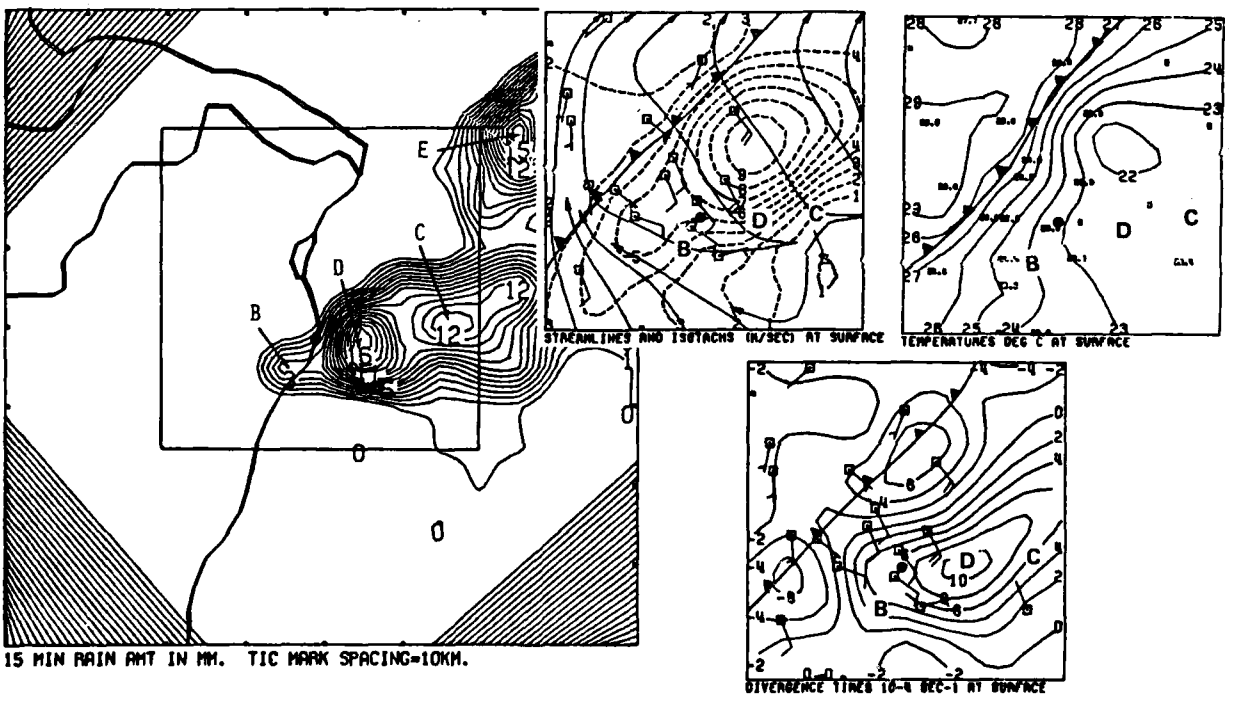

f. 1630 CST

Figure I15. Continued

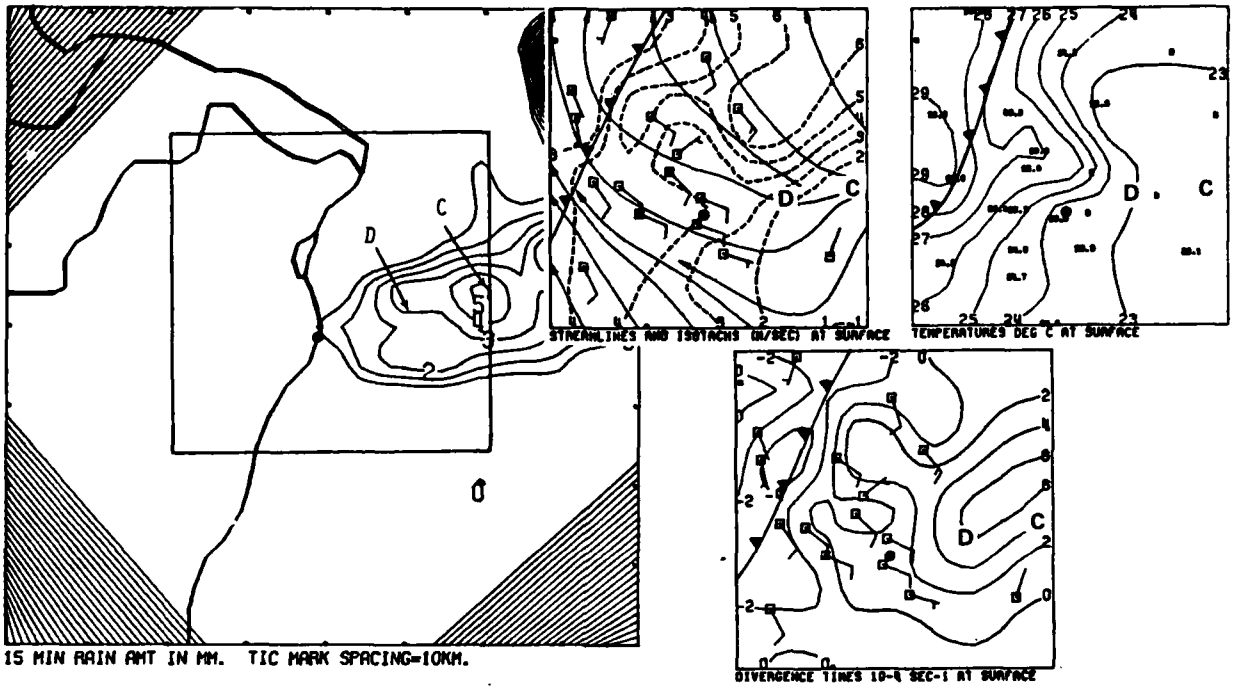

g. 1645 CST

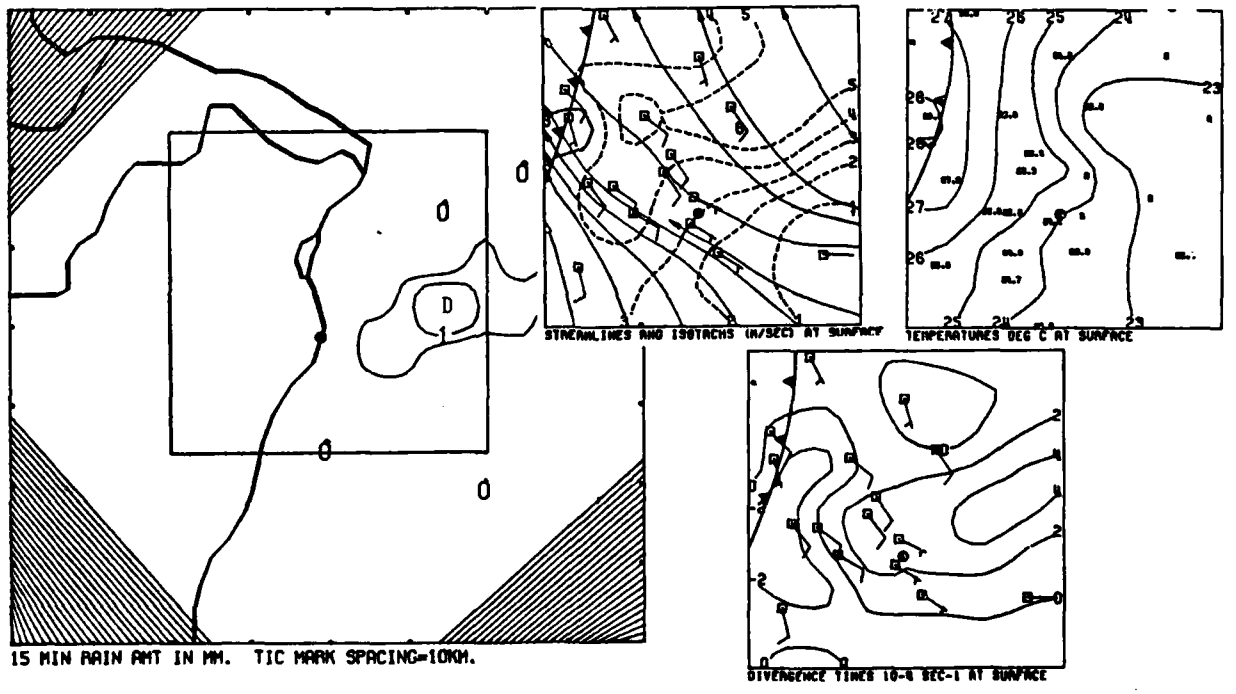

h. 1700 CST

Figure I15. Concluded

Cell D appeared 10 km east of the Arch at 1545 (Fig. I15c). An incipient cloudburst, this cell differed from Cells A, B, and C in that it produced a strong outflow at an early stage in its development. Its gust front pushed westward to interact with the convergence zone increasing the convergence to 6U.

Cell E (Fig. I15d) developed within an area of weak but persistent surface convergence that began at 1515 CST. It was also located where it could draw upon moisture plumed downwind from the areas of strong ascent at 1350 m at 1500 CST. Cells C and D had intensified explosively to cloudburst proportions. Their westward moving outflow continued to interact with the convergence zone to intensify the vertical displacements of moist air that would have been carried eastward into the storms by the winds aloft.

Cell F formed along the complex C D gust front at 1615 (Fig. I15e) to complete a line of strong thunderstorms that extended from location of maximum 1500 CST vertical motion (Cell B) downwind to the northeastern corner of the network (Cell E). Outflow from these major storms merged to form a northwestward moving gust front that had undercut the mesoscale convergence zone by 1615. Temperature contrasts up to 6C were found across the gust front.

Three stations near the intense rainstorms ceased transmission after 1600. Surface analyses with the remainder of the data identified the gust front in the temperature and wind fields as having pushed 15-20 km northwest of the storm complex at 1630 (Fig. I15f). Cell E had moved northeastward off the network and Cell F was dissipating. Two 6U convergence centers found along the gust front weakened to a single 4U center at 1645 (Fig. I15g). A center of 2U convergence remained along the western edge of the network at 1700 (Fig. I15h). No new raincells developed within the network after 1700 CST.

SUMMARY OF SHOWER DEVELOPMENTS ON 14 AUGUST

Weather systems on different motion scales combined to produce conditions favorable for precipitation over the St. Louis network on 14 August. A synoptic scale short wave trough with two embedded regional scale troughs were located west and north of St. Louis and, from qualitative pattern analysis, would have placed most of Missouri within a regime of weak positive vorticity advection and upward vertical motion.

The St. Louis network was located within the warm sector of a weak wave centered over Kansas with a stationary front extending across northern Missouri. The front did not directly influence the weather at St. Louis, however, a squall line spawned along the front moved into the network around 0730 (rain event 2) and later redevelopment triggered rain event 3. The vertical motions associated with the troughs aloft coupled with the vertical motions within the squall line and other convergence zones were sufficient to release the convective instability over parts of eastern Missouri.

The development of a mesoscale convergence zone over the network at 0600 CST preceded the squall line by 1.5 hrs. The reformation of the squall line began with a convergence zone at 1300 CST that persisted for 2.5 hrs before rainfall.

Raincell development over the St. Louis network was highly dependent upon the mesoscale convergence zones. Seven raincells during rain event 2 tended to form 15-20 km west of the intersection of the weak wind shift line preceding the squall line with the mesoscale convergence zone. The five raincells that formed within the network during rain event 3 were directly within the areas with current or previous surface convergence or within areas where moist air lifted within the convergence zone could have been advected into the storms by the winds above 500 m.

Table Il summarizes the cell strengths, convergence strengths, and convergence durations for the rain events 2 and 3 raincells. Seven raincells with strengths ranging from 1.5 mm to 24.0 mm formed over the network during the second period of rain. The average cell strength was 12.6 mm, the average convergence strength was 2.0U and the average duration was 15-min. Convergence preceded six of the seven raincells but only one had a duration exceeding 15-min. Two convergence centers with strengths and durations of, respectively, 2U (15-min) and 12U (60-min) were not associated with rainfall.

The spatial relationship between the convergence centers and the raincells was very good. Because of the short durations of the convergence centers (15-min or less for 6 of the 7 cells) the appearance of convergence centers was not considered to be predictive of the raincell development. Furthermore, there was no apparent relation between cell strength and convergence strength for these early morning storms.

The five rain event 3 storms that developed within the network had convergence durations that ranged from 0-195 min. Cell B formed within a stationary convergence zone that had persisted for 2.5 hrs. Convergence remained nearby for 75-min after cell B developed.

The raincells that formed during event 3 are also summarized in Table Il. One raincell had a strength of 61.0 mm and the average was 31.2 mm. The average convergence strength was 12.0U and the average duration was 66-min. Four of the five raincells were preceded by convergence which persisted for 30-min or longer. The fifth raincell was in a location to receive moisture that had been lifted within the convergence zone of the reactivating squall line and carried by the 500 m winds. There was one convergence center (16U and 60-min) that was not accompanied by rainfall.

The spatial relationship between the raincells and the convergence centers was very good. The convergence centers were also predictive of the location of raincell formation. There was no apparent relationship between the convergence strengths and the strengths of the raincells.

Table 11. Cell Strengths, Convergence Strengths, and Convergence Durations for the Rain Event 2 and 3 Raincells on 14 August.

Cell ID	Cell Strength	Convergence Strength	Convergence Duration
Rain Event 2			
A	24.0 mm	2U	15 min
B	8.0	2	15
C	18.0	2	15
D	12.0	0	0
E	12.0	4	30
F	13.0	2	15
G	1.5	2	15
Rain Event 3			
B	20.0	22	195
C	49.0	0	0
D	61.0	18	45
E	12.0	12	60
F	14.0	8	30

REFERENCES

Achtemeier, G. L., 1979: Evaluation of operational objective streamline methods. Mon. Wea. Rev., 107, 198-206.

_____, B. Ackerman, S. A. Changnon, P. Schickedanz, and R. G. Semonin, 1978: Illinois precipitation enhancement program (Phase 1) and design and evaluation techniques for High Plains Experiment. Atmospheric Sciences Section, Illinois State Water Survey, Final Report, Contract 14-06-D-7197, 210 pp.

_____, and G. M. Morgan, Jr., 1975: A short-term thunderstorm forecast system: step 1, exploitation of the surface data. Prep. 9th Conf. Sev. Loc. Storms, Norman, OK, Amer. Meteor. Soc., 18-24.

Ackerman, B., 1978: Regional kinematic fields in Summary of METROMEX, Vol. 2. Bulletin 63. Illinois State Water Survey, Urbana, IL, 165-205.

_____, 1979: METROMEX revisisted. Preprints Seventh Conf. Inadv. and Plan. Wea. Mod., Amer. Meteor. Soc., 26-27.

Anderson, C. E., and L. W. Uccellini, 1974: Studies of meteorological factors involved in the formation of severe local storms in the northeast Colorado region. Prep. 8th Conf. Sev. Loc. Storms, Denver, CO, Amer. Meteor. Soc., 84-89.

Byers, H. R.,and R. R. Braham, Jr., 1949: The Thunderstorm. U.S. Govt. Prtg. Off., Wash. DC (av. NITS) 287 pp.

Changnon, S. A., Jr., and G. M. Morgan, Jr., 1976: Design of an Experiment to Suppress Hail. Bulletin 61, ISWS/B-61/76, Illinois State Water Survey, Urbana, 53-73.

Copeland, R. C., and P. L. Hexter, 1957: The association of surface wind convergence with precipitation patterns. Proc. 6th Wea. Radar Conf., Cambridge, Amer. Meteor. Soc., 189-199.

Huff, F. A., 1977: Distribution of heavy raincells. In Summary of METROMEX, Vol. 1, Bulletin 63, Illinois State Water Survey, ISWS/BUL-62/77, 182-192.

Semonin, R. G., and S. A. Changnon, Jr., 1974: METROMEX: Summary of 1971-1972 results. Bull. Amer. Meteor. Soc., 55, 95-100.

Ulanski, S. L., and M. Garstang, 1978: The role of surface divergence and vorticity in the life cycle of convective rainfall. Part 1: Observations and Analysis. J. Atmos. Sci., 35, 1047-1062.

APPENDIX: QUALITY EVALUATION AND SELECTION OF THE ANALYSIS NETWORKS

Nancy E. Westcott

INTRODUCTION

The ability to correctly and consistently predict rainfall at a particular location in real time has long eluded the weather forecasting community. The lack of a densely instrumented network (e.g. 1/20 km^2) is largely responsible for this situation. Only coarse synoptic data are currently available to the forecaster. However, meso- and convective-scale measurements are needed to predict convective activity which is highly variable in space and time.

One of the basic objectives of the research under this project is to assess the predictive power of the ambient wind field with respect to convective midwestern rainfall. Concurrent rainfall and wind-field data, each with a fine spatial and temporal resolution, are required to accomplish this task. The following is a description of the development of a suitable data set from several diverse data bases and the selection of the analysis network to be used in the initial phase of the research. The St. Louis area was chosen as a test site for the initial studies in Illinois because extensive rainfall and wind data were readily accessible for the summer of 1975.

RAINFALL DATA

The rainfall data was collected from a high density (1/23 km^2) network operated by the Illinois State Water Survey (ISWS) during project METROMEX (Fig. 1). The measurements were recorded continuously on daily 8" charts from 222 weighing-bucket gages. Rainfall values could be read to about .01"/15 min. These charts were changed weekly. Thirteen weekly gages spaced throughout the network were used to identify the days on which the rain fell.

The week of 12-19 July 1975 was chosen as the case study "week." Eight periods of rain occurred during this time. The storms covered a wide range of durations, total accumulations and start times. Continuous 15-minute rainfall accumulations were calculated at each gage. The network distribution of rainfall was objectively analyzed on a 5 km x 5 km grid every 15-minutes during the rain periods. Two additional rain days - 30 July and 14 August were analyzed in the same way.

THE ORIGINAL WIND DATA

In order to discern the cells of divergent and convergent flow associated with the rainfall cells, an equally dense network of wind instruments is necessary. In the summer of 1975, 3 independent wind networks were operated by the U.S. EPA, the St. Louis Air Pollution Control Board and the Illinois State Water Survey. The data from these 3 diverse networks have been edited and merged into a single data base, according to the procedures and criteria described below.

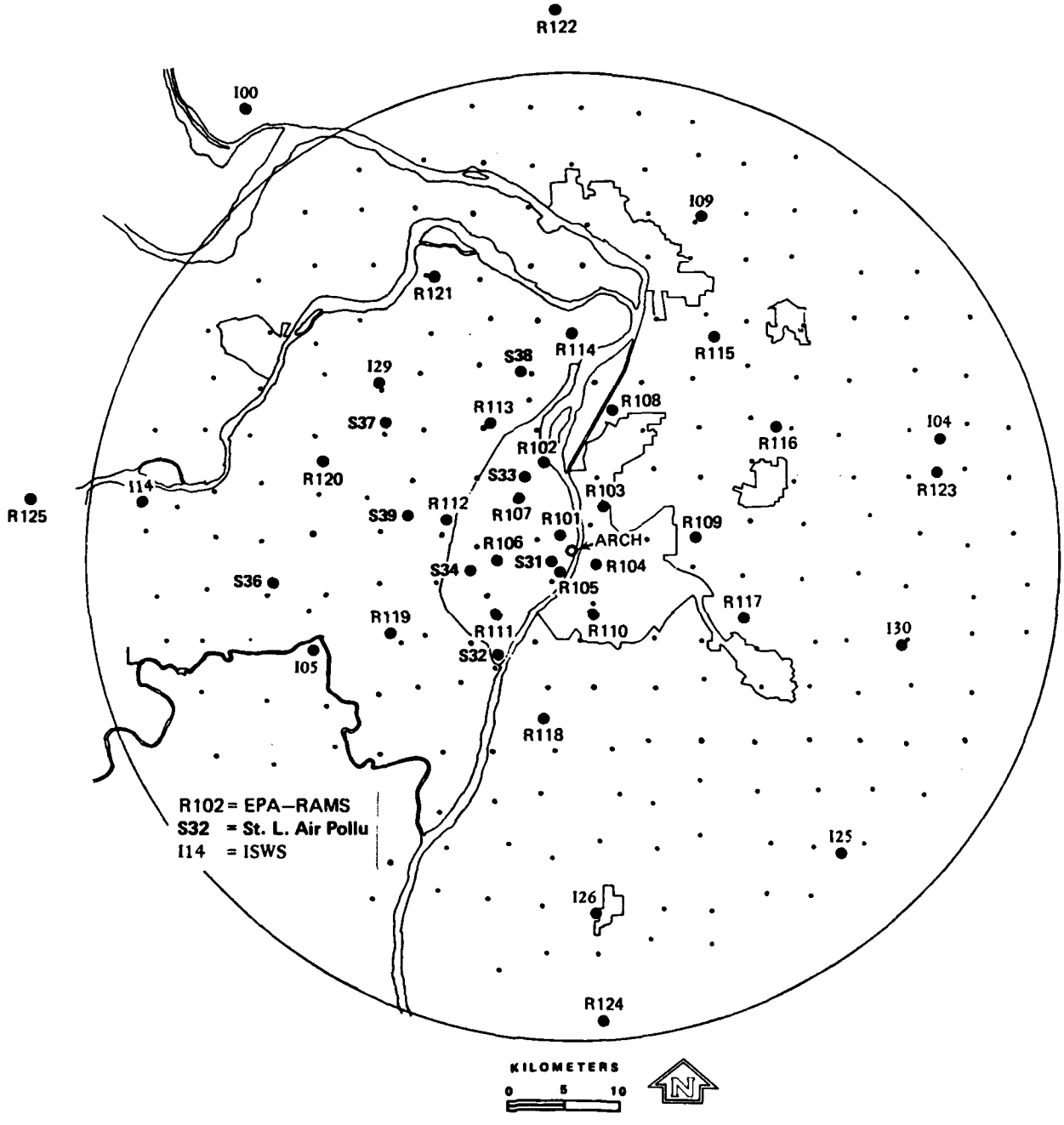

Figure 1. 1975 surface wind stations and raingage locations

At the outset, each station in the 3 networks was characterized as to general land-use category. The urban, rural or transitional classifications were based upon housing density, vegetative cover and proximity to urban influences (Table 1). The transitional areas were often suburban locations.

U.S. EPA Wind Network (RAMS)

The U.S. EPA maintained 25 surface stations and 4 upper air stations as part of the Regional Air Pollution Study during the summer of 1975. The station characteristics of the Regional Air Monitoring System (RAMS) ground-based instruments are summarized in Table 2, and their locations are given in Fig. 1.

The wind stations were arranged in a spiral pattern so that the urban area would contain the most dense array of instruments. The instruments were installed atop 10 and 30 meter towers. Of the seventeen 30 m towers, 9 were located in urban areas, 3 in a transitional zone and 5 in rural areas. Seven of the 10 m towers were located in the rural area surrounding St. Louis and one in the city.

The original measurements recorded on tape by the EPA consisted of 1-min readings of wind speed and direction, in units of meters-per-second (m/s) and degrees. The hours and minutes were recorded as Central Standard Time (CST).

Station 124, located in a rural area to the south of the city, has been excluded from the study as it recorded only 12 days of data during the summer.

St. Louis Air Pollution Control Board Network (STL)

The St. Louis Air Pollution Control Board has maintained a meteorological network since 1970 in conjunction with on-going air quality monitoring. The sensors were, in most cases, at tower heights of 5 to 10 meters. Two of the stations, however, were atop buildings; one at 115 m and the other at 20 m. At the outset, measurements from station 31, situated on the 115 m building were eliminated from the data set, and station 32 located on the 20 m building was designated as one of the group of 30 m towers. The locations of the stations in this network (designated STL) are presented in Fig. 1, and their characteristics in Table 2.

Table 1. Land Use Classification for the Surface Wind Networks.

Class	Vegetative Cover (percent)	Building Density (houses/km^2)
Urban	25-70	100 to > 800
Transitional	25-85	20 to 500
Rural	85-99	< 20

Table 2. The 42 RAMS, STL, ISWS Surface Wind Stations.

Station No.	Height AGL	Type	Status
US EPA RAMS NETWORK			
101	30	Urban	
102	30	Urban	Deleted
103	30	Trans	
104	30	Urban	Deleted
105	30	Urban	
106	30	Urban	Deleted
107	30	Urban	
108	10	Rural	
109	30	Rural	
110	10	Urban	
111	30	Urban	
112	30	Urban	
113	30	Urban	
114	10	Rural	
115	10	Rural	
116	10	Rural	
117	10	Rural	
118	10	Rural	
119	30	Trans	
120	30	Trans	Deleted
121	10	Rural	
122	30	Rural	Deleted
123	30	Rural	Deleted
124	30	Rural	Deleted
125	30	Rural	Deleted
STL AIR POLLUTION NETWORK			
31	115	Urban	Deleted
32	30	Urban	
33	10	Urban	
34	10	Urban	
36	5	Trans	
37	5	Urban	
38	5	Urban	Deleted
39	5	Urban	
ISWS WIND NETWORK			
00	5	Rural	Deleted
04	10	Rural	Deleted
05	3	Rural	
09	10	Trans	
14	3	Rural	Deleted
25	3	Rural	Deleted
26	8	Rural	Deleted
29	7	Trans	
30	5	Rural	Deleted

The original measurements were recorded on tape at 3-min intervals as easterly and westerly wind components, in units of 0.1 miles-per-hour and in CST.

Illinois State Water Survey Wind Network (ISWS)

During the summers of 1972-1975, the Illinois State Water Survey operated seven surface wind stations in the rural areas around St. Louis, as a part of the METROMEX project. Additional recorded wind data were available from the National Weather Service station at Lambert International Airport (station 29). Hourly observations were available from the U.S. Air Force weather station at Scott AFB (station 30), but not as continuous 15-min averages. Therefore, this station (ISWS 30) was excluded from the network. Further, during the summer of 1975, no data were recorded at station 25 in the far south, and station 14 in the far west was not functioning during the week chosen for study. Thus, the ISWS network was reduced to six stations. The possible stations for the final network numbered 37 (Table 1).

The original ISWS wind measurements were recorded at one minute intervals on strip charts. Prior to this study 10-min averages were estimated graphically once an hour. These averages were used in the quality control study. Additional processing was later done so that continuous 15-min averages would be available for use in the divergence analysis. The averaging was done by eye in both cases, with speed to the nearest integer mile-per-hour and direction to a 16-point compass or better. Later vector components were computed from these 10- and 15-min graphical averages. The components and the observed wind speed were converted to meters-per-second, and time to CST, for conformity with the RAMS and STL data.

DEVELOPMENT OF THE WIND DATA SET

Averaging Computations

Prior to the merging of the wind data sets, and to the performance of an objective analysis upon the data, a quality control check was necessary to ensure that the RAMS, STL and ISWS data were compatible and that each station had functioned properly.

The ten-min averages of ISWS wind speeds and directions which were calculated graphically once an hour for the summer, were used in the quality check. The RAMS 1-min values and the STL 3-min values were averaged both vectorially and arithmetically for 15-min intervals. The two sets of averages for the RAMS and STL were calculated to determine the magnitude of the differences in speed which would occur due to the averaging method.

These 15-min wind speed averages were further averaged arithmetically for daily, monthly and seasonal periods. Very little difference was found between the daily, monthly and summer arithmetic means and standard deviations computed from the 15-min arithmetic and vector speeds ($\sim$ .4 m/s or $<$ 20% difference). This indicates that on a 10 to 15-min basis, the vector and arithmetic averages are comparable. This also indicates that the graphical estimation on the ISWS records of the 10- and 15-min averages should be compatable with the RAMS and STL averaging techniques.

When taking the vector mean of the 10- and 15-min averages on a daily, monthly and seasonal basis, the shift in wind direction becomes an important consideration. The vector mean wind speed at each station decreases in going from daily to monthly to seasonal averaging. Particularly on a monthly and seasonal basis where the winds are from all 4 quadrants (range of 360°), arithmetic averaging should be employed. The difference in monthly and summer vector and arithmetic means is on the order of 1 to 4 m/s, with little difference on whether 15-min arithmetic or vector averages are used as the base value.

As for the wind direction calculations, the computational algorithm for arithmetically averaging winds works well over a 15-min period. The algorithm, however, omits cases where the winds are from 4 different quadrants. Therefore, daily, monthly and seasonal wind averages must be calculated vectorially from either U_{15} and V_{15}, or from arithmetically averaged 15-min wind speed and direction converted to -U and -V components. Very little difference is found between wind directions computed arithmetically, as opposed to being computed vectorially, for short periods. The advantage to averaging direction arithmetically is that standard deviation can also be computed.

Stratification

Monthly and seasonal averages of wind speed and direction are necessary variables in checking the quality of measurements from the wind stations. They are useful indicators of the presence of systematic discrepancies at individual stations. Additional stratification can be made to accentuate bias in the data, namely, stratification by day and night and by rain-days (or-nights) and non-rain-days.

Local effects caused by the topographic setting of the station may dominate at night under the presence of nocturnal cooling and lower wind speeds, and mask the station's performance. At lower wind speeds (< 1 m/s) the instrument response time is lengthened and the resolution of speed and direction lessens. The 24-hour day was therefore broken into daytime (0700-1900 CST) and nighttime hours (1900-0700 CST). The period 0700-1900 CST in rural areas is generally one of positive temperature changes and 1900-0700 CST is one of negative temperature changes (Hilberg, 1978).

Since higher, more variable winds are expected during rain periods, the days were further divided into rain and no-rain groups. If rain began anytime during the hours of 0700 and 1845 CST, the whole day was declared a rain period, and likewise for the night hours. If the rain continued for more than 2 hours into the next day or night period, that period was also declared a rain period. If rain continued for less than 2 hours, the following period was classified as non-rain. This lag time of 2 hours was instigated under the assumption that as a storm ends, it tapers off, and the wind ceases to be so erratic. For this reason, inclusion in the rain category of these periods when rain was decreasing is unnecessary and lessens the sample size of non-rain days.

After stratifying by day and night, and then further into wet and dry categories, the number of samples in each block was very small. The amount of data at each station also varied widely. In the quality evaluation, emphasis

was placed mainly on the results for the day-night stratification, and the results for the second order, rain - no rain stratification was given less weight due to small sample sizes. Means and standard deviations of wind speed have been calculated for daily, monthly and summer, daytime and nighttime, wet and dry periods.

Frequency Distributions

The final preparation prior to the evaluation of station quality was the development of frequency distribution tables for the 10- and 15-min averages of wind speed and direction. Eight categories of wind direction were examined: 45° intervals, centered on integral multiples of 45°. Eleven groups of wind speed were selected as shown in Table 3. The frequencies were computed only for the daytime and nighttime summer samples.

The 2-way frequency distributions provided information on the sample size and percent in each speed and direction block, each speed-alone block and each direction-alone block. Values for the 15-min arithmetic and vector averages of speed and direction were tabulated as were wind roses for each station.

The frequency counts of wind speed indicated that 2 stations (STL 32 and RAMS 118) had some unusually high wind speeds. This led to the discovery of several days of bad data which were eliminated. This table also made it clear that the STL and the RAMS stations never recorded zero wind speeds, whereas the ISWS stations did.

Table 3. Wind Speed and Direction Categories.

Wind Speed (m/s)	Wind Direction(o)	
0.0	N	337-21
0.01 - 0.5	NE	22-66
0.51 - 1.0	E	67-111
1.01 - 2.5	SE	112-156
2.51 - 5.0	S	157-201
5.01 - 10.0	SW	202-246
10.01 - 15.0	W	247-291
15.01 - 20.0	NW	292-336
20.01 - 25.0		
25.01 - 30.0		
> 30.0		

Summary

The following data sets were developed for each station:

1.) Means and standard deviations of wind speed and direction for daily, monthly and summer periods, stratified by a.) daytime and nighttime hours and b.) rain and non-rain situations.

2.) Plots of the daily (for 12-19 July 1975 only), monthly and summer averages of wind speed and direction for day and night stratification.

3.) Frequency tables of daytime and nighttime wind speed and wind direction for the 3-month period.

4.) Plots of the daytime summer wind roses (Fig. 2).

STATION QUALITY

The decision to retain or omit stations in the VIN network was based on the following criteria:

1.) The location with respect to other stations.

2.) The daytime, daily, monthly and summer mean wind speeds.

3.) The daytime daily mean wind direction for the study days.

4.) The daytime summer wind rose (Fig. 2).

Usually more than one criterion applied when a station was rejected.

Six stations were eliminated because of their remoteness from the more densely instrumented part of the network. Their inclusion would have resulted in highly variable station spacing in the network. The stations were RAMS 122, RAMS 123, RAMS 125, ISWS 00, ISWS 04, ISWS 26. Five of these stations also had either questionable wind speeds or wind directions.

The station mean daytime wind speeds were compared with the mean network wind speed on a daily (12-19 July 1975), monthly and summer basis. If the station mean was $\pm$ 1.0 m/s away from the network mean speed, the station was considered to be high or low for that period. Six stations had abnormally high speeds during the summer of 1975 and seven stations had abnormally low wind speeds.

Stations RAMS 122, RAMS 123, ISWS 00, ISWS 04 and ISWS 26, which had abnormal speeds, were already deleted from the data set because of their remote locations. Stations RAMS 102 and RAMS 106 were omitted because of their high wind speeds, and also because they were in an area of high station density. Their inclusion was not crucial to the analysis. Too few data were available for station ISWS 05, from which a reliable monthly and summer mean could be computed. It was left in for further consideration.

Because the remaining 5 stations were strategically located in the network, it was decided to adjust the wind speeds at RAMS 103, a 30 m tower down to 10 m, and the winds at the STL stations (5 m towers), effectively upward to 10 m, using a logarithmic wind profile. The decision to make the adjustments was difficult as the effects of tower height and geographic location at a station are interrelated and difficult to distinguish. The adjustment factor was calculated as the ratio of the log of the tower heights divided by the assumed roughness parameter, Z_o. For the rural and transitional towers, Z_o was .1 m; and 1 m for the urban areas. All of the 5

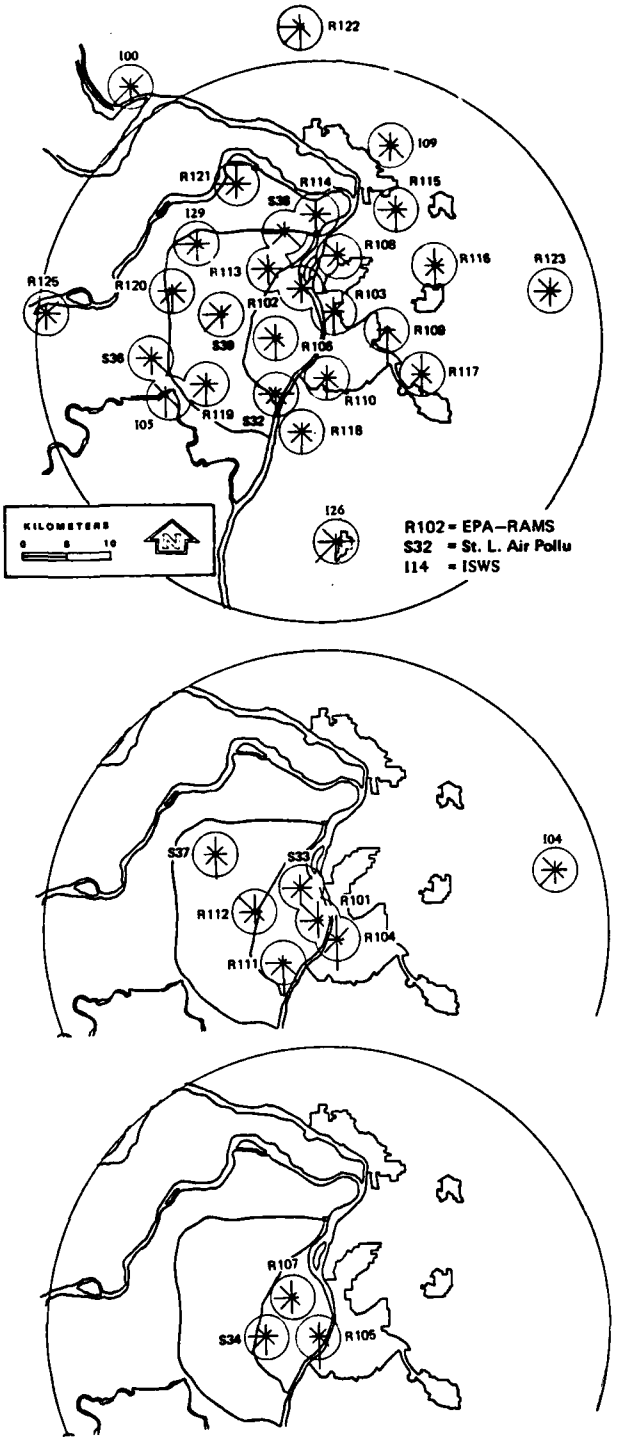

Figure 2. Summer daytime wind roses

meter towers (except ISWS 05) have been either deleted or have been adjusted ($\ln 10/1 \div \ln 5/1 = 1.43$). Only one of the 3 remaining rural or transitional 30 m towers was adjusted ($\ln 10/.1 \div \ln 30/.1 = .81$), however.

Twenty-nine stations remained in the data base before examining the characteristics of the wind direction at the stations. In viewing the daily network mean wind direction during the study week, 8 stations were found to have questionable means. These stations and their frequency of deviation from the network mean are presented in Table 4. Two stations (R102 and R122) had already been deleted on the basis of other criteria.

Two of the eight stations (RAMS 112 and STL 39) showed a systematic and consistent difference in direction from their neighbors. The wind directions at these stations were corrected for the study week by the subtraction of the indicated bias: station RAMS 112 (-50^{o}); station STL 39 (-42^{o}). Station RAMS 120 often deviated from its neighboring stations but showed no systematic bias, and thus was omitted from the network.

Stations RAMS 113 and ISWS 09 also showed some problem with the daily wind direction but were retained because of 1.) their critical placement in the network, 2.) they were never off by two or more standard deviations and 3.) their summer wind roses were acceptable (Fig. 2). Station ISWS 05 was retained because of its crucial location, and because the sample sizes for the daily, monthly and summer averages were small and could have been the cause of the anomalous behavior.

The final elimination criteria was based on the summer wind rose plots (Fig. 2). At 11 stations, the frequency of direction was deficient or in excess by two standard deviations from the network mean for a particular quadrant (Table 5). Stations RAMS 102, STL 39 and ISWS 26 have already been either corrected or deleted. Station RAMS 104 and STL 38 were omitted; RAMS 104 because of obvious channeling in the river valley and STL 38 because of poor southern exposure. RAMS 101, RAMS 105, RAMS 109, RAMS 111 and STL 32 were retained as they appeared acceptable during the study week. However, the roses at these stations were considered in analyzing the wind fields.

In summary, Table 6 is a list of the stations and their status and deficiencies. Sixteen of the original 42 were deleted, leaving 26 in the final surface wind network (Fig. 3). Of the remaining stations, RAMS 109 and ISWS 05 needed close attention in the analysis.

Table 4. Number of Days When Mean Direction is ± 2 Standard Deviations from Network Mean.

Station	No. >2σ from net mean	No. >1σ, <2σ from net mean	Total >1σ	Total Possible
R102	1	5	6	8
R112	3	2	5	5
R113	0	5	5	7
R120	1	2	3	3
R122	2	1	3	4
S39	6	1	7	8
I05	0	1	1	2
I09	0	2	2	8

Table 5. Quadrant Where Frequency of Direction is >2 Standard Deviations from the Mean.

Station	Deficient Quadrant	Excess Quadrant
R101	NE-E-SE	N-NW-W
R102		NE
R104		N Channeling
R105		S Channeling
R109	NW-N-NE	S-SW-W
	W-NW-N	SE-S-SW
	N-NE-E	S
		S-SW-W
R111	NW-N-NE	SE-S-SW
S32		E
S38	S	SE Poor S exposure
S39	E-SE-S	NW-W-SW
I05	N-NE-E	W Channeling
I26	SW-W-NW	
	SW	

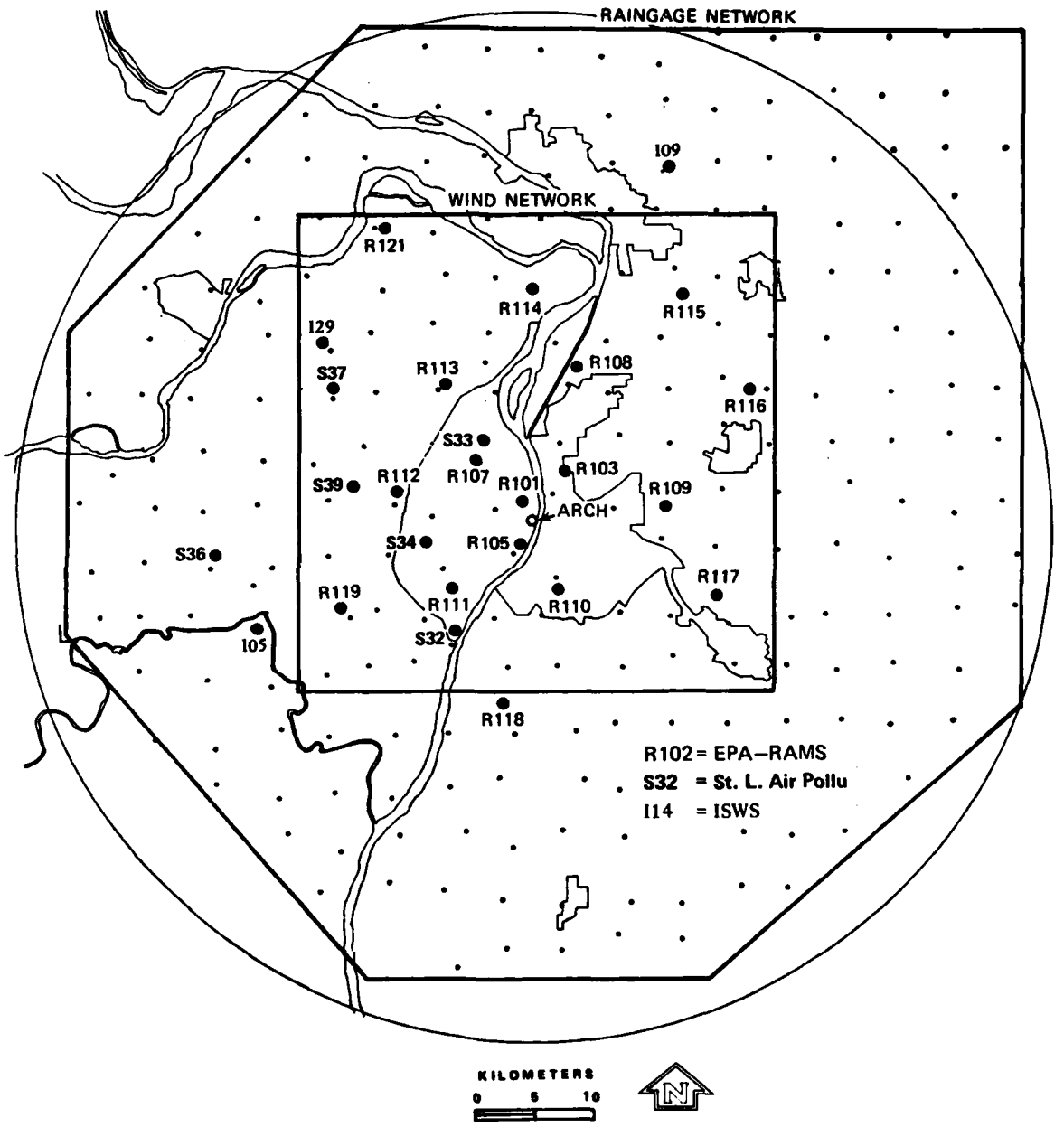

Figure 3. Final surface wind and raingage networks

Table 6. Status of the 42 RAMS, STL, ISWS surface wind stations after screening for inclusion for the objective analysis.

	quality	omitted or adjusted	location	month & seasonal wind speed	daily wind direction	summer wind rose
RAMS 101	fair					few east winds
102	bad	0	close to neighbor	high	small non-systematic error	excess NE winds
103	good	A		high-adjusted		
104	--	0	close to neighbor			channeling
105	fair					channeling
106	bad	0	close to neighbor	high		
107	good					
108	good					
109	poor			high		few northly winds
110	good					
111	fair					few northly winds
112	good	A			50^{o} bias-adjusted	
113	fair				small non-systematic error	
114	good					
115	good					
116	good					
117	good					
118	good					
119	good					

Table 6. Continued

		quality	omitted or adjusted	location	month & seasonal wind speed	daily wind direction	summer wind rose
RAMS	120	bad	0			non-systematic error	
	121	good					
	122	--	0	out of VIN area	high	small non-systematic error	
	123	--	0	out of VIN area	high		
	124	missing data	0	out of VIN area			
RAMS	125	--	0	out of VIN area			
STL	31	115m tower	0				
	32	fair					excess of E winds
	33	good					
	34	good					
	36	good	A		low-adjusted		
	37	good	A		low-adjusted		
	38	bad	0		low		poor southern exposure
STL	39	fair	A		low-adjusted	42^{o} off-adjusted	
ISWS	00	--	0	out of VIN area	low		
	04	--	0	out of VIN area	low		
	05	poor				small non-systematic error	channeling
	09	fair				small non-systematic error	

Table 6. Continued

		quality	omitted or adjusted	location	month & seasonal wind speed	daily wind direction	summer wind rose
ISWS	14	missing data	0				
	25	missing data	0				
	26	--	0	out of VIN area	low		excess SW, W winds
	29	good	0				

Reference

Hilberg, S. D., 1978: Diurnal Temperature and Moisture Cycles, in Summary of METROMEX, Vol. 2: Causes of Precipitation Anomalies, Bulletin 42, Illinois State Water Survey, Urbana, pp. 25-42.